eman ta zabal zazu

Universidad del País Vasco
Euskal Herriko Unibertsitatea

Universidad del País Vasco / Euskal Herriko Unibertsitatea
Facultad de Medicina y Enfermería
Departamento de Neurociencias

Microglial Phagocytosis/Apoptosis Uncoupling in Epilepsy: Mechanisms and Detrimental Consequences

Tesis doctoral para optar al grado de Doctor, presentada por:

Oihane Abiega Etxabe
2017

Directora de Tesis:

Dra. Amanda Sierra

Esta tesis doctoral ha sido realizada gracias al disfrute de una beca del Programa Predoctoral de Formación de Personal Investigador No Doctor del Departamento de Educación, Política Lingüística y Cultura del Gobierno Vasco durante el periodo 2013-2016.

El trabajo experimental ha sido financiado con becas del ministerio de Economía y Competitividad (http://www.mineco.gob.es), fondos FEDER (BFU2012-32089 y RYC- 2013-12817) (SAF2012-40085 y RYC- 2012-11137), becas del Gobierno Vasco (http://www.euskadi.eus/gobierno-vasco/departamento-desarrollo-economico-competitividad/ inicio/) (Saiotek S-PC 12UN014) y fondos start-up de Ikerbasque.

TABLE OF CONTENTS

TABLE OF CONTENTS

1. ABBREVIATIONS 3

2. RESUMEN/SUMMARY 9

3. INTRODUCTION 25

3.1. INTRODUCTION TO MICROGLIA 25

3.2. MICROGLIAL FUNCTIONS 26

3.2.1. Motility 27

3.2.1.1. *Motility regulation* 28

3.2.1.1.1. *ATP* 28

3.2.1.1.2. *Neurotransmitters* 29

3.2.1.1.3. *Other signals* 30

3.2.2. Proliferation 31

3.2.3. Inflammation 33

3.2.3.1. *Pro-inflammatory cytokines* 34

3.2.3.2. *Anti-inflammatory cytokines* 35

3.2.4. Phagocytosis 36

3.2.4.1. *Synaptic pruning* 37

3.2.4.2. *Amyloid β* 38

3.2.4.3. *Axonal and myelin debris* 39

3.2.4.4. *Dead cells* 40

3.2.4.4.1. *Apoptotic cells* 40

3.2.4.4.2. *Necrotic cells* 41

3.2.4.4.3. *Functional consequences of the phagocytosis of apoptotic cells* 41

3.3. STAGES OF APOPTOTIC CELL PHAGOCYTOSIS AND MECHANISMS OF REGULATION: "FIND-ME", "EAT-ME", AND "DIGEST-ME" 43

3.3.1. "Find-me" stage 43

3.3.2. "Eat-me" stage 45

3.3.3. "Digest-me" stage 46

3.4. MICROGLIAL PHAGOCYTOSIS OF APOPTOTIC CELLS IN PHYSIOLOGICAL CONDITIONS . 47

3.5. MICROGLIAL PHAGOCYTOSIS IN PATHOLOGICAL CONDITIONS: THE CASE OF EPILEPSY... 49

3.5.1. Introduction to epilepsy 49
3.5.2. Focal epilepsies: Mesial temporal lobe epilepsy (MTLE) 50
3.5.3. Generalized epilepsies: Progessive myoclonus epilepsy of Unverricht-Lundborg type 51
3.5.4. Pathological features of epilepsy 52
3.5.4.1. *Excitotoxicity* 53
3.5.4.2. *Inflammation* 53
3.5.5. Microglial phagocytosis and epilepsy 55

4. HYPOTHESIS AND OBJECTIVES 59

5. EXPERIMENTAL PROCEDURES 63

5.1. ANIMALS 63
5.2. SURGICAL PROCEDURES 64
5.2.1. Intrahippocampal injections 64
5.2.2. EEG recordings 65
5.3. CELL CULTURES 65
5.3.1. Organotypic hippocampal slice cultures 65
5.3.2. NE-4C cell line 66
5.3.3. Primary microglia cultures 66
5.4. PHAGOCYTOSIS ASSAY 67
5.5. IMMUNOFLUORESCENCE 67
5.5.1. Brain tissue sections and hippocampal organotypic cultures 67
5.5.2. Primary microglial cultures 68
5.5.3. Antibodies 68
5.6. IMAGE ANALYSIS 69
5.7. PHAGOCYTOSIS ANALYSIS 69
5.8. LIVE IMAGING 71
5.8.1. Two-photon imaging on acute hippocampal slices 71
5.8.2. Two-photon imaging on the living cortex 71
5.9. ELECTROPHYSIOLOGY 73

5.10. FACS SORTING 74

5.11. RNA ISOLATION AND RTqPCR 74

5.11.1. RNA isolation and RT 74

5.11.1.1. *Hippocampus* 74

5.11.1.2. *FACS sorted microglia* 75

5.11.2. qPCR 75

5.11.3. Primers 75

5.12. STATISTICAL ANALYSIS 76

6. RESULTS 81

6.1. MICROGLIAL PHAGOCYTOSIS IS COUPLED TO CELL APOPTOSIS IN PATHOLOGICAL CONDITIONS IN VITRO AND IN VIVO 81

6.1.1. Microglial phagocytosis is coupled to cell apoptosis during excitotoxicity in vitro 81

6.1.2. Microglial phagocytosis is coupled to cell apoptosis during acute inflammation in vivo 84

6.1.3. Microglial phagocytosis is coupled to cell apoptosis during chronic inflammation in vivo 85

6.2. MICROGLIAL PHAGOCYTOSIS IMPAIRMENT IN VIVO IN A PHARMACOLOGICAL MODEL OF EPILEPSY: MESIAL TEMPORAL LOBE EPILEPSY (MTLE) 87

6.2.1. Acute impairment of microglial phagocytosis following seizures in vivo 87

6.2.1.1. *Intrahippocampal injection of KA causes mesial temporal lobe epilepsy (MTLE) and an increase in dead cells in the hippocampus in vivo* 87

6.2.1.2. *Microglial phagocytosis is acutely impaired in the hippocampus during MTLE seizures* 88

6.2.1.3. *Microglial phagocytosis impairment is not compensated by other cell types in the hippocampus* 90

6.2.1.4. *Microglial phagocytosis is acutely impaired in the hippocampus and in the cortex during MTLE seizures* 91

6.2.2. Microglial phagocytosis impairment is related to reduced motility 93

6.2.3. Microglial phagocytosis impairment is triggered by widespread atp release during seizures 95

6.2.3.1. *Microglial phagocytosis impairment is not directly mediated by KA on microglia* 95

6.2.3.2. *Seizures trigger ATP-mediated microglial activation and phagocytosis impairment in vitro* 96

6.2.3.3. *ATP impairs microglial phagocytosis in vitro* 99

6.2.3.4. *ATP impairs microglial phagocytosis in vivo* 102

6.2.3.5. *ATP induced phagocytosis impairment is unrelated to pannexin channel expression on apoptotic cells* 106

6.2.4. Seizures lead to the accumulation of non-phagocytosed apoptotic cells in vivo ... 108

6.2.5. Microglial phagocytosis impairment correlates with inflammation 112

6.3. MICROGLIAL PHAGOCYTOSIS-APOPTOSIS UNCOUPLING IN VIVO IN A GENETIC MODEL OF EPILEPSY: PROGRESSIVE MYOCLONUS EPILEPSY OF UNVERRICHT-LUNDBORG TYPE (EPM1) 114

6.3.1. Microglial phagocytosis is severely uncoupled from apoptosis during seizures in vivo in a model of genetic epilepsy 114

6.3.1.1. *Microglial phagocytosis is uncoupled from apoptosis in cystatin B knock-out mice, a model of progressive myoclonus epilepsy* 114

6.3.1.2. *Microglial proliferation and multinuclearity is increased in Cstb KO mice at PND30 in vivo* 116

6.3.1.3. *Microglial phagocytosis-apoptosis uncoupling is not compensated by astrocytes in Cstb KO mice at PND30 in vivo* 117

6.3.1.4. *Early hippocampal atrophy in PND30 Cstb KO mice in vivo* 118

6.3.2. Microglial phagocytosis-apoptosis uncoupling precedes seizure development in vivo in a model of genetic epilepsy 119

6.3.2.1. *Microglial phagocytosis-apoptosis uncoupling precedes seizure development in Cstb KO mice in vivo* 119

7. DISCUSSION 125

7.1. MICROGLIAL PHAGOCYTOSIS IS COUPLED TO APOPTOSIS IN HEALTH AND DISEASE .. 125

7.1.1. Microglial phagocytosis is fast and efficient in physiological conditions 125

7.1.2. Microglial phagocytosis is coupled to apoptosis in pathological conditions 126

7.1.3. Microglia have a large phagocytic reservoir 126

7.2. SEIZURES INDUCE A MICROGLIAL PHAGOCYTOSIS-APOPTOSIS UNCOUPLING IN EPILEPSY 127

7.2.1. Microglial phagocytosis is uncoupled from apoptosis following seizures in vivo in a pharmacological and a genetic model of epilepsy 127

7.2.2. Microglia remain the most determinant phagocytes during phagocytosis-apoptosis uncoupling in MTLE and EPM1 mice 128

7.2.3. Microglial multinucleation in EPM1 mice 129

7.2.4. Microglial phagocytosis-apoptosis uncoupling could be a widespread phenomenon in the epileptic brain 129

7.3. MECHANISMS OF MICROGLIAL PHAGOCYTOSIS-APOPTOSIS UNCOUPLING IN MTLE . 130

7.3.1. Microglial phagocytosis impairment is unrelated to a direct effect of KA on microglia 130

7.3.2. Microglia sense seizures via ATP 130

7.3.3. Disruption of ATP gradients impairs microglial phagocytosis 131

7. 3.4. ATP induced loss of microglial phagocytosis efficiency is unrelated to microglial viability 132

7.3.5. Pannexin expression is unrelated to microglial phagocytosis impairment 133

7.3.6. Microglial phagocytosis impairment is related to reduced motility 133

7.3.7. Additional mechanisms in microglial phagocytosis impairment 134

7.4. MECHANISMS OF MICROGLIAL PHAGOCYTOSIS-APOPTOSIS UNCOUPLING IN EPM1 134

7.4.1. Microglial phagocytosis-apoptosis uncoupling is unrelated to seizures in EPM1 mice 134

7.4.2. Effects of the lack of cystatin B on microglial phagocytosis 135

7.5. MICROGLIAL PHAGOCYTOSIS IMPAIRMENT HAS DETRIMENTAL CONSEQUENCES FOR THE BRAIN 137

7.5.1. Microglial phagocytosis impairment correlates with the development of an inflammatory response in MTLE 137

7.5.2. Microglial phagocytosis impairment induces a delayed clearance of apoptotic cells in MTLE 138

7.6. MICROGLIAL PHAGOCYTOSIS MODULATION AS A NOVEL THERAPEUTIC TOOL IN NEURODEGENERATION AND BRAIN INJURY 139

8. CONCLUSIONS 145

9. BIBLIOGRAPHY 149

1 ABBREVIATIONS

1. ABBREVIATIONS

4-AP	4-aminopyridine
AA	Arachidonic acid
ACAMPs	Apoptotic cells-associated cellular patterns
ACSF	Artificial cerebrospinal fluid
act-casp3	Activated caspase 3
AD	Alzheimer's disease
ADP	Adenosine diphosphate
ALA	α-linolenic acid
AMP	Adenosine monophosphate
AMPA	α-amino-3-hydroxy-5-methyl-4-isoxazolepropionic acid
AP	Anteroposterior
ApoE	Apolipoprotein E
APP	Amyloid precursor protein
ATP	Adenosine triphosphate
ATPγS	Adenosine 5'-O-(3-thio)triphosphate
AU	Arbitrary units
Aβ	Amyloid beta
BAI-1	Brain-specific angiogenesis inhibitor 1
bal	Balanced
BAPTA	1,2-bis(o-aminophenoxy)ethane-N,N,N',N'-tetraacetic acid
BBB	Blood-brain barrier
BBG	Brilliant blue G
BrdU	Bromo-deoxyuridine
BSA	Bovine serum albumin
CA1	Cornu ammonis 1
CA2	Cornu ammonis 2
CA3	Cornu ammonis 3
CatB	Cathepsin B
CatS	Cathepsin S
CD11b	Cluster of differentiation molecule 11B
cDNA	Complementary DNA
CNS	Central nervous system
CR3	Complement receptor 3
CSF	Colony stimulating factor
Csf1r	Colony stimulating factor 1 receptor
Cstb	Cystatin B
Cx	Cortex
CX3CR1	Fractalkine receptor
CXC3CL1	Fractalkine
d	Day
DAP12	DNAX-activation protein of 12 kD
DAPI	4',6-diamidino-2-phenylindole
def	Deficient

DG	Dentate gyrus
DIV	Day in vitro
DMEM	Dulbecco's Modified Eagle's Medium
DNA	Deoxyribonucleic acid
DNAse	Deoxyribonuclease
do	Days old
Dpi	Days post-injection
DPN	Día post-natal
DV	Dorsoventral
E	Embryonic day
EDTA	Ethylenediaminetetraacetic acid
EEG	Electroencephalography
EGFP	Enhanced green fluorescent protein
ELT	Epilepsia del lóbulo temporal
ELTM	Epilepsia del lóbulo temporal mesial
EMP	Epilepsia mioclónica progresiva
EMP1	Epilepsia mioclónica progresiva tipo 1/Enfermedad de Unverricht-Lundborg
ENTPDases	Ectonucleotidases
EPM1	Progressive myoclonus epilepsy type 1/ Unverricht-Lundborg disease
FA	Fatty acid
FACS	Fluorescence-activated cell sorting
FBS	Fetal Bovine Serum
FC	Fold change
Fc	Fragment crystallizable
GABA	Gamma amynobutyric acid
GABAA	Gamma amynobutyric acid receptor A
GD	Giro dentado
GFAP	Glial fibrillary acidic protein
GFP	Green fluorescent protein
GM-CSF	Granulocyte-macrophage colony stimulating factor
GPR34	G protein-coupled receptor 34
GZ	Granular zone
h	Hours
HBSS	Hank's balanced salt solution
HEPES	4-(2-hydroxyethyl)-1-piperazineethanesulfonic acid
hGFAP	Human glial fibrillary acidic protein
HIV	Human immunodeficiency virus
hpi	Hours post-injection
Hsp60	Heat shock protein 60
i.p.	Intra-peritoneal
Iba1	Ionized calcium-binding adapter molecule 1
IL-1β	Interleukin 1 beta
IL-6	Interleukin 6
KA	Kainic acid, kainate
KO	Knock-out

L27A	60S ribosomal protein L27A
LA	Linolenic acid
LDL	Low density lipoprotein
LL	Laterolateral
LPC	Lysophosphatidylcholine
LPS	Bacterial lipopolysaccharides
M	Microglia
M-CSF	Macrophage colony stimulating factor
MEM	Minimum essential medium
MerTK	Mer tyrosine kinase
MFG-E8	Milk fat globule-epidermal growth factor
mg	Microglia
MIC-1	Macrophage inhibitory cytokine 1
min	Minutes
MIQE	Minimal Information for Publication of Quantitative Real Time Experiments
mo	Months-old
mol	Molecular layer
mpi	Months post-injection
mRNA	Messenger ribonucleic acid
MS	Multiple sclerosis
MTLE	Mesial temporal lobe epilepsy
NB	Neuroblast
ND	Not detected
NeuN	Neuronal Nuclei
NGF	Nerve growth factor
NGS	Normal goat serum
NMDA	N-methyl-D-aspartic acid
OAZ1	Ornithine decarboxylase antizyme
p53	Tumour protein 53
PBS	Phosphate buffered saline
PCR	Polymerase chain reaction
PFA	Paraformaldehyde
Ph	Phagocytosis
Ph/A	Phagocytosis/apoptosis
PI	Propidium iodide
PME	Progressive myoclonus epilepsy
PND	Postnatal day
POMC	Proopiomelanocortin
ppu	Parts per unit
PS	Phosphatidylserine
PUFA	Polyunsaturated fatty acid
qPCR	Quantitative polymerase chain reaction
RNA	Ribonucleic acid
RT	Room temperature
RTqPCR	Reverse transcription quantitative polymerase chain reaction

S1P	Sphingosine-1-phosphate
Sal	Saline
SEM	Standard error of the mean
SGZ	Subgranular zone
SIP	Solution of isotonic percoll
STP	Staurosporine
SVZ	Subventricular zone
t	Time
TGFβ	Transforming growth factor beta
TLE	Temporal lobe epilepsy
TNFα	Tumor necrosis factor alpha
TREM2	Triggering receptor expressed on myeloid cells-2
UDP	Uridine diphosphate
UTP	Uridine triphosphate
vATPases	Vacuolar ATPases
vEEG	Video-electroencephalogram
WT	Wild type
ZSG	Zona subgranular
Ω3	Omega 3 (Ω6, Ω7, Ω9)

2 RESUMEN/SUMMARY

2. RESUMEN

La microglía es el macrófago residente y el fagocito profesional del sistema nervioso central. Son células muy ramificadas con procesos altamente móviles que les permiten monitorizar constantemente el parénquima cerebral. Las dos funciones microgliales fundamentales son la inflamación y la fagocitosis. Como célula inmune del cerebro, la microglía es la encargada de iniciar la respuesta inflamatoria, caracterizada por la liberación de citoquinas pro- y anti-inflamatorias. La inflamación es una respuesta protectora para el cerebro que puede convertirse en perjudicial si no es controlada, como ocurre en muchas enfermedades neurodegenerativas. Por este motivo, el papel de la microglía en las enfermedades neurodegenerativas ha sido ampliamente considerado perjudicial. Sin embargo, la microglía ejerce otras funciones más benignas como fagocito profesional del cerebro.

La fagocitosis hace referencia al proceso mediante el que una célula se come a otra y está compuesta por tres fases: encontrar ("find-me"), engullir ("eat-me") y digerir ("digest-me"). La microglía puede fagocitar distintos tipos de material tanto en situaciones fisiológicas como patológicas, como sinapsis, restos de mielina y axones, y proteínas relacionadas con patologías como la beta amiloide (Aβ), modulando así la función cerebral y la homeostasis a varios niveles. En la presente tesis doctoral nos hemos centrado en la fagocitosis de células en proceso de apoptosis, o muerte celular programada. El reemplazamiento de células por otras nuevas es una parte central tanto del desarrollo embrionario como del mantenimiento diario de la homeostasis tisular. Por lo tanto la apoptosis es un proceso ubicuo en los organismos vivos. Los vastos números de células muertas demandan un sistema de limpieza eficiente del que se encarga la microglía a través de la fagocitosis de los restos celulares. La eliminación de células apoptóticas es muy importante, ya que si no son rápidamente fagocitadas, evolucionan a células necróticas secundarias, perdiendo la integridad de su membrana plasmática y liberando sus contenidos intracelulares tóxicos al medio extracelular. Esto podría tener consecuencias perjudiciales para el tejido circundante ya que se ha relacionado con la iniciación de la respuesta inflamatoria y con enfermedades autoinmunes. Por lo tanto, la rápida y eficiente eliminación de células muertas es crucial para el mantenimiento de la homeostasis tisular. Sin embargo, la fagocitosis microglial sigue siendo un proceso notoriamente desconocido, especialmente in vivo.

La eficiencia fagocítica microglial ha sido estudiada recientemente en condiciones fisiológicas en el nicho neurogénico hipocampal, donde un gran porcentaje de las células recién nacidas muere por apoptosis. En estas condiciones, la fagocitosis microglial es muy

eficiente ya que la microglía está fagocitando hasta un 90% de estas células apoptóticas recién nacidas en un momento dado. Además, desde que la microglía encuentra una célula apoptótica hasta que la digiere por completo transcurre 1.5h, demostrando que la fagocitosis es un proceso muy rápido. Es más, en condiciones fisiológicas solo un pequeño porcentaje de la microglía está fagocitando, lo que sugiere que estas células poseen un potencial fagocítico mucho mayor que podría ser explotado en condiciones en las que haya un gran incremento del número de células apoptóticas, como en el cerebro enfermo. De cualquier forma, la fagocitosis microglial de células apoptóticas en condiciones patológicas sigue siendo desconocida en cuanto a su eficiencia, sus mecanismos de ejecución, sus consecuencias beneficiosas o perjudiciales y su impacto en la homeostasis del tejido cerebral. En la presente tesis doctoral, nuestro objetivo ha sido analizar la eficiencia de la fagocitosis microglial en diferentes condiciones patológicas, como son la epilepsia y sus procesos patológicos subyacentes, para comprender como cada uno de estos procesos patológicos afecta al comportamiento fagocítico microglial.

Epilepsia es un término utilizado para describir un espectro de trastornos neurológicos caracterizados por convulsiones epilépticas (abrupta actividad neuronal anormal y sincronizada). La epilepsia es la tercera enfermedad crónica más común y afecta a entre 50 y 65 millones de personas en todo el mundo. Además de las convulsiones, los pacientes experimentan con frecuencia complicaciones como discapacidad cognitiva y trastornos psiquiátricos como la depresión. La epilepsia puede ser controlada por la medicación pero hoy en día no existe cura. Además, alrededor del 30% de pacientes son farmacorresistentes o refractarios a los actuales tratamientos farmacológicos disponibles. Por lo tanto, la epilepsia representa un serio problema de salud pública global. Depende de la región cerebral donde se inicia, la epilepsia puede ser clasificada como focal o generalizada. Las convulsiones focales o parciales tienen su inicio en un área concreta del cerebro, mientras que en las convulsiones generalizadas está involucrado el cerebro completo. El lóbulo temporal es la región más epileptogénica del cerebro, por lo que la epilepsia del lóbulo temporal (ELT), un tipo de epilepsia focal, es el tipo más común de epilepsia. La epilepsia del lóbulo temporal mesial (ELTM) es uno de los tipos de epilepsia mejor caracterizados y también la forma más común de epilepsia farmacorresistente, lo que obliga a muchos pacientes a someterse a una operación para extraer el hipocampo epiléptico como única alternativa para dejar de sufrir convulsiones. La administración hipocampal de kainato (KA) constituye uno de los modelos más replicables de ELTM. El KA es un agonista de receptores de glutamato y su administración reproduce las principales características histopatológicas y clínicas de la ELTM. Por otro lado, las

convulsiones generalizadas suelen estar provocadas por factores genéticos más a menudo que las focales. Dentro de este grupo están las epilepsias mioclónicas progresivas (EMPs), un grupo heterogéneo de trastornos hereditarios con una patogénesis muy desconocida y generalmente farmacorresitentes. La causa más común de EMP es la epilepsia mioclónica progresiva tipo 1 (EMP1) o enfermedad de Unverricht-Lundborg, un trastorno hereditario autosómico recesivo causado por mutaciones que derivan en la pérdida de función del gen de la cistatina B (Cstb), un inhibidor de las cisteína proteasas.

Los distintos tipos de epilepsia comparten características patológicas como la excitotoxicidad y la inflamación. La excitotoxicidad hace referencia a la muerte causada por una prolongada activación inducida por una liberación excesiva de glutamato. La inflamación se ha erigido durante los últimos años como posible causante de la patogénesis de la epilepsia, ya que muchas citoquinas son epileptogénicas. De hecho hay ensayos clínicos para combatir la epilepsia basados en la reducción de la producción de interleuquina-1β (IL-1β), una citoquina pro-inflamatoria clásica. Además, se ha visto que algunas señales fagocíticas de “find-me” que afectan a la motilidad basal y dirigida y sus receptores están sobreexpresados en modelos de epilepsia, como es el caso de la fractalquina y los receptores purinérgicos, que responden a adenosina trifosfato (ATP) y a sus metabolitos. Sin embargo, la eficiencia de la fagocitosis microglial durante epilepsia o durante sus procesos patológicos subyacentes, excitotoxicidad e inflamación, continúa siendo desconocida.

El objetivo de esta tesis doctoral es analizar la eficiencia fagocítica microglial en estos dos modelos patológicos (ELTM y EPM1), estudiar los mecanismos que controlan la regulación de la fagocitosis durante epilepsia y analizar las posibles consecuencias negativas de un bloqueo fagocítico para la homeostasis del cerebro.

Usando el giro dentado (GD) hipocampal como modelo, nuestro primer objetivo ha sido examinar la eficiencia fagocítica microglial en las condiciones patológicas que ocurren durante la epilepsia, excitotoxicidad e inflamación. Con este propósito hemos usado un modelo de excitotoxicidad in vitro utilizando cultivos organotípicos de hipocampo y modelos de inflamación aguda y crónica in vivo. También hemos estudiado la fagocitosis en un modelo farmacológico de ELTM inducido por administración intrahipocampal de KA in vivo. Todos los parámetros referentes a la eficiencia fagocítica microglial y a la apoptosis celular han sido directamente cuantificados en secciones de tejido tratadas mediante inmunofluorescencia y visualizadas con microscopía confocal. Además, hemos utilizando un nuevo set de parámetros desarrollado por nosotros para la cuantificación directa de estos procesos. En los modelos de excitotoxicidad e inflamación hemos observado una respuesta generalizada en la que la

microglía responde al incremento de células apoptóticas con un incremento en la fagocitosis microglial, es decir, la fagocitosis microglial está acoplada a la apoptosis (Ph/A coupling). Este acoplamiento se consigue mediante una combinación de tres estrategias diferentes: el reclutamiento de microglía fagocítica, el incremento del número de células apoptóticas que cada microglía fagocita (incremento de la capacidad fagocítica) y/o el incremento de los números de microglía. En cambio, en nuestro modelo farmacológico de ELTM in vivo la fagocitosis microglial está severamente impedida durante la fase aguda de la enfermedad (6h a 1 día después de la inyección de KA). Además, el bloqueo fagocítico no solo ocurre en el GD, sino también en otras áreas del hipocampo y de la corteza. Por último, el bloqueo fagocítico microglial no está compensado por otros tipos de células como astrocitos y neuroblastos, lo que convierte a la microglía en el fagocito más determinante en el hipocampo de los ratones ELTM a 1 día post inyección (1dpi).

Nuestro segundo objetivo ha sido analizar cómo las convulsiones afectan al comportamiento fagocítico microglial. Para ello hemos investigado los potenciales mecanismos que subyacen al bloqueo fagocítico en el GD durante la fase aguda del ELTM. Como nuestros resultados muestran que un gran porcentaje de células apoptóticas no fagocitadas están a gran distancia del proceso microglial más cercano, hipotetizamos que podría haber un defecto en la motilidad microglial que estuviera causando el bloqueo fagocítico. Para analizar la motilidad de los procesos microgliales hemos utilizado un modelo ex vivo (rodajas agudas de ratones inyectados con KA) y un modelo in vivo (corteza cerebral situada sobre el hipocampo de ratones inyectados con KA) y hemos visualizado la microglía mediante microscopía de 2 fotones. El KA induce una bajada de la motilidad basal de la microglía a 1dpi en ambos modelos, lo que explica parcialmente el defecto en la fagocitosis microglial de células apoptóticas que observamos durante las convulsiones. Para saber si el KA afecta directamente a la fagocitosis microglial hemos determinado el efecto del KA en la fagocitosis en rodajas organotípicas de hipocampo y en cultivos primarios de microglía a los que añadimos células apoptóticas. El KA no provoca un bloqueo fagocítico de células apoptóticas en las rodajas, seguramente debido a que el KA no induce convulsiones en este modelo in vitro. Los resultados en los cultivos microgliales muestran que el KA provoca una pequeña reducción en el porcentaje de microglía fagocítica. En conjunto, estos resultados apuntan a que el fuerte bloqueo fagocítico microglial que observamos in vivo tras la inyección de KA no es debido a un efecto directo del KA sobre la microglía.

Una molécula que podría actuar como mediadora entre las convulsiones y la microglía es el ATP extracelular, una señal de “find-me” bien conocida que es liberada por células

apoptóticas para atraer a la microglía. El ATP también es liberado durante convulsiones de forma masiva por neuronas y astrocitos. Debido a que el ATP extracelular es degradado muy rápidamente a sus metabolitos, hemos recurrido a un método indirecto para determinar la acción del ATP liberado durante convulsiones sobre la microglía in vitro. Dado que la microglía detecta el ATP a través de varios receptores ionotrópicos (P2X) y metabotrópicos (P2Y), hemos utilizado el brilliant blue G (BBG), un antagonista de amplio espectro de receptores P2X para analizar mediante técnicas electrofisiológicas si la liberación de ATP debido a las convulsiones afecta directamente a la microglía. En estas condiciones, la aplicación de BBG bloquea parcialmente las corrientes catiónicas entrantes en la microglía a través de los canales regulados por ATP, lo que demuestra que la microglía detecta las convulsiones vía ATP. Para determinar si la respuesta electrofisiológica microglial producida por el cóctel correlaciona con un bloqueo fagocítico, hemos analizado la fagocitosis microglial en rodajas organotípicas de hipocampo tratadas con el cóctel. Hemos observado que las convulsiones bloquean per se la fagocitosis microglial, lo que apunta al ATP como mediador del bloqueo fagocítico que observamos en ELTM in vivo. Por lo tanto, hipotetizamos que una liberación masiva de ATP por parte de neuronas y/o astrocitos durante las convulsiones interferiría con el ATP liberado por células apoptóticas, acabando con los microgradientes de ATP que guían a la microglía. Para probar esta hipótesis hemos analizado si el incremento de ATP induce un bloqueo fagocítico per se. Para ello hemos utilizado altas concentraciones de ATP en rodajas organotípicas de hipocampo y en el hipocampo in vivo. En estas condiciones, la eliminación de los gradientes de ATP bloquea la fagocitosis microglial in vitro e in vivo, sugiriendo que el ATP es un mecanismo subyacente clave en el bloqueo fagocítico microglial en nuestro modelo de ELTM y muy posiblemente en otros modelos de epilepsia.

Nuestro tercer objetivo ha consistido en analizar si el bloqueo fagocítico microglial que ocurre durante el ELTM experimental tiene consecuencias nocivas para el tejido cerebral. Primero hemos analizado si el bloqueo fagocítico microglial induce una acumulación de células apoptóticas no fagocitadas en el hipocampo in vivo. Como la mayoría de las células apoptóticas a 1dpi están localizadas en la zona subgranular (ZSG), donde se encuentra el nicho neurogénico hipocampal, hemos estudiado el efecto de las convulsiones en la supervivencia de las células recién nacidas de 3 días de edad. Para ello hemos utilizado un paradigma de administración semi-acumulativa de BrdU antes de la inyección de KA y hemos cuantificado la cantidad de células BrdU positivas vivas y apoptóticas. Hemos observado que el incremento del número de células apoptóticas en ELTM es debido a la acumulación de células apoptóticas no fagocitadas en el hipocampo. Por otro lado, se ha visto que la fagocitosis microglial de

células apoptóticas es activamente anti-inflamatoria in vitro, por lo que hipotetizamos que el bloqueo fagocítico microglial podría correlacionar con el desarrollo de una respuesta inflamatoria. Con este propósito, hemos analizado la expresión de un panel de citoquinas pro- y anti-inflamatorias mediante RTqPCR en tejido hipocampal y microglía hipocampal aislada de ratones inyectados con KA. Las citoquinas inflamatorias están sobreexpresadas tanto a nivel tisular como en la microglía, siguiendo un patrón paralelo al del desarrollo del bloqueo fagocítico microglial a través del tiempo. Por lo tanto, estos resultados muestran que el perfil inflamatorio coincide con el perfil del bloqueo de la eficiencia fagocítica microglial en ELTM.

Nuestro cuarto objetivo ha sido comprobar si el bloqueo fagocítico microglial que observamos en ELTM se da también en otros tipos de epilepsia. Para ello, hemos utilizado un modelo genético de epilepsia generalizada, EMP1, en el que hemos analizado la eficiencia fagocítica microglial in vivo en el GD de ratones Cstb KO a día postnatal 30 (DPN30), la edad en la que comienzan a sufrir convulsiones. Hemos observado que la microglía trata de equilibrar el incremento de la apoptosis proliferando, reclutando más microglía fagocítica y aumentando la capacidad fagocítica de cada célula, al contrario de lo que pasa en ELTM, donde la microglía se vuelve no fagocítica. Sin embargo, esta respuesta microglial insuficiente provoca un desacople de la fagocitosis y la apoptosis en los ratones Cstb KO, como ocurre en ELTM. Para conocer si el desacople microglial estaba compensado otras células en ratones EPM1 a DPN30, hemos cuantificado la fagocitosis astrocitaria. Nuestros resultados muestran que los astrocitos no fagocitan células apoptóticas en ratones Cstb KO, por lo que la microglía sigue siendo el fagocito más relevante en el hipocampo de estos ratones a DPN30, en concordancia con lo que observamos en ELTM. Por último, para comprender más a fondo los mecanismos que regulan la fagocitosis microglial en los ratones con EMP1, hemos analizado si el desacople fagocítico que vemos en los ratones Cstb KO es debido a las convulsiones o a la pérdida de Cstb per se. Para ello hemos analizado la fagocitosis en el DG de ratones Cstb KO a DPN14, edad que precede al comienzo de las convulsiones. Tal y como ocurre a DPN30, hay un intento fallido por parte de la microglía de compensar el incremento en el número de células apoptóticas. Por lo tanto, el desacople entre apoptosis y fagocitosis precede al comienzo de las convulsiones en ratones Cstb KO, apuntando al Cstb como posible regulador de la fagocitosis microglial. Además, ya que la microglía expresa altos niveles de Cstb, estos resultados sugieren que la microglía podría estar contribuyendo al desarrollo de la patología en EMP1.

En conclusión, nuestros resultados demuestran que en el cerebro epiléptico la microglía no está simplemente reaccionando al daño neuronal sino que su función fagocítica básica está bloqueada. Teniendo en cuenta que la muerte neuronal y la inflamación son

aspectos importantes de todas las más importantes enfermedades neurodegenerativas como isquemia, Alzheimer, Parkinson y esclerosis múltiple, aumentar la fagocitosis microglial podría servir para controlar el daño tisular y la inflamación como nueva estrategia para acelerar la recuperación del cerebro. Además, hemos observado que la eficiencia fagocítica microglial afecta de forma crítica a las dinámicas de la apoptosis, hecho que aboga por el análisis rutinario la eficiencia fagocítica microglial en trastornos neurodegenerativos.

2. SUMMARY

Microglia are the resident macrophages and professional phagocytes of the central nervous system (CNS). These highly motile cells constantly monitor the brain parenchyma fulfilling their two fundamental functions: inflammation and phagocytosis. Phagocytosis refers to the cellular process of eating and consists on three different stages: finding, engulfing, and digesting the phagocytic cargo, which are differentially regulated by “find-me”, “eat-me”, and “digest-me” signals, respectively. Microglia can phagocytose all kinds of cargo during physiological and pathological conditions. However, in this PhD thesis we have focused in the phagocytosis of cells undergoing apoptosis, or programmed cell death. Apoptosis is an ubiquitous process in organisms and an essential part of development and everyday tissue homeostasis. Importantly, if apoptotic cells are not rapidly phagocytosed they evolve to secondary necrotic cells, losing the integrity of their plasma membrane and spilling over their toxic intracellular contents, which might exert detrimental consequences for the surrounding tissue. Thus, the rapid and efficient clearance of apoptotic cells is crucial for the maintenance of tissue homeostasis.

Importantly, the efficiency of microglial phagocytosis in physiological conditions has been recently established in the neurogenic cascade of the hippocampus, where a large percentage of the newborn cells undergo apoptosis and are efficiently phagocytosed by microglia. Moreover, only a small proportion of microglia are engaged in phagocytosis, suggesting that they hold a large phagocytic reservoir to face great increases in apoptotic cell numbers. However, microglial phagocytosis of apoptotic cells in pathological conditions in vivo remains unknown. In this PhD thesis, we will focus on the role of microglia in epilepsy.

Epilepsy is a term used to describe a spectrum of neurological disorders characterized by spontaneous epileptic seizures. Epilepsy is the third most common chronic brain disorder, and seizures can be controlled but cannot be cured by medication. Importantly, about 30% of patients are pharmacoresistant. Thus, epilepsy is a significant health concern worldwide. According to the brain region where seizures initiate, they can be classified as focal or generalized. Mesial temporal lobe epilepsy (MTLE), a focal pharmacoresistant epilepsy, is one of the best-characterized and most frequent type of epilepsy. One of the most reliable MTLE models is the intrahippocampal administration of kainate (KA), a glutamate receptor agonist which mimics all the main histopathological and clinical features of MTLE. Generalized epilepsies include progressive myoclonus epilepsies (PMEs), pharmacoresistant epilepsies with a poorly understood pathogenesis. The most common cause of PME is epilepsy myoclonus

type 1 (EPM1), a genetic disorder caused by loss-of-function mutations in the cystatin B gene (Cstb), an inhibitor of cysteine proteases.

These different types of epilepsies share two common pathological features, excitotoxicity and inflammation. Excitotoxicity refers to cell death caused by a prolonged activation due to excessive glutamate release. Inflammation is caused by the increased inflammatory mediator release during epilepsy, and has gained attention as a possible underlying contributor to the pathogenesis of seizures, as many cytokines are epileptogenic. Phagocytic "find-me" signals and their receptors, such as CX3CL1 and purinergic receptors, which respond to adenosine triphosphate (ATP) and its metabolites have also been found to be upregulated in epilepsy models. Nevertheless, microglial phagocytosis efficiency during epilepsy or during its underlying pathological processes, excitotoxicity and inflammation, remains unknown. Therefore, the goal of this PhD thesis has been to analyze microglial phagocytosis efficiency in these two pathological models, MTLE and EPM1. We have also assessed the mechanisms underlying the regulation of phagocytosis during epilepsy, as well as analyzing the possible detrimental consequences of a phagocytosis impairment for brain tissue homeostasis.

Using the hippocampal DG to quantify phagocytosis, our first aim was to examine the microglial phagocytosis efficiency during excitotoxicity and inflammation. For this purpose, we used an in vitro excitotoxicity model using organotypic hippocampal slices, and acute and chronic inflammation models in vivo. We also assessed phagocytosis in a pharmacological model of MTLE in vivo, induced by intrahippocampal administration of KA. We show evidence of a widespread response of microglia to apoptotic challenge induced by excitotoxicity or inflammation in which microglial phagocytosis remains tightly coupled to apoptosis, i.e., a rise in apoptotic cell numbers is matched with an increase in microglial phagocytosis. Hence, in these conditions there is phagocytosis/apoptosis coupling (Ph/A coupling). We also show that this coupling is achieved by a combination of three different strategies: recruiting more microglial cells to be phagocytic, increasing the phagocytic capacity of each cell (the number of apoptotic cells each microglia engulfs), and/or increasing microglial numbers. Unexpectedly, microglial phagocytosis is severely impaired in our pharmacological model of MTLE in vivo during the acute phase of the disease (6h to 1 day after KA injection) in the DG and other areas of the hippocampus and in the cortex. Importantly, the microglial phagocytosis impairment is not compensated by other cell types (astrocytes, neuroblasts), which renders the impaired microglia the most determinant phagocyte in the hippocampus of MTLE mice at 1dpi.

Our second aim was to understand how seizures affect microglial behavior and thus, we investigated the potential mechanisms underlying the phagocytosis impairment in the DG during the acute phase of KA induced MTLE. Because many apoptotic cells were localized far away from microglia, we hypothesized that there could be a possible defect in microglial surveillance and/or targeting of apoptotic cells, caused by an impaired motility. Using live-imaging in acute hippocampal slices from KA injected mice and in the cortex of KA injected mice in vivo, we show that KA induces a decrease in basal microglial motility 1 day after KA injection, which partially explains the defect in microglial phagocytosis of apoptotic cells observed after seizures. To further assess if KA was directly affecting microglial behavior, we determined the effect of KA on microglial phagocytosis in hippocampal slices and primary microglia fed with apoptotic cells. Importantly, KA does not impair microglial phagocytosis of apoptotic cells in hippocampal slices and induces a very small reduction in the percentage of phagocytic primary microglia. Therefore, the strong impairment of microglial phagocytosis that we observe in vivo after KA injection is unlikely due to a direct effect of KA on microglia.

The extracellular ATP could be an alternative mediator between seizures and microglia. ATP is a well known “find-me” signal released by apoptotic cells and is also released during seizures, from neurons and astrocytes. Because extracellular ATP is very rapidly degraded into its metabolites, we resorted to indirectly determine the action of ATP released during seizures on microglia using acute hippocampal slices treated with a seizure inducing epileptogenic cocktail and a broad ionotropic purinergic receptor inhibitor. Electrophysiological measurements shows that the purinergic inhibitor partially blocks large inward currents in microglia, thus indicating that microglia sense seizures via ATP. To determine whether the cocktail induced electrophysiological microglial response correlated with a phagocytosis impairment, we assessed microglial phagocytosis using hippocampal organotypic slices treated with the epileptogenic cocktail. We show that seizures per se impair microglial phagocytosis, pointing towards ATP as the mediator of the phagocytosis impairment we observe in experimental MTLE in vivo. Thus, we hypothesized that a widespread release of ATP by neurons and/or astrocytes during seizures would interfere with the ATP released by apoptotic cells, disrupting ATP microgradients. To prove this hypothesis we disrupted ATP microgradients using high concentrations of ATP in hippocampal slices and in the hippocampus in vivo. In accordance, ATP greatly impairs microglial phagocytosis in vitro and in vivo suggesting that ATP is a main underlying cause of the early phagocytosis impairment in experimental MTLE.

Our third aim was to assess whether the microglial phagocytosis impairment during pharmacologically induced MTLE would have detrimental consequences for the brain. Thus,

we first tested whether the phagocytosis impairment induced an accumulation of non-phagocytosed apoptotic cells in the hippocampus in vivo. As the majority of apoptotic cells at 1 day after KA are located in the SGZ, where new neurons are born, we studied the effect of seizures on the apoptosis and survival of 3 day old (3do) newborn cells using a semi-cumulative BrdU administration paradigm before the KA injection. Importantly, the rise of apoptotic cell numbers in the SGZ induced by KA is largely due to accumulation of the non-phagocytosed newborn cells that underwent apoptosis in physiological conditions. Thus, microglial phagocytosis impairment causes the accumulation of uncleared apoptotic cells in the hippocampus. Moreover, as microglial phagocytosis of apoptotic cells has previously been shown to be actively anti-inflammatory in vitro, we hypothesized that the microglial phagocytosis impairment could correlate with the development of an inflammatory response. For this purpose, we analyzed the expression of pro- and anti-inflammatory cytokines by RTqPCR in hippocampal tissue samples and in acutely isolated hippocampal microglia from KA injected mice. We show that inflammatory cytokines are upregulated both at the tissue level and in isolated microglia. Thus, the profile of inflammation coincides with the profile of the impaired phagocytosis efficiency in MTLE.

Our fourth aim was to extend our observations on the microglial phagocytosis impairment to other types of epilepsy. Thus, we focused on a genetic model of epilepsy, EPM1. For this purpose, we assessed microglial phagocytosis efficiency in vivo in the DG of Cstb KO mice at the seizure onset age, postnatal day 30 (PND30). In these conditions, microglia try to balance the increase in apoptosis by proliferating, recruiting more phagocytic cells, and increasing the phagocytic capacity of each cell, contrary to what happens in MTLE, where microglia mainly become non-phagocytic. Nevertheless, the insufficient microglial response leads to a phagocytosis-apoptosis uncoupling in Cstb KO mice, resembling our results in MTLE. Moreover, microglial phagocytosis impairment is not compensated by astrocytes in PND30 Cstb KO mice, similarly to what we observe in MTLE. To further understand the mechanisms regulating microglial phagocytosis, we assessed whether the phagocytosis-apoptosis uncoupling in Cstb KO mice was due to seizures or to the loss of Cstb per se by analyzing phagocytosis in the DG of Cstb KO mice at PND14, an age preceding seizure onset. We show a failed attempt by microglia to compensate the increase in apoptosis identical to the impairment in Cstb KO mice at PND30. Thus, these results demonstrate that the microglial phagocytosis impairment precedes seizure development in Cstb KO mice, pointing at Cstb as a possible regulator of microglial phagocytosis. Furthermore, as microglia expresses high levels

of Cstb, these results suggest that microglia might be contributing to the development of the pathology in EPM1.

In conclusion, our results prove that in the epileptic brain microglia are not merely “reactive” to the neuronal damage but have their basal phagocytic function impaired. Because neuronal death and inflammation are hallmarks of all major neurodegenerative diseases, harnessing microglial phagocytosis may serve to control tissue damage and inflammation as a novel strategy to accelerate brain recovery. Moreover, these results demonstrate that the efficiency of microglial phagocytosis critically affects the dynamics of apoptosis and urge to routinely assess the microglial phagocytosis efficiency in neurodegenerative disorders.

3 INTRODUCTION

3. INTRODUCTION

3.1. INTRODUCTION TO MICROGLIA

Microglia are the resident macrophages and professional phagocytes of the central nervous system (CNS). Moreover, they are the unique population of resident immune cells in the brain and thus, the major orchestrators of the innate immune response (Sierra et al., 2013). Microglia are part of the glial cells, alongside with astrocytes, oligodendrocytes, and ependymal cells, and they account for 5–12% of the total glial cell population in the brain (Gomez-Nicola and Perry, 2015). First described by Pío del Río-Hortega in 1919 (Tremblay et al., 2015), microglia are highly ramified cells and are randomly distributed in close proximity with each other, but with little overlap between the processes of neighbouring cells (Graeber, 2010). Microglia are broadly distributed through the brain (Lawson et al., 1990), although their density and morphology are region-specific, and they are more abundant in the gray than in the white matter (Lawson et al., 1990).

During embryonic development, all glial cells except microglia originate from the ectodermal layer of the early embryo, one of the three primary germ layers. In contrast, microglia have a mesodermal origin and are generated in the yolk sac during embryogenesis at embryonic day 7.5 (E7.5) in the mouse, when hematopoietic stem cells in the yolk sac become primitive macrophages and then migrate into the developing CNS to become microglia (Aguzzi et al., 2013; Casano and Peri, 2015; Ginhoux and Prinz, 2015). Unlike other yolk sac- derived macrophages, microglia are not replaced during the postnatal period and later life by liver- or bone marrow-derived macrophages (Hoeffel et al., 2012).

Thus, microglia belong to the monocyte-macrophage linage, and as such they play central roles to survey and regulate the microenvironment to support homeostasis during brain development and under normal and pathological conditions (Prinz and Priller, 2014). Nevertheless, microglia are not just brain macrophages, as shown by their cell-specific gene expression signatures, distinct ontogeny and differential functions, which are totally adapted to their environment (Butovsky et al., 2012; Gautier et al., 2012; Ginhoux et al., 2010; Kierdorf et al., 2013; Prinz and Priller, 2014; Schulz et al., 2012). We will cover the wide arrange of microglial functions in the next section.

3.2. MICROGLIAL FUNCTIONS

As the most susceptible sensors of changes in the brain, microglia fulfill a wide range of functions (Ginhoux et al., 2013; Nayak et al., 2014). During develoment, microglia can promote either cell death or cell survival depending on the microenvironment and interactions with other cell types (Czeh et al., 2011; Hanisch and Kettenmann, 2007; Mallat and Chamak, 1994; Ueno et al., 2013). Moreover, microglia may play a role in regulating neurogenesis during development, although direct evidence is still missing (Antony et al., 2011; Cunningham et al., 2013; Swinnen et al., 2013). However, during adulthood, microglia contribute to neurogenesis through the clearance of excessive newborn neurons by phagocytosis, both in the hippocampus (Sierra et al., 2010) and in the subventricular zone (Fourgeaud et al., 2016). Moreover, during pathological conditions such as aging and neurodegenerative diseases, microglial-derived pro-inflammatory cytokines are considered detrimental for adult neurogenesis, although the relative contribution of microglia versus other types of cells involved in the inflammatory response remains unknown (Sierra and Tremblay, 2014). Microglia may also be involved in developmental astrogliogenesis, due to the sequential appearance of microglia and astrocytes in the same regions during CNS development (Aquino et al., 1996; Fox et al., 2004; Kalman and Ajtai, 2001; Monier et al., 2006; Voigt, 1989), although the functional relationship between these cells has not been determined. Importantly, the production of pro-inflammatory mediators by neuroinflammatory microglia induces the appearance of reactive astrocytes, which lose the ability to promote neuronal survival, outgrowth, and synaptogenesis, and induce the death of neurons and oligodendrocytes (Liddelow et al., 2017). Microglia may also play a role in myelination by producing several growth factors that control proliferation and survival of oligodendrocytes and their precursors (Park et al., 2001). Moreover, there might also be a relationship between microglia and vasculogenesis, as microglia can be found in temporal and spatial association with developing vasculature (Imamoto and Leblond, 1978; Rezaie et al., 1997; Rezaie et al., 2005), although the functional implications of co-localization have not been clearly defined to date (Arnold and Betsholtz, 2013). Furthermore, several studies suggest that microglia may also contribute to synapse formation (Coull et al., 2005; Parkhurst et al., 2013), maturation (Paolicelli et al., 2011; Zhan et al., 2014), function, and plasticity (Paloneva et al., 2000; Roumier et al., 2004; Roumier et al., 2008; Walker and Lue, 2013). Thus, new roles for microglia in the brain are emerging and will be further studied in the future.

However, in this thesis we have focused in the two fundamental microglial functions, inflammation and phagocytosis, due to their central role in the response of microglia to

pathological conditions. We will also tackle microglial motility and proliferation, as they are essential for phagocytosis because they affect microglial surveillance capacities and are key features for exerting microglial functions in a localized manner. We will cover all these functions in more depth in the next sections.

3.2.1. Motility

One of the most characteristic features of microglia is the high motility if their processes. In the healthy adult brain, microglia are present as so-called ‘‘ramified microglia’’ with highly branched processes (Koizumi et al., 2013). The basic morphology of cortical microglia in physiological conditions, as described in mice, is generally represented in a complex branch order as follows: the first branch order, usually between seven and nine main processes, which extend directly from the cell soma; the second branch order are medium processes, which branch from the main processes to several shorter and thinner processes; and the third branch order fine processes, which are mostly devoid of expression of ionized calcium-binding adapter molecule 1 (Iba-1), a macrophage marker (Baron et al., 2014). Similar to the typical morphological properties of microglia in the healthy mouse cortex, microglia in the healthy zebrafish brain are also highly branched with dynamic processes, which end with stick-like or bulbous tips (Peri and Nusslein-Volhard, 2008; Sieger and Peri, 2013).

Importantly, microglial processes are constantly and rapidly monitoring their immediate surroundings by extension and retraction (Davalos et al., 2005; Nimmerjahn et al., 2005), and are morphologically plastic with considerable motility, presenting a similar rate of extension and retraction of around 1.5 µm/min (Nimmerjahn et al., 2005). In contrast, the small-shaped soma of microglial cells has been shown to remain still overtime, and only 5% of the cells move at 1–2 µm/h (Nimmerjahn et al., 2005). This constant movement of microglial processes while the soma remains stationary is called microglial motility (Hristovska and Pascual, 2015).

Microglial motility can be classified into two modes: baseline surveillance, with apparently random non-directed process movements; and microglial chemotaxis, a response to cell or tissue damage, with highly targeted movements of microglial processes toward the injury site (Madry and Attwell, 2015). Interestingly, microglial baseline surveillance operates isotropically, with process extensions and retractions in all directions, whereas chemotaxis is anisotropic and involves process retraction on one side of the microglial cell and process extension on the other side (Madry and Attwell, 2015) (**Figure 1**).

Microglial cells are the most dynamic brain cells, as no other cells display such morphological plasticity in vivo. The dynamism of microglial processes in vivo has also been confirmed in the mouse spinal cord and retinal explants (Davalos et al., 2005; Lee et al., 2008), and in the zebrafish embryo (Peri and Nusslein-Volhard, 2008). It has been suggested that these dynamic microglial prolongations entirely survey the brain every few hours (Nimmerjahn et al., 2005). This surveying capability of microglia is of paramount importance to rapidly register any environmental changes caused by cellular death, toxicity or injury in the brain, thus allowing them to rapidly act as required (Koizumi et al., 2013).

3.2.1.1. *Motility regulation*

Microglial motility requires cytoskeletal rearrangements, and therefore, microglia have high amounts of filamentous actin (Capani et al., 2001). Agents blocking actin polymerization such as cytochalasin B or latrunculin B inhibit both microglial baseline surveillance and chemotaxis in acute brain slices (Hines et al., 2009). Besides cytoskeleton rearrangement requirements, microglia are equipped with a rich repertoire of sensing receptors (Kettenmann et al., 2011), which allow them to respond to a variety of chemotactic triggers (Andreasson et al., 2016), such as the extracellular nucleotide adenosine triphosphate (ATP), neurotransmitters, and others (Madry and Attwell, 2015) (**Figure 1**).

3.2.1.1.1. *ATP*

A key regulator of microglial morphology and baseline dynamics identified in recent years is the extracellular nucleotide ATP, a neuro- and gliotransmitter. ATP is released by neurons and astrocytes into the extracellular space and is rapidly degraded by extracellular ectonucleotidases to adenosine 5'-diphosphate (ADP), adenosine monophosphate (AMP), and adenosine, and each of them signal to microglia on a plethora of promiscuous receptors: P2X receptors (ionotropic, activated by ATP), P2Y receptors (metabotropic, activated by ATP and ADP), and P1 receptors (metabotropic, activated by adenosine). Interestingly, disruption of ATP-dependent signalling in the presence of the ATP/ADP hydrolyzing enzyme apyrase decreases the basal motility of microglial processes in vivo (Davalos et al., 2005), while application of ATP increases basal motility and cell complexity in mouse retinal explants, an ex vivo model with minimal CNS damage (Fontainhas et al., 2011). ATP is also involved in microglial chemotaxis because focal applications of ATP cause a striking extension of microglial processes towards the source of ATP in vivo and in brain slices (Davalos et al., 2005; Dissing-Olesen et al., 2014), while process outgrowth persists as long as ATP is applied (Dissing-Olesen et al., 2014). In addition, ATP critically mediates microglial chemotaxis towards sites of

increased neuronal activity in vivo (Eyo et al., 2014; Li et al., 2012). Therefore, ATP and its metabolites are key regulators of microglial motility (**Figure 1**).

Importantly, the effects of ATP on microglial motility can be mediated through other mechanisms. In addition to inducing microglial chemotaxis, activation of P2Y purinergic receptors also elicits an outward K^+ current in microglia in acute brain slices. This current can be blocked with the non-selective K^+ channel antagonist quinine abolishing ATP chemotaxis, suggesting its importance in ATP/ADP-mediated microglial motility (Wu et al., 2007). Moreover, blocking volume-sensitive chloride channels prevents microglial chemotaxis in acute brain slices, while microglial baseline motility is unaffected (Hines et al., 2009). Volume regulation may be essential for microglial cell processes navigating through narrow extracellular spaces. Volume-sensitive chloride channels (and channels with similar pharmacology, like transmembrane channels pannexins (Dahl et al., 2013), also mediate ATP release from cells (Mitchell et al., 1998). Thus, ATP signalling can be modulated through these pathways.

3.2.1.1.2. *Neurotransmitters*

Another relevant signalling pathway regulating microglial process length and motility involves glutamate and gamma amynobutiric acid (GABA), the main excitatory and inhibitory neurotransmitters in the brain, respectively (Dissing-Olesen et al., 2014; Fontainhas et al., 2011). Although initial studies failed to demonstrate any effect of local application of glutamate and GABA on microglial motility (Chen et al., 2010; Nimmerjahn et al., 2005; Wu and Zhuo, 2008), it has been found that glutamatergic and GABAergic neurotransmission modulate microglial morphology and motility in retinal explants: GABA application decrease microglial motility, whereas bicuculline, a competitive antagonist of $GABA_A$ receptors, increases both the size and basal velocity of microglial processes, although application of glutamate alone does not change any of the above parameters (Fontainhas et al., 2011). Increases in neuronal activity evoked by glutamate or its analogues N-methyl-D-aspartate (NMDA), α-amino-3-hydroxy-5-methyl-4-isoxazolepropionic acid (AMPA), or kainic acid (KA), or by blocking GABAergic inhibition, lead to microglial process extension and enhanced baseline motility, whereas block of AMPA receptors has the opposite effect (Dissing-Olesen et al., 2014; Eyo et al., 2014; Fontainhas et al., 2011; Nimmerjahn et al., 2005).

However, recent studies suggest that glutamate and GABA do not exert a direct effect over microglial motility, but through the modulation of extracellular levels of ATP and its metabolites. Indeed, in microglia in acute brain slices or retinal explants, only extracellular

nucleotides such as ATP, ADP, and uridine diphosphate (UDP) evoke inward membrane currents through ionotropic P2X receptors and outward potassium currents via G protein-coupled (P2Y) purinergic receptors (Arnoux et al., 2013; Avignone et al., 2008; Boucsein et al., 2003; Fontainhas et al., 2011; Ulmann et al., 2013; Wu et al., 2007; Wu and Zhuo, 2008), whereas other neurotransmitters (glutamate, GABA, glycine, acetylcholine, dopamine, or noradrenaline) generate no current (Avignone et al., 2008; Boucsein et al., 2003; De Simoni et al., 2008; Eyo et al., 2014; Wu et al., 2007; Wu and Zhuo, 2008). These results are in agreement with the discovery that ionotropic glutamatergic receptors are not present on microglial processes and soma when assessed by immunofluorescence in retinal explants (Fontainhas et al., 2011). Thus, neuronal activity-evoked changes in microglial morphology and baseline motility are most likely not due to direct neurotransmitter signaling from active neurons to microglia, but rather are indirectly mediated by local rises of extracellular nucleotide concentrations (**Figure 1**).

3.2.1.1.3. *Other signals*

Besides neurotransmitters, there are other signals which can regulate microglial motility. One of such signals is the chemokine fractalkine (CXC3CL1), a chemotactic factor for microglia (Réaux-Le Goazigo et al., 2013). In retinal explants, CX3CR1 knock-out leads to reduced microglial baseline surveillance and chemotaxis (Liang et al., 2009). Thus, CXC3CL1 signaling promotes microglial motility. Another potent inducer of microglial chemotaxis is the plasma protein fibrinogen, acting via its CD11b/CD18 receptor (integrin αMβ2) (**Figure 1**), in diseases with blood-brain barrier (BBB) disruption such as multiple sclerosis (MS), or small haemorrhages (Davalos et al., 2012), as shown in an in vivo model of MS and by injecting physiological concentrations of fibrinogen into the intact brain. Knocking out the binding motif of the CD11b/CD18 receptor led to smaller clusters of microglia around blood vessels, and reduced axonal damage (Davalos et al., 2012). In contrast to the few in vivo studies, numerous other chemoattractants have been shown to induce chemotaxis of cultured microglia in vitro, including various chemokines, tissue complement, and growth factors (Cross and Woodroofe, 1999; Forstreuter et al., 2002; Nolte et al., 1996).

The variety of signals regulating microglial motility confirms that a fine regulation of motility is of paramount importance, as it allows microglia to accurately sense their surroundings and rapidly respond to any relevant extracellular cues. Moving their processes or migrating if necessary, microglia will reach any area of the brain and locally exert their various functions as required. Importantly, microglial cell numbers can also greatly affect the rest of

their functions. Microglial population numbers are controlled by proliferation, a process which we will cover next.

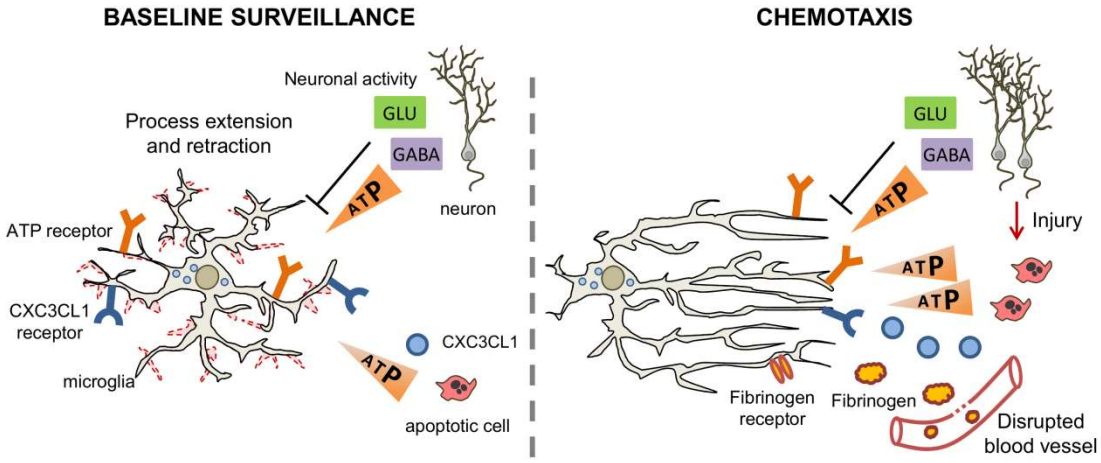

Figure 1. Microglial motility regulation. Microglial cells are the most dynamic brain cells, constantly and rapidly moving their processes to monitor their immediate surroundings. Microglial motility can be classified as baseline surveillance, with apparently random non-directed process movements; and microglial chemotaxis, a response to cell or tissue damage, with highly targeted movements of microglial processes toward the injury site. Ramified surveying microglia are equipped with a repertoire of sensing receptors to respond to a variety of chemotactic triggers. Purinergic receptors respond to ATP, a key regulator of microglial baseline surveillance. Focal applications of ATP induce chemotaxis towards the source of ATP, causing a directed extension of microglial processes. ATP also mediates microglial chemotaxis towards sites of increased neuronal activity in vivo, and mediates the effect of neurotransmitters Glu and GABA on microglial motility. The chemokine CXC3CL1 also modulates microglial baseline surveillance and chemotaxis. In addition, the plasma protein fibrinogen, acting via its CD11b/CD18 receptor (integrin αMβ2), is another potent inducer of microglial chemotaxis in diseases with BBB disruption.

3.2.2. Proliferation

Cell proliferation results in an increase of the number of cells, and is defined by the balance between cell divisions and cell loss. The goal of cell proliferation is double: first, it is a fundamental process to maintain cell populations, as it counteracts the effects of cell loss caused by cell death or differentiation; second, it is a key response to increase the numbers of a given cell population when needed. While other microglial responses have been widely studied, proliferation is still not well characterized (Shankaran et al., 2007).

In the case of microglia, the homeostatic maintenance of the microglial population during an organism's lifetime is achieved through proliferation. In the adult mice in physiological conditions there is a highly dynamic but tightly regulated control of microglial cell numbers (Askew et al., 2017). Microglia display a high proliferation rate which is temporally

and spatially coupled to microglial apoptosis, resulting in the maintenance of a relatively steady number of cells from early postnatal stages through to aging (Askew et al., 2017). Moreover, different brain regions show differences in microglial self-renewal rates which correlate with the proliferation of other CNS cells in the respective environment, albeit at a lower rate compared to that of other brain cells (Tay et al., 2017). Furthermore, the high microglial proliferation enables the microglial population to be formed without a contribution from circulating progenitors and it accounts for several rounds of renewal of the whole population during the organism's lifetime (Askew et al., 2017).

Microglia can also undergo proliferation and increase in numbers in response to injury (Grady et al., 2003; Graeber et al., 1988; Liu et al., 2001; Marlatt et al., 2014). Importantly, the expansion of the microglial population during neurodegeneration is almost exclusively dependent upon proliferation of resident cells (Gomez-Nicola et al., 2013; Gomez-Nicola and Perry, 2015; Li et al., 2013). Microglial proliferation has been shown to occur in many neurodegenerative diseases such as in different models of MS (Remington et al., 2007), in mice models and post-mortem samples from patients with Alzheimer's disease (AD) (Gomez-Nicola et al., 2013; Gomez-Nicola, 2014; Kamphuis et al., 2012; Marlatt et al., 2014), in axonal lesion models (Dissing-Olesen et al., 2007), in ischemia (Zhang et al., 2009), and in epilepsy models (Nitecka et al., 1984). In a model of acute neurodegeneration (facial nerve axotomy), microglia quickly shift from the random proliferation observed in homeostatic circumstances toward selected clonal expansion leading to clusters of daughter cells (Tay et al., 2017). Furthermore, there is a dual mechanism of microglial cell removal for the restoration of the homeostatic microglial network after facial nerve axotomy: first, egress of excess microglia from the area of CNS pathology into nearby compartments and, second, their local cell death by apoptosis (Tay et al., 2017). Microglia also proliferate during neuroinflammation, and their numbers return to normal again via apoptosis once the inflammation is resolved (Stebbing et al., 2015). Inhibition of proliferation, coupled with inflammatory mediator production inhibition, has been found to be neuroprotective in a rat model of ischemia (Zhang et al., 2009), and the ablation of microglial proliferation in a stroke model has been shown to lead to a larger stroke lesion area and increased neuronal death (Lalancette-Hebert et al., 2007). Thus, these results point at proliferating resident microglia as crucial for a better outcome in cerebral ischemia (Cipriani et al., 2014). However, the beneficial or detrimental role of microglial proliferation in brain homeostasis in different pathologies in the short and long run still remains to be elucidated.

Interestingly, multinucleated microglia, or cells with multiple nuclei sharing their cytoplasm, are related to both proliferation and inflammation. Microglial multinucleation

results from incomplete mitosis because it is caused by nucleokinesis without cytokinesis due to a failure of abscission, followed by reversal of the earlier stages of cytokinesis (Hornik et al., 2014). Moreover, this unresolved nucleokinesis has been shown to be induced by inflammation in primary microglia in vitro (Lee et al., 1993; Suzumura et al., 1999). During chronic inflammation as a result of persistent infection or foreign bodies, macrophages can form multinucleated giant cells (MGCs) (McNally and Anderson, 2005; Quinn and Schepetkin, 2009). MGCs derived from microglia have been implicated in a variety of brain pathologies. In particular, human immunodeficiency virus (HIV)-associated dementia is mediated by HIV-infected microglia, which become MGCs, but how these infected multinucleate microglia cause dementia is unclear (Ghorpade et al., 2005; Nardacci et al., 2005). Microglia also form MGCs in the spinal cord of rats expressing a mutant Cu/Zn superoxide dismutase gene, modelling amyotrophic lateral sclerosis in humans (Fendrick et al. 2007). Amyloid-β (Aβ) related angiitis, is associated with an accumulation of microglia and MGCs containing intracellular deposits of Aβ (Melzer et al. 2012). Whether Aβ can induce microglia to form MGCs is unknown. In addition, MGCs derived from microglia accumulate in the brain with age (Hart et al. 2012). However, the function, dysfunction or lack of function of MGCs is unclear (McNally and Anderson 2011). Multinucleate microglia induced in vitro in a microglial cell line have been found to behave similarly to mononucleate microglia, but are larger and have a higher capacity to phagocytose large beads and cells (Hornik et al., 2014). Interestingly, multinucleate microglia have a disproportionately higher capacity to phagocytose the larger beads, and a substantially increased ability to phagocytose dead and live cells, relative to mononucleate microglia (Hornik et al., 2014). Nevertheless, the consequences of microglial multinucleation on their functions in vivo remain unknown.

Thus, microglial proliferation is a process that can greatly affect the outcome of key microglial functions in a population level. One of such functions is inflammation, which we will cover next in more depth.

3.2.3. Inflammation

As the innate immune cells of the brain, one of the main roles of microglia is to initiate an inflammatory response. Inflammation is a protective response of the body to harmful stimuli (Ferrero-Miliani et al., 2007). The classical signs of inflammation are heat, pain, redness, swelling and loss of function. Inflammation is considered a mechanism of the innate immune system because it is a generic response given to any pathological stimulus. In contrast, the mechanisms of adaptive immunity are specific to each pathogen (Alberts et al., 2002). The

function of inflammation is to eliminate the initial cause of cell injury, clear out dead cells and tissues damaged from the original insult and the inflammatory process, and to initiate tissue repair (Lucas et al., 2006).

Inflammation can be triggered by a variety of stimuli including pathogens, such as bacteria, fungi, parasites, and viruses (Nayak et al., 2014). Nevertheless, pathogens very rarely enter the brain parenchyma, thanks to the blood brain barrier, a highly selective semipermeable membrane formed by endothelial cells, which separates the circulating blood from the brain parenchyma (Pardridge, 2005). Thus, inflammation is more commonly induced by other triggers such as brain injury, disease associated proteins, environmental toxins, and uncontrolled death (Block and Hong, 2005).

When subjected to an inflammatory stimulus, microglia respond by releasing a variety of soluble factors, such as pro- and anti-inflammatory cytokines, chemokines, complement proteins, free radicals, and trophic factors (Nayak et al., 2014). Among these, cytokines play a central role. Cytokines are a class of proteins which regulate inflammation, constituting a diverse group of pro- and anti-inflammatory factors modulating cellular activities such as growth, survival, differentiation, and neuronal excitability (Vilček, 2003). Cytokine binding to its receptors in neurons and glia triggers a cascade of signalling events that regulate various cellular functions such as cell adhesion, cytokine secretion, cell survival, apoptosis, angiogenesis, and proliferation (Devi, 2000). Importantly, microglia are not the only source of these cytokines, but they can also be released by astrocytes, oligodendrocytes, endothelial cells and even neurons (Benveniste, 1992; Cámara-Lemarroy et al., 2010; Watkins and Maier, 2002).

Cytokines are broadly categorized as pro-inflammatory or anti-inflammatory (**Figure 2**).

3.2.3.1. *Pro-inflammatory cytokines*

Pro-inflammatory cytokines play a role in initiating the inflammatory response. The most extensively studied pro-inflammatory cytokines are interleukin 1 beta (IL-1β), tumour necrosis factor α (TNFα), and interleukin 6 (IL-6) (Vezzani et al., 2011) (**Figure 2**). Brain inflammation has been reported in all acute and chronic neurodegenerative diseases, such as AD, Parkinson's, stroke, MS, epilepsy, etc, and even in mood disorders (Amor et al., 2010; Vezzani et al., 2011). In these conditions, IL-1β, TNFα, and IL-6 are first expressed in microglia and astrocytes, and cytokine receptor expression is upregulated in microglia, astrocytes and neurons (Vezzani and Granata, 2005). Interestingly, there are other less known pro-inflammatory cytokines, such as M-CSF (macrophage colony stimulating factor), which is

involved in the microglial phagocytosis impairment observed in brain tumours (Gabrusiewicz et al., 2011; Jinushi et al., 2007).

Although the functions of many inflammatory mediators remain unknown, clear evidence exists for a detrimental role of pro-inflammatory cytokines in many brain pathologies. In fact IL-1β and TNFα are known to induce excitotoxicity, or cell death provoked by over-activation of glutamatergic receptors, by elevating intracellular and extracellular glutamate levels in human and rat primary neuron cultures in vitro (Ye et al., 2013). Moreover, the facilitatory role of TNFα in glutamate excitotoxicity is mediated by inhibition of astrocytic glutamate transporters, thus blocking glutamate re-uptake from the extracellular space (Pickering et al., 2005). Additionally, TNFα has direct effects on glutamate transmission, as it increases the expression of glutamatergic AMPA receptors on synapses (Pickering et al., 2005). As a result of regulating neuronal neurotransmitter functions IL-1β is epileptogenic (Vezzani et al., 2013b) as we will discuss later in "Section 3.5. Pathological features of epilepsy". Importantly, pro-inflammatory cytokines exert further detrimental effects when they diffuse into the bloodstream attracting leukocytes to the site of inflammation and upregulate the expression of cellular adhesion molecules, which are necessary for leukocytes to attach and migrate into the brain (Engelhardt, 2008), an invasion that can be potentially detrimental (Greve and Zink, 2009). Thus, prolonged pro-inflammatory cytokine release exerts detrimental effects during brain pathologies (**Figure 2**).

3.2.3.2. *Anti-inflammatory cytokines*

Anti-inflammatory cytokines are instrumental for controlling both the extent and the duration of tissue inflammation. They play a role in controlling the pro-inflammatory cytokine response (Opal and DePalo, 2000) and induce the resolution of the inflammatory processes, thus preventing the occurrence of detrimental effects associated with chronic inflammation (Vezzani et al., 2013b) (**Figure 2**). TGFβ is one of the best known anti-inflammatory cytokines (Ruocco et al., 1999). TGFβ production induces a potent intrinsic protective response during pathological conditions in the brain (Ruocco et al., 1999), and it has been suggested to protect neurons against apoptosis, excitotoxicity and possibly Aβ neurotoxicity (Vivien and Ali, 2006). However, anti-inflammatory cytokines can also exert detrimental effects. TGFβ has been linked to epileptogenesis (Vezzani et al., 2013b) and macrophage inhibitory cytokine 1 (MIC-1) is involved in the microglial phagocytosis impairment observed in brain tumours (Wu et al., 2010).

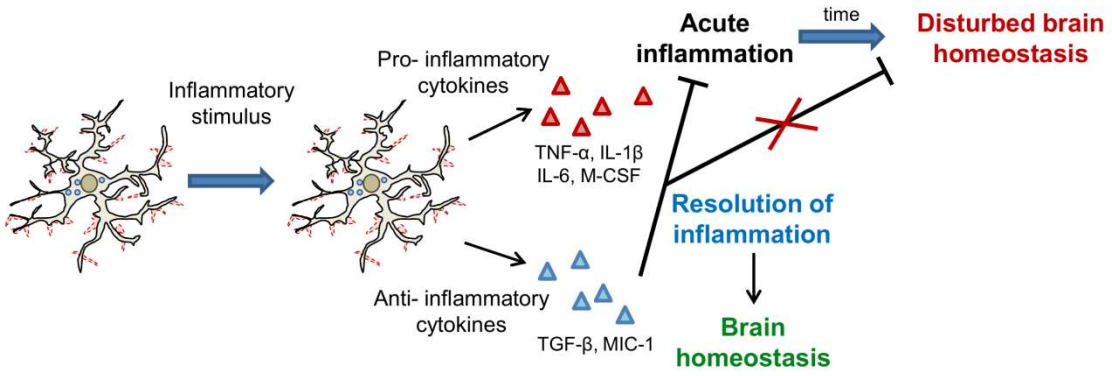

Figure 2. Inflammation. Inflammation is a protective response of the body to harmful stimuli and it is initiated by microglia in the brain. When subjected to an inflammatory stimulus, microglia release pro- and anti-inflammatory cytokines. Importantly, microglia are not the only source of these cytokines, but they can also be released by astrocytes, oligodendrocytes, neurons, endothelial cells, perivascular and meningeal macrophages, and infiltrating immune cells. Pro-inflammatory cytokines (IL-1β, TNFα, IL-6, M-CSF) contribute to the development of acute inflammation, a fundamental response to protect the brain. However, pro-inflammatory cytokines can also contribute to the generation of an uncontrolled or prolonged inflammation that is potentially harmful, and if sustained long enough can result in chronic inflammation, a major cause of cellular damage. Anti-inflammatory cytokines (TGFβ, MIC-1) modulate the pro-inflammatory cytokine response controlling both the extent and the duration of tissue inflammation by resolving inflammatory processes, thus preventing the occurrence of detrimental effects associated with chronic inflammation.

Overall, pro-inflammatory cytokines contribute to the development of acute inflammation, a fundamental response generated to protect the brain against harmful stimuli such as microbe or virus infections (Cherry et al., 2014). Nevertheless, these cytokines can also contribute to the generation of an uncontrolled or prolonged inflammation that is potentially harmful, and if sustained long enough can result in chronic inflammation, a major cause of cellular damage (Cherry et al., 2014) (**Figure 2**). This is particularly relevant in neurodegenerative diseases, where chronic inflammation is common (Frank-Cannon et al., 2009). As the main releasers of inflammatory mediators in the brain, microglial involvement in neurodegenerative diseases has been extensively studied and widely considered detrimental (Ransohoff, 2016). Nevertheless, microglia exert other more benign function which has attracted less attention, as the brain professional phagocytes.

3.2.4. Phagocytosis

Phagocytosis refers to the cellular process of eating (Sierra et al., 2013). It describes the recognition, engulfment, and degradation of large (>0.5 μm), particulated organisms or structures (Mukherjee et al., 1997), and, is mostly performed by specialized, professional phagocytes: tissue macrophages, dendritic cells (DCs), and neutrophils. In the brain, microglia

are the professional phagocytes. Additionally, other cells such as astrocytes (Magnus et al., 2002) and neuroblasts (Lu et al., 2011) can be recruited to perform phagocytosis, although they are not as efficient as microglia and can delay phagocytosis for several hours in vitro (Magnus et al., 2002; Parnaik et al., 2000). Together with inflammation, phagocytosis composes the first line of defence against pathogens by the innate immune system and also helps to initiate the more pathogen-specific adaptive immune response through antigen-presentation to T lymphocytes (Litman et al., 2005).

Phagocytosis comprises three different phases: “find-me”, the stage in which microglial processes find the phagocytic target; “eat-me”, the stage where a direct microglia-target contact is established via a receptor-ligand interaction and recognition and engulfment take place; and “digest-me”, the stage in which the phagocytic cup closes forming the phagosome, which further evolves into a phagolysosome to execute the degradation of the target (Savill et al., 2002) (**Figure 3**). Importantly, microglial phagocytosis could be potentially modulated if changes occur in any of these three stages. The phagocytic phases and their regulators will be covered in more depth in the upcoming ”Section 3.3. Stages of apoptotic cell phagocytosis and mechanisms of regulation”.

Importantly, microglia have been shown to phagocytose all kinds of cargo during physiological and pathological conditions, thus affecting brain function and homeostasis at many different levels. Microglial phagocytic targets include specific brain structures and molecules such as synapses, axonal and myelin debris, and pathology-related proteins such as Aβ (Sierra et al., 2013), and other targets shared with macrophages, such as microbes and dead cells (Diaz-Aparicio et al., 2016).

3.2.4.1. *Synaptic pruning*

During the development of the nervous system, more synapses form than are ultimately required, and remodelling is thus needed to achieve precise wiring of brain circuits. Synapse remodelling refers to the elimination (or “pruning”) of unnecessary synapses and the strengthening of remaining synapses (Zuchero and Barres, 2015). Microglia may play a role in shaping structural features of synaptic connections within neural circuits during development and following injury by phagocytosing pre- and post-synaptic components.

Microglia constantly contacts synapses (Tremblay et al., 2010; Wake et al., 2009). In the postnatal hippocampus, specific presynaptic and postsynaptic proteins have been identified inside microglial processes following synaptic contacts (Paolicelli et al., 2011) and there is evidence of increased phagocytosis of synaptic debris by microglia after enhanced

developmental plasticity in the visual cortex (Tremblay et al., 2010). Moreover, there is direct, quantified evidence of microglia phagocytosing synapses (mostly, presynaptic elements) in the developing visual system (Schafer et al., 2012). These data support a novel role for microglia in monitoring synapses in the healthy developing brain (Sierra et al., 2013).

Microglia-synapse interactions are also observed in several neurodegenerative diseases. In the ischemic cortex, microglia-synapse contacts become markedly prolonged (Wake et al., 2009), but only a minority of boutons disappear after being contacted by microglia and phagocytosis is not observed (Wake et al., 2009). Importantly, a reduction in the function and number of synapses is an early event in the pathogenesis of AD, Huntington's disease, and other neurodegenerative diseases (Perry et al., 2010). C1q, the initiating protein of the classical complement cascade, and microglia have been found to mediate synapse loss in mouse models of early AD (Hong et al., 2016). Moreover, viral infection of adult hippocampal neurons induces complement mediated elimination of presynaptic terminals in a murine West Nile virus disease model (Vasek et al., 2016). Therefore, these and similar studies hint at a relationship between microglia and synaptic and cognitive defects in neurodegenerative diseases, but further investigation is needed to demonstrate a direct link and underlying mechanisms (Miyamoto et al., 2013).

3.2.4.2. *Amyloid β*

In addition to the uncertain role of microglial phagocytosis in synaptic pruning, microglia might also phagocytose Aβ deposits. Aβ is a small peptide produced by proteolytic cleavage from amyloid precursor protein (APP) by β- and γ-secretases. The most pathogenic form of Aβ forms fibrils, insoluble aggregates found in amyloid plaques in the brains of AD patients (Xu and Ikezu, 2009). Due to the location of microglia surrounding plaques in human and in mouse models of AD, microglia was proposed to phagocytose Aβ (Paresce et al., 1996). Indeed, microglia phagocytoses Aβ in vitro (Liu et al., 2012; Liu et al., 2005; Paresce et al., 1996) and Aβ also induces a positive microglial chemotaxis in vivo (Huang et al., 2010; Meyer-Luehmann et al., 2008), which can explain the positioning of microglia around plaques. Nevertheless, microglia has not been observed to phagocytose Aβ in vivo. Although Aβ internalization by microglia has been documented in organotypic hippocampal slices (Hellwig et al., 2015) and in vivo (Bolmont et al., 2008), others report incomplete processing of Aβ (Grathwohl et al., 2009; Krabbe et al., 2013; Spangenberg and Green, 2017). In support of the latter, in APP mice, a model of AD, the size of the Aβ plaques remained constant and no evidence of phagocytosis or plaque clearance was obtained using multiphoton microscopy imaging (Meyer-Luehmann et al., 2008). In agreement, a detailed 3D reconstruction of

microglia and amyloid fibrils in APP mutated mice in vivo showed no Aβ within microglia (Stalder et al., 2001). In addition, depletion of microglia in three different AD mouse models has no effect on fibrillar or soluble Aβ accumulation, indicating that microglia are not responsible for Aβ clearance in these models (Grathwohl et al., 2009; Spangenberg and Green, 2017). Furthermore, microglia from old mutant APP/presenilin 1 mice have a decreased expression of phagocytic genes and increased expression of pro-inflammatory cytokines (TNFα, IL-1β, IL-6), compared with wild type mice (Hickman et al., 2013). Moreover, the BBB is partially disturbed in AD patients, facilitating the extravasation of circulating monocytes (Lai and McLaurin, 2012). Macrophages have higher Aβ capacity intake than microglia in vitro (Lai and McLaurin, 2012), and ablation experiments have suggested that the Aβ burden is cleared by blood-borne macrophages, but not resident microglia (Simard et al., 2006). Hence, the role of microglia in Aβ phagocytosis in vivo is yet to be elucidated.

3.2.4.3. *Axonal and myelin debris*

Microglia have been shown to phagocytose axonal debris after nerve injury in the brain, where this debris is considered one of the obstacles for axonal outgrowth. Nevertheless, the phagocytosis of axonal debris has only been shown in vitro (Sierra et al., 2013). Indeed, in cortical rat explants where growing neurites were sectioned, debris was cleared by microglia (Jin and Yamashita, 2016; Tanaka et al., 2009). Additionally, in a compartmentalized co-culture model, different treatments induced axonal degeneration and microglia rapidly cleared the axonal debris (Hosmane et al., 2012). In both set ups, axonal debris (lacking myelin) had a detrimental effect on axon regrowth, which was prevented by microglial phagocytosis (Hosmane et al., 2012; Tanaka et al., 2009), suggesting that enhancing microglial phagocytosis could be a novel therapeutical tool in traumatic brain injuries.

However, more attention has been put into the mechanisms of myelin debris clearance. In physiological conditions, myelin pieces are gradually released from aging myelin sheaths and are subsequently cleared by microglia (Safaiyan et al., 2016). With age, myelin fragmentation increases and leads to the formation of insoluble, lipofuscin-like lysosomal inclusions in microglia, contributing to microglial senescence and immune dysfunction in aging (Safaiyan et al., 2016). Myelin debris clearance is particularly important during MS and in spinal cord and nerve injuries. In spinal cord injury, the degeneration of the severed axons is followed by degradation of myelin and apoptosis of myelinating cells, oligodendrocytes (Crowe et al., 1997). This provokes the accumulation of myelin debris (Stys et al., 2012), which interferes with axonal regeneration and repair, rendering myelin clearance mandatory for recovery

(Wang et al., 2002). However, contrary to the peripheral nervous system, myelin clearance after injury is very inefficient in the CNS, due to microglial poor phagocytosing capabilities together with poor or slow recruitment of macrophages (Gaudet et al., 2011). However, myelin debris is still observed in the human spinal cord years after the injury (Buss et al., 2004). Microglia phagocytose myelin to some extent in mouse models of MS (Nielsen et al., 2009). Importantly, a microglial phenotype supportive of remyelination has been described in a cuprizone induced mouse model of MS, where myelin-phagocytosing microglia express genes involved not only in phagocytosis but also in the activation, migration, proliferation, and differentiation of oligodendrocyte precursor cells (Olah et al., 2012). While it remains to be directly assessed whether myelin phagocytosis triggers this remyelination-supportive phenotype, this data suggests that the beneficial consequences of enhancing microglial phagocytosis of myelin may be two-fold: clearing myelin and facilitating remyelination (Sierra et al., 2013).

3.2.4.4. *Dead cells*

Besides specific brain structures and molecules, microglia engulf another type of phagocytic cargo throughout their whole lifespan, in both physiological and pathological conditions: dead cells. Next, apoptotic and necrotic cell death will be discussed.

3.2.4.4.1. *Apoptotic cells*

Apoptosis, or programmed cell death, is an ubiquitous process in organisms. The turnover of old cells to be replaced by new cells is a central part of both embryonic and postnatal development and of everyday tissue homeostasis (Arandjelovic and Ravichandran, 2015). Apoptosis is thought to account for the majority of turnover cells in physiological conditions (Nagata et al., 2010). Brain development is a very wasteful process characterized by extensive neuronal apoptosis, which continues through adulthood in the neurogenic niches in healthy brain, where the majority of newborn neurons die long before reaching the mature neuron state (Sierra et al., 2010). Moreover, apoptosis is a key feature in most of the neurodegenerative diseases (Mattson, 2000).

Apoptosis can occur via two main mechanisms: the extrinsic or the intrinsic pathway (Barber, 2001; Taylor et al., 2008). While the extrinsic pathway is activated by signalling through cell surface death receptors, the intrinsic pathway is activated by cellular death and mitochondrial damage (Reubold and Eschenburg, 2012). However, both pathways converge on the activation of the executioner caspases (caspases 3, 6 and 7), which induce the morphological and biochemical changes associated with apoptosis (Taylor et al., 2008).

Morphological changes include cellular shrinkage with cytoplasm condensation, cap-shaped chromatin masses lying against the nuclear membrane, nuclear condensation (pyknosis), nuclear fragmentation (karyorrhexis), and the subsequent formation of membrane-confined apoptotic bodies containing a variety of cytoplasmic organelles and nuclear fragments (Eidet et al., 2014; Krysko et al., 2008; Poon et al., 2014). Importantly, the integrity of the plasma membrane is maintained up to an advanced stage of the death process (Marín-Teva et al., 2014). Biochemically, apoptosis is characterized by transient exposure of phosphatidylserine (PS), a phospholipid that resides in the inner side of the cytoplasmic membrane and is transiently translocated to the external surface during early apoptosis (Krysko et al., 2008). However, it has been proposed that the crucial feature of apoptosis in vivo is that it leads to the recognition and engulfment of intact cells or membrane-bound apoptotic bodies by phagocytes (Savill et al., 2002).

3.2.4.4.2. *Necrotic cells*

Death by necrosis is also an important component of many brain diseases. Necrosis remains an obscure process, and the molecular details of its execution are not well-known (Sierra et al., 2013). Necrosis is morphologically characterized by swelling of the organelles (endoplasmic reticulum, mitochondria) and the cytoplasm, followed by collapse of the plasma membrane and lysis of the cells (Krysko et al., 2008; Zong and Thompson, 2006), with spillover of cellular contents in the extracellular space (Savill et al., 2002). Two main forms have been recognized: accidental necrosis, an uncontrolled type of pathological cell death (Zong and Thompson, 2006), lacking underlying signalling events and occurring under extreme physic-chemical conditions, such as abrupt anoxia, sudden shortage of nutrients, and exposure to heat or detergents (Krysko et al., 2008; Savill et al., 2002); and necrosis-like programmed cell death, such as necroptosis, well defined as a viral defence mechanism, allowing the cell to undergo “cellular suicide” in a caspase-independent fashion in the presence of viral caspase inhibitors (Vanden Berghe et al., 2014), and without chromatin condensation (Leist and Jaattela, 2001).

3.2.4.4.3. *Functional consequences of the phagocytosis of apoptotic cells*

The vast amounts of cell death that can occur during physiological or pathological conditions mandate an active and efficient cleanup system. Microglia are the cells in charge of phagocytosing these dead cells. If apoptotic cells are not rapidly phagocytosed, they evolve to secondary necrotic cells, losing the integrity of their plasma membrane and spilling over their intracellular contents (Poon et al., 2014). This has detrimental consequences for the

surrounding tissue, as the leakage of intracellular contents is toxic for the tissue and may be responsible for the initiation of inflammation (Poon et al., 2014) or autoimmune diseases (Nagata et al., 2010) (**Figure 3**). Importantly, injecting apoptotic cells in the inflamed peritoneum in vivo leads to their clearance by peripheral macrophages and induces an increase in anti-inflammatory cytokine production (Huynh et al., 2002). Moreover, in vitro clearance of apoptotic neutrophils by monocytes treated with bacterial lipopolysaccharides (LPS) actively suppresses the initiation of inflammatory and immune responses, in part through the release of anti-inflammatory cytokines (Byrne and Reen, 2002). The anti-inflammatory role of phagocytosis in microglia has only been explored in vitro and involves the release of anti-inflamamtory cytokines such as TGFβ and trophic factors such as NGF (nerve growth factor) (De Simone et al., 2003; Fraser et al., 2010) that may potentially facilitate the functional recovery of the surrounding compromised neurons (Diaz-Aparicio et al., 2016). Thus, the rapid and efficient clearance of the cell corpses is crucial for the maintenance of tissue homeostasis.

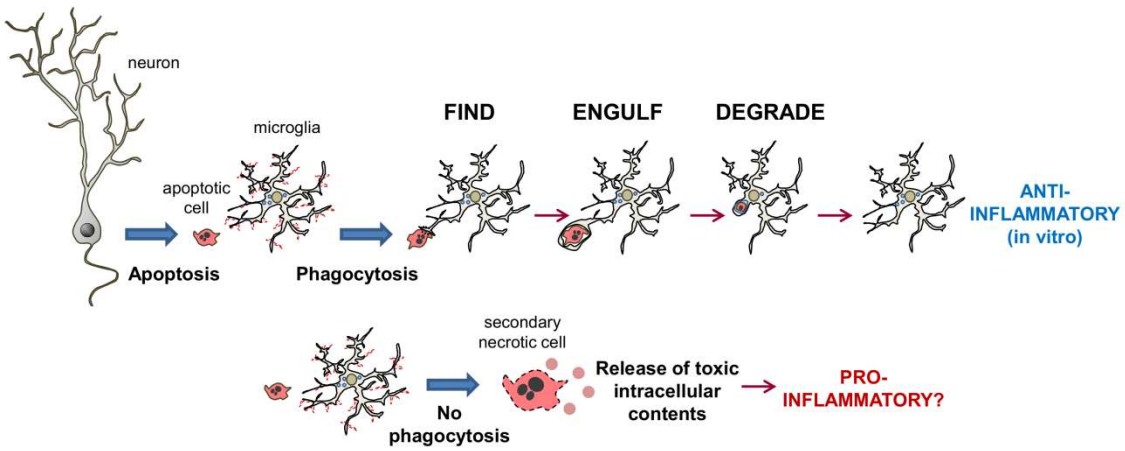

Figure 3. Phagocytosis of apoptotic cells and functional consequences. Phagocytosis refers to the cellular process of eating and it describes the recognition, engulfment, and degradation of large (>0.5 µm), particulated organisms or structures. Apoptosis, or programmed cell death, is an ubiquitous process in organisms. Importantly, phagocytosis of apoptotic cells is actively anti-inflammatory in vitro. Nevertheless, if apoptotic cells are not rapidly phagocytosed they evolve to secondary necrotic cells, losing the integrity of their plasma membrane and spilling over their toxic intracellular contents, a process that could be harmful for the surrounding brain tissue and could also trigger an inflammatory response. Thus, the rapid and efficient clearance of the cell corpses is crucial for the maintenance of tissue homeostasis.

Although the clearance of apoptotic cells has obvious implications for the correct functioning of the brain in health and disease, and is a well described process in peripheral inflammatory diseases, microglial phagocytosis of apoptotic cells remains a notoriously unexplored process in vivo, in terms of its efficiency in pathological conditions, its mechanisms

of execution, its beneficial or detrimental consequences, and its ultimate impact in maintaining tissue homeostasis (Sierra et al., 2013). The goal of this thesis is to analyze microglial phagocytosis and apoptosis in the brain in pathological conditions, focusing on epilepsy. Moreover, we also assessed the mechanisms regulating microglial phagocytosis and the effects of a phagocytosis impairment in the brain.

3.3. STAGES OF APOPTOTIC CELL PHAGOCYTOSIS AND MECHANISMS OF REGULATION: "FIND-ME", "EAT-ME", AND "DIGEST-ME"

In recent years significant progress has been made in understanding the steps involved in apoptotic cell clearance in vivo. First, apoptotic cells release "find-me" signals that attract microglia. Once microglia have reached the dead cells they recognize them via "eat-me" signals and proceed to engulf them, undergoing extensive cytoskeletal rearrangements (Arandjelovic and Ravichandran, 2015; Sierra et al., 2013). Finally, the "digest-me" stage takes place, where microglia close the phagocytic cup, forming the phagosome and then proceeding to the degradation of the apoptotic cells in the lysosomal compartment (Diaz-Aparicio et al., 2016; Hochreiter-Hufford and Ravichandran, 2013; Sierra et al., 2013) (**Figure 4**).

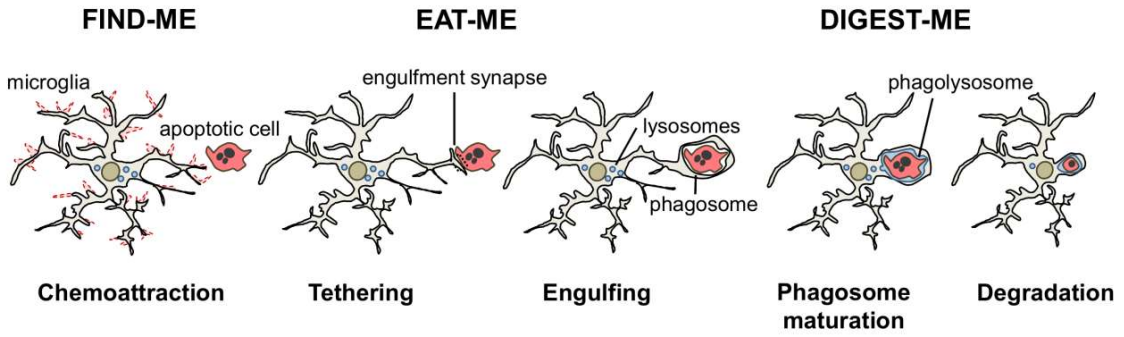

Figure 4. Three-step model of microglial phagocytosis. In physiological conditions, microglial processes are highly motile and respond to chemoattractant molecules released by damaged or apoptotic cells ("find-me" signals) such as fractalkine and the extracellular nucleotide ATP. Next, an engulfment synapse is formed between a series of microglial receptors and their ligands in the membrane of the apoptotic cell ("eat-me" signals), leading to the tethering and engulfing of the apoptotic cell in a phagosome. The phagosome becomes mature by fusing with lysosomes and other organelles, and the apoptotic cell is fully degraded in the phagolysosome in less than 2h. Adapted from (Sierra et al., 2013).

3.3.1. "Find-me" stage

Given their broad distribution throughout the brain and their highly motile processes, microglia can fortuitly encounter apoptotic cells and begin the phagocytic process.

Nevertheless, for an efficient clearance of apoptotic cells, microglia need to be guided to the target cells. Therefore, the release of "find-me" signals by apoptotic cells is critical to recruit microglia to the dying cells. Apoptotic cells can release several different "find-me" signals. These include the chemokine fractalkine, the lipids lysophosphatidylcholine (LPC) and sphingosine-1-phosphate (S1P), and extracellular nucleotides (ATP, UTP) (Arandjelovic and Ravichandran, 2015; Elliott et al., 2009; Gude et al., 2008; Lauber et al., 2003; Sierra et al., 2013; Truman et al., 2008).

CXC3CL1 is highly expressed in neurons, while its receptor, CX3CR1 is only expressed by microglia in the healthy brain (Eyo et al., 2016; Jung et al., 2000; Mizutani et al., 2012). In physiological condition CX3CL1 is tethered to the neuronal membrane, but when the cell undergoes apoptosis, CX3CL1 is cleaved releasing an extracellular soluble fragment that acts as a chemotactic factor for microglia (Noda et al., 2011; Sokolowski et al., 2014; Truman et al., 2008). Another "find-me" signal released by apoptotic cells is LPC (Lauber et al., 2003), a phospholipid which promotes microglial precursor entry into the brain in zebrafish embryos (Xu et al., 2016). The effects of S1P, another lipid secreted by apoptotic cells which stimulates chemotaxis (Gude et al., 2008), have not been studied on microglia yet (Hochreiter-Hufford and Ravichandran, 2013).

Importantly, extracellular nucleotides have gained a lot of attention in the past years, due to their strong effect on microglia (Elliott et al., 2009). The extracellular nucleotides ATP and uridine 5'-triphosphate (UTP) are released by apoptotic cells to attract phagocytes (Elliott et al., 2009). One route through which nucleotides are released from apoptotic cells in vitro is through pannexin1 channels (Chekeni et al., 2010). Most ATP receptors are expressed by microglia (Crain et al., 2009; Domercq et al., 2013), and besides the already mentioned effects of ATP and its metabolites on microglial motility, they have also been found to regulate phagocytosis (Fang et al., 2009; Orr et al., 2009). Exposure of primary microglia to a high concentration of ATP or a P2X7 agonist induced a reduction of phagocytosis of fluorescent latex microbeads, while knockdown or blockade of P2X7 efficiently restored phagocytotic activity (Fang et al., 2009). Moreover, LPS-treated primary microglia showed a decrease in particle uptake when treated with agonists of A2A, a type of P1 receptor (Orr et al., 2009), suggesting that A2A stimulation may modulate substrate engulfment by activated microglia. Similarly, uridine diphosphate (UDP), the product of degradation of UTP by extracellular ectonucleotidases, acts on microglial P2Y6 receptors to facilitate phagocytosis of microspheres both in vitro and in vivo (Koizumi et al., 2007). Thus, extracellular nucleotides might also regulate microglial phagocytosis of apoptotic cells in vivo.

Once the phagocyte has reached the target a direct cell membrane contact is established via a receptor-ligand interaction and the “eat-me” stage of phagocytosis takes place (Sierra et al., 2013).

3.3.2. “Eat-me” stage

The eating stage of phagocytosis involves the recognition and engulfment of the apoptotic cell by microglia (Sierra et al., 2013). Phagocytes are equipped with an array of receptors which enable them to recognize “eat-me” signals expressed by their targets and discriminate them from living cells (which express “don’t-eat-me” signals) (Ravichandran, 2010; Savill et al., 2002). Some of these receptors serve to tether the phagocyte and the target together while others trigger internalization (Underhill and Goodridge, 2012).

The receptors for apoptotic cell clearance belong to one main type: Apoptotic cells-associated cellular patterns (ACAMPs). The main exponent of ACAMPs is PS, a cell membrane lipid of the inner layer which is exposed in the outer leaflet of the cell membrane during apoptosis. Detection of ACAMPs, is mediated directly by several receptors, including brain-specific angiogenesis inhibitor 1 (BAI-1) (Armstrong and Ravichandran, 2011), and by bridging molecules such as milk fat globule-epidermal growth factor (MFG-E8). Another important receptor that signals internalization is triggering receptor expressed on myeloid cells-2 (TREM2), preferentially expressed in microglia in the brain (Hickman and El Khoury, 2014; Hickman et al., 2013) whose signalling mechanisms are unknown, but TREM2-deficint mice and cells have shown that TREM2 is able to suppress inflammatory cytokine production (Ito and Hamerman, 2012; Takahashi et al., 2005; Wang et al., 2015; Zhong et al., 2015) and facilitate phagocytosis of latex beads by primary microglia (Takahashi et al., 2005) and apoptotic cells by BV2 microglial cell line (Kawabori et al., 2015). TREM2 is known to interact with the signalling adapter protein named DNAX-activation protein of 12 kD (DAP12) (Paloneva et al., 2002), mostly expressed by microglia in the brain (Hickman and El Khoury, 2014; Hickman et al., 2013). However its ligand in apoptotic cells remains elusive. Several candidates have been proposed, namely, anionic oligosaccharides such as bacterial lipopolysaccharides (Daws et al., 2014; Quan et al., 2008), lipoproteins like low density lipoprotein (LDL) and apolipoproteins like apolipoprotein E (ApoE) (Atagi et al., 2015; Yeh et al., 2016), extracellular nucleic acids (Kawabori et al., 2015), and heat shock protein 60 (Hsp60) (Stefano et al., 2009). Hsp60 is exposed in the surface of apoptotic cells (Goh et al., 2011) and increases the in vitro phagocytic activity of a microglial cell line enriched in TREM2 (Stefano et al., 2009). Other apoptotic cell phagocytosis receptor is Mer tyrosine kinase (MerTK), well known for its immunosuppressive signaling (Caberoy et al., 2012). Importantly, adult mice deficient in

microglial MerTK exhibit a marked accumulation of apoptotic cells specifically in the neurogenic regions of the CNS (Fourgeaud et al., 2016). Another apoptotic cell phagocytosis receptor is the G protein coupled receptor GPR34 (Preissler et al., 2015). Interestingly, microglia show reduced phagocytosis activity in both retina and acutely isolated cortical slices of GPR34-deficient mice (Preissler et al., 2015).

In addition to the direct recognition of the targets by microglial cell membrane receptors, engulfment can also be triggered by soluble opsonins, molecules that bind to receptors signalling internalization in the microglia. Antibodies such as immunoglobulin G and proteins of the complement system such as C3b, bind to phagocyte Fc receptors and complement receptor 3 (CR3), respectively, and mediate phagocytosis (Underhill and Goodridge, 2012). The level of expression of the receptors involved in phagocytosis may change under different stimuli such as inflammation (Falsig et al., 2008) but it is not known whether they ultimately impact the efficiency of microglial phagocytosis.

These receptors and their targets closely interact in what has been termed “engulfment synapse” or “phagocytic synapse” (Dustin, 2012; Ravichandran, 2010; Underhill and Goodridge, 2012). Similar in size (0.5 µm in diameter) and purpose (close cell–cell contact) to its immunological and neural counterparts, phagocytic synapses are specialized regions of the membrane where the apoptotic cell and the phagocyte interact through microclusters of receptors. In contrast to the immunological synapse and the synapses formed between neurons, phagocytic synapses are short-lived and last only a few minutes (Dustin, 2012). Once the contact is established, phagocytic synapses initiate a series of intracellular pathways that lead to the remodelling of the phagocyte cytoskeleton through actin polymerization and membrane composition, triggering the formation of pseudopodia that form a phagocytic cup engulfing the target (Lee et al., 2007). Of the complex process of signal transduction and formation of the phagocytic cup, very little is known in microglia.

3.3.3. “Digest-me” stage

The phagocytic cup closes up forming the phagosome around the target. To execute the degradation of the target, phagosomes go through a process of maturation in which they fuse sequentially with early and late endosomes, and lysosomes, to form phagolysosomes (Desjardins et al., 1994). These phagolysosomes contain hundreds of proteins, including hydrolases such as cathepsins to digest the target; and proton pumps such as vacuolar ATPases (vATPases) to acidify the medium (Garin et al., 2001). The acidic pH found in phagolysosomes (pH ≤ 5) is essential for the lysosomal degradation capabilities, as it is optimal for most

hydrolases. Interestingly, the signalling associated with the acidic Ph of lysosomes deactivates the generation of radicals from the oxidative burst (Li et al., 2010). Again, the process of phagosome formation and cargo degradation has been barely addressed in microglia. Live imaging showed that in the nematode C. elegans microglial vATPases are required for phagosome–lysosome fusions and consequently to degrade cargo (Peri and Nusslein-Volhard, 2008). Further research is necessary to delineate the mechanisms of degradation of apoptotic cells by microglia.

Moreover, the location where the actual degradation of the phagocytosed cargo occurs remains unexplored. Phagocytosis is commonly performed by terminal or en passant branches of ramified, surveillant microglia (Peri and Nusslein-Volhard, 2008; Sierra et al., 2010). Interestingly, live imaging experiments show that phagosomal cups are retrogradely transported to the cell soma in the mouse neocortex (Nimmerjahn et al., 2005), and small puncta of apoptotic cell material are observed within branches of ramified microglia in fixed adult hippocampus, indirectly suggesting their transport (Sierra et al., 2010). Moreover, direct evidence of retrograde transport of cargo-containing phagosomes has been observed in C.elegans (Peri and Nusslein-Volhard, 2008). Collectively, these data indirectly suggest a yet unexplored role of the cytoskeleton in transporting the phagosome for the degradation of the engulfed apoptotic material.

Thus, apoptotic cell phagocytosis can be regulated at many different stages. Changes in any of these phases could potentially affect phagocytic efficiency. Next, we will discuss microglial apoptotic cell phagocytosis in physiological conditions.

3.4. MICROGLIAL PHAGOCYTOSIS OF APOPTOTIC CELLS IN PHYSIOLOGICAL CONDITIONS

Apoptosis can be ubiquitously found throughout the whole lifespan in the neurogenic niches of the brain: the subventricular zone (SVZ), located throughout the lateral walls of the lateral ventricles, which generates interneurons populating the olfactory bulb; and the subgranular zone (SGZ) of the hippocampus, in which newborn cells integrate locally as mature granule cells in the granular zone of the dentate gyrus (DG). In physiological conditions a large percentage of these newborn cells undergo apoptosis in the SGZ (Sierra et al., 2010) (**Figure 5**). This constitutive apoptosis found in the DG constitutes a good model to establish the baseline of microglial phagocytosis of apoptotic cells in physiological conditions and thus, to assess the

changes in the efficiency of phagocytosis under different pathological conditions. In this thesis we will assess microglial phagocytosis in the hippocampal DG.

Importantly, the physiological efficiency of microglial phagocytosis in the DG has been established before. Microglia are present in the SGZ and are physically intimate with all components of the adult hippocampal neurogenic cascade, which allows them to phagocytose the apoptotic newborn cells (Sierra et al., 2010). In fact, 90% of all newborn apoptotic cells are phagocytosed by microglia in the SGZ in physiological conditions as observed with immunofluorescence staining and confocal microscopy (Sierra et al., 2010). Moreover, the whole phagocytic process takes place very rapidly in physiological conditions, in under 1.5h (Sierra et al., 2010) (**Figure 5**). Importantly, aging does not alter microglial phagocytic efficiency (Sierra et al., 2010). Therefore, microglia are very efficient phagocytes in the healthy DG through the lifespan. Moreover, in physiological conditions only a small proportion of microglia are in the process of phagocytosing at a given time, suggesting that these cells hold a large phagocytic reservoir that could be summoned in conditions where apoptotic cell numbers greatly increase, such as in the diseased brain (Sierra et al., 2010).

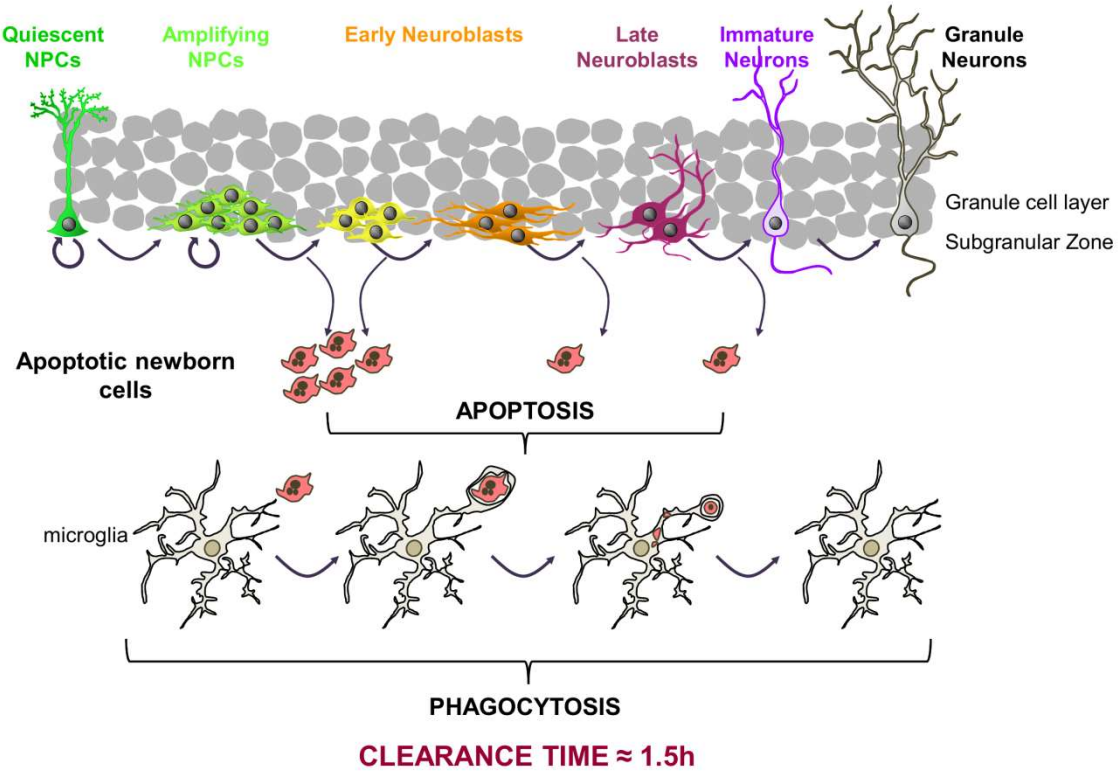

Figure 5. Microglial phagocytosis of apoptotic cells in physiological conditions. In the adult hippocampus, neuroprogenitor cells in the SGZ of the DG give rise to newborn neuroblasts. However, only a small subset of these cells integrates into the hippocampal circuitry as mature neurons, because the majority undergo death by apoptosis before becoming neuroblasts. Importantly, these apoptotic newborn cells are rapidly cleared out through phagocytosis by ramified microglia present in the adult

SGZ. The whole phagocytic process takes place very rapidly in physiological conditions, in under 1.5h, and is undeterred by increased age. Adapted from (Sierra et al., 2010).

Nevertheless, the efficiency of microglial phagocytosis in vivo during pathological conditions remains unknown. In this PhD thesis, our objective has been to analyze microglial phagocytosis in epilepsy and in its underlying pathological events, excitotoxicity and inflammation, to understand how each specific pathological process might affect microglial phagocytosis.

3.5. MICROGLIAL PHAGOCYTOSIS IN PATHOLOGICAL CONDITIONS: THE CASE OF EPILEPSY

3.5.1. Introduction to epilepsy

Epilepsy is a term used to describe a spectrum of neurological disorders characterized by spontaneous epileptic seizures, which are abrupt abnormal synchronized neuronal activities (Fisher et al., 2005; Savage, 2014). Epilepsy is the third most common chronic brain disorder, affecting between 50 and 65 million people globally (Thurman et al., 2011). Importantly, because of the reorganization of neural circuits and activities in the brain in response to seizures, patients frequently experience further complications such cognitive impairment, and psychiatric and mood disorders such as depression (Jensen, 2011). Moreover, patients with epilepsy have been reported to exhibit increased mortality of 2–10 years earlier than the general population (Gaitatzis et al., 2004). Thus, epilepsy is a significant health concern for the human population.

Epilepsy presents thousands of etiologies of known risk factors (such as genetic risk factors) and unknown risk factors (Eyo et al., 2017). It may arise due to a brain infection, trauma, ischemia, tumor, neurodegenerative disease, or genetic predisposition (Ahl et al., 2016). Importantly, epilepsy can be controlled but cannot be cured by medication (Rassendren and Audinat, 2016), and about 30% of patients are pharmacoresistant, or refractory to currently available pharmacological treatments (Schuele and Luders, 2008). Moreover, treatment is frequently associated with undesirable side effects. Thus, there is a strong need for developing new treatment strategies to ameliorate the progression and/or limit the detrimental consequences of the disease (Eyo et al., 2017).

According to the brain region where seizures initiate, they can be classified as focal or generalized (Fisher et al., 2017). Focal or partial seizures are initiated from one area of

the brain and may induce a plethora of symptoms often correlated to the function or lack of function of that particular brain region (Ahl et al., 2016). Generalized seizures involve the whole brain at once and the patients experience disturbed consciousness and often tonic-clonic muscle movements (Ahl et al., 2016), which implies rigidity and shaking of extremities.

3.5.2. Focal epilepsies: Mesial temporal lobe epilepsy (MTLE)

The temporal lobe is the most epileptogenic region of the human brain (Tatum, 2012) and thus, temporal lobe epilepsy (TLE), is the most common form of epilepsy (Crespel et al., 2002). TLE is a group of disorders that predominantly involves dysregulation of hippocampal function caused by neuronal hyperexcitability (Schwartzkroin, 1986). Mesial temporal lobe epilepsy (MTLE) is one of the best-characterized types of epilepsy (Tatum, 2012) as well as the most common form of pharmacoresistant epilepsy (Duveau et al., 2016), and therefore many patients require resection of the epileptic hippocampus (Quirico-Santos et al., 2013). Human pathophysiological features of MTLE include unprovoked seizures and hippocampal sclerosis, including cell death, gliosis, inflammation, and granule cell dispersion (Babb et al., 1995; Bouilleret et al., 1999; Heinrich et al., 2006; Kralic et al., 2005; Nitta et al., 2008). Importantly, hippocampal sclerosis is thought to have a predominantly acquired causation (Shorvon, 2011), which implies that MTLE is mostly an acquired disease, secondary to other pathological situations such as brain injury (Cendes, 2005).

Experimental epilepsy models have been developed primarily in rodents. The most ubiquitous models include chemically induced models using the glutamatergic agonist KA (Ben-Ari and Lagowska, 1978) or pilocarpine, a muscarinic receptor agonist (Vezzani, 2009). Both chemoconvulsants induce hippocampal sclerosis and are recognized to mimic salient histopathological and clinical features of human MTLE.

Pilocarpine is usually administered systemically though it is sometimes coupled with lithium pre-treatment to lower the threshold for seizure-induction (Eyo et al., 2017). In this model the homeostatic balance of neuronal excitation–inhibition is tipped toward increased excitability presumably at least in part by increase in glutamate release and sustained NMDA receptor activation (Priel and Albuquerque, 2002; Smolders et al., 1997). KA induces seizures via activation of KA glutamate receptor subtypes (Ben-Ari and Cossart, 2000) and AMPA receptors, as a partial agonist (Fritsch et al., 2014). KA can be administered either systemically or intracerebrally, via injection into the hippocampus or the amygdala (Levesque and Avoli, 2013). Importantly, intrahippocampal KA is one of the best models to mimic MTLE as it replicates the major pathophysiological features of the disease, such as recurrent seizures and

hippocampal sclerosis, and shows similar electroencephalogram (EEG) histopathology and synaptic reorganization (Bouilleret et al., 1999). Moreover, intrahippocampal KA administration shows the lowest percentage of death among the different administration methods (Levesque and Avoli, 2013). Additionally, intrahippocampal KA administration is more replicable than systemic administration particularly in C57 mice (McKhann et al., 2003). Intrahippocampal KA leads to hypersynchronized excitatory neuronal activity which if prolonged, results in neuronal death (Eyo et al., 2017). Although a complex interplay of KA and non-KA glutamate receptors have been implicated in the mechanism of KA induced seizures, the cornu ammonis 3 (CA3) region of the hippocampus is recognized to be extremely susceptible due to a high density of specific kainate receptors in this region (Levesque and Avoli, 2013). Besides affecting the hippocampus, KA-induced MTLE also affects other regions of the brain like the ipsilateral cortex (Sierra et al., 2015). Due to its reliability and lower mortality rate than pilocarpine (Curia et al., 2008; Levesque and Avoli, 2013), we will use intrahippocampally administered KA to model MTLE.

3.5.3. Generalized epilepsies: Progessive myoclonus epilepsy of Unverricht-Lundborg type

Generalized epilepsies are more likely to involve genetic factors than focal epilepsies (Ferraro et al., 2012). Among this group are progressive myoclonus epilepsies (PMEs), a heterogeneous group of inherited disorders with a poorly understood pathogenesis which are generally pharmacoresistant (Tegelberg et al., 2012). In this PhD thesis, we will focus on the most common cause of PME: Unverricht-Lundborg disease (epilepsy myoclonus type 1, EPM1), an autosomal recessively inherited disorder caused by loss-of-function mutations in the cystatin B gene (Cstb), which encodes an inhibitor of cysteine proteases (Joensuu et al., 2008; Lalioti et al., 1997; Pennacchio et al., 1996). These proteases include lysosomal cysteine cathepsins, which show an increased activity that has been related to EPM1 pathogenesis (Rinne et al., 2002). In particular, cathepsin B (CatB) shown to induce neuronal apoptosis in the context of neurodegenerative diseases (Gan et al., 2004; Kim et al., 2007; Kingham and Pocock, 2001) has been specially linked to the pathogenesis of EPM1. Importantly, microglia is known to be a major source of CatB in the brain (Hayashi et al., 2013; von Bernhardi et al., 2015; Wendt et al., 2008). However, the precise role of Cstb and the mechanisms by which its loss leads to EPM1 remain poorly understood. Pathophysiological features of EPM1 include severe stimulus-sensitive myoclonus, a brief involuntary twitching of muscles, and generalized tonic-clonic seizures, and other neurologic symptoms such as ataxia, lack of movement coordination,

and dysarthria, a motor disorder during speech, which appear as the disease progresses (Kalviainen et al., 2008; Koskiniemi et al., 1974; Norio and Koskiniemi, 1979).

The Cstb-deficient, or Cstb knock-out (KO) mouse (Pennacchio et al., 1998) is a widely used model to study EPM1 (Franceschetti et al., 2007; Maher et al., 2014; Manninen et al., 2014; Shannon et al., 2002; Tegelberg et al., 2012). These mice recapitulate the key clinical features of the disease, characteristic of EPM1 patients: the mice develop myoclonus by one month and progressive ataxia by six months of age (Pennacchio et al., 1998). Consistent with findings in human patients (Koskenkorva et al., 2012; Manninen et al., 2013; Mascalchi et al., 2002), there is progressive atrophy, cortical thinning, and neuron and white matter loss in the brain of Cstb KO mice affecting particularly the cerebellum and the thalamocortical system (Koskenkorva et al., 2012; Manninen et al., 2013; Pennacchio et al., 1998; Tegelberg et al., 2012). Interestingly, the earliest neuropathological finding in Cstb KO mice is the altered microglial morphology, at two weeks of age. This is followed by the activation of astrocytes, myoclonus, and progressive neuronal degeneration from one month onwards (Tegelberg et al., 2012). Gene-expression profiling has revealed an upregulation of genes associated with immune-system processes in the cerebellum of Cstb KO mice at one month, and has led to the discovery of alterations in GABAergic signaling already at one week of age (Joensuu et al., 2014). In detail, findings implying a diminished number of GABAergic pre- and postsynaptic terminals, decreased inhibition, and reduced ligand binding to GABAA receptors were identified in the cerebellum of Cstb KO mice (Joensuu et al., 2014). Thus, Cstb KO mice constitute a solid model of EPM1.

In spite of the different ethiopathological origin, these different types of epilepsies share some common pathological features that we will assess next in more depth.

3.5.4. Pathological features of epilepsy

The hyperactivity of neural circuits that underlies epilepsy is thought to arise from an imbalance wherein excitatory neurotransmission predominantly through glutamatergic signalling is increased and inhibitory neurotransmission predominantly through GABA-ergic signalling is decreased (Dalby and Mody, 2001; Sharma et al., 2007). Due to the neuronal hyperactivity there is neuronal damage, and an exaggerated immune response (Ekdahl et al., 2003; Kan et al., 2012; Legido and Katsetos, 2014; Ravizza et al., 2011), as microglia release pro- and antiinflammatory mediators during the acute innate immune response in the brain following seizures (Pernhorst et al., 2013). Moreover, astrocytes change their activity state and exhibit disturbed buffering capacity of ions and glutamate uptake (Crunelli et al., 2015). In

addition to the innate immune reaction, seizures may cause blood-brain barrier dysfunction and activation of vascular-associated and blood-derived immune cells (Legido and Katsetos, 2014).

Next, we will cover the excitotoxicity and inflammation processes happening during epilepsy in more depth.

3.5.4.1. *Excitotoxicity*

Excitotoxicity refers to cell death caused by a prolonged activation due to excessive glutamate release (Pickering et al., 2005). Excitotoxicity is common to many neurodegenerative diseases, such as epilepsy, ischemia, Parkinson's, AD and MS (Dong et al., 2009) can provoke death by apoptosis or necrosis, depending on its intensity (Bonfoco et al., 1995). Excitotoxicity is a complex process which mainly affects neurons and oligodendrocytes (Matute et al., 2001; Wang and Qin, 2010), and it is normally initiated by activation of glutamatergic ionotropic channels, NMDA, AMPA and KA by endogenous excitotoxins (high concentrations of glutamate); or exogenous excitotoxins (glutamate agonists NMDA and KA). When glutamatergic receptors get over-activated by continuous stimulation, high levels of calcium ions (Ca^{2+}) enter the cell (Jaiswal et al., 2009) and activate a number of enzymes which go on to damage the cytoskeleton, membrane, and DNA, finally provoking cell death (Orrenius et al., 2003).

3.5.4.2. *Inflammation*

Inflammation is an intrinsic feature in pharmacoresistant epilepsies of different etiology (Vezzani et al., 2011). In adult rats and mice, induction of recurrent short seizures or status epilepticus by chemoconvulsants or electrical stimulation triggers a rapid induction of inflammatory mediators in brain regions of seizure activity onset and propagation (Fabene et al., 2010; Vezzani et al., 2008; Yoshikawa et al., 2006) (**Figure 6**). Moreover, immunohistochemical studies on rodent brains after induction of status epilepticus demonstrate subsequent waves of inflammation during the epileptogenic process, involving various cell populations. After seizures, proinflammatory cytokines (IL-1β, TNFα, and IL-6) are expressed in microglia and astrocytes, and cytokine receptor expression is upregulated in microglia, astrocytes, and neurons (Vezzani and Granata, 2005). As in human epileptic brain specimens, brain tissue from rodents with experimental chronic TLE contains both astrocytes and microglia expressing inflammatory mediators (Crespel et al., 2002; Dube et al., 2010; Ravizza et al., 2008). Evidence for brain vessel inflammation associated with BBB breakdown is also prevalent (Fabene et al., 2008; Marchi et al., 2007; Ravizza et al., 2008). Thus, brain

inflammation induced by status epilepticus develops further during epileptogenesis and persists in chronic epileptic tissue, thereby supporting the idea that inflammation might be intrinsic to—and perhaps a biomarker of—the epileptogenic process (Dube et al., 2010; Majores et al., 2004). Importantly, an inhibitor of IL-1β is already undergoing clinical trials to be used as a treatment for epilepsy (Vezzani et al., 2010).

In fact, inflammation has gained recognition as a crucial contributor to the etiopathogenesis of epilepsy, among several other CNS disorders (Vezzani et al., 2011). Despite the widespread acknowledgement of the glutamate and GABA imbalance during epilepsy, therapeutic antiepileptic strategies targeting these mechanisms have proved insufficient in a significant proportion of patients (Kwan and Brodie, 2006). Thus, the role for inflammation and inflammatory mediators has become increasingly appreciated and is a focus of current research (Choi and Koh, 2008; Vezzani et al., 2013a).

Importantly, many inflammatory cytokines are known to be neurotoxic and involved in the epileptogenic process by promoting neuronal hyperexcitability during epilepsy (Vezzani et al., 2011) (**Figure 6**).

Among pro-inflammatory cytokines, IL-1β exerts excitatory effects in various brain regions (Vezzani et al., 2013b). In particular, IL-1β reduces synaptically-mediated GABA inhibition in area CA3 of the hippocampus (Wang et al., 2000; Zeise et al., 1997) and increases CA1 neuron excitability by reducing NMDA channel- and voltage-gated calcium channel-induced outward current (Zhang et al., 2010). This cytokine also potentiates NMDA receptor function in cultured hippocampal neurons (Lai et al., 2006; Viviani et al., 2003), by enhancing NMDA-mediated Ca2+ influx (Viviani et al., 2003). Thus, IL-1β contributes to excitotoxicity and epileptogenesis.

Among anti-inflammatory cytokines, TGFβ is upregulated in many epileptogenic conditions (Szelényi, 2001), and is potentially involved in epileptogenesis. Serum albumin, the most abundant class of plasma protein in the blood, and an inducer of post-injury epilepsy (Weissberg et al., 2015) binds to the TGFβ receptor and activates TGFβ signalling when extravasated through a dysfunctional BBB, a hallmark of brain injuries and neurodegenerative diseases (Cacheaux et al., 2009; Ivens et al., 2007). Accordingly, transcriptome analysis shows a similar transcription modulation pattern in animals exposed to BBB dysfunction, serum-derived albumin or following direct brain exposure to physiological levels of TGFβ (Vezzani et al., 2013b). In fact, TGFβ up-regulation is part of the inflammatory response in the hippocampus of rats undergoing status epilepticus (Aronica et al., 2000). Importantly, blocking

TGFβ signalling in an albumin induced model of epileptogenesis reversed inflammation and transcriptional patterns associated with activated glia and prevented the development of epileptiform activity (Vezzani et al., 2013b). However, the detailed mechanisms and cellular pathways bridging TGFβ signalling to seizures in different cell types within the neurovascular network are still a matter of investigation (Vezzani et al., 2013b).

3.5.5. Microglial phagocytosis and epilepsy

Importantly, phagocytic "find-me" signals and their receptors have been found to be upregulated in epilepsy models. CX3CL1 is upregulated in the serum and cerebrospinal fluid of epileptic patients as well as in a lithium-pilocarpine rat model (Ali et al., 2015). Furthermore, a corresponding increase in CX3CL1 receptor expression is detected between 1 and 6 h and begins to decline by 3 days following seizures (Ali et al., 2015; Yeo et al., 2011). However, following intrastriatal KA treatment, fractalkine receptor expression remained unchanged in microglia despite evident neuronal loss (Hughes et al., 2002). In addition to CX3CL1 signalling, purinergic signalling is now known to be critical in epileptogenesis. Purinergic receptors are upregulated on microglia following experimental seizures (Avignone et al., 2008) (**Figure 6**). P2X7 receptor shows an increased immunohistochemical expression in microglia in rats 24h after intraperitoneal KA injection (Rappold et al., 2006). Moreover, upregulation of P2X7 among other P2X and P2Y receptors (P2Y6 and P2Y12) has been confirmed by quantitative polymerase chain reaction (qPCR) and functional electrophysiology in mice 24h after intraperitoneal KA injection (Avignone et al., 2008). In addition, microglial lysosomal proteases, CatB, D, and S increase following seizures in rats 2 days after systemic KA injection (Akahoshi et al., 2007; Banerjee et al., 2015). Together, these studies highlight the dramatic upregulation of microglial purinergic receptors, cytokines, and proteases following seizures (Eyo et al., 2017).

Nevertheless, microglial phagocytosis efficiency during epilepsy or during its underlying pathological processes, excitotoxicity and inflammation, remains unknown. The goal of this PhD thesis is to assess microglial phagocytic efficiency in all these pathological models. We will also determine the possible mechanisms that modulate phagocytosis during epilepsy, as well as analyzing the possible detrimental consequences of a phagocytosis impairment for brain tissue homeostasis.

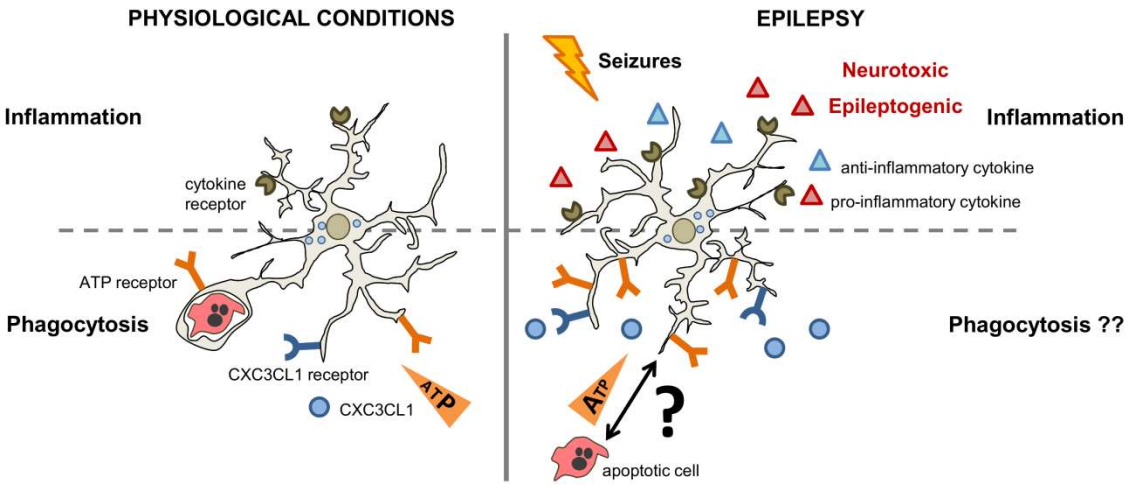

Figure 6. Microglial functions in epilepsy. In the epileptic brain, seizures upregulate the expression of pro- and anti-inflammatory cytokines and their receptors in microglia. Many inflammatory cytokines are known to be neurotoxic and involved in the epileptogenic process by promoting neuronal hyperexcitability during epilepsy. Importantly, some phagocytic "find-me" signals and their receptors are upregulated in microglia during epilepsy. However, the efficiency and modulation of microglial apoptotic cell phagocytosis during epilepsy remains unknown.

4 HYPOTHESIS AND OBJECTIVES

4. HYPOTHESIS AND OBJECTIVES

Microglial phagocytosis is very rapid and efficient in physiological conditions. Thus, we hypothesize that this efficiency could be maintained in pathological conditions where apoptotic cell numbers increase, such as excitotoxicity, acute and chronic inflammation, and pharmacologically induced epilepsy. Additionally, since microglial phagocytosis of apoptotic cells has been found to correlate with the induction of an anti-inflammatory response in microglia in vitro, we also hypothesize that microglial phagocytosis impairment would have detrimental consequences for the maintenance of tissue homeostasis. Additionally, analyzing the mechanisms driving a microglial phagocytosis impairment could open the venue to the generation of new therapies to harness microglial phagocytosis in disease.

Aim 1. To test the efficiency of microglial phagocytosis in the diseased brain in different pathological conditions. For this purpose, we will use an in vitro model of excitotoxicity using hippocampal slice cultures, and in vivo models of acute and chronic inflammation and pharmacologically induced epilepsy by KA intrahipocampal injection. All parameters regarding microglial phagocytosis efficiency will be quantified by immunofluorescence in mouse tissue sections imaged by confocal microscopy.

Aim 2. To analyze the mechanisms inducing a microglial phagocytosis impairment in a model of pharmacologically induced epilepsy. For this purpose we will test whether the phagocytosis impairment is due to deficits in microglial motility using 2-photon microscopy in acute hippocampal slices ex vivo and in the cortex of epileptic mice in vivo. We will also test whether the impairment is mediated by or due to a direct effect of KA on microglia using hippocampal slices and primary microglial cultures. Finally, we will test whether the impairment is mediated by ATP on microglia, in vivo and in organotypic hippocampal slices.

Aim 3. To analyze the effects of the microglial phagocytosis impairment during pharmacologically induced epilepsy. For this purpose we will test whether the phagocytosis impairment induces an accumulation of non-phagocytosed apoptotic cells in the hippocampus in vivo. We will also test whether the phagocytosis impairment correlates with an increase in tissue inflammation, using RTqPCR to analyze cytokine RNA expression from hippocampus homogenates and from FACS sorted hippocampal microglia.

Aim 4. To analyze if the microglial phagocytosis impairment occurs in a model of genetic epilepsy. For this purpose we will test whether there is a microglial phagocytosis impairment in a model of genetic epilepsy (Cstb KO) in the hippocampus in vivo, before and after the onset of seizures.

5 EXPERIMENTAL PROCEDURES

5. EXPERIMENTAL PROCEDURES

5.1. ANIMALS

Mice were housed in 12:12h light cycle with ad libitum access to food and water. All procedures followed the European Directive 2010/63/EU, NIH guidelines, and Canadian Council on Animal Care guidelines, and were approved by the Ethics Committees of the University of the Basque Country EHU/UPV (Leioa, Spain; CEBA/205/2011, CEBA/206/2011, CEIAB/82/2011, CEIAB/105/2012), Bordeaux University (protocol number 5012094-A), and Southampton University (in accordance with U.K. Home Office licensing; project license 30/3056); the Baylor College of Medicine Institutional Animal Care and Use Committee (Houston, TX, USA; AN- 5004); and the Animal Care Committee of Université Laval (protocol number 2013102-1). Unless otherwise stated, mice were 8 weeks old at the time of the KA injection.

All experiments were performed in fms-EGFP (MacGreen) mice, except the analysis of tissue cytokines by reverse transcription quantitative polymerase chain reaction (RTqPCR) and the analysis of microglial motility, which were performed in C57BL/6 (Harlan, Boxmeer, the Netherlands) and CX3CR1$^{GFP/+}$ mice, respectively. In both fms-EGFP (Sasmono et al., 2003; Sierra et al., 2007) and CX3CR1$^{GFP/+}$ mice (Jung et al., 2000), all microglia express the green fluorescent reporter. Fms-EGFP mice express the green reporter under the colony stimulating factor 1 receptor (Csf1r) and CX3CR1$^{GFP/+}$ mice have one allele of the CX3CR1 gene (fractalkine receptor) replaced by the GFP reporter gene. Analysis of phagocytosis by non-professional phagocytes was done in POMC-EGFP mice (Overstreet et al., 2004) in which enhanced green fluorescent protein (EGFP) is expressed in newborn granule cells in the dentate gyrus (DG) under the transcriptional control of proopiomelanocortin (POMC); hGFAP-GFP mice (Zhuo et al., 1997) in which GFP is expressed under the control of the astrocyte-specific glial fibrillary acidic protein (GFAP) human promoter; and nestin-GFP mice (Encinas et al., 2006; Mignone et al., 2004), in which GFP is expressed under the regulatory elements of the intermediate filament nestin, expressed in neural stem and progenitor cells. Analysis of phagocytosis in a genetic model of epilepsy was done in Cstb KO mice, constitutive knock-outs (KO) of the cystatin B (Cstb) gene, which encodes an inhibitor of cysteine proteases. All mice used were in a C57BL/6 background, except experiments with fatty acid diets, which were performed in CD-1 Swiss mice. Omega 3 (Ω3) deficient (containing 6% fat in the form of sunflower oil, rich in linoleic acid) or omega 3 balanced (containing a mixture of different oils rich in alpha-linolenic acid) diets were given immediately after mating and through gestation

and lactation (Mingam et al., 2008); both diets were isocaloric and only their lipid composition was different, as shown in the following table.

FATTY ACIDS	Ω3 BALANCED DIET	Ω3 DEFICIENT DIET
16:0	22.6	7.3
18:0	3.3	4.1
other saturated FAs	1.8	1.6
total saturated FAs	**27.7**	**13.0**
16:1 Ω7	0.2	0.2
18:1 Ω9	57.9	28.1
18:1 Ω7	1.5	0.9
other monounsaturated FAs	0.4	0.2
total monounsaturated FAs	**60.0**	**29.4**
18:2 Ω6 (LA)	10.6	57.4
20:4 n Ω6 (AA)	ND	ND
total Ω6 polyunsaturated FAs	**10.7**	**57.4**
18:3 Ω3 (ALA)	1.6	0.2
total Ω3 PUFAs	**1.6**	**0.2**
total PUFAs	**12.3**	**57.6**

Table 1. Fatty acid composition of the dietary lipids. Percentage (in weight) in saturated, monounsaturated, omega 6 (Ω6) polyunsaturated and omega 3 (Ω3) polyunsaturated fatty acids, as determined by gas chromatography. AA, arachidonic acid; ALA, α-linolenic acid; FAs, fatty acids; LA, linolenic acid; ND, not detected (under the limit for the detection by gas chromatography, <0.05%); PUFAs, polyunsaturated fatty acids.

5.2. SURGICAL PROCEDURES

5.2.1. Intrahippocampal injections

Induction of epilepsy was achieved by intrahippocampal injection of kainic acid (KA, Sigma-Aldrich, St Louis, MO, USA) a kainate receptor agonist (Bouilleret et al., 1999). In brief, mice were intraperitoneally anesthetized with ketamine/xylazine (10/1 mg/kg) and received a

single dose of the analgesic buprenorphine (1mg/kg) subcutaneously. The hair over the scalp was shaved and povidone iodine was applied. The animal was positioned in the stereotaxic apparatus, and an incision was cut in the skin over the scalp to localize Bregma (intersection of the coronal suture and the sagittal suture). Next, a 0.6mm whole was drilled at coordinates taken from Bregma: anteroposterior (AP) -1.7mm, laterolateral (LL) -1.6mm. A pooled glass microcapillary was inserted at -1.9mm dorsoventral (DV), and 50nL of saline or KA (20mM) were delivered into the right hippocampus using a microinjector (Nanoject II, Drummond Scientific, Broomal, PA, USA). Adenosine triphosphate (ATP; 1µl; 10, 100mM; Sigma) and ATPγS (1µl; 100mM; Tocris) a non-degradable form of ATP, were injected directly into the DG as pH-balanced solutions at coordinates AP -1.7mm, LL -1.4mm, DV -2.3mm. After waiting 2min to evade reflux, the microcapillary was retracted, and the mice sutured and maintained in a thermal blanket until recovered from anesthesia.

5.2.2. EEG recordings

Some saline and KA injected mice were implanted with platinum iridium, Teflon-coated deep electrodes (PlasticsOne, Roanoke, VA, USA) immediately after intrahippocampal injection. Four recording electrodes were positioned at -1.6mm AP, +1.8mm LL, -1.8mm DV (left hippocampus); -1.6mm AP, -1.8mm LL, -1.8mm DV (right hippocampus); -0.1mm AP, -1.8mm LL, -2mm DV (right cortex): -0.1mm LL, +1.8mm LL, -2mm DV (left cortex). The reference electrode was placed at the frontal lobe at +0.1mm AP, +0.1mm LL, - 0.5mm DV, and the ground electrode was positioned over the cervical paraspinal area (Sierra et al., 2015). Four hours after implantation, every two days for the next week, and once a week for another 7 weeks, mice were attached to a Nicolet video-electroencephalogram (vEEG) system (NicView 5.71, CareFusion, San Diego, CA, USA), and were recorded in 4h sessions.

5.3. CELL CULTURES

5.3.1. Organotypic hippocampal slice cultures

Organotypic hippocampal slice cultures were prepared as described previously (Vinet et al., 2012) with minor modifications. 7 day-old fms-EGFP pups were decapitated and the brains extracted and placed in cold Hank's balanced salt solution (HBSS). Both hippocampi were dissected and cut into 350µm slices using a tissue chopper (McIlwain). Slices in good condition (with whole and visible DG and cornu ammonis (CA) and without cuts or damaged borders) were then selected and transferred to 0.4 µm culture plate inserts (Millipore), each

containing 4 slices. These membranes were placed in six well plates, each well containing 1ml of fresh hippocampal organotypic culture medium. The medium consisted of 50% Neurobasal medium supplemented with 0.5% B27, 25% horse serum, 1% Glutamax, 1% penicillin/streptomycin (all from Gibco) and 1% glucose solution in HBSS. Culture medium was changed the first day after doing the culture and every 2 days afterwards. Slices were kept in culture for 7 days before performing the experiments. For induction of excitotoxicity, hippocampal slices were treated with media containing 50µM N-methyl-D-aspartic acid (NMDA), a glutamate agonist, and 10µM glycine, an NMDA receptor co-agonist, at in vitro day 7 for 4h; another batch of slices were then placed in fresh culture medium for another 24h. For KA experiments, hippocampal slices were treated with media containing 1mM KA (Sigma) for 6h. For ATP experiments, hippocampal slices were treated with media containing 300µM and 1mM ATP (Sigma) for 4h. For experiments with the epileptogenic cocktail, hippocampal slices were treated for 1h with either vehicle (oxygenated (95% O_2/5% CO_2) artificial cerebrospinal fluid (ACSF), pH7.4, containing 124mM NaCl, 25mM $NaHCO_3$, 1.25mM NaH_2PO_4, 2.5mM KCl, 2.5mM $CaCl_2$, 1.3mM $MgCl_2$, and 10mM D-glucose) or proepileptogenic cocktail (oxygenated ACSF, with high K^+ (8mM), low Mg^{2+} (0.25mM) and 4-aminopyridine (4-AP, 100µM)(Hsiao et al., 2014). Propidium iodide (PI, 5µg/ml, Sigma) a marker of necrosis, was added to the cultures in the last hour of the treatment.

5.3.2. NE-4C cell line

NE-4C (American Type Culture Collection), a mouse neural stem cell line derived from the cortex of 9do tumour protein 53 (p53, a tumour suppressor gene) knock-out embryos was used for the phagocytic assay experiments. NE4C cells were grown as an adherent culture in Poly-L-lysine-coated (15µl/ml, Sigma) culture flasks covered with 10-15ml of medium. The medium consisted on Minimum Essential Medium (MEM, Gibco), supplemented with 1% Glutamax, 2,5% Fetal Bovine Serum (FBS) and 1% penicillin/streptomycin (all from Gibco). When confluency was reached, cells were trypsinized and replated at 1:4.

5.3.3. Primary microglia cultures

Primary microglia cultures were performed as previously described (Moussaud and Draheim, 2010). Postnatal day 0-1 (PND0-PND1) fms-EGFP mice pup brains were extracted and the meninges were removed in HBSS (Hyclone) under a magnifying scope. The olfactory bulb and cerebellum were discarded and the rest of the brain was then mechanically disrupted and enzymatically digested with papain (20U/ml, Sigma), a cysteine protease enzyme, and deoxyribonuclease (DNAse; 150U/µl, Invitrogen) for 15min at 37ºC. The homogenization was

helped by carefully pipetting throughout the process. The resulting cell suspension was then filtered through a 40µm nylon cell strainer (Fisher) and transferred to a 50ml Falcon tube quenched by 5ml of 20% FBS (Gibco) in HBSS. Afterwards, the cell suspension was centrifuged at 200g for 5min, the pellet was resuspended in 1ml Dulbecco's Modified Eagle's Medium/F12 (DMEM/F12, Gibco) complemented with 10% FBS and 1% Penicillin-Streptomycin (Gibco), and plated in Poly-L-Lysine-coated (15µl/ml, Sigma) culture flasks with a density of two brains per flask. Medium was changed every 3-4 days and enriched with granulocyte-macrophage colony stimulating factor (5µg/ml GM-CSF, Sigma), which promotes microglial proliferation. After confluence (at 37°C, 5% CO_2 for approximately 14 days), microglia cells were harvested by shaking at 100rpm, 37°C, for 4h. Isolated cells were counted and plated at a density of 80.000cell/well on poly-L-lysine-coated glass coverslips resting in 24-well plates. Microglia were allowed to adhere for at least 24h before phagocytosis experiments.

5.4. PHAGOCYTOSIS ASSAY

Primary microglia cells were fed for 3h with NE-4C cells. NE-4C were previously labeled with the membrane marker CM-DiI (5µM; 10min at 37°C, 15min at 4°C; Invitrogen) and treated with staurosporine (STP, 10µM, 4h; Sigma) an inhibitor of protein kinases that induces apoptosis (Lawrie et al., 1997). This treatment resulted in 27.4% ± 8.5% of apoptotic and 1.2% ± 0.9% of necrotic NE-4C cells, as determined by flow cytometry analysis with Annexin V (apoptosis marker) and PI (necrosis marker); and in 35.0% ± 6.1% of apoptotic cells with pyknotic/karyorrhectic nuclear morphology determined with 4',6-diamidino-2-phenylindole (DAPI) in immunofluorescent assays (data not shown). Apoptotic NE-4C cells were added to the microglial cultures in a 10:1 proportion approximately. For the KA treatment, microglia were pre-treated with 1mM KA (Sigma) for 2h before adding the apoptotic cells and remained present for the 3h of the phagocytosis assay, accounting for a total of 5h of KA treatment (Christensen et al., 2006).

5.5. IMMUNOFLUORESCENCE

5.5.1. Brain tissue sections and hippocampal organotypic cultures

Mice were anesthetized with 2,5% avertine and transcardially perfused with 30ml of PBS followed by 30 ml of 4% paraformaldehyde (PFA). The brains were removed and postfixed with the same fixative for 3h at room temperature (RT), then washed in phosphate buffered

saline (PBS) and kept in cryoprotectant at -20ºC. Six series of 50µm-thick sections per mouse brain hemisphere were sagitally cut using a Leica VT 1200S vibrating blade microtome (Leica Microsystems GmbH, Wetzlar, Germany). Hippocampal organotypic slices were fixed in 4% formaldehyde for 40 min and then stored in PBS at 4ºC. Fluorescent immunostaining was carried out following standard procedures (Sierra et al., 2010). Free-floating vibratome sections or organotypic slices were incubated in permeabilization solution (0.3% Triton-X100, 0.5% BSA in PBS; all from Sigma) containing 5% normal goat serum (NGS) for 1h at RT with gentle shaking, and then incubated overnight with the primary antibodies diluted in the permeabilization solution at 4ºC. For BrdU (bromo-deoxyuridine) staining, an antigen retrieval protocol was performed on the sections, consisting on incubation in 2M HCl for 15min at 37ºC and then washing with 0.1M sodium tetraborate for 10min at RT prior to staining with the primary antibodies. After overnight incubation with primary antibodies, brain sections were thoroughly washed with 0,3% triton in PBS. Next, the sections were incubated with fluorochrome-conjugated secondary antibodies and DAPI (5mg/ml; Sigma) diluted in the permeabilization solution for 2h at RT. After washing with PBS the sections and organotypic cultures were mounted on glass slides with DakoCytomation Fluorescent Mounting Medium (DakoCytomation, Carpinteria, CA).

5.5.2. Primary microglial cultures

Primary microglial cultures were fixed for 10min in 4% formaldehyde and then stored in PBS at 4ºC. Coverslips with primary microglial cultures were blocked in 1% NGS (Sigma), 0.2% Triton X-100 in PBS for 30min. The cells were then incubated with primary antibodies in 0.2% Triton X-100 PBS for 1h at RT, washed in PBS and incubated in the secondary antibodies containing DAPI (5mg/ml) in the same solution for 1h at RT. Finally, cell containing coverslips were mounted on glass slides with DakoCytomation Fluorescent Mounting Medium.

5.5.3. Antibodies

The following antibodies were used: chicken anti-GFP (1:750; Aves Laboratories); mouse anti-NeuN (neuronal nuclei) (1:1000; EMD Millipore Corporation); rabbit anti-activated-caspase-3 (1:100; Cell Signaling Technology); rabbit anti-cfos (1:1000; Santa Cruz Biotechnologies); rabbit anti-Ki67 (1:1000; Vector Laboratories); rabbit anti-Iba1 (1:1000; Wako Chemicals); rat anti-BrdU (1:300; AbD Serotec), rat anti-CD11b (1:200, Serotec). Secondary antibodies coupled to AlexaFluor 488, Rodhamine Red X, or AlexaFluor 647 were purchased from Molecular Probes or from Jackson Immunoresearch.

5.6. IMAGE ANALYSIS

All fluorescence immunostaining images were collected using an Olympus Fluoview or a Leica SP8 laser scanning microscope using a 40X oil-immersion objective (in vivo experiments and primary cultures) or a 60X oil-immersion objective (organotypic slice experiments) and a z-step of 0.7µm. All images were imported into Adobe Photoshop 7.0 (Adobe Systems Incorporated, San Jose, CA) in tiff format. Brightness, contrast, and background were adjusted equally for the entire image using the "brightness and contrast" and "levels" controls from the "image/adjustment" set of options without any further modification. 3D-rendering of phagocytic microglial cells was performed using ImageSurfer (NIH) or ImageJ (Fiji distribution). Quantitative analysis of apoptosis and phagocytosis was performed using unbiased stereology methods as previously described (Sierra et al., 2010). For mouse tissue sections, 2-3 20µm-thick z-stacks located at random positions containing the DG were collected per hippocampal section, and a minimum of 6 sections per series were analyzed. For organotypic cultures, 3 20µm-thick random z-stacks of the DG were collected per hippocampal slice. For primary cultures, over 10 random z-stacks were obtained per coverslip.

5.7. PHAGOCYTOSIS ANALYSIS

Apoptotic cells were defined based on their nuclear morphology after DAPI staining as cells in which the chromatin structure (euchromatin and heterochromatin) was lost and appeared condensed and/or fragmented (pyknosis/karyorrhexis); they also co-localized with activated-caspase-3, a well-known marker of apoptosis (Green and Llambi, 2015). Phagocytosis was defined as the formation of an enclosed, three-dimensional pouch of microglial processes surrounding an apoptotic cell. In tissue sections and organotypic cultures, the number of apoptotic cells, phagocytosed cells, $BrdU^+$ cells, and microglia were estimated in the volume of the DG contained in the z-stack (determined by multiplying the thickness of the stack by the area of the DG at the center of the stack using ImageJ (Fiji)). To obtain the absolute numbers (in tissue sections), this density value was then multiplied by the volume of the septal hippocampus (spanning from -1mm to -2.5mm in the anteroposterior axes, from Bregma; approximately 6 slices in each of the 6 series), which was calculated using Fiji from a Zeiss Axiovert epifluorescent microscope images collected at 20X. In organotypic cultures, the number of apoptotic cells and microglia in the DG was given as a density, over a 200.000μm^3 volume (roughly, a 100x100μm^2 area of 20µm of thickness). In primary cultures, the percentage of phagocytic microglia was defined as cells with pouches containing NE-4C nuclei

and/or CM-DiI particles. The following formulae were used to estimate microglial phagocytosis efficiency in tissue or organotypic cultures:

Ph index: proportion of apoptotic cells completely engulfed by microglia

Ph index = $\frac{apo^{Ph}}{apo^{tot}}$

where apo^{Ph} is the number of apoptotic cells phagocytosed and apo^{tot} is the total number of apoptotic cells.

Ph capacity: proportion of microglia with one or more phagocytic pouches, each containing one apoptotic cell.

Ph capacity = $\frac{mg^{Ph1}+2\ x\ mg^{Ph2}+3\ x\ mg^{Ph3}\ldots+n\ \ x\ mg^{Phn}}{mg}$

where mg^{Phn} is the proportion of microglia with n phagocytic pouches and mg is the number of microglial cells.

Ph/A coupling: phagocytosis/apoptosis ratio.

Ph/A coupling = $\frac{Ph\ capacity\ x\ microglia}{apo^{tot}}$

Where apo^{tot} is the total number of apoptotic cells.

Clearance time: average time at the population level for an apoptotic cell to be eliminated by microglia.

Clearance time =$\frac{apo^{tot}(t2)x\ \Delta t}{\Delta BrdU}$

where apo^{Ph} is the number of apoptotic cells phagocytosed; Δt is the diference between the two time points analyzed and ΔBrdU is the change in the number of BrdU marked cells in those time points.

5.8. LIVE IMAGING

5.8.1. Two-photon imaging on acute hippocampal slices

Brain slices were obtained from CX3CR1$^{GFP/+}$ mice aged 2 months old (mo) 1 day post-injection (dpi) or 7dpi of KA or saline. As we previously described (Madore et al., 2013), animals were quickly anesthetized with isoflurane, their brains were extracted and 300 µm-thick coronal slices were made using a Vibratome (VT1000S, Leica, Nanterre, France). Slices were then stored at RT (20 to 23°C) for one hour before imaging in an oxygenated ACSF containing 126mM NaCl, 2.0mM $CaCl_2$, 2.0mM $MgCl_2$, 2.5mM KCl, 1.25mM NaH_2PO_4, 26mM $NaHCO_3$, 10mM glucose, 1mM ascorbic acid, 4mM sodium pyruvate, and saturated with 95% O_2 and 5% CO_2 (310 ± 5 mOsm). Slices were transferred to a recording chamber and perfused with oxygenated ACSF at a rate of 1-3ml/min and maintained at 25°C with an inline heater. Two-photon imaging was performed with a laser-scanning microscope Leica DMLFSA TCS SP2 on an upright stand (Leica Microsystems, Mannheim, Germany) coupled to a femtosecond pulsed Ti:Sapphire laser (Mira 900, Coherent Laser Group, Santa Clara, CA, USA). The laser was tuned to the excitation wavelength for GFP (900 nm) and there was no photobleaching nor was there any evidence of cellular damage during extensive scanning to obtain time lapse images. The laser intensity was carefully monitored in all instances and kept comparable between all experiments. A HCX IR Apo L 25X NA 0.95 (Olympus) water-immersion objective lens was used. Imaging was done at depths in brain slices >50µm and up to 100µm. The mean depth for imaging lesions was 75µm. Voxel size was adjusted to 0.1x0.1µm and z-stacks were taken in 1µm steps. The mean scan time for z-stack was approximately 45s. 3D reconstruction of microglia, and automated assessment of the number of branches was performed using the "filament tracer program" (Matlab algorithm) of Imaris 7.6 (Bitplane AG), after correction for drift in x- and y-axis (Stackreg (Thevenaz et al., 1998) and Multistackreg (Busse) plugins, Fiji) and drift in z-axis ("correct 3D axis", Fiji module of Imaris 7.6). This allowed us to isolate each microglial process and to follow its length modification all along the recording period. In both saline- and KA-injected animals, we analyzed 4-5 cells (distributed through the hilus and the DG) per animal and 3-4 animals per group.

5.8.2. Two-photon imaging on the living cortex

Live imaging was performed using two-photon imaging as previously described (Tremblay et al., 2010). 2mo CX3CR1$^{GFP/+}$ mice were injected with saline or KA as explained previously. 24h later, mice were anesthetized with isoflurane. The hair above the skull was shaved and ethanol and povidone iodine were applied to disinfect. Next, the skin was cut and

the skull above the motor cortex was exposed and cleaned with ethanol and ferric oxide, which dry the periosteum and allow its removal. Then the skull was dried and glued to a thin metal plate and a small patch (1mm^2) was carefully thinned to an approximately 20- to 30-mm thickness, using a high-speed dental drill (Osada Inc) and a microsurgical blade. Drilling was interrupted every 20 seconds, and sterile saline was applied on the skull to prevent heat-induced damage. Next, the mice were placed under an Olympus two-photon microscope FV1000MPE equipped with a Ti:Sapphire laser (Mai Tai DeepSee; Spectra Physics) tuned to 920 nm for transcranial imaging. A 25X water-immersion lens (1.05 N.A.; Olympus) was used throughout the imaging session. Z stacks taken 1µm apart were acquired every 1.5min for 13.5 min (10 time frames). Microglial motility was analyzed using several plugins in Fiji. In brief, images were registered using the "Affine" algorithm of the "MultiStack" plugin and aligned by using the "Correct 3D drift" plugin (Parslow et al., 2014). Background was subtracted using a difference of Gaussians and bleaching was corrected using the "Histogram Matching" algorithm of the "Bleach Correction" plugin (Miura et al., 2014). The motility was automatically determined using a self-developed ImageJ macro that estimated the 3D length of previously selected processes, and calculated the motility as the absolute difference of length between two consecutive frames divided by the time interval (1.5min). For automatic measurement of the length process, each selected process was reoriented vertically in the xy plane and the intensity profiles of horizontal lines run through the length of the process were obtained in each z-slice.

Intensity profiles were used to determine the x and z coordinates of the borders of the process in each line based on three parameters: background intensity, the difference between the maximum intensity and the pixels flanking the maxima, and the inflexion points of the intensity profiles. x and z coordinates of the borders were used to calculate the center of the process in each horizontal plane (xz planes). Then, the length of the 3D skeleton of the process in each time frame was calculated as the summation of the distances between each pair of center points located in consecutive xz planes. The following formulae were used to calculate the mean motility of a process:

$$z_C = \frac{z_U + z_B}{2}$$

Where z_C, z_U and z_B are the coordinates of the center, the upper z-slice and the bottom z-slice containing the process, respectively.

$$x_C = \frac{x_R + x_L}{2}$$

Where x_C, x_R and x_L are the coordinates of the center, the right border and the left border of the process, respectively. If z_c-slice was virtual (i.e., not an integer):

$$x_R = \frac{x_{R_{(z_c-0.5)}} + x_{R_{(z_c+0.5)}}}{2}$$

$$x_L = \frac{x_{L_{(z_c-0.5)}} + x_{L_{(z_c+0.5)}}}{2}$$

Once the coordinates of the center of the vertically aligned process had been defined in the X and Z planes, its length was estimated:

$$length = \sum_{i=y_0}^{y_{n-1}} \sqrt{(y_{i+1} - y_i)^2 + (x_{c_{y_{i+1}}} - x_{c_{y_i}})^2 + (z_{c_{y_{i+1}}} - z_{c_{y_i}})^2}$$

Where y_0 and y_{n-1} are the y coordinates of the first and last horizontal lines, respectively, containing pixels with intensities above the background. Finally, the process motility was estimated:

$$motility = \frac{\sqrt{(length_{f+1} - length_f)^2}}{1.5}$$

Where f is time frame, and 1.5 corresponds to the 1.5min of the time interval between consecutive frames. Mean motilities were used for analysis. Mean protraction and retraction of a process were calculated as the mean of the motilities from consecutive frames (f and f+1) where the length of the process was increased or decreased, respectively.

5.9. ELECTROPHYSIOLOGY

Hippocampal slices (300µm) were cut with a vibratome (Leica) from PND20-PND30 fms-EGFP mice in oxygenated (95% O_2/5% CO_2) ACSF, pH7.4, that contained 124mM NaCl, 25mM $NaHCO_3$, 1.25mM NaH_2PO_4, 2.5mM KCl, 2.5mM $CaCl_2$, 1.3mM $MgCl_2$, and 10mM D-glucose. Slices were allowed to recover for at least 1h and were then transferred to a 37°C chamber with continuous flow (1mL/min) of oxygenated ACSF. To induce epileptiform activity, cells were perfused with high K^+ (8mM), low Mg^{2+} (0.25mM) and 4-aminopyridine (4-AP, 100µM) (Hsiao et al., 2014). Extracellular field potential recordings were performed in the CA1 pyramidal layer to monitor epileptiform activity, using glass electrodes (1MΩ) filled with ACSF. Epileptiform activity was induced both in the DG and CA1, but the amplitude of the spikes was considerably larger in CA1 and thus EGFP-expressing microglial cells were simultaneously patch-clamped recorded in this region in whole-cell configuration with recording pipettes (7-

10MΩ) filled with a solution containing 135mM KCl, 4mM NaCl, 0.7mM $CaCl_2$, 10mM BAPTA, 10mM HEPES, 4mM Mg-ATP and 0.5mM Na_2-GTP (pH 7.2).

5.10. FACS SORTING

For cytokine expression experiments, microglial cells were isolated from brains as described previously (Sierra et al., 2007). 2mo fms-EGFP mice were anesthetized, perfused with saline and decapitated in order to isolate the hippocampus. The hippocampi were then dissected and placed in enzymatic solution (116mM NaCl, 5.4mM KCl, 26mM $NaHCO_3$, 1mM NaH_2PO_4, 1.5mM $CaCl_2$, 1mM $MgSO_4$, 0.5mM EDTA, 25mM glucose, 1mM L-cysteine) with papain (20U/ml) and DNAse I (150U/µl, Invitrogen) for digestion at 37°C for 15 min. 4 hippocampi from saline or KA-injected mice were collected per replica, with a total of 4 replicas. After homogenization, tissue clogs were removed by filtering the cell suspension through a 40µm nylon strainer to a 50ml Falcon tube containing 5ml of HBSS with 20% heat inactivated FBS, to stop the enzymatic reaction of papain. For further enrichment of microglia, myelin was removed by using a Percoll gradient. For this purpose, cells were centrifuged at 200g for 5min and resuspended in 20% Solution of Isotonic Percoll (20% SIP; in HBSS), obtained from a previous stock of SIP (9 parts Percoll per 1 part PBS 10X). Then, each sample was layered with HBSS poured very slowly by fire-polished pipettes. Afterwards, gradients were centrifuged for 20min at 200g with minimum acceleration and no brake so the interphase was not disrupted. Then the myelin containing interphase was removed, cells were washed in HBSS by centrifuging at 200g for 5min and pellet was resuspended in 500µl of sorting buffer (25mM HEPES, 5mM EDTA, 1% BSA, in HBSS). Microglia cell sorting was performed by fluorescence activated cell sorting (FACS) using FACS Jazz (BD), in which the population of green fluorescent cells was selected, collected in Lysis Buffer (Qiagen) containing 0.7% 2-mercaptoethanol and stored at -80°C until processing.

5.11. RNA ISOLATION AND RTqPCR

5.11.1. RNA isolation and RT

5.11.1.1. *Hippocampus*

The right (injected) hippocampus of wild type (WT) mice was rapidly isolated immediately after intraaortic perfusion with cold PBS under tribromoethanol overdose, and stored at -80°C until processed. Total ribonucleic acid (RNA) was isolated using a roto-stator

homogenizer and Qiagen RNeasy Mini Kit (Alcobendas, Spain), following manufacturer's instructions, including a DNAse treatment step to eliminate genomic deoxyribonucleic acid (DNA) residues. RNA was quantified in a Nanodrop 2000, and 1.5µg were retrotranscribed using random hexamers (Invitrogen) and Superscript III Reverse Transcriptase kit (Invitrogen), following manufacturer's instructions in a Veriti Thermal Cycler (Applied Biosystems, Alcobendas, Spain).

5.11.1.2. *FACS sorted microglia*

RNA from FACS-sorted microglia was isolated by Rneasy Plus micro kit (Qiagen) according to the manufacturer instructions, and the RNA was retrotranscribed using an iScript advanced complementary DNA (cDNA) Synthesis Kit (Biorad) following manufacturer's instructions in a Veriti Thermal Cycler.

5.11.2. qPCR

Quantitative Polymerase Chain Reaction (qPCR) was performed following MIQE guidelines (Minimal Information for Publication of Quantitative Real Time Experiments (Bustin et al., 2009)). Three replicates of 1.5µl of a 1:3 dilution of cDNA were amplified using Power SybrGreen (Biorad) for whole hippocampus experiments or SsoFast EvaGreen Supermix (Biorad) for FACS-sorted microglia experiments in a CFX96 Touch Real-Time PCR Detection System (Biorad). The amplification protocol for both enzymes was 3min 95ºC, and 40 cycles of 10sec at 95ºC, 30sec at 60ºC. Primers were designed to amplify exon-exon junctions using Primer Express (Applied Biosystems) or PrimerBlast (NIH) to avoid amplification of contaminating genomic DNA, and their specificity was assessed using melting curves and electrophoresis in 2% agarose gels.

5.11.3. Primers

Primers were designed using Primer express (Thermo Fisher Scientific). Primer sequences are listed in **Table 2**.

For each set of primers, the amplification efficiency was calculated using a standard curve of 1:2 consecutive dilutions, and was used to calculate the relative amount using the following formula:

$$\Delta\Delta Ct = (1 + eff.target\ gene)\exp(Ct\ sample - Ct\ control)/(1 + eff.reference\ gene)\exp(Ct\ sample - Ct\ control)$$

GENE	GENE BANK	AMPLICON SIZE	SEQUENCE
Reference genes			
OAZ-1	NM_008753	51	Fwd AGCGAGAGTTCTAGGGTTGCC Rev CCCCGGACCCAGGTTACTAC
L27A	BC086939	101	Fwd TGTTGGAGGTGCCTGTGTTCT Rev CATGCAGACAAGGAAGGATGC
Cytokines			
IL-1β	NM_008361	152	Fwd CAACCAACAAGTGATATTCTCCATG Rev GATCCACACTCTCCAGCTGCA
IL-6	NM_031168	141	Fwd GAGGATACCACTCCCAACAGACC Rev AAGTGCATCATCGTTGTTCATACA
TGFβ1	NM_011577	51	Fwd GCAGTGGCTGAACCAAGGAG Rev TGAGCGCTGAATCGAAAGC
TNFα	NM_013693	179	Fwd CATCTTCTCAAAATTCGAGTGACAA Rev TGGGAGTAGACAAGGTACAACCC
CSF	NM_007778	51	Fwd GTCCTGCAGCAGTTGATCGA Rev GGCAATCTGGCATGAAGTCTC
MIC-1	NM_011819	52	Fwd TCAGTCCAGAGGTGAGATTGGG Rev TTGACGCGGAGTAGCAGCTG

Table 2. Primer sequences. Primer sequences for cytokine expression analysis by qPCR.

Two independent reference genes (or housekeeping genes) were compared: L27A, which encodes a ribosomal protein of the 60S subunit (Sierra et al., 2007) and OAZ-1, which encodes ornithine decarboxylase antizyme, a rate-limiting enzyme in the biosynthesis of polyamines and recently validated as reference gene in rat and human (Kwon et al., 2009). The expression of L27A and OAZ-1 remained constant independently of time and treatments (data not shown), validating their use as reference genes. In all experiments, the pattern of mRNA expression was similar using the assigned couple of reference genes, and in each experiment the reference gene that rendered lower intragroup variability was used for statistical analysis.

5.12. STATISTICAL ANALYSIS

SigmaPlot (San Jose, CA, USA) was used for statistical analysis. For the analysis of cytokine mRNA expression, a logarithmic transformation was performed to comply with

ANOVA assumptions (normality and homocedasticity) (Sierra et al., 2007). The analysis of cytokine and apoptotic cell expression was evaluated by 2-way ANOVA or the corresponding non-parametrical test (Kruskal-Wallis). When interaction between factors (time x treatment) was found, a 1-way ANOVA test of all groups was performed instead to determine the overall effect of each factor. In all cases, all-pairwise multiple comparisons (Holm-Sidak method or Tukey test) were used as a posthoc test to determine the significance between groups in each factor. Only $p<0.05$ is reported to be significant. Data is shown as mean ± SEM (standard error of the mean).

6 RESULTS

6. RESULTS

6.1. MICROGLIAL PHAGOCYTOSIS IS COUPLED TO CELL APOPTOSIS IN PATHOLOGICAL CONDITIONS IN VITRO AND IN VIVO

6.1.1. Microglial phagocytosis is coupled to cell apoptosis during excitotoxicity in vitro

Microglial phagocytosis has been shown to be very efficient at eliminating apoptotic cells in the dentate gyrus (DG) in physiological conditions (Sierra et al., 2010) but this efficiency has never been tested in pathological conditions. Thus, to assess whether the phagocytosis efficiency was maintained in different conditions we exposed microglia to different pathological models both in vitro (in organotypic hippocampal slices and primary cultures) and in vivo.

First, we investigated the response of microglial phagocytosis to excitotoxicity, one of the underlying pathological events occurring in epilepsy, were cell death is caused by excessive stimulation by neurotransmitters such as glutamate. For this purpose we used N-methyl-D-aspartate (NMDA), a glutamate agonist which causes excitotoxicity and seizures in vivo (Toscano et al., 2008), but only causes excitotoxicity in organotypic hippocampal slice cultures (Vinet et al., 2012) possibly due to the absence of the complete hippocampal circuit. Organotypic cultures are a useful approach for pharmacological studies as they partially preserve the structure and connectivity of the original tissue and maintain a physiological environment where all cell types are present (Gahwiler et al., 1997). Moreover, there is basal apoptotic death occurring in organotypic slices, which allowed us to establish the baseline of microglial phagocytosis in the DG this in vitro model. Thus, we induced excitotoxicity with a 4h treatment of NMDA (50µM) in postnatal organotypic hippocampal cultures of fms-EGFP mice, in which all microglia express the green fluorescent reporter (Sierra et al., 2007) (**Figure 7**). Apoptosis was determined by aberrant nuclear morphology, as visualized with the DNA dye DAPI, defined as pyknotic (condensed nuclei) and karyorrhectic (fragmented nuclei) cells. Necrosis was determined by retention of propidium iodide (PI), a DNA intercalating agent that is not extruded by cells with a disrupted cytoplasmic membrane, a hallmark of necrosis (Krishan, 1975). Microglial phagocytosis was assessed by the appearance of phagocytic pouches, i.e., apoptotic nuclei totally encircled by microglia (**Figure 7A**). In physiological conditions in vivo, microglia phagocytose apoptotic cells with pouches located at the tip of their processes in a “ball and chain” configuration or by en passant branches (Sierra et al., 2010). Nevertheless, microglia present a less ramified and more hypertrophic morphology in

organotypic slices, where phagocytosis can be seen to be carried out by microglial somas, with the phagocytic pouches located close to the microglial nuclei (**Figure 7A**).

The number of apoptotic cells increased significantly after 4 hours (4h) of NMDA treatment compared to non-treated controls and returned to basal levels 24h later, while the number of necrotic cells stayed unchanged (**Figure 7B**). The basal *phagocytic index* (Ph index), i.e., the proportion of apoptotic cells completely engulfed by microglia, was 13 ± 2% in control organotypic slices (**Figure 7C**) and remained stable in response to NMDA. Microglia responded to the increased number of apoptotic cells by rising their *phagocytic capacity* (Ph capacity), i.e., the proportion of microglia with one or more phagocytic pouches, each containing one apoptotic cell (Sierra et al., 2010), and there were more phagocytic microglia overall, some of them with up to 7 pouches (**Figure 7D, E**), while the number of microglia remained unchanged (**Figure 7F**). Thus, the increase of net phagocytosis (number of microglia multiplied by their phagocytic capacity) matched the increase in apoptosis, as determined by the *phagocytosis/apoptosis coupling ratio* (Ph/A coupling). The Ph/A coupling was similar between control and NMDA-treated slices (**Figure 7G**). Although the Ph coupling was maintained between the treatments indicating a balance between the change in phagocytosis and apoptosis, the Ph index showed that only 13 ± 2% of apoptotic cells were phagocytosed in controls, much less than in adults in physiological conditions (90-100%) (Sierra et al., 2010). Thus, to assess the effects of the tissue culturing on microglial phagocytosis we assessed the Ph index in postnatal day 7 (PND7) and PND14 mice (**Figure 7H, I**) the ages when organotypic cultures were made (PND7) and were used for experiments (PND14= PND7+7 days in vitro (DIV)). The Ph index was higher in the postnatal DG in vivo (60-70%; **Figure 7I**) at both ages comparing to the control organotypic slices. These data are evidence of changes induced by culturing the tissue. In summary, these results show that NMDA treatment increased apoptotic cell numbers in the DG and microglia responded increasing its Ph capacity proportionally, thus maintaining the apoptosis-microglial phagocytosis coupling.

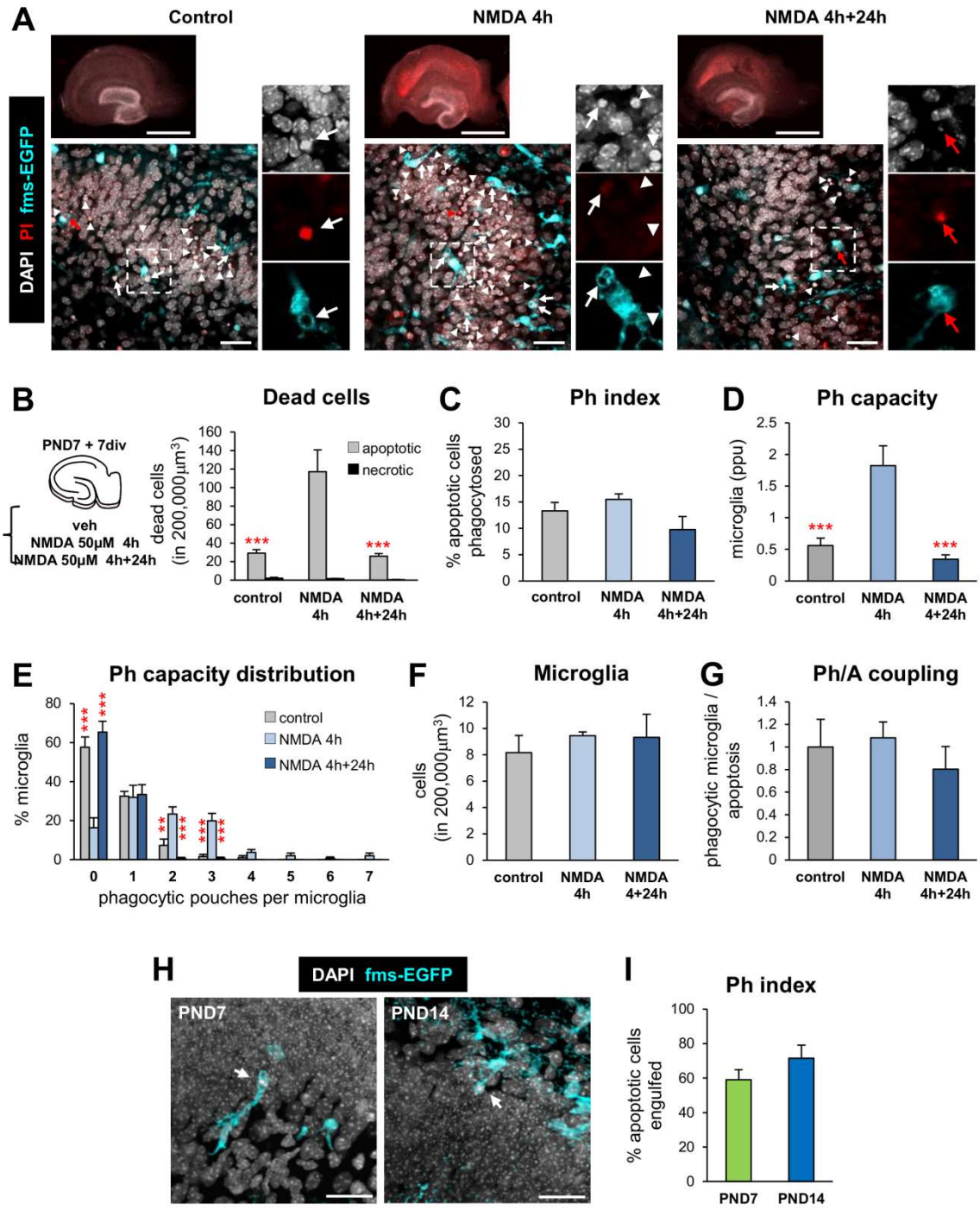

Figure 7. Microglial phagocytosis is coupled to apoptosis during in vitro excitotoxicity. (**A**) Representative epifluorescence (whole hippocampus view in the upper panels) and confocal (remaining panels) images of the DG in hippocampal organotypic cultures treated with media (control; n=6), media with NMDA (50µM) for 4h (NMDA 4h; n=3), or media with NMDA 4h and fresh media for another 24h (NMDA 4h+24h; n=3). Normal or apoptotic (pyknotic/karyorrhectic) nuclear morphology was visualized with DAPI (white), microglia by the transgenic expression of fms-EGFP (cyan) and membrane permeability (characteristic of necrotic cells) by propidium iodide (PI, red). High magnification inserts show a phagocytosed secondary apoptotic cell (pyknotic, PI^+; left panel, arrow); primary apoptotic cells (pyknotic, PI^-), phagocytosed or not (arrow and arrow heads, respectively, central panel); and phagocytosed necrotic (non-pyknotic, PI^+; red arrow, right panel). (**B**) Number of dead apoptotic

(primary and secondary together) and necrotic cells in 200,000µm^3 of the DG in organotypic slices treated with NMDA. (**C**) Ph index in organotypic slices (% of apoptotic cells phagocytosed) treated with NMDA. (**D**) Weighted Ph capacity of microglia (in parts per unit, ppu). (**E**) Histogram showing the Ph capacity of microglia (in % of cells). (**F**) Number of microglial cells in 200,000µm^3 of the DG. (**G**) Ph/A coupling (in fold-change) in organotypic slices treated with NMDA. (**H**) Representative confocal z-stack projections of the DG of the hippocampus at postnatal day 7 (PND7) and PND14 of fms-EGFP mice. Arrows show phagocytosed apoptotic cells. (**I**) Ph index in the DG at PND7 and 14 (in % of apoptotic cells; n=3-4 per group). Bars represent mean ± SEM. * indicates $p<0.05$, ** indicates $p<0.01$, and *** indicates $p<0.001$ by Holm-Sidak posthoc test (after one-way ANOVA was significant at $p<0.05$) (B-G) or by 1-tail Student´s t-test (I). Only significant effects are shown. Scale bars=1mm (A, upper pannel), 30µm (A, lower pannel), 50µm (H). z=16.8µm (H).

6.1.2. Microglial phagocytosis is coupled to cell apoptosis during acute inflammation in vivo

To further test microglial phagocytosis efficiency in vivo we used the hippocampal DG. Importantly, the baseline of microglial phagocytosis was established in the DG (Sierra et al., 2010). The subgranular zone (SGZ) of the DG is one of the two regions of the brain where neurogenesis is found all throughout adulthood. In physiological conditions a large percentage of the newborn cells undergo apoptosis in the neurogenic cascade (Sierra et al., 2010). This constitutive apoptosis found in the DG allowed us to establish the baseline of microglial phagocytosis and thus, to assess the changes in the efficiency of apoptotic cell phagocytosis under different pathological conditions.

We first investigated whether an exogenous inflammatory challenge known to activate the microglial inflammatory response interfered with microglial phagocytosis in the DG. Importantly, inflammation is another pathological feature of epilepsy (Vezzani et al., 2011). As the orchestrators of the innate immune response in the brain, microglia are the first cells to respond to infectious stimuli (Kettenmann et al., 2011). We induced acute neuroinflammation by peripheral (intraperitoneal, i.p.) administration of bacterial lipopolysaccharides (LPS) (1 mg/kg). LPS stimulates microglia to express proinflammatory cytokines that peak at 3h and return to basal levels by 24h (Sierra et al., 2007). We previously found that at 8h of LPS treatment in 1 month old (mo) mice (**Figure 8A**), the Ph index remained stable (96 ± 2 vs 93 ± 1% of apoptotic cells engulfed in control vs LPS, respectively (Sierra et al., 2010), even though there was a 242% ± 44% increase in apoptotic cells compared to control animals (**Figure 8B**) (Sierra et al., 2010). Microglia responded to the increase in apoptosis by proportionally raising their phagocytic capacity (**Figure 8C**), without increasing their number (**Figure 8D**). As a result, the Ph/A coupling ratio (**Figure 8E**) remained unchanged. Thus, these results indicate that in

the young adult DG the phagocytosis efficiency of microglia was maintained during acute inflammatory challenge.

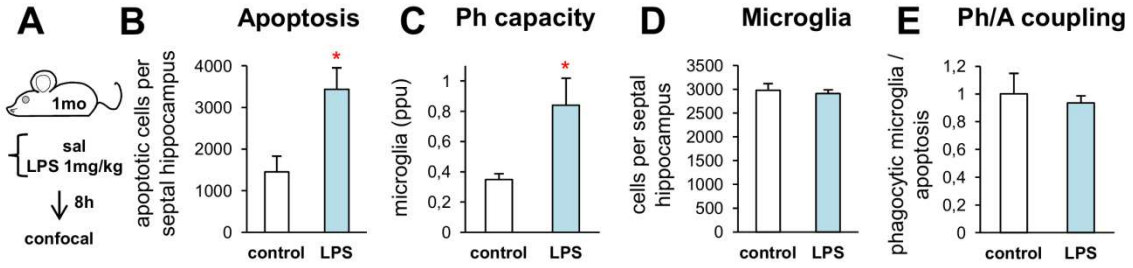

Figure 8. Microglial phagocytosis is coupled to apoptosis during acute inflammation in vivo. (**A**) Experimental design of C57BL/6 fms-EGFP 1mo mice injected systemically with LPS (1mg/kg; n=5) or vehicle (saline; n=4) 8h prior to sacrifice. (**B**) Number of apoptotic (pyknotic/karyorrhectic) cells per septal hippocampus. This graph is reprinted with permission of Elsevier from (Sierra et al., 2010). (**C**) Weighted Ph capacity of microglia (in parts per unit, ppu) in control and LPS mice. (**D**) Number of microglial cells per septal hippocampus in control and LPS mice. (**E**) Ph/A coupling in the 1mo mouse hippocampus (in fold change) during acute inflammatory challenge. Bars represent mean ± SEM. * indicates $p<0.05$ and ** indicates $p<0.01$ by 1-tail Student´s t-test.

6.1.3. Microglial phagocytosis is coupled to cell apoptosis during chronic inflammation in vivo

As microglia managed to maintain their phagocytosis efficiency during acute inflammation, we assessed whether a chronic inflammatory challenge would affect phagocytosis efficiency. In order to induce chronic inflammation we fed young mice during embryonic and postnatal development with a diet deficient in anti-inflammatory omega 3 (Ω3) polyunsaturated fatty acids (Mingam et al., 2008). Today's western diets have excessive amounts of Ω6 polyunsaturated fatty acids and a very low Ω3/Ω6 ratio. This imbalance promotes the pathogenesis of many diseases, including inflammatory and autoimmune diseases, whereas increased levels of Ω3 exert immunosuppressive effects (Simopoulos, 2002). In order to study the effects of chronic inflammation on phagocytosis, we fed mice along gestation and postnatal development until PND21 with either a balanced (Ω3:Ω6, 1:5; Ω3 bal) or deficient (Ω3-Ω6, 1:15; Ω3 def) Ω3 diet (**Figure 9A**). Unlike what we observed in organotypic slices, the morphology of microglial phagocytosis was very similar to that found in physiological conditions in vivo, in which microglia phagocytose apoptotic cells in a "ball and chain" configuration or by en passant branches (**Figure 9A**). In Ω3 deficient mice there was an increase in apoptosis in the DG (**Figure 9A, B**), in accordance with data showing that Ω3 has an anti-apoptotic effect in different pathological conditions (Calandria et al., 2009; Sinha et al., 2009).

Interestingly, the Ph index remained unaltered in Ω3 deficient mice compared to mice fed with an Ω3 balanced diet (**Figure 9C**). The increase in apoptosis was matched by a partial increase in the Ph capacity and an increase in the number of microglial cells (**Figure 9D-F**), ultimately resulting in the maintenance of the Ph/A coupling (**Figure 9G**). Thus, both after excitotoxic challenge in vitro and acute and chronic inflammatory challenge in vivo, both pathologies concurring in epilepsy, microglial phagocytosis remained tightly coupled to apoptosis.

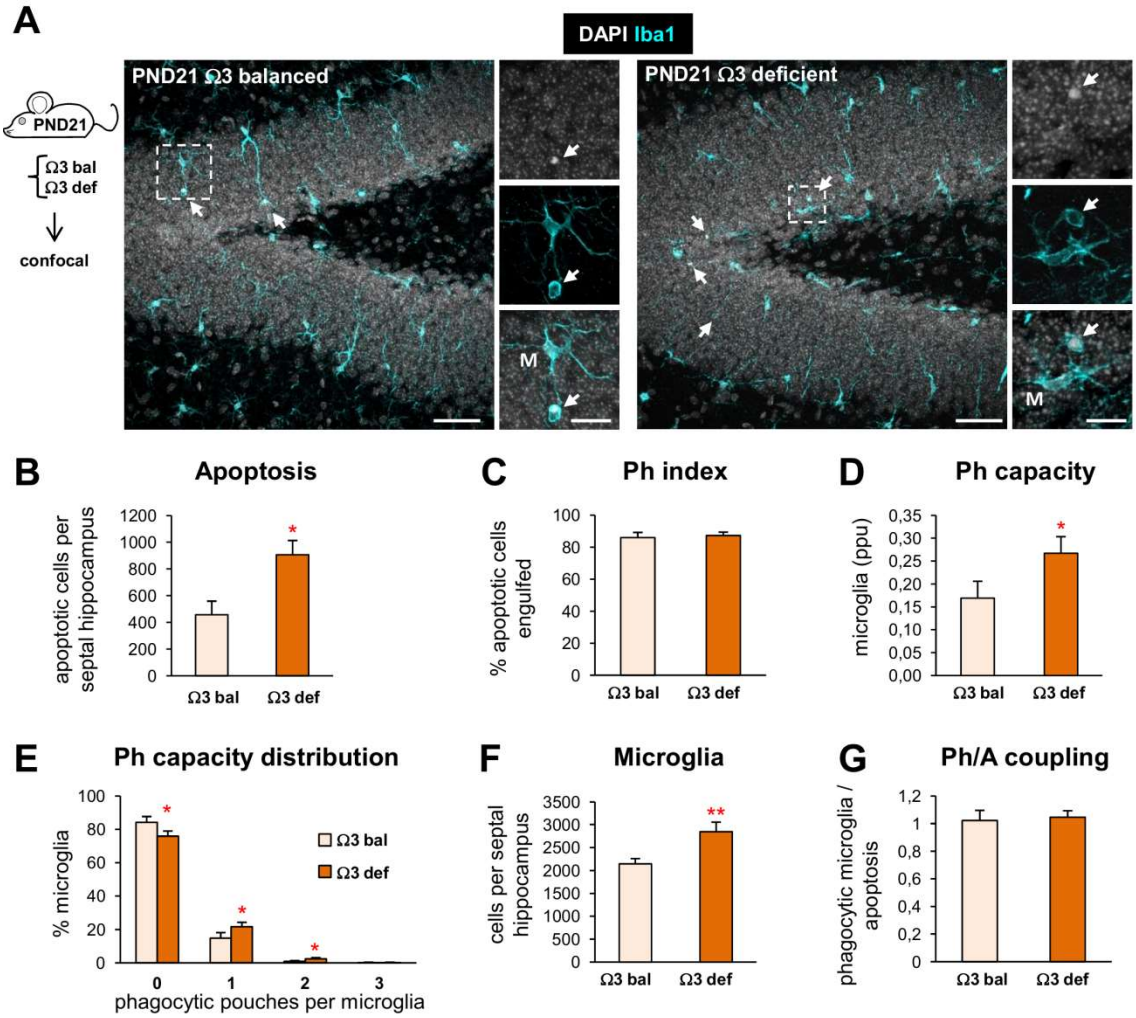

Figure 9. Microglial phagocytosis is coupled to apoptosis during chronic inflammation in vivo. (**A**) Experimental design and representative confocal z-stacks of the DG of PND21 Swiss mice fed during gestation and lactation until PND21 with a diet balanced (Ω3 bal; n=7) or deficient (Ω3 def; n=7) in Ω3 polyunsaturated fatty acids. Microglia were labeled with ionized calcium-binding adapter molecule 1 (Iba1, cyan) and apoptotic nuclei were detected by pyknosis/karyorrhexis (white, DAPI). Arrows point to apoptotic cells engulfed by microglia (M). Scale bars=50µm; z=22.5µm. (**B**) Number of apoptotic (pyknotic/karyorrhectic) cells per septal hippocampus in mice fed with Ω3 balanced and deficient diets. (**C**) Ph index in the PND21 hippocampus (in % of apoptotic cells) in mice fed with Ω3 balanced and deficient diets. (**D**) Weighted Ph capacity of microglia (in ppu) in PND21 mice. (**E**) Histogram showing the Ph capacity distribution of microglia (in % of cells) in PND21 mice. (**F**) Total number of microglial cells

(Iba1^{+}) per septal hippocampus in PND21 mice. (**G**) Ph/A coupling in PND21 mice. Bars represent mean ± SEM. * indicates p<0.05 and ** indicates p<0.01 by 1-tail Student´s t-test.

6.2. MICROGLIAL PHAGOCYTOSIS IMPAIRMENT IN VIVO IN A PHARMACOLOGICAL MODEL OF EPILEPSY: MESIAL TEMPORAL LOBE EPILEPSY (MTLE)

6.2.1. Acute impairment of microglial phagocytosis following seizures in vivo

6.2.1.1. *Intrahippocampal injection of KA causes mesial temporal lobe epilepsy (MTLE) and an increase in dead cells in the hippocampus in vivo*

The above results suggest that microglia have a substantial reservoir for phagocytosis, as they could reach their maximum Ph capacity by recruiting up to 100% microglia to be phagocytic, by inducing each microglia to phagocytose more apoptotic cells, and/or by increasing the total number of microglia. To test this potential, we challenged microglia in an in vivo model of mesial temporal lobe epilepsy (MTLE), in which seizures concur with excitotoxicity and inflammation. MTLE is one of the best-characterized types of epilepsy (Tatum, 2012) and a type of focal epilepsy in which seizures originate in the hippocampus and related structures (Sharma et al., 2007). To model MTLE, we injected the glutamate analog kainic acid (KA) (Bouilleret et al., 1999). KA induces seizures via activation of two subtypes of ionotropic glutamate receptors: kainate receptors and AMPA receptors (as a partial agonist) (Fritsch et al., 2014) located presynaptically in GABAergic terminals (Cossart et al., 2001) and postsinaptically in glutamatergic neurons (Lerma, 2003). To mimick MTLE we injected KA (20mM, 50nL) intrahippocampally (**Figure 10 and Figure R11**). Intrahippocampal administration of KA induced an episode of prolonged continuous seizure activity (status epilepticus) that lasted 4-6h. All animals reached level 3-4 class seizures according to the Racine scale (Racine, 1972), and the development of spontaneous recurrent seizures was monitored for up to 7 weeks (**Figure 10A**) (Sierra et al., 2015). Apoptosis was most consistently induced in the septal hippocampus (spanning from -1mm to -2.5mm in the anteroposterior axis, from Bregma; data not shown), and thus quantifications were restricted to that area. We quantified the absolute number of apoptotic cells (determined by pyknosis/karyorrhexis and/or activated caspase 3 staining) along a time course from 6h post-injection (6hpi) to 7 days post-injection (dpi) (**Figure 10B, C**). In the DG apoptotic cells were mainly located in the SGZ at 1dpi suggesting that the cells in the neurogenic cascade were the most affected by the KA triggered seizures at that time point. The number of apoptotic cells significantly increased

starting from 1dpi and up to 7dpi relative to controls (**Figure 10C**). Thus, KA generated seizures increased the number of dead cells mainly in the neurogenic niche of the DG.

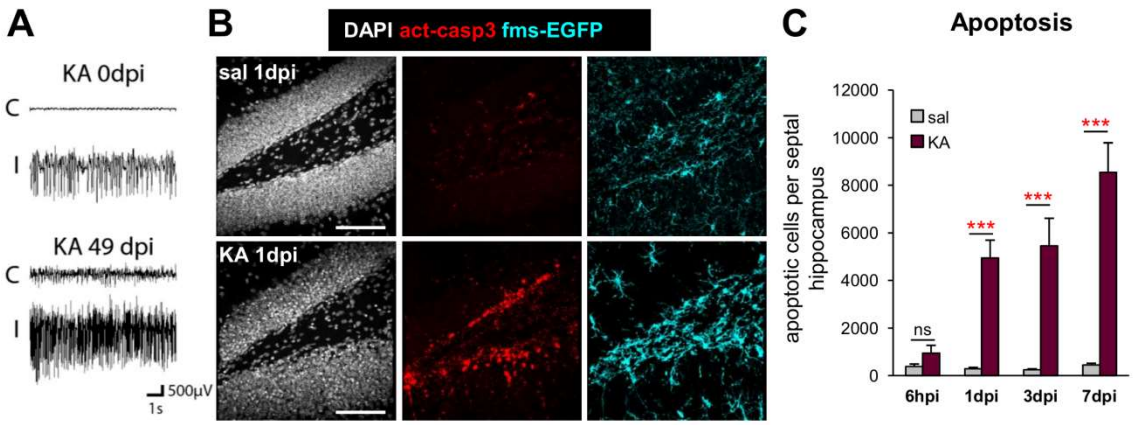

Figure 10. Intrahippocampal injection of KA causes MTLE seizures in vivo and an increase in apoptotic cell numbers in the subgranular zone (SGZ) of the hippocampus. (**A**) Hippocampal electroencephalographic (EEG) recordings of mice injected in the ipsilateral side (I) with KA (50nL, 20mM) during status epilepticus (0 days post-injection, dpi) and during a spontaneous seizure occurring in the chronic phase of MTLE (49dpi). The contralateral hippocampus (C) is shown for comparison purposes. (**B**) Representative confocal z-stacks of saline (sal) and KA (1dpi) hippocampi labeled with DAPI (nuclear morphology, white), activated caspase 3 (act-casp3^{+}, red, for apoptotic cells), and fms-EGFP (cyan, microglia). (**C**) Number of apoptotic cells (pyknotic/karyorrhectic and act-casp3^{+}) in the septal DG (n=3-9 per time point and treatment). Bars represent mean ± SEM. * indicates $p<0.05$, ** indicates $p<0.01$, and *** indicates $p<0.001$ by one-way ANOVA (C, where a significant interaction time x treatment was found) were significant at $p<0.05$. Scale bars=50µm. z=25µm (B).

6.2.1.2. *Microglial phagocytosis is acutely impaired in the hippocampus during MTLE seizures*

As microglial phagocytosis-apoptosis coupling was maintained in phagocytic challenges induced by excitotoxicity and acute and chronic inflammation, both processes concurring in epilepsy, we asked whether the increase in the number of apoptotic cells induced by seizures would also be matched by an increase in phagocytosis. Unexpectedly, we found limited evidence of phagocytosis, with many non-phagocytosed apoptotic cells located very close to microglia, which showed thickened processes (**Figure 11A-C**). In fact, the Ph index significantly dropped at 6hpi and 1dpi (**Figure 11D**). We further analyzed the characteristics of this phagocytosis impairment in the DG. We found a decreased Ph capacity in the KA injected mice at both 6hpi and 1dpi compared to controls, related to a smaller proportion of microglia with phagocytic pouches (**Figure 11E, F**). While no significant changes in total microglial numbers were found (**Figure 11G**), there was a significant decrease in the microglial density in the KA injected mice at 1dpi (**Figure 11H**), which can be attributed to the increase in the DG volume,

which is due to granule cell dispersion (**Figure 11I**), typical of both human and mouse MTLE (Haas and Frotscher, 2010). As a result of the decreased Ph capacity induced by KA, the Ph/A coupling ratio dramatically decreased at both time points (**Figure 11J**). In summary, in contrast to what we found in excitotoxicity and inflammation where the increase in apoptotic cell numbers was matched by a boost in microglial phagocytosis, we found a severe phagocytosis impairment in the KA induced apoptotic challenge as early as 6hpi.

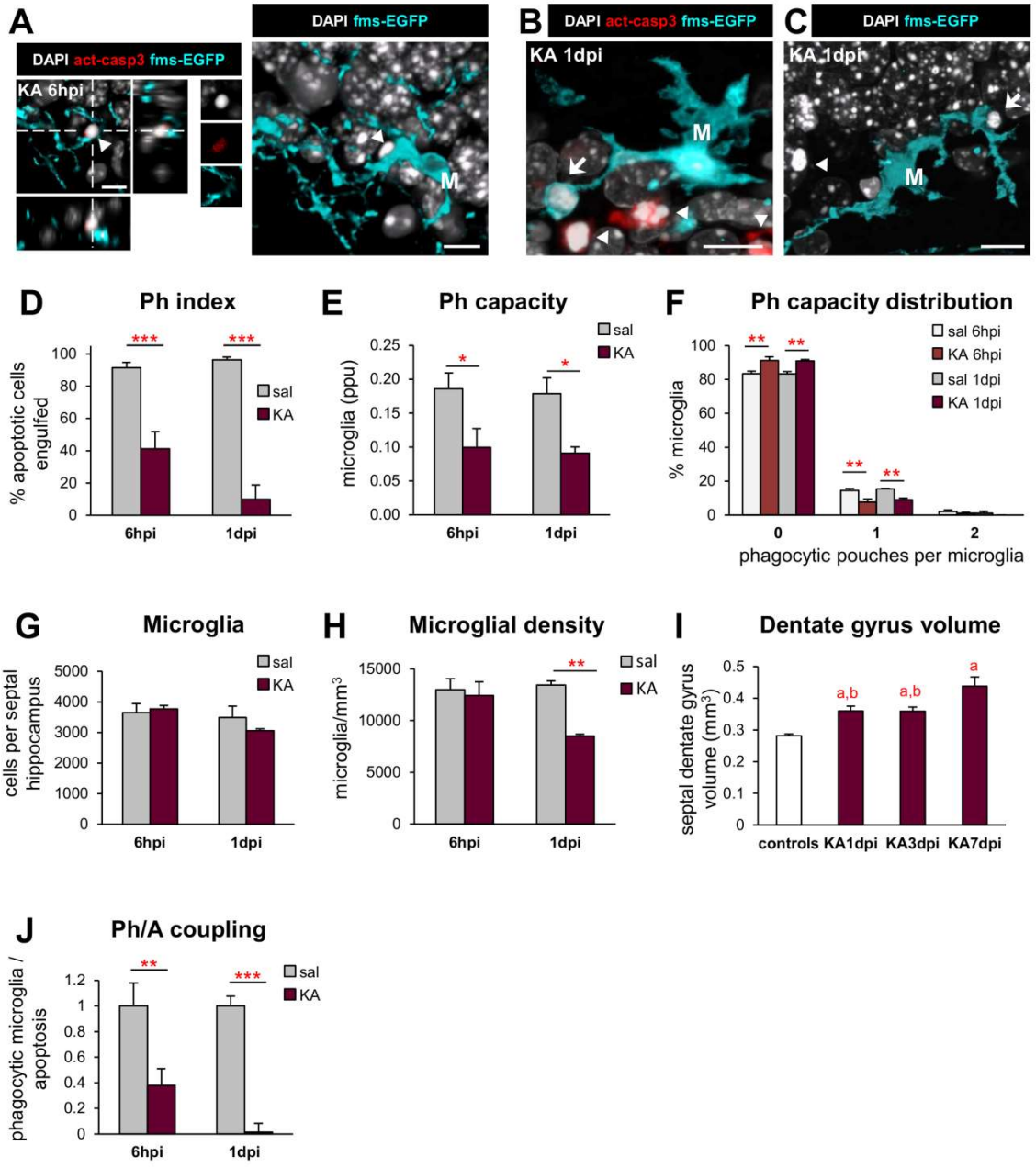

Figure 11. Microglial phagocytosis is acutely impaired in the hippocampus due to MTLE seizures in vivo. (**A**) Representative confocal image of a non-phagocytosed apoptotic (pyknotic and act-casp3^{+}, arrowhead) cell in the SGZ (orthogonal projection, left; and 3D-rendered image, right) in the septal DG of mice treated with KA at 6 hpi. M, microglial cell body. (**B**) Representative 3D-rendered confocal z-stack of apoptotic (pyknotic and act-casp3^{+}) cells, phagocytosed (arrow) or not (arrowheads) in the

septal DG of mice treated with KA at 1dpi. M, microglial cell body. (**C**) Representative 3D-rendered confocal z-stack of apoptotic (pyknotic), non-phagocytosed cells (arrowheads) in the DG of mice treated with KA at 1dpi. The arrow points to a semi-engulfed apoptotic cell. M, microglial cell body. (**D**) Ph index of microglia (in % of apoptotic cells) in the septal DG 6h and 1d after sal/KA. (**E**) Weighted Ph capacity of microglia (in ppu) in the septal DG 6h and 1d after sal/KA. (**F**) Histogram showing the Ph capacity distribution of microglia (in % of cells) in the septal DG 6h and 1d after sal/KA. (**G**) Total number of microglial cells (fms-EGFP^{+}) in the septal DG 6h and 1d after sal/KA. (**H**) Density of microglia (cells/mm^{3}) in saline and KA-injected mice (n=3-5 per group). At 1dpi, KA induced a significant decrease in the density of microglia. (**I**) Volume of the septal dentate gyrus (mm^{3}) in saline and KA-injected mice (n=3-5 per group). The volume occupied by the dentate gyrus was assessed in the septal hippocampus (spanning from -1mm to -2.5mm in the anteroposterior axes, from Bregma) in control animals (injected with saline, pooled from different time points for robustness) or after injection of KA at 1, 3 and 7 dpi (no changes after 6hpi were found). (**J**) Ph/A coupling (in fold change) in the septal DG 6h and 1d after sal/KA. Bars represent mean ± SEM except in K, where they indicate the sum of cells in each distance slot. * indicates p<0.05, ** indicates p<0.01, and *** indicates p<0.001 by Holm-Sidak posthoc test after two-way ANOVA (E-H, J), one-way ANOVA (D, where a significant interaction time x treatment was found) or Dunn´s posthoc test after Kruskal-Wallis (L) were significant at p<0.05. Scale bars=10µm (A-C). z=13.9µm (A), 14.1µm (B), 8.4µm (C).

6.2.1.3. *Microglial phagocytosis impairment is not compensated by other cell types in the hippocampus*

Because seizures impaired microglial phagocytosis we assessed whether other resident cells endowed with phagocytic potential could compensate the impairment. This could be achieved by the recruitment of astrocytes (Magnus et al., 2002) or neuroblasts (Lu et al., 2011), which do not normally phagocytose hippocampal apoptotic cells in resting conditions (Sierra et al., 2010)**.** To test this hypothesis, we used transgenic mice in which the expression of fluorescent reporters is controlled by cell-type specific promoters, i.e., hGFAP (human glial fibrillary acidic protein, for astrocytes), and POMC (proopiomelanocortin, which in the hippocampus is only expressed in neuroblasts) (Overstreet et al., 2004). We found that both cell types were engaged in phagocytosis after 1dpi of KA, but nonetheless, they only engulfed a small proportion of the apoptotic cells compared to microglia (**Figure 12**). Therefore, even at 1dpi after KA when microglial phagocytosis of apoptotic cells accounted only for 10% of the apoptotic cells, microglia remained the most determinant phagocyte in the hippocampus.

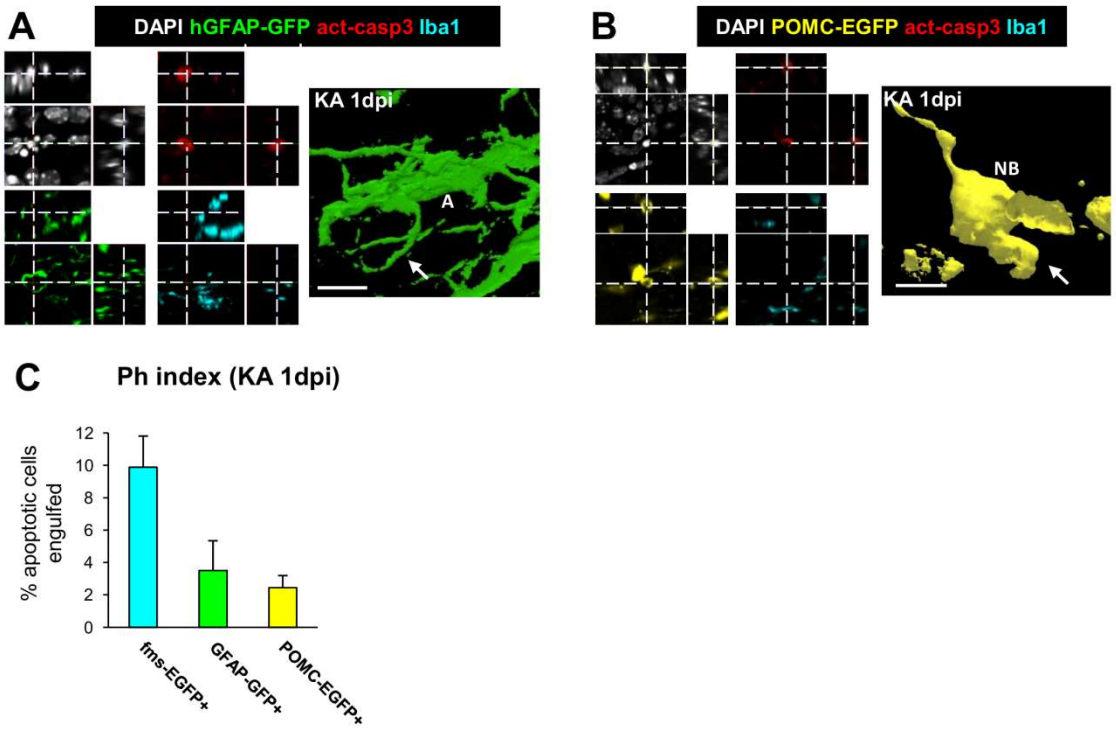

Figure 12. Microglial phagocytosis impairment is not compensated by other cell types. (**A**) Representative orthogonal projection (upper panel) and 3D-rendered image (lower panel) of a confocal z-stack showing an apoptotic cell (pyknotic, white, DAPI) expressing activated-caspase 3 (act-casp3$^+$, red) phagocytosed by a hGFAP$^+$ astrocyte (A, green), nearby a microglial cell (Iba1$^+$, cyan). Arrow, phagocytic pouch. (**B**) Representative orthogonal projection (upper panel) and 3D-rendered image (lower panel) of a confocal z-stack showing an apoptotic cell (pyknotic, white, DAPI) expressing activated-caspase 3 (act-casp3$^+$, red) phagocytosed by a POMC$^+$ neuroblast (NB, yellow), nearby a microglial cell (Iba1$^+$, cyan). Arrow, phagocytic pouch. (**C**) Ph index of microglia, astrocytes and neuroblasts (in %) at 1dpi after the injection of KA (n=3-4 per group). At 1dpi, the impaired microglia remained the major phagocytic cell in the hippocampus, as it engulfed a higher percentage of apoptotic cells. Bars represent mean ± SEM. Scale bars=10µm. z=11.9µm.

6.2.1.4. *Microglial phagocytosis is acutely impaired in the hippocampus and in the cortex during MTLE seizures*

To determine whether microglial phagocytosis was affected in areas other than the hippocampal DG we assessed the phagocytosis efficiency in nearby regions. Besides affecting the hippocampus, KA-induced MTLE also affects other regions of the brain like the ipsilateral cortex, which also develops seizures as early as 4hpi (Sierra et al., 2015). Accordingly, we found a consistently low Ph index in the cornu ammonis 1 (CA1) and CA3 regions of the hippocampus, as well as in the adjacent somatosensory cortex at 1dpi after KA (**Figure 13**). In these regions, apoptosis was undetectable in control conditions, and thus the basal Ph index could not be estimated. Therefore, the microglial phagocytosis impairment surpassed the limits of the DG and hippocampus during MTLE.

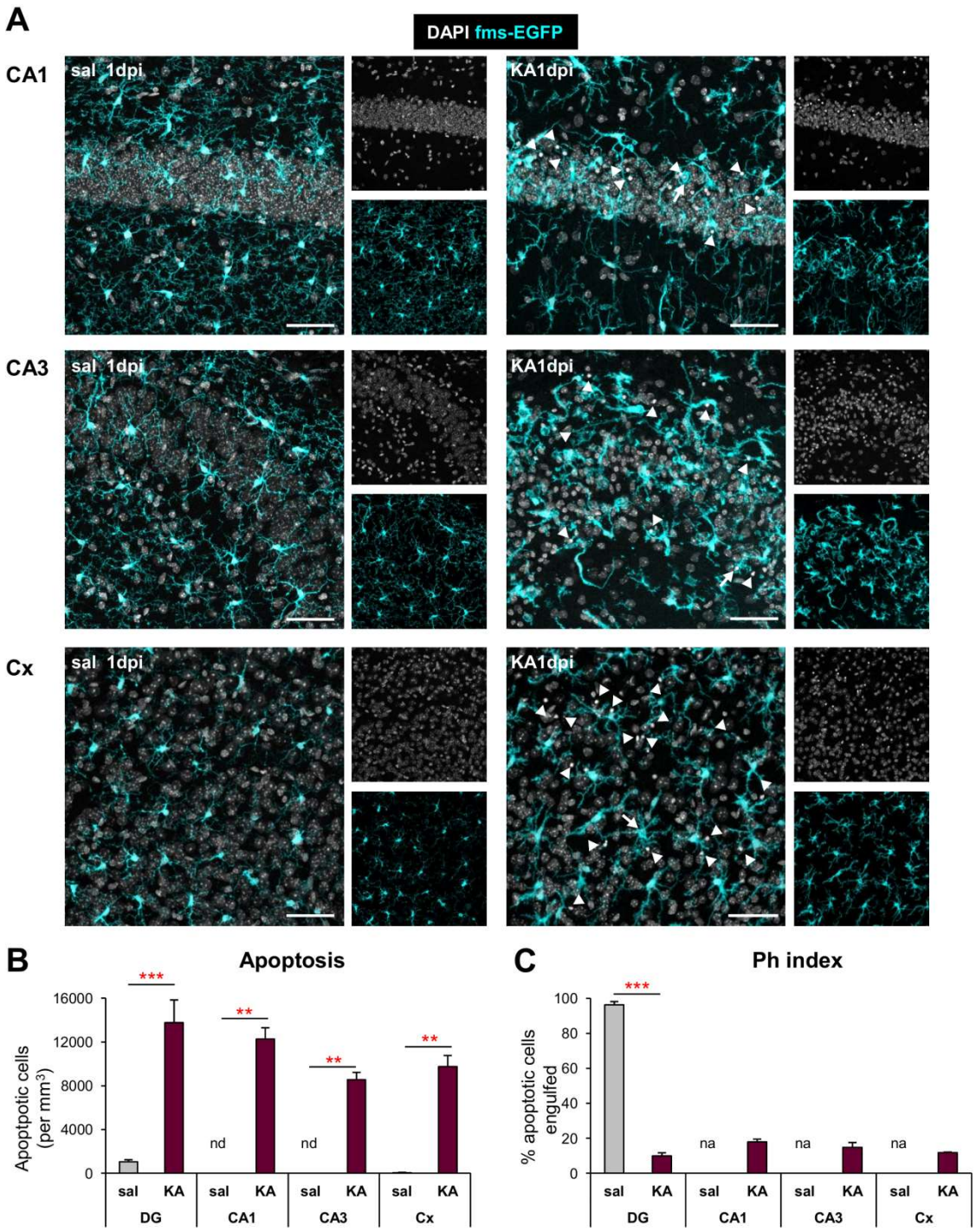

Figure 13. Microglial phagocytosis is acutely impaired in hippocampal CA and in the somatosensory cortex due to MTLE seizures in vivo. (**A**) Representative confocal z-stack projections of the CA1 and CA3 regions of the hippocampus, and cortex (Cx) of 2mo fms-EGFP mice injected with saline (left panels) or KA (right panels) at 1dpi. Apoptotic cells (pyknotic, white, DAPI; arrowheads) are largely absent in control conditions but present in KA-treated mice in the three regions. Some apoptotic cells were phagocytosed (arrows) by microglia (fms-EGFP^{+}, cyan) but most were not (arrowheads). (**B**) Density of apoptotic (pyknotic/karyorrhectic and act-casp3+) per mm^{3} (n=3 per region and treatment). (**C**) Ph index (in % of apoptotic cells) in the different brain regions after KA. nd, not detected; na, not applicable. Bars represent mean ± SEM. ** indicates p<0.01, and *** indicates p<0.001 by Student t-test. Scale bars=50µm. z=18.2µm (except in CA1 KA1dpi=20.3µm, CA3 sal 1dpi=17.5µm and Cx KA 1dpi=19.6µm).

6.2.2. Microglial phagocytosis impairment is related to reduced motility

To understand how seizures were affecting microglial behaviour we investigated the potential mechanisms underlying the phagocytosis impairment in the DG during the acute phase of KA induced epilepsy. Such impairment occurred as early as 6hpi, before a significant increase in the number of apoptotic cells and decreased microglial density were detectable at 1dpi (**Figure 10C and Figure 11H**). Interestingly, we observed that in the KA mice many non-phagocytosed apoptotic cells were localized in direct apposition to a microglial process (**Figure 11A-C**). While in control mice the average distance between an apoptotic cell and the closest microglial process was 1.3 ± 0.3 μm, this was increased significantly at 6hpi and 1dpi following KA challenge (**Figure 14A**). In KA-treated mice at 1dpi 25% of non-phagocytosed apoptotic cells were 3-10 μm away, and up to 15% were over 10μm away from a microglial process (**Figure 14B**). These results suggested two potential mechanisms for the phagocytosis impairment: a defect in recognition and phagocytosis initiation (which would result in apoptotic cells apposed to microglia but not phagocytosed); and a defect in microglial surveillance and/or targeting of apoptotic cells (which would result in far-off apoptotic cells).

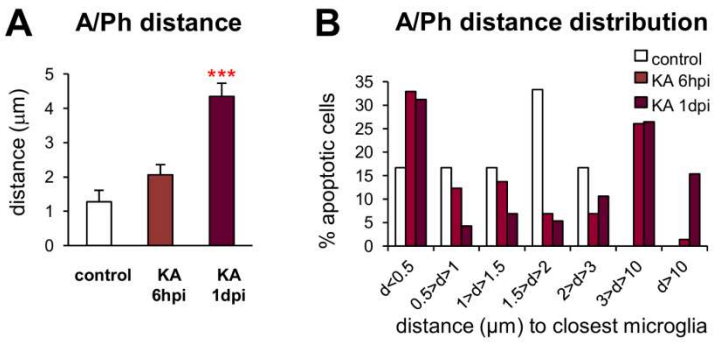

Figure 14. Distance between microglial processes and apoptotic cells increases during MTLE. (**A**) Average distance (d; in μm) between apoptotic nuclei and the closest (perpendicular) microglial process. Apoptotic cells were analyzed from 3 animals per group (n=6, 73, and 189 cells for control, KA 6hpi and KA 1dpi, respectively). (**B**) Histogram showing the distribution of the distance (in μm) of apoptotic cells (in %) to microglial processes in the septal DG 6h and 1d after sal/KA. KA. Bars represent mean ± SEM. * indicates $p<0.05$, ** indicates $p<0.01$, and *** indicates $p<0.001$ by Dunn´s posthoc test after Kruskal-Wallis (A) were significant at $p<0.05$.

We explored the possibility of a defect in microglial surveillance and/or targeting of apoptotic cells and reasoned that the impaired targeting could result from an impaired motility of the microglial processes (**Figure 15**), among other possible mechanisms. To assess the motility of microglial processes we resorted to an ex vivo approach using acute hippocampal slices and 2-photon microscopy. Acute brain slices were obtained from 2 mo CX3CR1-EGFP

mice, in which microglia express the green reporter (Sasmono et al., 2003; Sierra et al., 2007). Acute brain slices were prepared 1dpi after injection of KA or saline and were imaged in a 2-photon microscope (Madore et al., 2013; Tremblay et al., 2010). As predicted, KA induced a 22% decrease in basal microglial motility at 1dpi, mostly due to a decreased retraction of their processes (**Figure 15A-C**), which could lead to a decreased surveillance capacity. To further test the impairment of microglial motility, we imaged the living cerebral cortex overlying the hippocampus, where we had previously detected the phagocytosis impairment (**Figure 12A**). 2 mo CX3CR1-EGFP mice were injected with either KA or sal and at 1dpi the cortex was imaged by 2-photon microscopy. In the living cortex of KA-injected mice, microglia showed a 37% decrease in their basal motility compared to saline-injected mice, which affected both the retraction and protraction (**Figure 15D-F**). Therefore, this reduced motility partially explained the defect in microglial phagocytosis of apoptotic cells observed after seizures.

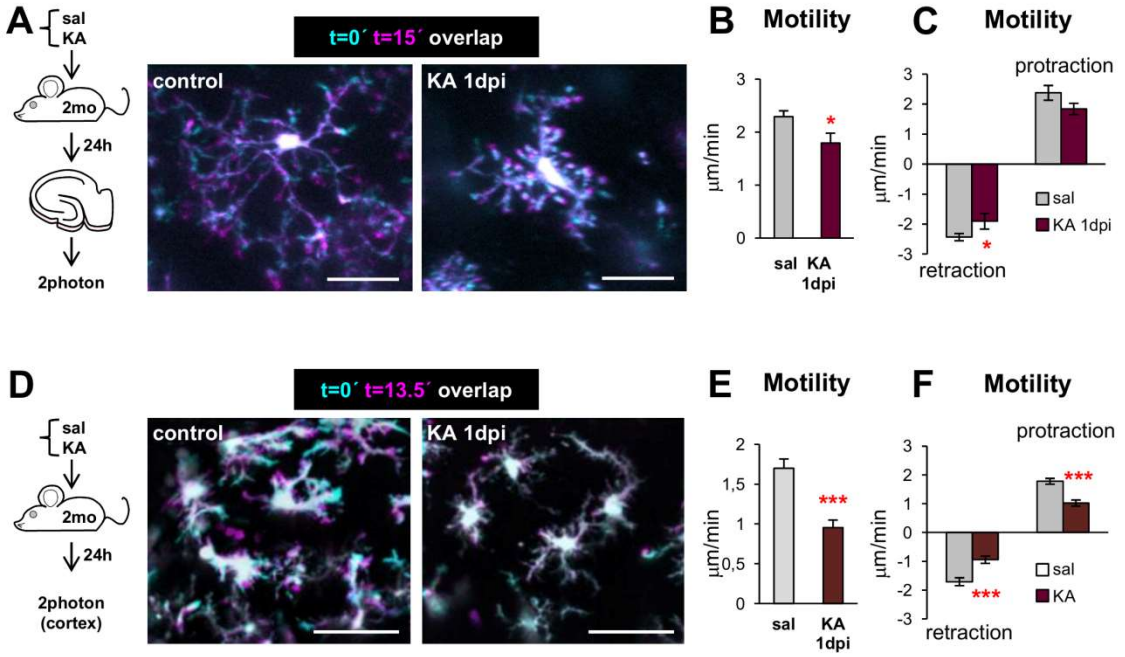

Figure 15. MTLE induced phagocytosis impairment is related to reduced motility. (**A**) Experimental design and representative projections of 2-photon microscopy images of microglia at time 0 (t0) (cyan) and 15min later (magenta) from the DG of acute hippocampal slices from control and KA-injected CX3CR1$^{GFP/+}$ mice (1dpi). (**B**) Motility of microglial processes by 2-photon microscopy in acute slices from CX3CR1$^{GFP/+}$ mice after in vivo injection of KA (1dpi; n=4-5 cells from 3-4 mice per group). (**C**) Retraction and protraction of microglial processes by 2-photon microscopy in acute slices from CX3CR1$^{GFP/+}$ mice after in vivo injection of KA (1dpi). (**D**) Experimental design and representative projections of 2-photon images of microglia at t0 (cyan) and 13.5min (magenta) in the cortex of controls and KA-treated CX3CR1$^{GFP/+}$ mice (1dpi). (**E**) Motility of microglial processes by 2-photon microscopy in the living cortex of CX3CR1$^{GFP/+}$ mice after the injection of KA (1dpi; n=6 cells from 3 mice per group). (**F**) Retraction and protraction of microglial processes by 2-photon microscopy in the living cortex of CX3CR1$^{GFP/+}$ mice after the injection of KA. Bars represent mean ± SEM. * indicates p<0.05, ** indicates p<0.01, and *** indicates p<0.001 by Student´s t-test (A, C, D). Scale bars=20µm (A), 50µm (D). z=50µm (A), 40µm (D).

6.2.3. Microglial phagocytosis impairment is triggered by widespread atp release during seizures

6.2.3.1. *Microglial phagocytosis impairment is not directly mediated by KA on microglia*

KA could be acting directly on microglia to cause the observed phagocytosis impairment. As KA acts on neurons through both KA and AMPA receptors (Lerma, 2003), we assessed whether microglia expressed indeed any glutamate receptor in vivo, a matter under discussion (Beppu et al., 2013; Domercq et al., 2013; Eyo et al., 2014; Fontainhas et al., 2011; Kaindl et al., 2012; Wu and Zhuo, 2008). To assess the expression of these receptors in microglial cells in vivo we used reverse transcription quantitative polymerase chain reaction (RTqPCR) from fluorescence activated cell sorting (FACS)-sorted microglia. We found a residual expression of most ionotropic and metabotropic glutamate receptor subunits, which was unlikely sufficient to form functional receptors (Abiega et al., 2016), in agreement with previous studies that have shown the lack of functional receptors in microglia in acute hippocampal slices (Wu and Zhuo, 2008) or retinal explants (Fontainhas et al., 2011). To further assess if KA was directly affecting microglia we determined the effect of KA in organotypic slices and primary cultures (**Figure 16**). We tested the effect of KA (1mM) for 6h in hippocampal organotypic slices (**Figure 16A-F**), and found that apoptosis had a tendency to decrease that was not significant (**Figure 16B**). The Ph index remained unchanged (**Figure 16C**), while the Ph capacity decreased (**Figure 16D**) and microglial numbers remained stable (**Figure 16E**). Consequently, the Ph/A coupling was maintained in KA treated organotypic hippocampal cultures (**Figure 16F**). Therefore, KA did not directly impair microglial phagocytosis of apoptotic cells, likely because KA did not induce seizures in vitro, at least in short treatments (6h in total). These results are in accordance with studies showing a lack of functional AMPA receptor in resting microglia in acute brain slices (Wu and Zhuo, 2008). Finally, we tested the direct effect of KA on microglia in an in vitro model of phagocytosis, in which primary cultures of microglia derived from PND0 mice were fed with NE-4C, a brain neuroectodermal stem cell line, previously treated with staurosporine to induce apoptosis. There, KA only produced a small but significant reduction in the percentage of phagocytic microglia (**Figure 16G-I**), in accordance with studies reporting that some AMPA and KA receptor subunits are expressed in cultured microglial cells (Hagino et al., 2004; Noda et al., 2000). Therefore, the strong impairment of microglial phagocytosis that we observed in vivo after KA injection was unlikely due to a direct effect of KA on microglia.

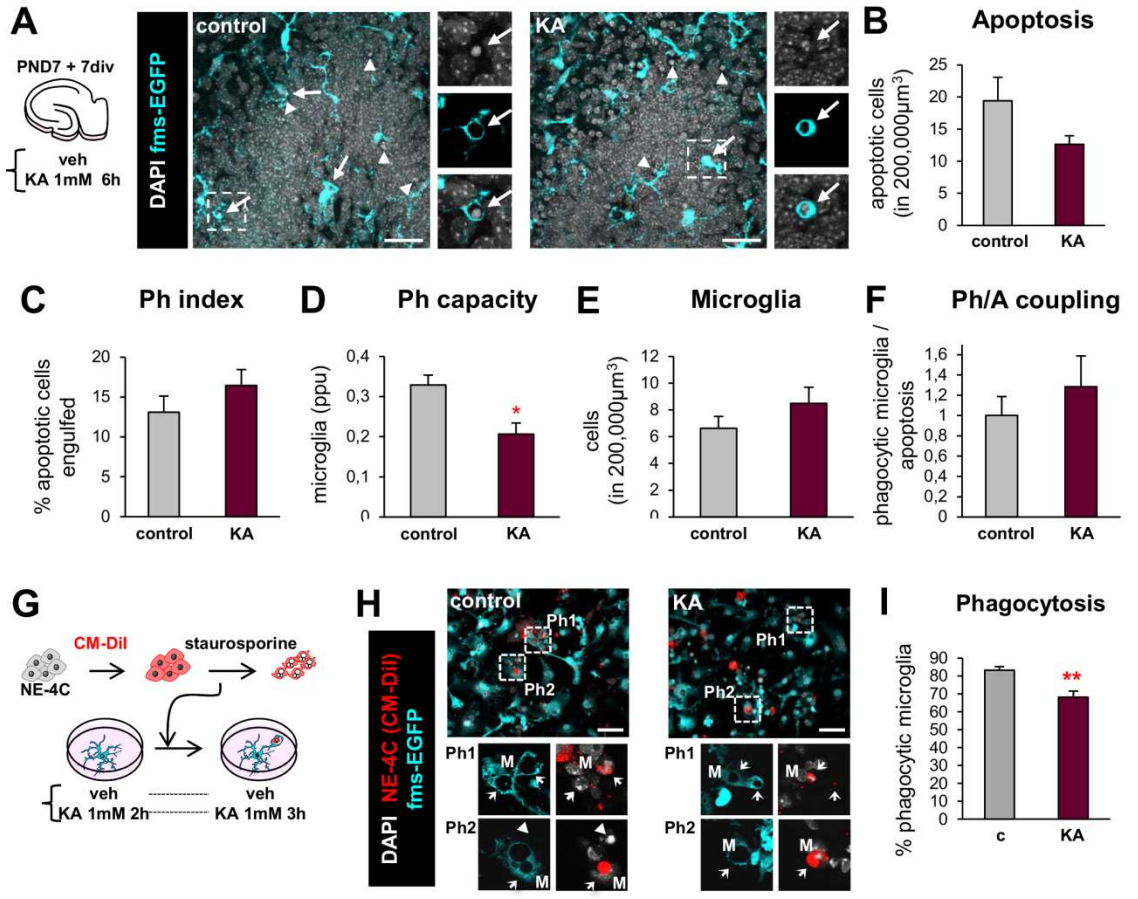

Figure 16. Phagocytosis impairment is not directly mediated by KA on microglia. (**A**) Experimental design and representative projections of confocal z-stacks of organotypic slices from fms-EGFP mice treated with vehicle (control) or KA (1mM) for 6h. Arrowheads, non-phagocytosed pyknotic cells; arrows, phagocytosed pyknotic cells. (**B**) Number of apoptotic cells (pyknotic/karyorrhectic) in the DG of organotypic slices treated with vehicle or KA (n=3 in controls, n=5 in KA). (**C**) Ph index (in % of apoptotic cells) in the DG of organotypic slices treated with vehicle or KA. (**D**) Weighted Ph capacity (in ppu) in the DG of organotypic slices treated with vehicle or KA. (**E**) Microglial density (in cells in 200000µm^3) in the DG of organotypic slices treated with vehicle or KA. (**F**) Ph/A coupling (in fold-change) in the DG of organotypic slices treated with vehicle or KA. (**G**) Experimental design to test the effect of KA on microglial phagocytosis in primary cultures in vitro. Primary microglial cultures were pre-treated with KA (1mM) for 2h prior to adding apoptotic NE-4C cells (treated with 5µM CM-DiI for 25min and 1µM staurosporine for 4h). NE-4C cells were left in culture with microglia for another 3h in the presence or absence of KA. (**H**) Representative confocal z-stacks of fms-EGFP$^+$ microglia phagocytosing apoptotic (pyknotic) CM-DiI$^+$ NE-4C cells. Arrowheads, non-phagocytosed pyknotic cells; arrows, phagocytosed pyknotic CMDiI$^+$ cells. (**I**) Percentage of phagocytic microglia in cultures (n=2 independent experiments in triplicate). Bars represent mean ± SEM. ** indicates p<0.01 by Student´s t-test (I). Scale bars= 30µm (A, H). z=6.3µm (C, G).

6.2.3.2. *Seizures trigger ATP-mediated microglial activation and phagocytosis impairment in vitro*

Because KA was not directly affecting microglia, we searched for an alternative mediator between seizures and microglia. The extracellular adenosine triphosphate (ATP) was

a strong candidate, as it is a well-known microglial chemoattractant (Davalos et al., 2005). Importantly, ATP is released by apoptotic cells to attract microglia (Elliott et al., 2009) but it is also released during seizures, either from neurons or from astrocytes (Dale and Frenguelli, 2009; Santiago et al., 2011). In the extracellular space ATP is rapidly degraded by ectonucleotidases to adenosine diphosphate (ADP) and adenosine monophosphate (AMP) (Zimmermann, 1999). Therefore, direct methods for measuring extracellular ATP such as the luciferin-luciferase assay (Crouch et al., 1993) or extracellular measurements with microelectrode biosensors (Heinrich et al., 2012; Llaudet et al., 2003) are very complicated to perform in a mouse brain in vivo. Thus, we resorted to indirectly determine the action of ATP released during seizures on microglia in vitro. For this purpose we used acute hippocampal slices and organotypic hippocampal slices and treated them with a seizure inducing epileptogenic cocktail**.** The cocktail contained high K^+ which increases the extracellular amount of K^+ inducing cell depolarization (Rutecki et al., 1985), and low Mg^{2+}, a physiological blocker of NMDA channels, which avoids their inactivation and induces seizures (Traub et al., 1994). The cocktail also contained 4-aminopyridine (4-AP), a non-selective blocker of voltage-dependent potassium channels, which acts inhibiting the uptake of extracellular potassium by astrocytes (Luhmann et al., 2000) (**Figure 17 and Figure 18**).

First, we assessed whether the seizures induced by the epileptogenic cocktail were affecting microglia via ATP. Microglia senses ATP via a plethora of receptors such as P2X ionotropic receptors and P2Y metabotropic receptors (Domercq et al., 2013). Thus, we used brilliant blue G (BBG), a broad purinergic P2X receptor antagonist to assess whether the seizure induced release of ATP was directly affecting microglia. For this purpose we used PND20-30 acute hippocampal slices treated with either epileptogenic cocktail in the presence or absence of BBG (**Figure 17**). We recorded field recordings to register seizures and assessed microglial currents by patch-clamp. We observed that the cocktail induced a depolarizing response in microglia with a latency of 11 ± 2min (**Figure 17A-D**). Importantly, this result is in accordance with data showing that after K+ induced depolarization the maximum ATP release is reached in approximately 9min in rat hippocampal slices (Heinrich et al., 2012). Furthermore, we observed that when BBG was applied alongside the cocktail the large inward currents in microglia were partially blocked (**Figure 17A-D**), indicating a cationic current through ATP regulated channels. To assess if BBG was altering the cocktail-induced seizures, we recorded the field potential before and after BBG and found that BBG did not alter the frequency or amplitude of the epileptic discharges (**Figure 17E-G**). Due to the complexity and workload involved, the complete pharmacology to assess the individual effect of all ATP, ADP

and adenosine receptors on microglial phagocytosis will be completed in the future. Overall, this data demonstrated that microglia sense seizures via ATP.

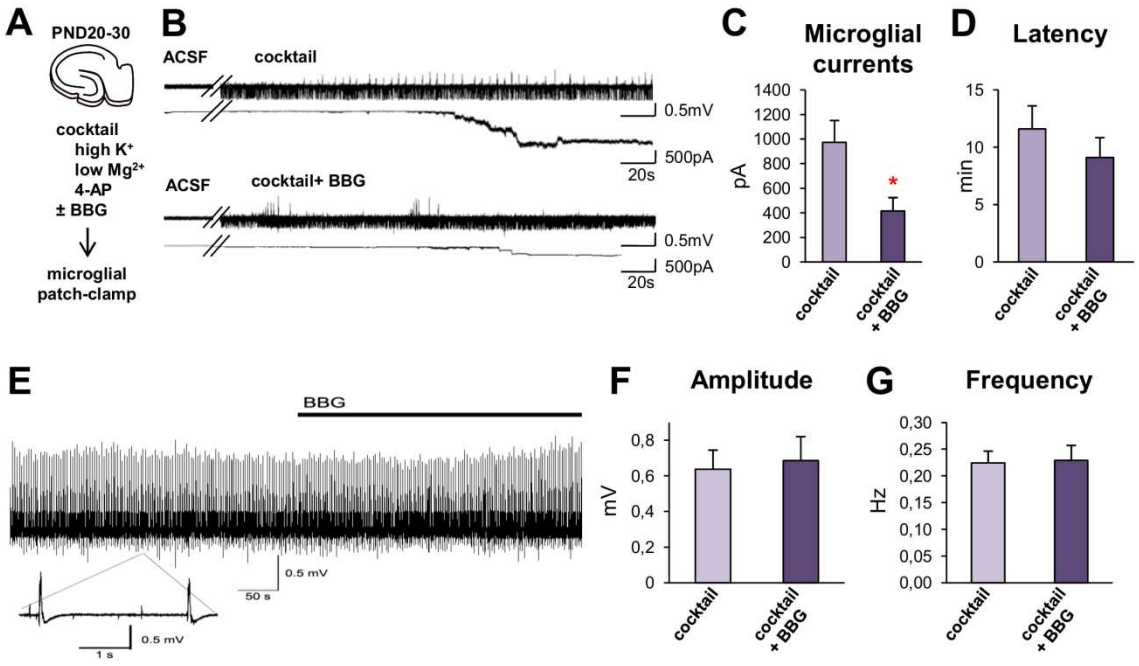

Figure 17. Seizures trigger ATP-mediated microglial activation. (**A**), Experimental design used to induce seizures in acute hippocampal slices with an epileptogenic cocktail that included high K^+, low Mg^{2+} and 4-aminopyridine (4-AP) in ACSF, in the presence or absence of the broad P2X receptor antagonist BBG (5μM). (**B**) Seizure activity was recorded in CA1, where it had higher amplitude than in the DG. Top, extracellular recording (mV) and bottom, simultaneous microglia patch clamp recording (pA) before and after seizure induction in the absence or in the presence of BBG. (**C**) Patch-clamp currents (in pA) induced in microglia by the seizure activity after the epileptogenic cocktail in the absence (control, n=18 cells) or presence of the P2X antagonist BBG (n=11 cells). (**D**) Latency (in minutes) of the currents induced in microglia by the seizure activity. (**E**) Extracellular recording of the seizure activity induced by the epileptogenic cocktail before and after the purinergic antagonist BBG was added in acute hippocampal slices. (**F**) Spike amplitude (in mV) induced by the epileptogenic cocktail. (**G**) Spike frequency (in Hz) induced by the epileptogenic cocktail. Bars represent mean ± SEM. * indicates $p<0.05$, ** indicates $p<0.01$, and *** indicates $p<0.001$ by Student´s t-test (B).

Finally, we determined whether the cocktail induced electrophysiological microglial response would correlate with a phagocytosis impairment. We treated hippocampal organotypic slices with the epileptogenic cocktail for 1h (**Figure 18**) and found that apoptotic cell numbers increased (**Figure 18B**). Similarly to what we observed in MTLE, the Ph index decreased (**Figure 18C**), while both the Ph capacity (**Figure 18D, E**) and microglia (**Figure 18F**) remained unchanged. Consequently, the Ph/A coupling was lost in the cocktail treated slices (**Figure 18G**). Thus, this data showed that seizures affected microglia via ATP, impairing microglial phagocytosis. These results further confirmed our in vivo data indicating that MTLE

seizures per se impaired phagocytosis and pointed towards ATP as the mediator of this phagocytosis impairment.

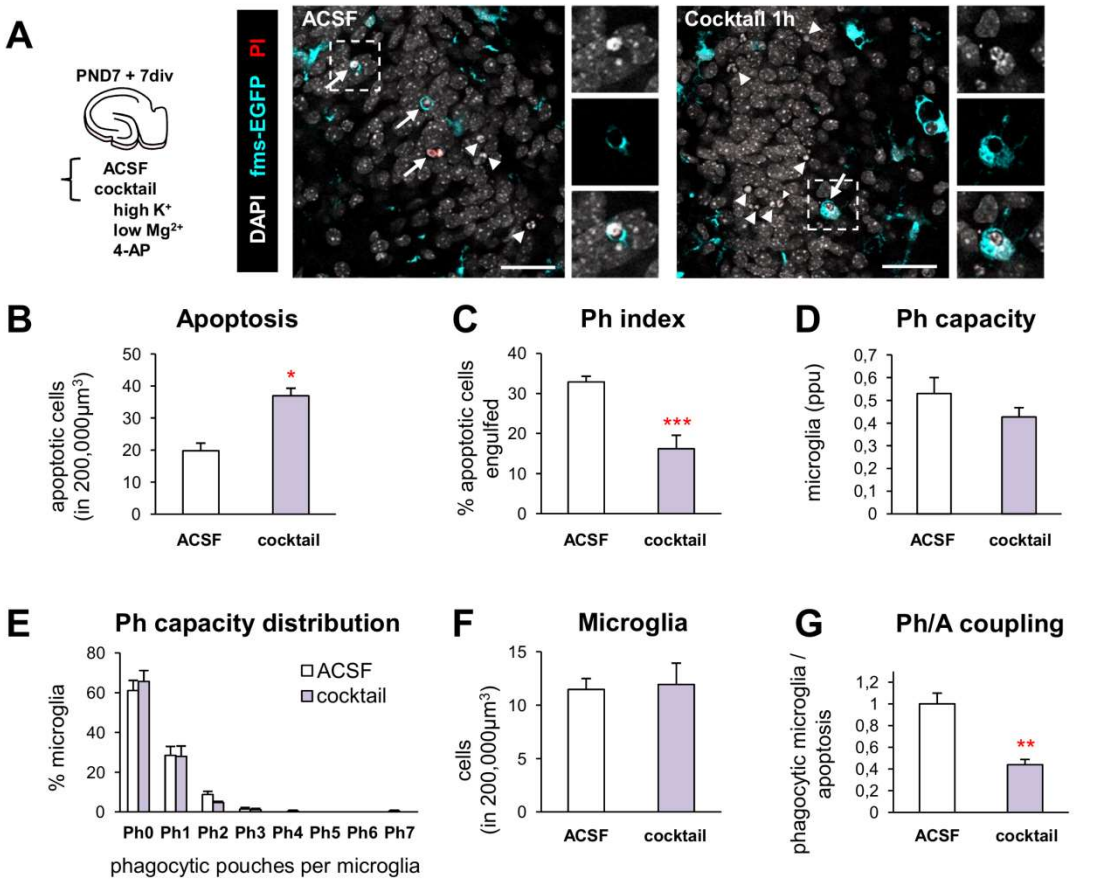

Figure 18. Microglial phagocytosis is acutely impaired in vitro due to seizures induced by a proepileptogenic coktail. (**A**) Experimental design and representative images of the DG of hippocampal organotypic slices treated with ACSF (control, n=3) or an epileptogenic cocktail (high K^+, low Mg^{2+}, 4-AP; n=3) for 1h. Normal or apoptotic (pyknotic/karyorrhectic) nuclear morphology was visualized with DAPI (white), microglia by the transgenic expression of fms-EGFP (cyan), and membrane permeability (characteristic of necrotic cells) by PI (red). High magnification inserts show details of phagocytosed apoptotic cells in the two conditions. Arrows, phagocytosed cells; arrowheads, non-phagocytosed cell. (**B**) Number of dead apoptotic cells in 200000µm^3 of the DG in organotypic slices treated with the epileptogenic cocktail. (**C**) Ph index in organotypic slices (% of apoptotic cells phagocytosed) treated with the epileptogenic cocktail. Note that the Ph index in ACSF-treated slices is higher than in organotypic culture media-treated slices (**Figure 7**). (**D**) Weighted Ph capacity of microglia (in parts per unit, ppu). (**E**) Histogram showing the Ph capacity of microglia (in % of cells). (**F**) Number of microglial cells. (**G**) Ph/A coupling (in fold-change) in organotypic slices treated with the epileptogenic cocktail. Bars represent mean ± SEM. * indicates p<0.05 and ** p<0.01 by Student´s t-test. Scale bars=30µm.

6.2.3.3. *ATP impairs microglial phagocytosis in vitro*

Our results with epileptogenic cocktail treated organotypic slices pointed at seizure released ATP as one of the mechanisms underlying the microglial phagocytosis impairment.

Thus, we hypothesized that a widespread release of ATP by neurons and/or astrocytes during seizures would interfere with the ATP released by apoptotic cells, disrupting ATP microgradients. Indeed, it has been shown that disrupting ATP gradients by saturating the cortical tissue with a high concentration bath of ATP affects microglial motility through a decrease of the extension rate of microglia towards a laser-induced lesion (Davalos et al., 2005). Therefore, we assessed whether an increase in ATP would induce a phagocytosis impairment per se. We tested the hypothesis that large concentrations of ATP would disrupt the local "find-me" gradients in hippocampal organotypic slices and impair phagocytosis (**Figure 19**). Bathing the slices in ATP (1mM) significantly increased the number of apoptotic cells in the slice (**Figure 19A, B**) but the Ph index was substantially decreased (**Figure 19C**), as a result of decreased Ph capacity (**Figure 19D, E**) and decreased microglial density (**Figure 19F**). Therefore, the increase in the number of apoptotic cells was possibly due both to direct neuronal death (Skaper et al., 2010; Wang et al., 2004) and to a block of microglial phagocytosis. We did not observe microglial apoptosis induced by ATP, but instead, microglia migrated towards the edges of the slice, an effect that we attribute to the chemotactic nature of ATP. Ultimately, the Ph/A coupling was lost (**Figure 19G**). Overall, these data indicated that ATP impaired microglial phagocytosis and suggested that ATP was the underlying cause of the early phagocytosis impairment in experimental MTLE.

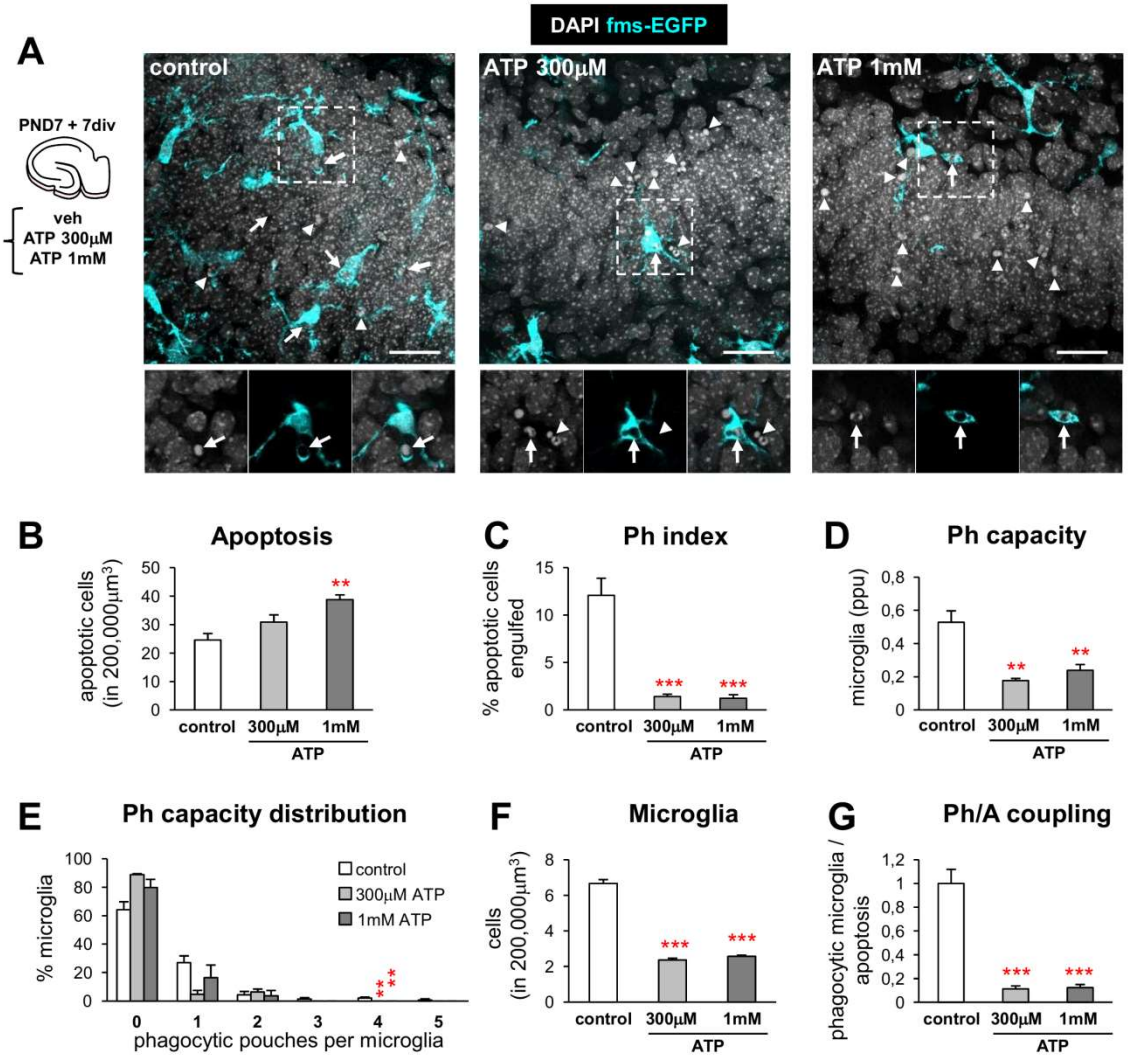

Figure 19. ATP impairs microglial phagocytosis in hippocampal slices in vitro. (**A**) Experimental design and representative projections of confocal z-stacks of fms-EGFP hippocampal organotypic slices treated with vehicle (control) or ATP (300µM and 1mM) for 4h. Normal or apoptotic (pyknotic/karyorrhectic) nuclear morphology was visualized with DAPI (white) and microglia by the transgenic expression of fms-EGFP (cyan). The high magnification inserts show single images of apoptotic cells phagocytosed by microglia (arrows) or not phagocytosed (arrowheads). (**B**) Number of apoptotic cells in a 200000µm^3 volume containing the DG in organotypic slices treated with control medium or ATP (n=3 animals, 12 slices per group). (**C**) Ph index in organotypic slices (in %) treated with control medium or ATP. (**D**) Weighted Ph capacity (in ppu) in organotypic slices treated with control medium or ATP. (**E**) Histogram showing the Ph capacity of microglia distribution (in % of cells) in organotypic slices treated with control medium or ATP. (**F**) Number of microglia in organotypic slices treated with control medium or ATP. (**G**) Ph/A coupling (in fold-change) in organotypic slices treated with control medium or ATP. Bars represent mean ± SEM. * indicates p<0.05, ** indicates p<0.01, and *** indicates p<0.001 by Holm-Sidak posthoc test after one-way ANOVA (B-G) was significant at p<0.05. Scale bars=30µm. z=6.3µm.

6.2.3.4. *ATP impairs microglial phagocytosis in vivo*

After proving that widespread ATP release impaired microglial phagocytosis in vitro we assessed the effect of both ATP and its non-degradable analog ATPγS on microglial phagocytosis at 2hpi in vivo (**Figure 20**). We injected a relatively high dose (100mM) compared to conventional doses used in vitro, as in our organotypic slices experiments, to account for their diffusion through the whole hippocampus (spanning an area of several cubic mm). No signs of cell death or shrinkage to a potential osmosis imbalance were observed at the injection site in spite of the high osmolarity of the injected solutions (phosphate buffered saline (PBS): 286mmol/kg; ATP: 473mmol/kg; ATPγS: 635mmol/kg), likely because of their diffusion over the hippocampal parenchyma. No changes in the volume of the DG were found (data not shown). ATP, but not ATPγS, resulted in increased numbers of apoptotic cells in the DG (**Figure 20A, B**). Both treatments induced a significant reduction of the Ph index (**Figure 20C**) and the Ph capacity (**Figure 20D, E**), without altering the number of microglia (**Figure 20F**), ultimately resulting in a strong reduction of the Ph/A coupling (**Figure 20G**). Nonetheless apoptotic microglia could be occasionally observed in the ATP (126 ± 46 apoptotic microglia per septal hippocampus) but not in the ATPγS- treated DG.

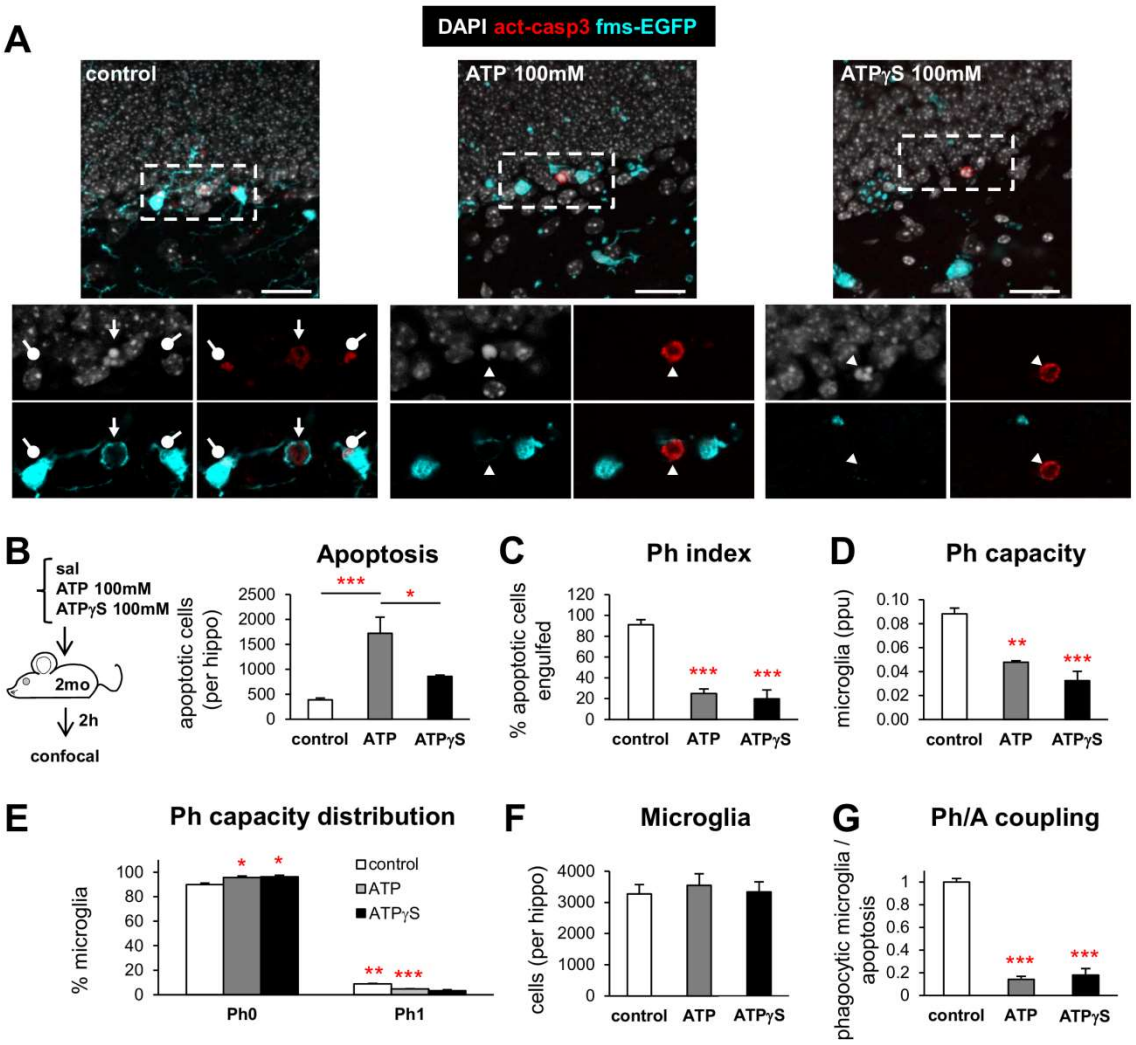

Figure 20. ATP impairs microglial phagocytosis in vivo. (**A**) Representative confocal z-stacks of saline, 100mM ATP and 100mM ATPγS (2hpi) DG labeled with DAPI (nuclear morphology, white), activated caspase 3 (act-casp3$^+$, red, for apoptotic cells), and fms-EGFP (cyan, microglia). Arrow points to a phagocytosed apoptotic cell, whereas arrowheads point to non-phagocytosed apoptotic cells. Activated-caspase 3 puncta within microglia are labeled with a round-ended arrow. (**B**) Experimental design (100mM of ATP and ATPγS, 2h; n=3-4 per group) and number of apoptotic cells (pyknotic/karyorrhectic and act-casp3$^+$) in the septal DG treated with ATP. (**C**) Ph index in the septal DG (in % of apoptotic cells) treated with ATP. (**D**) Weighted Ph capacity of hippocampal microglia (in ppu) in the septal DG treated with ATP. (**E**) Histogram showing the Ph capacity distribution of microglia (in % of cells) in the septal DG treated with ATP. (**F**) Total number of microglial cells (fms-EGFP$^+$) in the septal DG treated with ATP. (**G**) Ph/A coupling (in fold change) in the septal DG treated with ATP. Bars represent mean ± SEM, * indicates $p<0.05$, ** indicates $p<0.01$, and *** indicates $p<0.001$ by Holm-Sidak posthoc test after one-way ANOVA were significant at $p<0.05$. Scale bars=50µm, z= 11.9µm (control, ATP), 9.8µm (ATPγs). Inserts are single plane images of the corresponding confocal z-stacks.

The 2h 100mM ATP treatment provoked a noticeable alteration in microglial morphology with processes retraction throughout the septal hippocampus, largely restricted to the DG (**Figure 21A**). The injected volume was larger than in the KA injections (1µl vs 50nL)

and thus the cortical damage was more apparent while the hippocampus was preserved (**Figure 21A**).

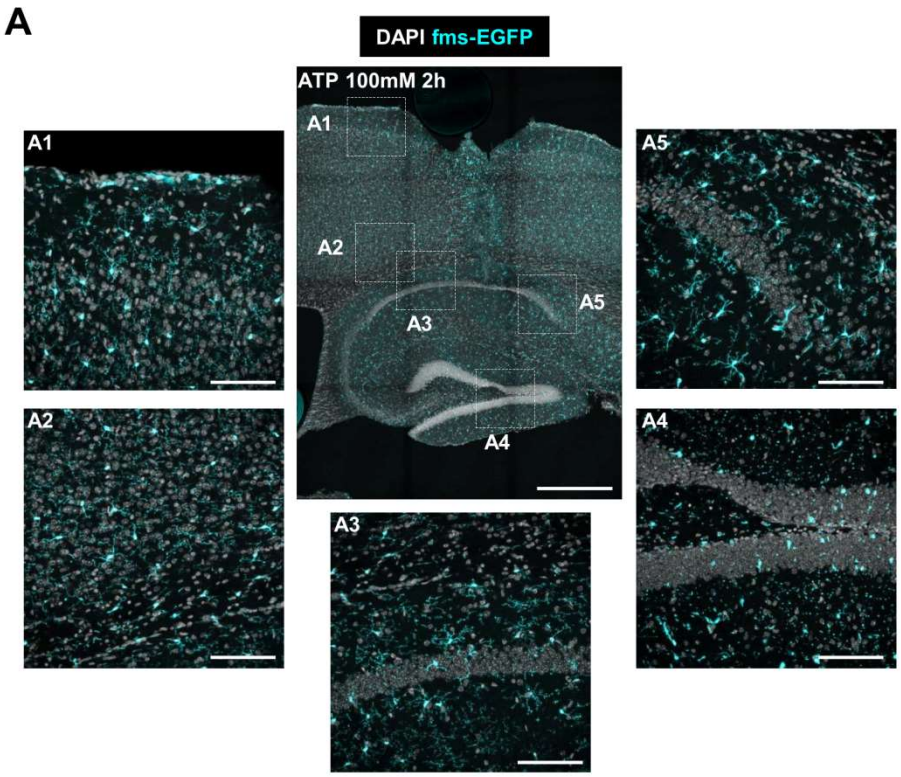

Figure 21. Effect of ATP in vivo. (**A**) Tiled confocal z-stack of the injection site in ATP-injected mice (100mM, 2h). Nuclei are shown with DAPI (white) and microglia is visualized with fms-EGFP (cyan). Inserts show details of the cortex (**A1**, **A2**), CA3 (**A3**), DG (**A4**) and CA1 (**A5**). Scale bars=500µm (A, tiled image), 100µm (A, details). z=25.2µm (A, tiled image), 16.8µm (A, details).

To disregard the possibility that changes in phagocytosis efficiency in ATP-treated mice were the result of reduced microglial viability, we performed a second experiment with 10mM (304mmol/kg) and 100mM ATP. It is also important to note that, as the average clearance time is 1.2-1.5h (Sierra et al., 2010), at 2hpi we could detect only a fraction of the cells that had impaired recognition, as the cells that started phagocytosis before the injection would still be in the process of degrading the apoptotic cell. Thus, we analyzed microglial phagocytosis at a later time point (4hpi) to allow microglia to either die or recover, and to let them further progress in the phagocytosis. In contrast, in this later time point degradation of the injected ATP by ectonucleotidases was more likely. At 4hpi, both 10 and 100mM ATP increased the number of apoptotic cells in the DG (**Figure 22A, B**) and as expected, the phagocytosis impairment indicated by the drop in the Ph index was more obvious in mice treated with the higher dose (**Figure 22C**)**.** Following 100mM ATP, the Ph index dropped and the Ph capacity remained constant, indicating a recovery from the 2hpi likely because of a wash-out or

degradation of the injected ATP (**Figure 22D, E**). No changes in the volume of the DG were found (data not shown). The number of microglia decreased after the ATP 100mM treatment (**Figure 22F**), indicating the expected loss of viability. Microglial apoptosis was observed at 100mM ATP (34 ± 16 apoptotic microglia per septal DG) but not at 10mM ATP. Furthermore, at 10mM ATP the Ph index dropped and the Ph capacity increased but not sufficiently to counteract the increase in apoptosis. Moreover, microglial numbers were not affected (**Figure 22F**). Ultimately, the Ph/A coupling was decreased (**Figure 22G**). Thus, the changes in phagocytosis efficiency in ATP-treated mice were not the result of reduced microglial viability. Overall, these results showed that ATP impaired microglial phagocytosis and pointed at this molecule as a main mechanism underlying MTLE induced phagocytosis impairment.

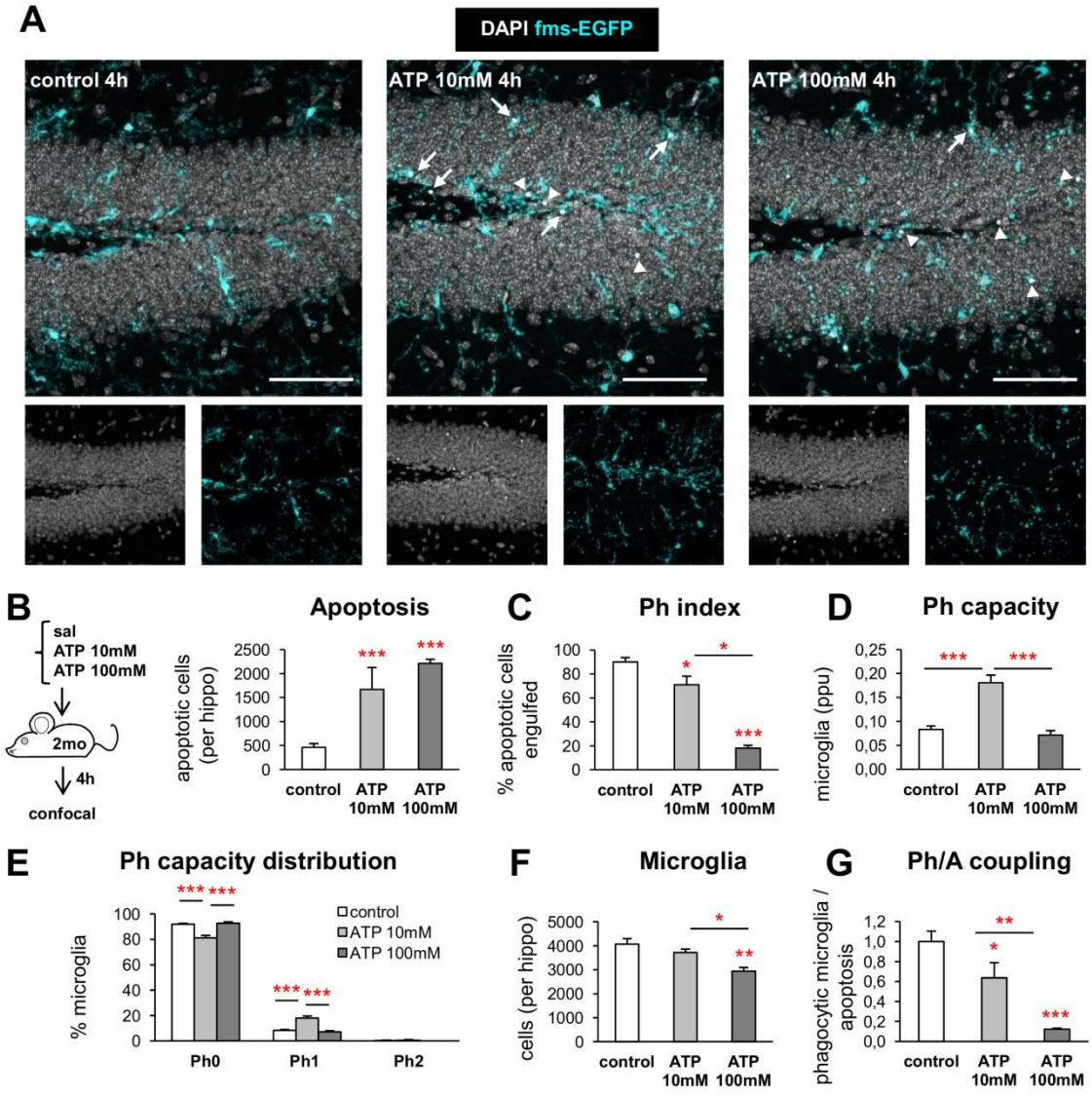

Figure 22. ATP induced changes in phagocytosis efficiency are not the result of reduced microglial viability. (**A**), Representative confocal z-stack of the DG in mice injected with vehicle (control) or ATP (10 or 100mM) at 4hpi. (**B**) Experimental design (10 and 100mM ATP, 4h; n=3-4 per group) and number of apoptotic cells (pyknotic/karyorrhectic and act-casp3^{+}) in the septal DG treated with ATP. (**C**) Ph index in

the septal DG (in % of apoptotic cells) treated with ATP. (**D**) Weighted Ph capacity of hippocampal microglia (in ppu) in the septal DG treated with ATP. (**E**) Histogram showing the Ph capacity distribution of microglia (in % of cells) in the septal DG treated with ATP. (**F**) Total number of microglial cells (fms-EGFP^{+}) in the septal DG treated with ATP. (**G**) Ph/A coupling (in fold change) in the septal DG treated with ATP. Bars represent mean ± SEM, * indicates $p<0.05$, ** indicates $p<0.01$, and *** indicates $p<0.001$ by Holm-Sidak posthoc test after one-way ANOVA were significant at $p<0.05$. Scale bars=500µm (A, tiled image), 100µm (A, details). z=25.2µm (A, tiled image), 16.8µm (A, details).

6.2.3.5. *ATP induced phagocytosis impairment is unrelated to pannexin channel expression on apoptotic cells*

We finally tested the alternative hypothesis that impaired recognition in epileptic mice was due to a defective ATP signaling from apoptotic cells, possibly due to an altered expression of pannexin, a major route through which ATP is released (Chekeni et al., 2010) (**Figure 23**). However, we found a low expression of pannexin throughout the hippocampus and no expression in apoptotic cells, either phagocytosed or not, both in control or KA-treated mice (**Figure 23**). Thus, in the hippocampus apoptotic cells may signal to microglia via mechanisms unrelated to pannexin channels. Overall, the results obtained with ATPγs (100mM, 2h) and ATP (10mM, 4h) in vivo confirmed our in vitro data and demonstrated that disrupting ATP gradients impaired microglial phagocytosis.

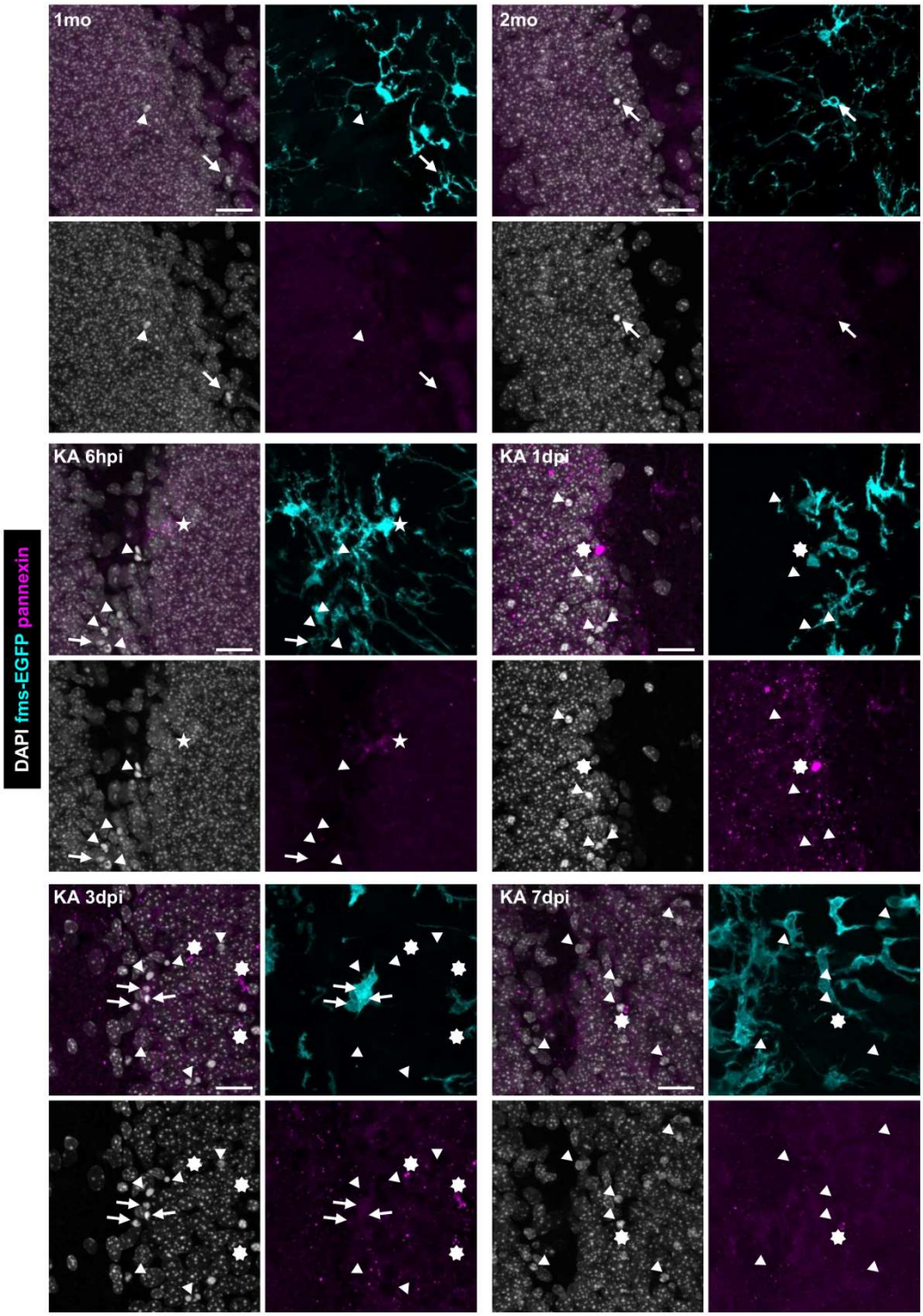

Figure 23. Expression of pannexin in the DG along the KA time course. Representative confocal z-stack projections of the DG in control (1 and 2 mo) and KA-injected mice from 6 hpi to 7 dpi showing the low expression of pannexin (magenta) in granule neurons (white, DAPI) and microglia (cyan, fms-EGFP) in the DG. Pannexin was expressed at low levels by granule neurons in control mice, and appeared in puncta on their surface along the time course after KA was injected (7-point stars), and could occasionally be diffusely expressed in microglia (5-point star at 6 hpi). Pannexin expression was largely absent in apoptotic cells, either phagocytosed (arrows) or non-phagocytosed (arrowheads) in control

and KA mice. We found some cases of non-phagocytosed apoptotic cells labelled with puncta of pannexin at 7 dpi (7-point star at 7 dpi). Scale bars = 20µm. z = 14.7µm.

6.2.4. Seizures lead to the accumulation of non-phagocytosed apoptotic cells in vivo

We then reasoned that the impairment in microglial phagocytosis should result in an accumulation of apoptotic cells. To directly test this hypothesis, we estimated the clearance time, of well-identified cell populations undergoing apoptosis. Our data showed that the majority of apoptotic cells at 1dpi after KA were located in the SGZ (**Figure 10B**), the niche where new neurons are born, in agreement with previous publications showing that seizures lead to apoptosis of newborn cells (Ekdahl et al., 2001; Ekdahl et al., 2003). Thus, we studied the effect of KA-induced seizures on the apoptosis and survival of newborn cells, and focused on their previously identified early (3 days old, do) and late (8do) critical periods of survival (Sierra et al., 2010; Tashiro et al., 2006) (**Figure 24**). In order to study the survival and apoptosis of the 3do and 8do newborn cell populations, a single injection of the thymidine analog bromo-deoxyuridine (BrdU, 150mg/kg) was administered 2 or 7 days prior to the injection of saline or KA, and mice were sacrificed 1 day later (KA 1dpi) (**Figure 24A**). 8do cells were naturally less abundant than 3do cells, reflecting the decreased survival of newborn cells. Unexpectedly, we found no significant changes in the number of 3 and 8do $BrdU^+$ cells, indicating that KA did not affect their survival (**Figure 24B**).

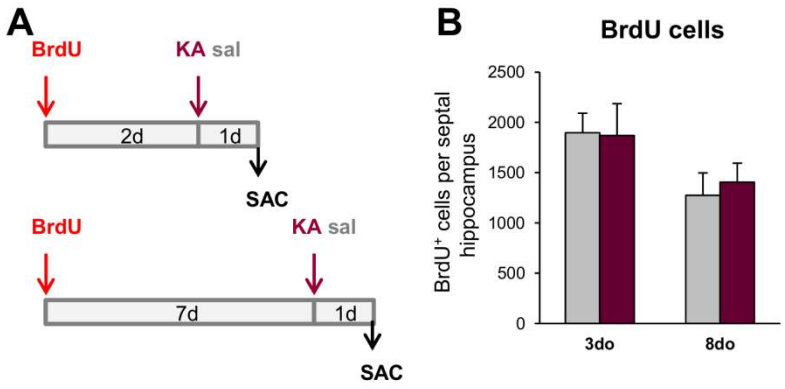

Figure 24. Survival of newborn cells 1dpi after KA. (**A**) Experimental design to test the effect of KA on 3do (upper panel) and 8do (lower panel). (**B**) Number of $BrdU^+$ cells per septal hippocampus in saline or KA injected mice (n=3-5 per group). Bars represent mean ± SEM.

To increase the probability of observing apoptotic $BrdU^+$ cells, we switched to a semi-cumulative BrdU administration paradigm and focused on the early critical period (3d) (**Figure**

24). We administered BrdU every 2h for 6h (**Figure 25A**) 2 days prior to KA injection and quantified the number of live and apoptotic $BrdU^+$ cells 1 day later (KA 1dpi) (**Figure 25B, C**). Again, we found no significant changes in the number of live $BrdU^+$ cells (**Figure 25D**), but a seemingly contradictory significant increase in the number of apoptotic $BrdU^+$ cells (**Figure 25E**). To exclude the possibility that an (undetectable) loss of $BrdU^+$ cells was compensated by their increased proliferation, we analyzed their reentry into the cell cycle by calculating the percentage of $BrdU^+$ cells expressing Ki67. We found no evidence of increased proliferation of the 3do $BrdU^+$ cell population due to KA injection, as the percentage of $BrdU^+$ cells co-labeled with the proliferation marker Ki67 remained unchanged between control and KA-injected mice (**Figure 25F and Figure 25H**). Together, these results demonstrate that the increase of apoptotic 3do $BrdU^+$ cells was not due to de novo apoptosis, but rather, to the accumulation of non-phagocytosed cells that were already undergoing apoptosis prior to the KA injection. Nonetheless, the apoptotic $BrdU^+$ fraction significantly decreased in KA mice (**Figure 25G**), suggesting that apoptosis preferentially targeted cell populations other than the 3do cells in the KA-injected hippocampus. Thus, the rise in apoptotic cells in KA at 1dpi was due both to an accumulation of non-phagocytosed 3do cells and de novo apoptosis of other populations.

For the 3do cells, we reasoned that if KA was not affecting their survival (as there was no change in the number of live $BrdU^+$ cells), the total number of apoptotic $BrdU^+$ cells (present and cleared) should be identical in both control and KA mice, and used this information to estimate the clearance time in KA mice. The number of cleared apoptotic cells, i.e., the number of apoptotic cells no longer present in the tissue and eliminated by phagocytosis, can be estimated using the clearance time formula (see Materials and Methods) and the estimated clearance time in physiological conditions of 1.5h (Sierra et al., 2010). To obtain the total number of apoptotic $BrdU^+$ cells (present and cleared), we estimated the number of cleared $BrdU^+$ apoptotic cells in saline mice and added it to the number of $BrdU^+$ apoptotic cells present in saline mice (**Figure 25I**). To obtain the estimated number of cleared cells in KA mice, we then subtracted the number of $BrdU^+$ apoptotic cells in KA mice from the above amount of total apoptotic $BrdU^+$ cells. This subtraction allowed us to estimate a new clearance time of 6.3h in KA mice (**Figure 25I**), which represents the average time at the population level required for an apoptotic cell to be eliminated by the dysfunctional microglia or the recruited astrocytes or neuroblasts. Furthermore, the decay in the Ph index predicted up to 52% of the variation in the number of apoptotic cells using a linear regression analysis ($p<0.001$) in all saline and KA mice used (6hpi and 1dpi) (**Figure 25J**), providing further evidence that the impairment in phagocytosis was linked to an accumulation of apoptotic cells.

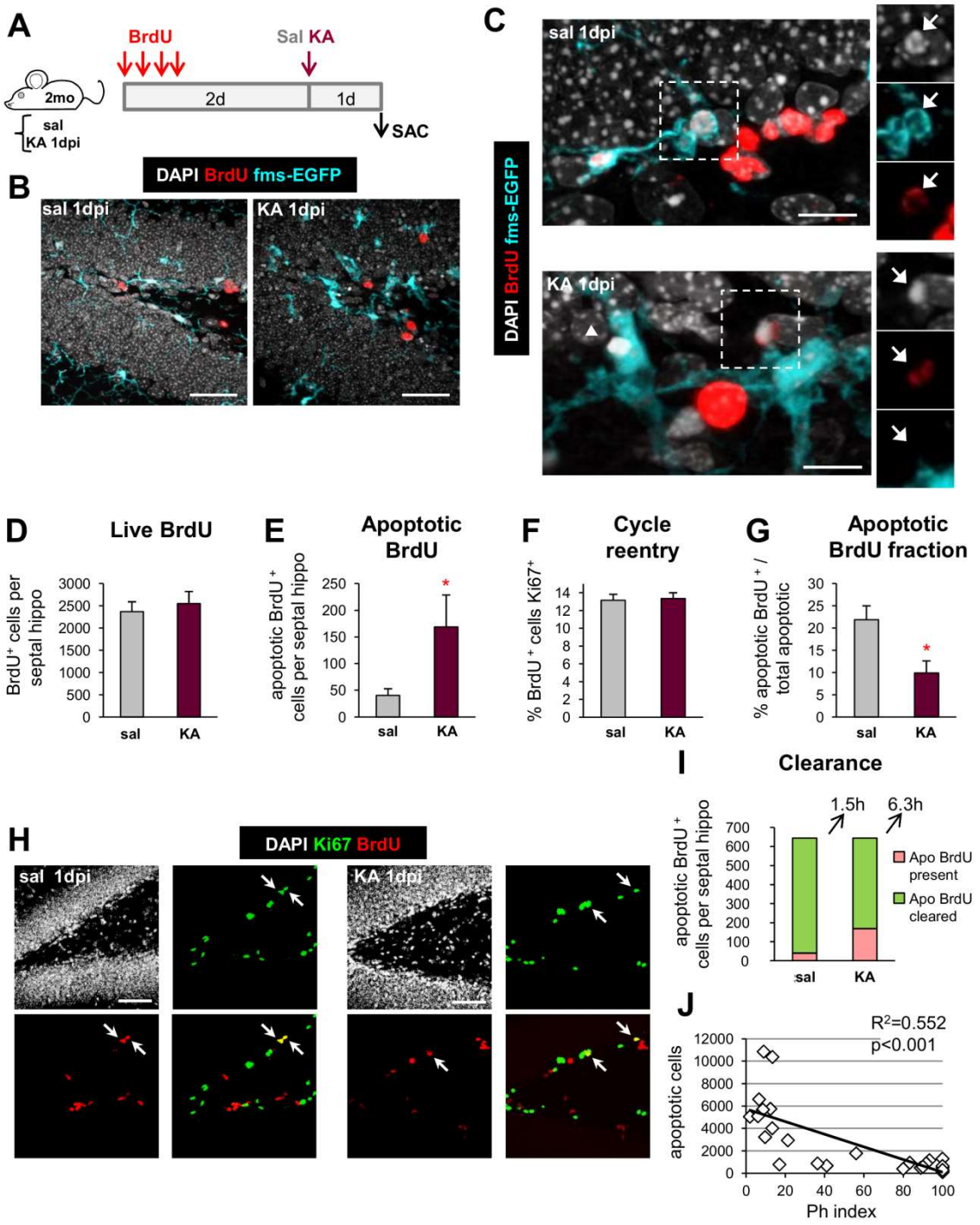

Figure 25. Microglial phagocytosis impairment leads to delayed clearance of apoptotic cells at 1dpi. (**A**) Experimental design used to analyze the survival of 3do cells after the injection of saline (n=7) or KA (n=8) in mice. (**B**) Representative confocal z-stacks of the DG of control and KA-injected mice (1dpi). The damage induced by KA was evidenced by the presence of cells with abnormal nuclear morphology (DAPI, white), and the altered morphology of microglia (fms-EGFP$^+$, cyan). (**C**) Representative confocal images of 3do apoptotic (pyknotic, DAPI, white) cells labeled with BrdU (red; arrows) in the SGZ of the hippocampus of saline and KA-injected mice at 1dpi. In the saline mouse, the BrdU$^+$ apoptotic cell, next to a cluster of BrdU$^+$ cells, was phagocytosed by a terminal branch of a nearby microglia (fms-EGFP, cyan), whose nucleus was also positive for BrdU. In the KA mouse, the apoptotic BrdU$^+$ cell was not phagocytosed by microglia. A nearby apoptotic cell (BrdU$^-$; arrowhead) was partially engulfed by microglia. (**D**) Total number of live 3do BrdU$^+$ cells (non-apoptotic) in the septal hippocampus after

treatment with KA. (**E**) Total number of apoptotic 3do $BrdU^+$ cells in the septal hippocampus after treatment with KA. (**F**) Percentage of 3do $BrdU^+$ cells that reenter cell cycle, assessed by their co-labeling with the proliferation marker Ki67 after treatment with KA. (**G**) Percentage of apoptotic $BrdU^+$ cells over total apoptotic cells in the septal hippocampus. (**H**) Representative projections of confocal z-stacks of the dentate gyrus of the hippocampus showing the co-localization between Ki67 (green) and BrdU (red), which had been injected 3 days before. (**I**) Estimated clearance of apoptotic cells in the septal hippocampus. The total number of apoptotic $BrdU^+$ (from E) present in the tissue was added to the number of estimated apoptotic $BrdU^+$ cells that had been cleared. In saline mice, this number was calculated using the clearance time formula shown in Methods with a clearance time of 1.5h (Sierra et al., 2010). As the total number of cells should be identical in saline and KA mice, the number of cleared apoptotic cells in KA mice was calculated as the difference between the total (in saline) and the number of present apoptotic cells (in KA). From here, we calculated a new clearance time using the same formula as in saline mice, of 6.3h. (**J**) Linear regression analysis of the relationship between apoptosis and phagocytosis (Ph index) in saline and KA-injected mice (6hpi and 1dpi). Bars show mean ± SEM. * indicates $p<0.05$, ** $p<0.01$, and *** $p<0.001$ by Student´s t-test (E, G). Scale bars=50μm (B), 20μm (C), 50μm (H). z=14μm (B), 12.6μm (C, sal), 15.4μm (C, KA), 28.7μm (H, saline), 25.2μm (H, KA).

Finally, we tested the effect of KA on apoptosis in young (2mo) and mature (6mo) animals, in which there are fewer neuroprogenitors and therefore fewer newborn cells (Encinas et al., 2011). Because in the SGZ, the vast majority of apoptotic cells are newborn cells (Sierra et al., 2010), we expected to see a reduction in SGZ apoptotic cells in older mice as a consequence of the reduced neurogenesis. After KA, both young and mature animals reached level 3-4 in the Racine scale and at 1dpi had a similar level and pattern of activation of the hippocampal circuitry (**Figure 26A, B**), as determined by staining with c-fos, an immediate early gene that has been used as an indirect marker of neuronal activation (Dragunow and Faull, 1989). In addition, at 1dpi after KA microglial phagocytosis was similarly impaired in 2 and 6mo mice (**Figure 26E**), but as expected, there were fewer SGZ apoptotic cells in 6mo than in 2mo mice (**Figure 26D**). This difference in apoptosis between young and mature mice could be attributed to the reduced proliferation and neurogenesis found in mature animals, confirming our hypothesis that the rise of apoptotic cells in the SGZ induced by KA was largely due to accumulation of the non-phagocytosed newborn cells that underwent apoptosis in physiological conditions.

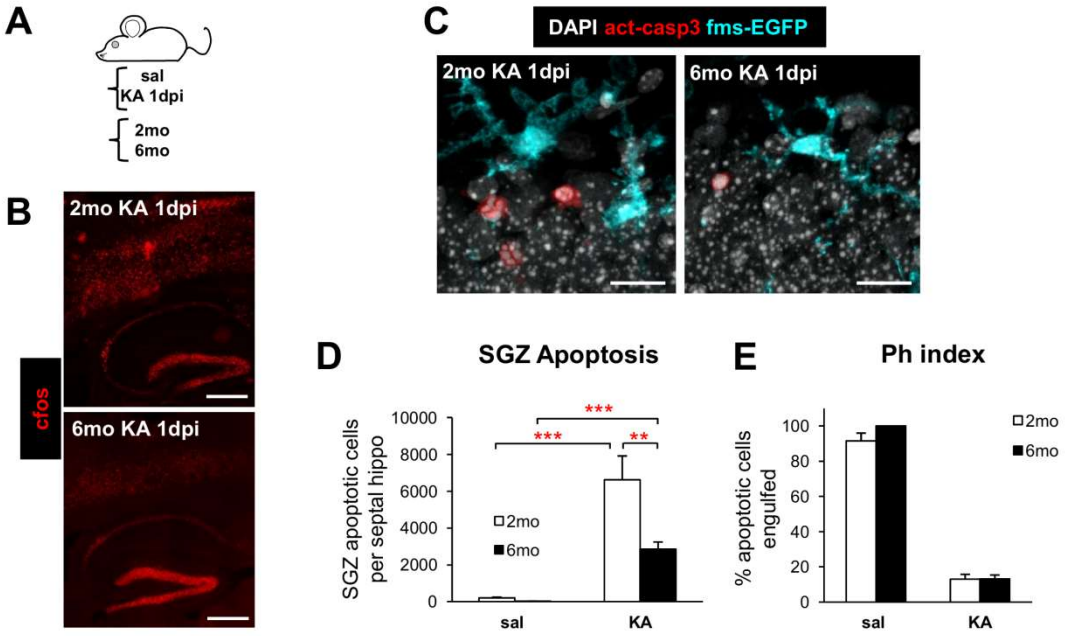

Figure 26. Effect of KA on SGZ apoptosis in young (2mo) and mature (6mo) mice. (**A**) Experimental design used to compare SGZ apoptosis induced by KA at 1dpi in young (2mo) and mature (6mo) mice. (**B**) Representative epifluorescent tiling image of the hippocampus and surrounding cortex of 2 and 6mo mice injected with KA at 1dpi stained with the neuronal activation marker c-fos. The same pattern of expression was found in young and mature mice throughout the DG, CA2, CA1 and the above cortex. (**C**) Representative confocal z-stacks of the apoptotic (pyknotic, white; act-casp3^{+}, red) cells in the SGZ of the hippocampus of 2mo and 6mo mice injected with KA (1dpi). (**D**) Total number of apoptotic cells in the SGZ of 2 and 6mo mice treated with saline or KA (1dpi; n=4-5 per group). (**E**) Ph index in the hippocampus (in % of apoptotic cells) in control and KA-injected mice at 2 and 6mo (n=4-5 per group). Bars show mean ± SEM. * indicates p<0.05, ** p<0.01, and *** p<0.001 by Holm-Sidak posthoc test after one-way ANOVA (M) was significant at p<0.05. Scale bars=500μm (B), 25μm (C). z=25μm (C).

6.2.5. Microglial phagocytosis impairment correlates with inflammation

As phagocytosis of apoptotic cells has previously been shown to be actively anti-inflammatory in vitro (De Simone et al., 2003), we assessed whether the microglial phagocytosis impairment correlated with the development of an inflammatory response. We tested this hypothesis by analyzing the expression of a panel of pro- and anti-inflammatory cytokines by RTqPCR in hippocampal tissue samples and in acutely purified hippocampal microglia along the time course (6hpi to 4 months post-injection (mpi)) (**Figure 27**). At the tissue level, we found that pro-inflammatory interleukin 1 beta (IL-1β) and interleukin 6 (IL-6) as well as anti-inflammatory macrophage inhibitory cytokine 1 (MIC-1) peaked at 1dpi and decreased afterwards up to 4mpi (**Figure 27A**), a pattern that mimicked the development of the phagocytosis impairment over time. In agreement, the average expression of these

cytokines as well as anti-inflammatory transforming growth factor β (TGFβ) correlated with the Ph index over the 4mpi time course (**Figure 27B**). We next compared the expression of these cytokines in FACS-sorted microglia from KA-treated mice. At 1dpi, microglia from KA mice expressed the highest levels of the pro-inflammatory tumor necrosis factor alpha (TNFα) and IL-6 (IL-1β showed a strong tendency but was not significant), as well as macrophage colony stimulating factor (CSF), and low levels of the anti-inflammatory TGFβ (MIC-1 showed a strong tendency but was not significant) compared to microglia from control mice. At 7dpi, microglia from KA mice expressed higher levels of IL-1β and TNFα, and lower levels of TGFβ (**Figure 27C**). These data demonstrated that the impaired microglia were in a pro-inflammatory state.

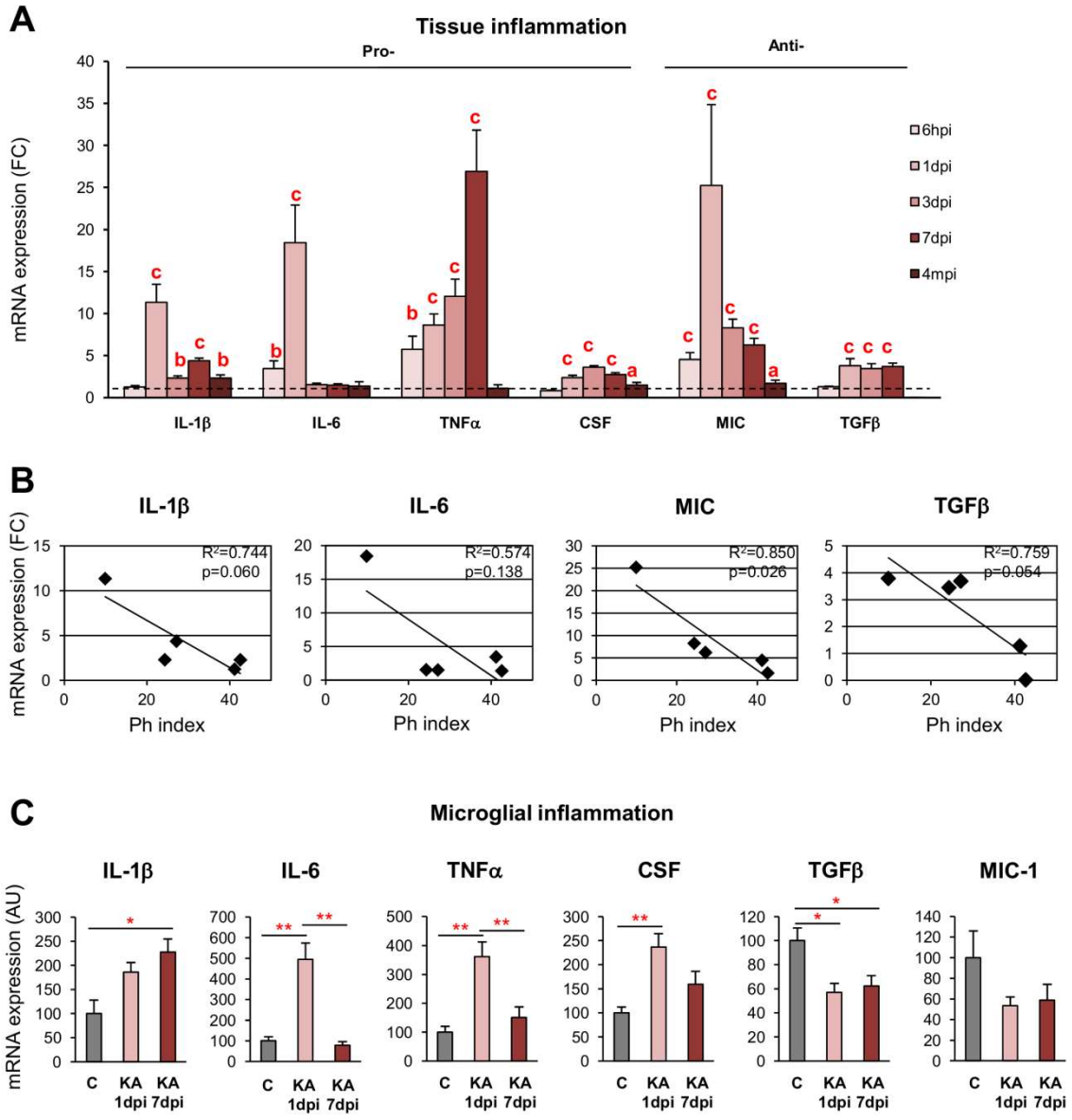

Figure 27. Phagocytosis impairment correlates with inflammation in mouse MTLE. (**A**) RTqPCR quantification of a panel of pro- and anti-inflammatory cytokines in the hippocampus of mice injected

with saline or KA over a time course. Expression was normalized with the reference gene ribosomal protein L27A (L27A) and expressed as fold change (FC) over the saline injected mice (dashed line). Data are shown as mean ± SEM. * indicates p<0.05, ** indicates p<0.01, and *** indicates p<0.001 by Holm-Sidak posthoc test compared to their respective time point controls, after one-way ANOVA was significant at p<0.05. The expression of the cytokines was linearized by a logarithmic transformation; only significant interactions are shown. (**B**) Linear regression analysis of the relationship between the average expression of tissue cytokines (IL-1β, IL-6, MIC-1, TGFβ) and average Ph index in KA-injected mice along the time course. The Ph index explained a large percentage of the variation of the expression of these cytokines, although significance at p=0.05 was only reached for MIC-1 likely due to the small number of time points analyzed. (**C**) RTqPCR quantification of a panel of pro- and anti-inflammatory cytokines in FACS-sorted fms-EGFP^{+} microglia.

6.3. MICROGLIAL PHAGOCYTOSIS-APOPTOSIS UNCOUPLING IN VIVO IN A GENETIC MODEL OF EPILEPSY: PROGRESSIVE MYOCLONUS EPILEPSY OF UNVERRICHT-LUNDBORG TYPE (EPM1)

6.3.1. Microglial phagocytosis is severely uncoupled from apoptosis during seizures in vivo in a model of genetic epilepsy

6.3.1.1. *Microglial phagocytosis is uncoupled from apoptosis in cystatin B knock-out mice, a model of progressive myoclonus epilepsy*

In summary, we have described that microglial phagocytosis and apoptosis can be either coupled (excitotoxicity in vitro and acute and chronic inflammation in vivo), or uncoupled (MTLE). To extend our observations on the microglial phagocytosis impairment to other types of epilepsy we focused on a genetic model of generalized epilepsy, Progressive Myoclonus Epilepsy of Unverricht-Lundborg type (EPM1). EPM1 is a hereditary neurodegenerative disorder characterized by severely incapacitating myoclonus, seizures and ataxia in which seizures arise from the whole brain at once. EPM1 is modeled in mice by constitutive knock-out (KO) of the cystatin B (Cstb) gene (Pennacchio et al., 1998). Cstb is an inhibitor of cysteine proteases such as cathepsin B (CatB), and is thought to play a role in protecting against proteases leaking from lysosomes (Turk et al., 2008)**.** Based on our results on MTLE we expected to find a phagocytosis impairment in Cstb KO mice at the age of myoclonus and seizures onset at PND30 (Tegelberg et al., 2012) (**Figure 28**).

At PND30, Cstb KO mice presented many apoptotic cells and hypertrophic microglia (**Figure 28A, B**). Compared to wild type (WT) mice, we found that Cstb KO mice had an increase in the total number of apoptotic cells (**Figure 28A-C**) and a severe decrease in the Ph index, with only

15% of the apoptotic cells engulfed (**Figure 28D**). The Ph capacity increased in Cstb KO mice (**Figure 28E, F**), as well as the total number of microglia, compared to WT mice (**Figure 28G**). Nonetheless, the compensatory mechanisms in Cstb KO mice were insufficient to match the increase in apoptotic cells, thus provoking a loss of the phagocytosis-apoptosis coupling (**Figure 28H**). These results evidenced an attempt of microglia to balance the increase in apoptosis, contrary to what happens in MTLE, where microglia mainly become non-phagocytic. Nevertheless and similarly to the outcome we observed in MTLE, the insufficient microglial response led to an apoptosis-phagocytosis uncoupling in Cstb KO mice.

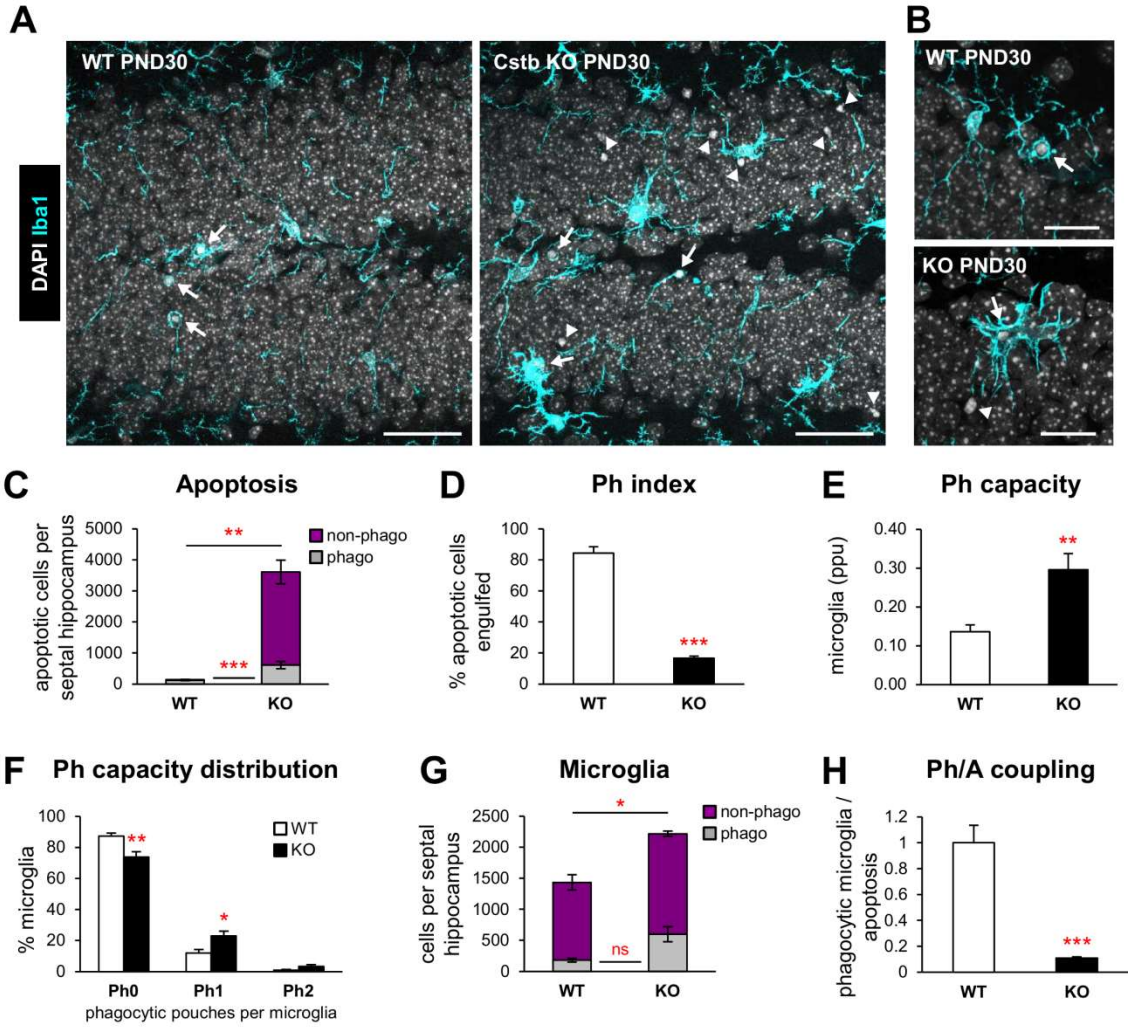

Figure 28. Microglial phagocytosis is uncoupled from apoptosis in Cstb KO mice, a model of progressive myoclonus epilepsy. (**A**) Experimental design and representative confocal z-stacks of the DG of PND30 WT (n=4) and Cstb KO (n=4) mice (C57BL/6 background). Microglia were labeled with Iba1 (cyan) and apoptotic nuclei were detected by pyknosis/karyorrhexis (white, DAPI). Arrowheads point to non-engulfed apoptotic cells and arrows point to apoptotic cells engulfed by microglia. (**B**) Representative confocal high magnification z-stack projections of miroglia from the DG of WT and Cstb KO mice at PND30. Arrowheads point to non-engufled apoptotic cells and arrows point to apoptotic cells engulfed by microglia. (**C**) Number of apoptotic (pyknotic/karyorrhectic) non-phagocytosed and phagocytosed cells per septal DG in PND30 WT and Cstb KO mice. (**D**) Ph index of microglia (in % of

apoptotic cells) in the septal DG of PND30 WT and Cstb KO mice. (**E**) Weighted Ph capacity of microglia (in ppu) in the septal DG of in PND30 WT and Cstb KO mice. (**F**) Histogram showing microglial Ph capacity distribution (in % of microglia) in the septal DG of in PND30 WT and Cstb KO mice. (**G**) Total number of non-phagocytic and phagocytic microglial cells ($Iba1^{+}$) per septal DG in WT and Cstb KO mice at PND30. (**H**) Ph/A coupling (in fold change) in the septal DG of PND30 WT and Cstb KO mice. Bars represent mean ± SEM. * indicates $p<0.05$ and ** indicates $p<0.01$ by 1-tail Student´s t-test. Scale bars=40µm (A), 20µm (B). z=7µm (A, B control), 3,5µm (B KO).

6.3.1.2. *Microglial proliferation and multinuclearity is increased in Cstb KO mice at PND30 in vivo*

As microglial numbers were increased in the DG of Cstb KO mice at PND30, we determined if this increase was due to microglial proliferation. For this purpose, we labeled the dividing cells using Ki67, a well-known marker of mitotic cells. In WT mice, Ki67 was expressed mainly in the SGZ (neuroprogenitors, presumably), whereas in Cstb KO mice it was more widespread throughout the DG including in microglia (**Figure 29A**). The percentage of proliferating (Ki67+) microglia was 0.8±0.5% in WT and increased to 8.3±1.1 in Cstb KO mice (**Figure 29C**). In addition, microglia showed thicker processes and enlarged somas in Cstb KO mice, mimicking what we observed at 3 and 7dpi in MTLE mice, where microglia had become multinucleated (Abiega et al., 2016). To assess whether the microglial morphology change was due to proliferation with an incomplete cytokinesis, we analyzed microglial multinuclearity in Cstb KO mice and quantified the percentage of cells with more than one nuclei (**Figure 29B**). Multinucleated cells were absent in WT mice but represented 13% of microglia in Cstb KO mice (**Figure 29D**). These results partially resembled our findings in MTLE at 3 and 7 dpi, where microglia proliferated and became multinucleated, but still had an impaired Ph capacity (Abiega et al., 2016).

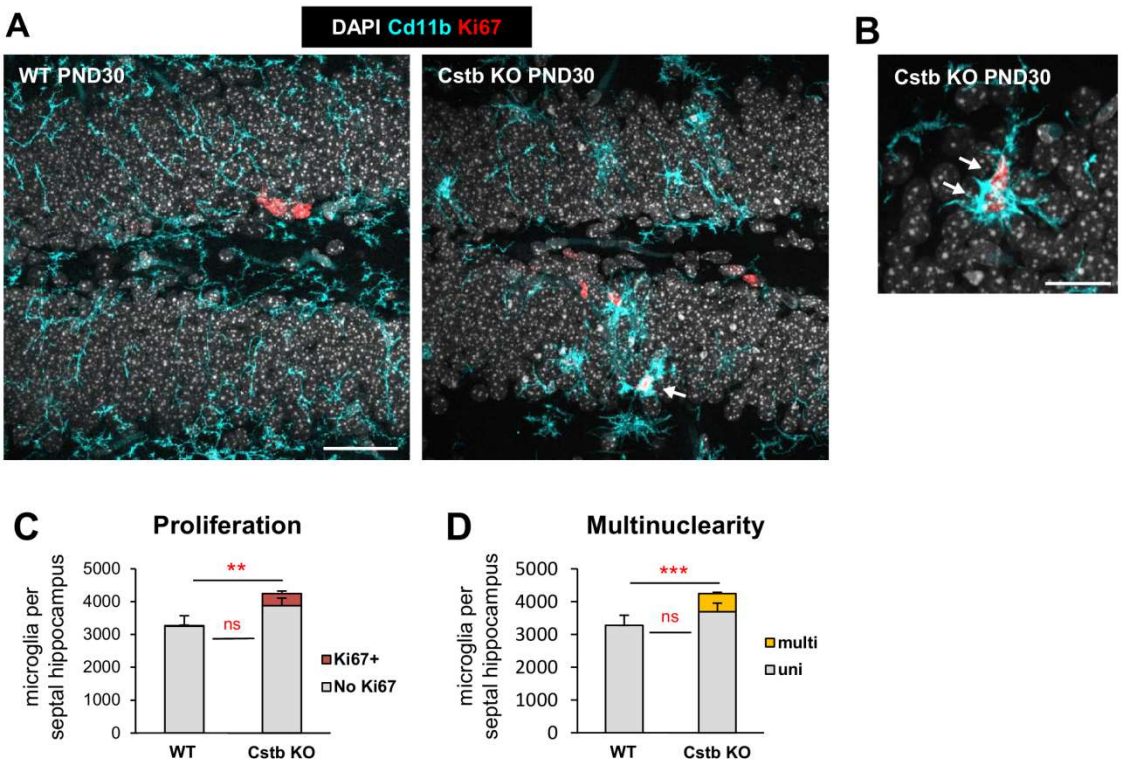

Figure 29. Microglial proliferation and multinuclearity is increased in Cstb KO at PND30 mice in vivo. (**A**) Representative confocal z-stacks of PND30 WT (n=4) and Cstb KO (n=4) hippocampal DG labeled with DAPI (nuclear morphology, white), Ki67 (red, for proliferating cells), and cluster of differentiation molecule 11B (CD11b, cyan, microglia). Arrow, $Ki67^+$ microglial nucleus. (**B**) Confocal z-stack high magnification inserts showing a bi-nucleated microglial cell ($Cd11b^+$, cyan) undergoing division ($KI67^+$, red) in PND30 Cstb KO mice. Arrows, $Ki67^+$ microglial nuclei. (**C**) Microglial proliferation (in KI67 positive or negative microglial numbers per septal hippocampus) in the DG of PND30 WT and Cstb KO mice. (**D**) Microglial mutlinuclearity (number of microglia containing one or more nuclei per septal hippocampus) in the DG of PND30 WT and Cstb KO mice. Bars represent mean ± SEM. * indicates $p<0.05$ and ** indicates $p<0.01$ by 1-tail Student´s t-test. Scale bars=40µm (A), 20 µm (B). z= 7µm (A), 3,5µm (B).

6.3.1.3. *Microglial phagocytosis-apoptosis uncoupling is not compensated by astrocytes in Cstb KO mice at PND30 in vivo*

Because microglial phagocytosis was not efficient enough to maintain the phagocytosis-apoptosis coupling, we assessed whether astrocytes performed phagocytosis to compensate the microglial impairment. For this purpose, we labeled them with glial fibrillary acidic protein (GFAP) and assessed the astrocytic Ph index (**Figure 30A**). We found an obvious morphology change in astrocytes which showed thicker processes, in accordance to the previously reported astrocytosis observed in PND30 Cstb KO mice (Tegelberg et al., 2012). However, we found no phagocytosis by astrocytes, concluding that the microglial phagocytosis

impairment observed was not compensated by astrocytes. Thus, microglia remained the most relevant phagocyte in the hippocampus of Cstb KO mice at PND30, similarly to what occurred in MTLE.

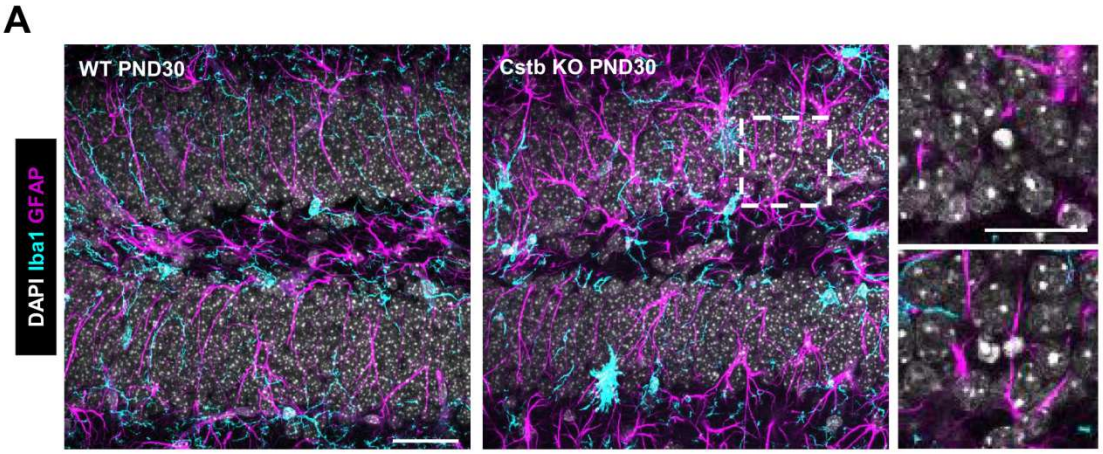

Figure 30. Microglial phagocytosis-apoptosis uncoupling is not compensated by astrocytic phagocytosis in PND30 Cstb KO mice in vivo. (**A**) Representative confocal z-stacks of PND30 WT and Cstb KO hippocampal DG labeled with DAPI (nuclear morphology, white), GFAP (magenta, astrocytes), and Iba1 (cyan, microglia). Cstb KO high magnification inserts show non-phagocytosed apoptotic cells (pyknotic, visualized with DAPI). Scale bars=40µm (A general views), 20 µm (A, high magnification inserts). z=7µm (A general views).

6.3.1.4. *Early hippocampal atrophy in PND30 Cstb KO mice in vivo*

Adult Cstb KO mice present several anatomical alterations including a region-specific neuronal loss in the primary somatosensory cortex at PND30 and regional atrophy and cortical thinning from P60 onward (Tegelberg et al., 2012). These anatomical changes can have a strong impact in the parameters we assess, as microglial and apoptotic total cell numbers and densities are influenced by changes in the DG volume. Thus, we assessed whether the hippocampus was affected in volume, cell density, or total cell numbers in Cstb KO mice at PND30 (**Figure 31**). We analyzed the septal and temporal regions of the DG separately, as they have different innervation (Thompson et al., 2008). We found no difference in the volume of the temporal DG, but the septal DG had a strong tendency to be smaller (P=0,052) (**Figure 31A**). This reduction in the septal DG volume could be related to either a higher granule cell density (with cells more packed) or a decrease of total granule cell numbers. To test these alternatives, we quantified the number of nuclei inside randomly chosen 1260 μm^3 volumes in the granular layer of the DG and found that there was no difference in the granule cell density in the septal DG of the Cstb KO mice (**Figure 31B**). Thus, the number of total granule cells decreased in the septal DG of the Cstb KO mice (**Figure 31C**). These results matched previous

data showing neuronal loss in the primary somatonsensory cortex at PND30 (Tegelberg et al., 2012), and pointed at a possible defect in the development of the hippocampus in Cstb KO mice.

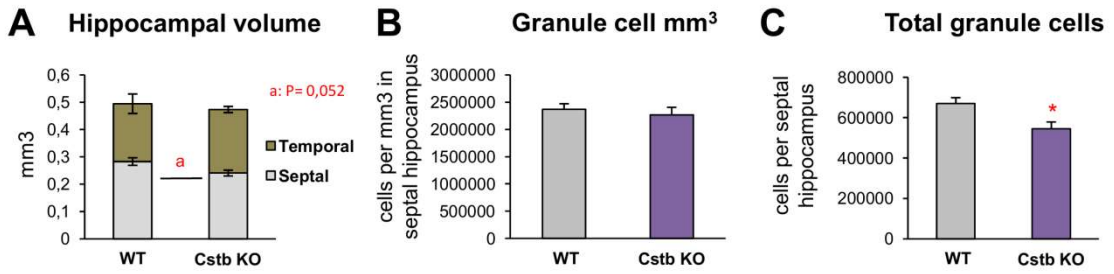

Figure 31. Early hippocampal atrophy in Cstb KO mice at PND30 in vivo. (**A**) Hippocampal volume (in mm^3) of the septal and temporal portions of the DG in PND30 WT and Cstb KO mice. (**B**) Granule cell density (in cells per mm^3 in the septal hippocampus) in the DG of PND30 WT and Cstb KO mice. (**C**) Total granule cells (per septal hippocampus) in the DG of PND30 WT and Cstb KO mice. Bars represent mean ± SEM. * indicates p<0.05 and ** indicates p<0.01 by 1-tail Student´s t-test. a= p=0,052.

6.3.2. Microglial phagocytosis-apoptosis uncoupling precedes seizure development in vivo in a model of genetic epilepsy

6.3.2.1. *Microglial phagocytosis-apoptosis uncoupling precedes seizure development in Cstb KO mice in vivo*

To further understand the mechanisms regulating microglial phagocytosis, we assessed whether the phagocytosis-apoptosis uncoupling in Cstb KO mice was due to the seizures or to the loss of Cstb per se. To test these alternatives, we analyzed phagocytosis in Cstb KO mice at PND14, age at which they show altered microglial morphology but have no seizures (Tegelberg et al., 2012). We found an increase in the total number of apoptotic cells, especially in non-phagocytosed apoptotic cells in Cstb KO mice compared to WT mice (**Figure 32A-E**). We also found a decrease in the Ph index, with only 40% of the apoptotic cells engulfed in Cstb KO mice (**Figure 32F**). The Ph capacity increased in Cstb KO mice (**Figure 32G, H**), as well as the total number of microglia, especially phagocytic microglia (**Figure 32I**). Nevertheless, the compensatory mechanisms in Cstb KO mice at PND14 were insufficient to match the increase in apoptotic cells, thus provoking a loss of the phagocytosis-apoptosis coupling (**Figure 32J**). These results show a failed attempt by microglia to compensate the increase in apoptosis identical to the impairment in Cstb KO mice at PND30.

To assess whether PND14 Cstb KO mice also presented a decreased hippocampus, we analyzed the volume of the septal and temporal regions of the DG (**Figure 32K**). Although the total hippocampal DG volume was maintained, we found that the temporal DG was larger in

PND14 Cstb KO mice, while the septal region was smaller compared to a WT mice. These differential volume changes in the two regions could be due to their different innervation (Thompson et al., 2008). The decrease in the septal DG volume in PND14 mice matched what we observed in PND30 mice and strongly suggested a possible defect in the development of the DG in Cstb KO mice.

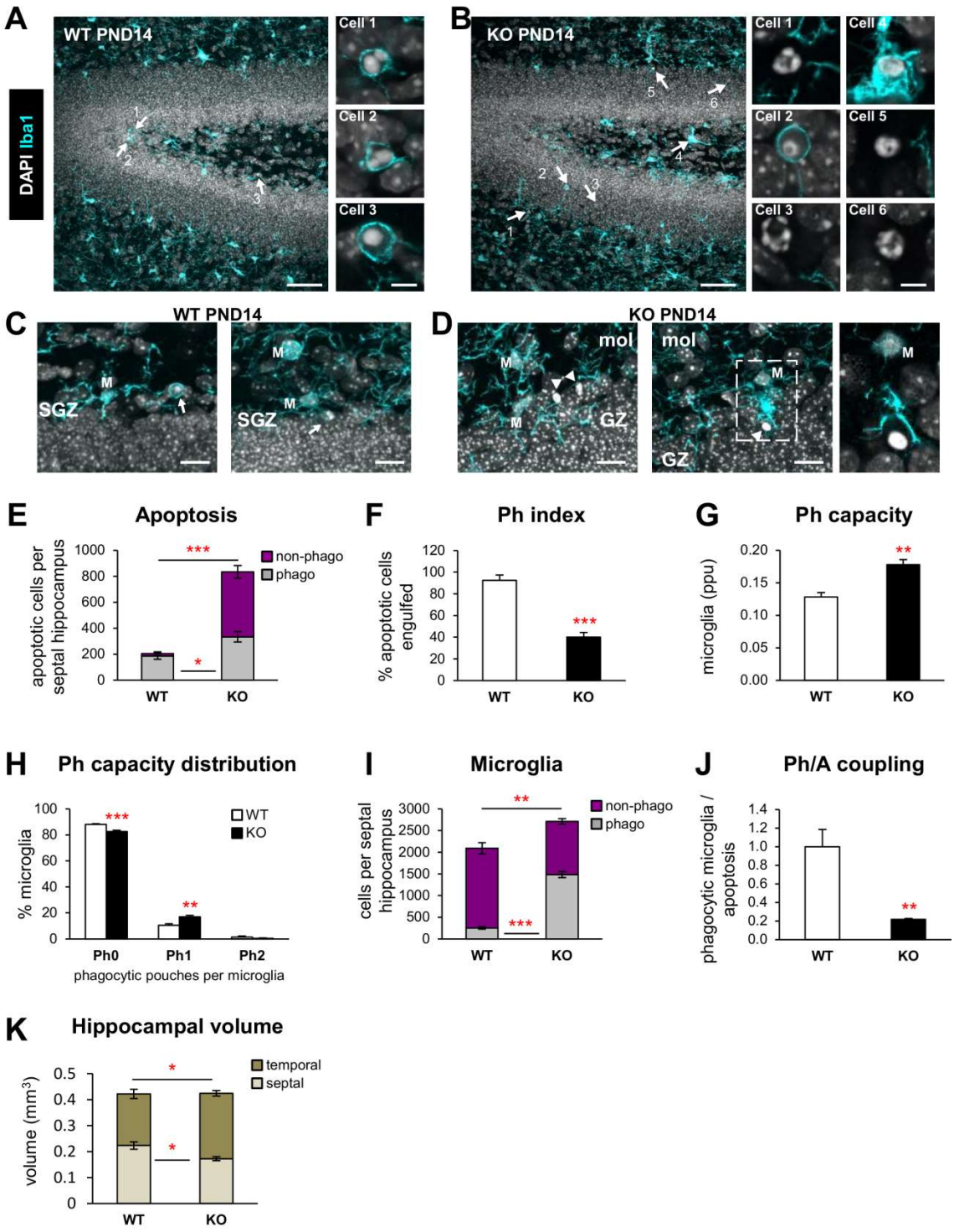

Figure 32. Microglial phagocytosis-apoptosis uncoupling precedes seizure development in Cstb KO mice in vivo. (**A, B**) Representative confocal z-stacks of the DG of PND14 WT (n=5) and PND14 Cstb KO

(n=5) mice (C57BL/6 background). Microglia were labeled with Iba1 (cyan) and apoptotic nuclei were detected by pyknosis/karyorrhexis (white, DAPI). Arrowheads point to non-engulfed apoptotic cells and arrows point to apoptotic cells engulfed by microglia. High magnification inserts show phagocytosed and non-phagocytosed nuclei. (**C**) Representative confocal z-stacks of apoptotic (pyknotic) cells phagocytosed (arrows) in the septal DG of PND14 WT KO mice. M, microglial soma; SGZ, subgranular zone. (**D**) Representative confocal z-stacks of apoptotic (pyknotic) cells non-phagocytosed (arrowheads) in the septal DG of PND14 Cstb KO mice. M, microglial soma; GZ, granular zone; mol, molecular layer. (**E**) Number of apoptotic (pyknotic/karyorrhectic) non-phagocytosed and phagocytosed cells per septal DG in PND14 WT and Cstb KO mice. (**F**) Ph index of microglia (in % of apoptotic cells) in the septal DG of PND14 WT and Cstb KO mice (**G**) Weighted Ph capacity of microglia (in ppu) in the septal DG of PND14 WT and Cstb KO mice. (**H**) Histogram showing microglial Ph capacity distribution (in % of microglia) in the septal DG of PND14 WT and Cstb KO mice. (**I**) Total number of microglial non-phagocytic and phagocytic cells ($Iba1^+$) per septal DG in PND14 WT and Cstb KO mice. (**J**) Ph/A coupling (in fold change) in the septal DG of PND14 WT and Cstb KO mice. (**K**) Hippocampal volume (in mm^3) of the septal and temporal portions of the DG in PND14 WT and Cstb KO mice. Bars represent mean ± SEM. * indicates $p<0.05$ and ** indicates $p<0.01$ by 1-tail Student´s t-test. Scale bars=50µm (A, B general views), 5µm (A, B inserts), 10µm (C, D). z=18.9µm (A, B), 9.8µm (C1), 16.1µm (C2), 11.2µm (D1), 12.6µm (D2).

Overall, these results demonstrate that the microglial phagocytosis impairment precedes seizure development in Cstb KO mice, pointing at Cstb as a possible regulator of microglial phagocytosis. Furthermore, these results suggest that microglia might be contributing to the development of the pathology in progressive myoclonus epilepsy.

7 DISCUSSION

7. DISCUSSION

Apoptosis is an ubiquitous process occurring in the brain both in physiological and pathological conditions. The dead cells must be quickly removed to avoid the further toxic effects they exert in the tissue. Microglia are in charge of removing these apoptotic cells by a process named phagocytosis, which implies finding, engulfing, and degrading the dead cells (Sierra et al., 2013). Even though microglial phagocytosis is a critical process to maintain tissue homeostasis, it remains widely unknown.

In this thesis we have assessed microglial phagocytosis in different pathological conditions using a novel set of parameters developed by us to quantify microglial phagocytosis both in vitro and in vivo. We have discovered a widespread response of microglia to apoptotic challenge induced by excitotoxicity or inflammation, in which microglia increase their phagocytic capacity proportionally to the increase in apoptosis. Thus, microglial phagocytosis and apoptosis are tightly coupled in these conditions (**Figure 33**).

Unexpectedly, we have found that microglial phagocytosis is uncoupled from apoptosis in two epilepsy models in mice: an in vivo model of mesial temporal lobe epilepsy (MTLE) induced by kainate (KA) administration and a genetic model of progressive myoclonus epilepsy 1 (EPM1) induced by genetic deletion of cystatin B (Cstb) (**Figure 33**). The mechanisms involved in the phagocytosis impairment and the similarities between both models will be discussed below. In addition, we have discovered that in MTLE the phagocytosis impairment induces a delayed clearance of apoptotic cells that leads to their accumulation, contributing to the damage of the tissue and correlating with the development of an inflammatory response. Our findings suggest that enhancing microglial phagocytosis could be a novel therapeutic strategy to control tissue damage and inflammation, and accelerate recovery in brain diseases.

7.1. MICROGLIAL PHAGOCYTOSIS IS COUPLED TO APOPTOSIS IN HEALTH AND DISEASE

7.1.1. Microglial phagocytosis is fast and efficient in physiological conditions

In contrast to the long-standing assumption that phagocytosis is executed only by ameboid-shaped microglia (Kettenmann 2007), we initially found that in physiological conditions, phagocytosis is efficiently enacted by unchallenged, ramified, surveillant microglia (Sierra et al., 2010). We used the adult hippocampal neurogenic cascade as a model to study microglial phagocytosis in vivo, because newborn neurons continuously undergo apoptosis

throughout adulthood in the neurogenic niche of the DG (Sierra et al., 2010), which allowed us to establish the baseline of microglial phagocytosis. We previously found that in physiological conditions the vast majority of apoptotic newborn cells are in the process of being engulfed by microglia (Ph index > 90%) through a ball-and-chain mechanism and a short clearance time (under 1.5h) (Sierra et al., 2010). This short clearance time implies that only 5% of the apoptotic cells that undergo apoptosis in a 24h period are visualized, as the rest of them are already degraded by microglia and are therefore undetectable. This is evident in the adult hippocampal neurogenic niche, where the majority of newborn cells undergo apoptosis but nonetheless very few apoptotic newborn cells are found (Dayer et al., 2003; Sierra et al., 2010). Thus, a speedy phagocytosis results in an underestimation of the total number of dead cells.

7.1.2. Microglial phagocytosis is coupled to apoptosis in pathological conditions

We have now studied the microglial response to phagocytic challenges induced by different pathological models and have found a generalized microglial response. When subjected to a phagocytic challenge induced by excitotoxicity in vitro or acute or chronic inflammation in vivo, microglia stood up to the increased apoptosis combining three different strategies: recruiting more phagocytic cells, increasing the phagocytic capacity of each cell, and/or increasing microglial numbers. The combination of these three adaptation strategies allowed microglia to boost their phagocytosis efficiency and match the apoptotic challenge, therefore maintaining the proportion between the change in phagocytosis and apoptosis. The phagocytosis-apoptosis coupling can be explained by the release and expression of “find-me” signals, such as adenosine triphosphate (ATP) and fractalkine (CXC3CL1) and “eat-me” signals, such as phosphatydilserine (PS) by the apoptotic cells (Sierra et al., 2013). Thanks to the different microglial phagocytic boosting strategies and the “find-me” and “eat-me” signals from apoptotic cells, the phagocytosis/apoptosis coupling was maintained in pathological conditions.

7.1.3. Microglia have a large phagocytic reservoir

We next assessed how much microglia phagocytosed in a given moment. In physiological conditions, the Ph index was normally around 90%, and two thirds of the total microglial cells remained non-phagocytic, while the remaining third was phagocytosing only one cell (Sierra 2010). Nevertheless, excitotoxicity and inflammation showed a shift from a majority of non-phagocytic microglia to a majority of phagocytic microglia, with a small

percentage of cells phagocytosing up to four apoptotic cells during in vivo acute inflammation (Sierra et al., 2010) and up to seven cells during excitotoxicity in organotypic slices. Nevertheless, more than 50% of microglial cells remained either non-phagocytic or phagocytosed only one cell in both pathologies, suggesting a large unexploited phagocytic capacity. Therefore, these data evidenced that microglia have an enormous reservoir for phagocytosis that could be reached by recruiting 100% of microglial cells to work at their maximum Ph capacity.

7.2. SEIZURES INDUCE A MICROGLIAL PHAGOCYTOSIS-APOPTOSIS UNCOUPLING IN EPILEPSY

Since microglia show a large phagocytic potential in both excitotoxicity and inflammation, pathologies which concur during epilepsy (Lee et al., 2008), we tested microglial phagocytosis in in vivo epilepsy. For this purpose, we used two different models: MTLE (induced by administration of KA), and EPM1 (induced by transgenic deletion of the Cstb gene).

7.2.1. Microglial phagocytosis is uncoupled from apoptosis following seizures in vivo in a pharmacological and a genetic model of epilepsy

There are many differences between MTLE and EPM1. MTLE is an acutely induced model of focal epilepsy. An adult mice is intrahippocampally injected with KA, which induces an episode of prolonged continuous seizure activity (status epilepticus) that starts at 4hpi and lasts 4-6h (Bouilleret et al., 1999). KA-injected mice develop chronic unprovoked seizures during several months (Sierra et al., 2015). In contrast, EPM1 is a chronic model of generalized epilepsy induced by transgenically knocking-out Cstb. These mice develop seizures starting at 1 month-old (mo). We first compared microglial morphology in adult MTLE (2mo) and post-natal day 30 (PND30) EPM1 mice. We found that both MTLE and PND30 EPM1 mice showed a change in microglial morphology, with cells showing thickened ramifications compared to their respective controls. PND30 EPM1 showed a more dramatic microglial morphology, with cells showing thickened somas and processes and a subset displaying even larger somas. In our recent paper we observed that microglia in 4mo MTLE mice presented a morphology similar to microglia in PND30 EPM1 mice (Abiega et al., 2016), probably due to the fact that both are models of chronic epilepsy.

We next examined apoptosis and phagocytosis in MTLE and PND30 EPM1 mice. In both cases seizures induced an increase in the number of apoptotic cells in the DG of the

hippocampus. To our surprise, in spite of their large phagocytic reservoir microglia failed to efficiently employ it to counteract the damage resulting from neuronal hyperactivity in both cases, thus resulting in a severe phagocytosis-apoptosis uncoupling. In MTLE, we found an impairment of microglial phagocytosis as early as 6 hours post-injection (hpi) and 1 day post-injection (dpi) after KA, in the acute phase of the disease and during status epilepticus. Importantly, this impairment was not simply an inability of microglia to cope with too much apoptosis because it occurred as early as 6 hpi after KA, before any significant accumulation of apoptotic cells took place. Moreover, microglia dispatched this amount of apoptosis in other conditions (for instance, bacterial lipopolysaccharides (LPS) in 1 mo mice) (Abiega et al., 2016; Sierra et al., 2010). In MTLE mice, microglial numbers did not increase and these mice showed a decreased Ph capacity, which provoked a net loss of phagocytosis and a severe phagocytosis-apoptosis uncoupling. PND30 EPM1 mice showed an increase in the total microglial numbers and a small increase in their Ph capacity, thus increasing the net phagocytosis. Nevertheless, this microglial phagocytic potentiation was insufficient to match the increase in apoptotic cell numbers in PND30 EPM1 mice, thus producing a phagocytosis-apoptosis uncoupling. Therefore, both pharmacologically and genetically induced seizures provoked a microglial phagocytosis-apoptosis uncoupling, but as a consequence of different microglial responses, showing a microglial phagocytosis impairment in MTLE and an insufficient phagocytic potentiation in PND30 EPM1 mice (**Figure 33**).

7.2.2. Microglia remain the most determinant phagocytes during phagocytosis-apoptosis uncoupling in MTLE and EPM1 mice

Since microglial phagocytosis was insufficient to balance the increased apoptotic cell numbers in both epilepsy models, additional phagocytosis performed by other phagocytes could have had a strong impact in the tissue. Microglia are the brain professional phagocytes, but other cell types can also perform phagocytosis, such as astrocytes (Magnus et al., 2002) or neuroblasts (Lu et al., 2011), which do not normally phagocytose hippocampal apoptotic cells in resting conditions (Sierra et al., 2010). These non-professional phagocytes delay phagocytosis for several hours (Parnaik et al., 2000) and engulf cells with much lower capacity (Magnus et al., 2002). Importantly, we observed that the MTLE-induced phagocytosis impairment was not compensated by recruiting neither astrocytes nor neuroblasts and PND30 EPM1 mice showed a complete lack of astrocytic phagocytosis. Thus, the importance of the microglial phagocytic dysfunction during seizure induced phagocytosis-apoptosis uncoupling became critical to the brain parenchyma, as the impaired microglia remained by far the most determinant phagocyte in the hippocampus of both EPM1 and acute MTLE mice.

7.2.3. Microglial multinucleation in EPM1 mice

Besides the changes in microglial morphology, we observed multinucleated microglia in PND30 EPM1 mice. Interestingly, we recently found that 3-7dpi after KA, MTLE mice also show multinucleated microglia, albeit in higher numbers than EPM1 (Abiega et al., 2016). Microglial multinucleation can be induced in vitro by inflammatory cytokines, resulting from incomplete cytokinesis (Hornik et al., 2014). We have observed that microglial multinucleation concurs with the development of an inflammatory response in MTLE mice (Abiega et al., 2016). In accordance, high expression of glial derived pro-inflammatory chemokines and cytokines have been reported in PND30 EPM1 mice (Joensuu et al., 2014), pointing at the possibility of inflammation inducing multinucleation in EPM1. Thus, the microglial multinucleation we observe in EPM1 could be a consequence of the inflammatory response that occurs during phagocytosis-apoptosis uncoupling in the hippocampus of PND30 EPM1 mice.

7.2.4. Microglial phagocytosis-apoptosis uncoupling could be a widespread phenomenon in the epileptic brain

KA-induced MTLE is known to affect other regions of the brain besides the DG, like the ipsilateral cortex, which also develops seizures as early as 4hpi (Sierra et al., 2015). Although the basal Ph index could not be quantified in these areas (as there is no apoptosis and therefore no phagocytosis of apoptotic cells in physiological conditions), we found that at 1dpi after KA microglial phagocytosis was as low in cornu ammonis 1 (CA1) and CA3 of the hippocampus and in the adjacent somatosensory cortex in MTLE as it was in the DG. Thus, our results showed that microglia responded to seizures with a similar phagocytosis impairment in different areas of the brain. We only studied microglial phagocytosis in the DG in PND30 EPM1 mice, but other studies show that the subset of microglia with enlarged somas that we observed in the hippocampal DG of these mice was also present in many other brain regions such as the cortex and the cerebellum (Tegelberg et al., 2012). Thus, these data suggest a possible microglial phagocytic dysfunction beyond the hippocampus in EPM1 mice. Altogether, these results suggested that the microglial phagocytic malfunction could be a widespread response throughout the brain parenchyma in both MTLE and EPM1.

Overall, our data on MTLE and PND30 EPM1 mice showed a severe microglial phagocytosis-apoptosis uncoupling in the DG of the hippocampus following seizures. The mechanisms underlying the uncoupling in each model will be discussed next.

7.3. MECHANISMS OF MICROGLIAL PHAGOCYTOSIS-APOPTOSIS UNCOUPLING IN MTLE

7.3.1. Microglial phagocytosis impairment is unrelated to a direct effect of KA on microglia

Since microglial phagocytosis was not impaired by inflammation nor by excitotoxicity per se, KA emerged as a possible microglial phagocytic modulator in MTLE. KA induces seizures via activation of KA and AMPA receptors (Fritsch et al., 2014), both of which are subtypes of ionotropic glutamate receptors. In our recent paper we showed that in vivo microglia expressed residual levels of ionotropic and metabotropic glutamate subunit mRNA, which are unlikely to form functional receptors (Abiega et al., 2016), in accordance with previous reports in microglia in acute hippocampal slices (Wu and Zhuo, 2008) and retinal explants (Fontainhas et al., 2011). In agreement, we showed that KA did not modulate microglial phagocytosis in organotypic cultures, in which it did not induce seizures. Interestingly it has been reported that some AMPA and KA receptor subunits are expressed in cultured microglial cells (Hagino et al., 2004; Noda et al., 2000) and in addition KA has been shown to induce membrane ruffling and morphological alterations in cultured microglia (Christensen et al., 2006), which would explain our results in primary cultures treated with KA, where it had a very small effect on phagocytosis of apoptotic cells. Therefore, our results showed that KA was not responsible for the microglial phagocytosis impairment in the absence of seizures, which led us to search for alternative mediators between neuronal hyperactivity and microglia.

7.3.2. Microglia sense seizures via ATP

A possible mediator of the effects of neuronal activity on microglia was extracellular ATP, which is released by neurons and astrocytes as neuro- and gliotransmitter (Dale and Frenguelli, 2009; Santiago et al., 2011). ATP signals to microglia on a plethora of promiscuous P2X (ionotropic) and P2Y (metabotropic) receptors and is degraded by extracellular ectonucleotidases to adenosine. Importantly, microglia express all types of purinergic receptors (Crain et al., 2009; Domercq et al., 2013). In retinal explants and acute hippocampal slices, neuronal glutamate signalling via NMDA receptor activation leads to the release of ATP which in turn alters microglial motility and morphology (Dissing-Olesen et al., 2014; Eyo et al., 2014; Fontainhas et al., 2011) and triggers microglial process convergence towards neuronal dendrites (Eyo et al., 2015). ATP is also released in large amounts during seizures in vivo and in vitro (Dale and Frenguelli, 2009; Santiago et al., 2011), and is rapidly degraded to adenosine diphosphate (ADP) and adenosine monophosphate (AMP) (Zimmermann, 1999), complicating

the use of in vivo direct methods for ATP measurement such as the luciferin-luciferase assay (Crouch et al., 1993) or microeletrode biosensors (Heinrich et al., 2012). Thus, we resorted to indirectly determine the action of ATP released during seizures on microglia in vitro by treating acute hippocampal slices with a seizure-inducing epileptogenic cocktail.

We showed that in vitro microglia acutely sensed seizures, resulting in large inward currents that depended at least partially on P2X receptors, similar to those observed in oligodendrocytes in vitro during oxygen and glucose deprivation induced ischemia, where enhanced ATP signalling is deleterious to oligodendrocytes (Domercq et al., 2010). Interestingly, we observed a delayed microglial response (11 min latency time) which is consistent with the time it takes to reach the maximum ATP release evoked by depolarization in acute slices (Heinrich et al., 2012). Thus, these results pointed at ATP as the mediator between seizures and microglia. Next, we assessed whether the epileptogenic cocktail would induce a phagocytosis impairment in hippocampal organotypic slices treated with the seizure inducing epileptogenic cocktail. Indeed, we found that microglial phagocytosis was impaired, mimicking our in vivo results in our MTLE model. Overall, this data demonstrated that microglia sensed seizures via ATP.

7.3.3. Disruption of ATP gradients impairs microglial phagocytosis

In addition to being a neuro- and gliotransmitter, ATP is a well-known “find-me” signal released by apoptotic cells (Elliott et al., 2009; Sierra et al., 2013) and mediates the rapid attraction of microglial processes towards laser-induced injuries (Davalos et al., 2005). Therefore, we hypothesized that the KA-triggered microglial phagocytosis impairment was consistent with a seizure-related widespread release of ATP that disrupted “find-me” signalling gradients and turned microglia “blinded” to apoptotic cells. Thus, we decided to assess whether ATP would cause a microglial phagocytosis impairment per se in the hippocampal DG, both in vitro and in vivo. In vitro experiments were performed using hippocampal organotypic slices treated with 1mM of ATP. Live imaging has shown that 1mM ATP affects microglial motility in vivo when applied locally in the cortex using a micropipette (Davalos et al., 2005), which has also been observed in vitro in mouse retinal explants (Fontainhas et al., 2011). 1mM ATP has also been shown to decrease phagocytosis in vitro in rat primary cultures (Fang et al., 2009). Treating organotypic slices with 1mM ATP for 4h severely impaired phagocytosis, mimicking the impairment observed in MTLE. Importantly, the high ATP concentration in the media did not induce microglial death, but provoked microglia to migrate towards the edges of the slices, in accordance with the strong chemotactic nature of ATP on microglia (Davalos et al., 2005).

To test the effect of ATP in vivo, we intrahippocampally injected 100mM ATP and 100mM of the non-degradable ATPγS for 2h and 10mM and 100mM ATP for 4h. Although the injected maximum dose was relatively high (100mM) compared to conventional doses used in vitro or in local application during in vivo imaging, this concentrations had to account for the diffusion of ATP and ATPγS through the whole hippocampus (spanning a volume of several mm^3). In addition, ectonucleotidase hydrolyzation of nucleotides occurs within a few hundred milliseconds in the extracellular space in rat brain slices (Cunha et al., 1998). Moreover, it has been shown that while ATP steady-state cytosolic concentration is high (5-10 mM), the extracellular concentration of ATP is very low (±10 nM), but CNS insults cause a pronounced release from damaged cells of mM concentrations of ATP (Trautmann, 2009). Thus, our use of mM ranges of ATP mimicked pathological ATP release concentrations in the brain, besides additionally compensating for its diffusion and degradation. At 2hpi of 100mM ATP and ATPγS microglial phagocytosis was severely impaired. Interestingly, ATP induced higher apoptotic cell numbers than ATPγS, possibly because the latter only affected ATP receptors, while the degradation of ATP into ADP and AMP would affect the whole plethora of purinergic receptors, having further toxic effects over surrounding cells (Robson et al., 2006). Overall, these data showed that in vivo ATP induced a severe microglial phagocytosis impairment that mimicked the results obtained in MTLE.

7.3.4. ATP induced loss of microglial phagocytosis efficiency is unrelated to microglial viability

To disregard the possibility that changes in phagocytosis efficiency in ATP-treated mice were the result of reduced microglial viability, we performed a second in vivo experiment injecting 10 and 100mM of ATP for 4h. As the average clearance time is 1.2-1.5h (Sierra et al., 2010), at 2hpi we could detect only a fraction of the cells that had impaired recognition, as the cells that started phagocytosis before the injection would still be in the process of degrading the apoptotic cell. Thus, we analyzed microglial phagocytosis at a later time point (4hpi) to allow microglia to either die or recover, and to let them further progress in the degradation of ingested cells. In contrast, this later time point propitiated a further degradation of the injected ATP by ectonucleotidases. As we expected, ATP 100mM treatment induced a drop in the numbers of microglia, indicating a decrease of microglial viability. In addition the Ph/A coupling was lost. Nevertheless, in the 10mM ATP treatment microglia did not die and its numbers remained stable while the Ph/A coupling was lost, showing that the ATP induced changes in microglial phagocytosis efficiency were not due to the loss of microglial viability.

7.3.5. Pannexin expression is unrelated to microglial phagocytosis impairment

Finally, we tested whether the impaired recognition in epileptic mice was due to a defective ATP signalling from apoptotic cells, possibly due to an altered expression of pannexin, one route through which ATP is released (Chekeni et al., 2010). The low expression of pannexin in hippocampal apoptotic cells pointed at an alternative signalling mechanism between apoptotic cells and microglia. Chemotherapeutic drugs have been shown to activate a pannexin independent pathway for ATP release from apoptotic Jurkat cells in the presence of a broad caspase inhibitor (Boyd-Tressler et al., 2014). Although this alternative ATP mechanism has not been studied in the brain yet, our results suggest that apoptotic cells might release ATP through similar pannexin independent mechanisms.

7.3.6. Microglial phagocytosis impairment is related to reduced motility

We observed a large proportion of microglia located far away from the apoptotic cells in MTLE mice at 6hpi and 1dpi, suggesting a reduction in surveillance capacity, which was in agreement with our hypothesis that seizures caused an ATP overflow that induced microglial blinding. The decreased surveillance could be related to a loss of microglial density in the DG of MTLE mice or, alternatively, it could result from decreased microglial motility. Interestingly, we found a lower microglial density in the DG of MTLE mice at 1dpi, but there were no changes in the total number of microglia. In fact, the reduction in microglial density was due to an obvious increase in the volume of the DG (Abiega et al., 2016). Nevertheless, we found a decreased overall motility of microglia in both acute hippocampal slices and in the living cortex of MTLE animals at 1dpi. The level of motility impairment observed in the cortex in vivo was higher than in the acute hippocampal slices, possibly because the released ATP was washed out during the slice preparation. Our results of motility impairment are to some extent in disagreement with a recent study in acute hippocampal slices, in which intraperitoneal KA injection produced no difference in microglial processes velocity but there was a puzzling increase in the area of the explored territory of each process 48h after the injection (Avignone et al., 2015). This occurred in spite of the increased purinergic signalling of microglia in this model (Avignone et al., 2008) and the well-established chemoattractant role of ATP in these lesions (Davalos et al., 2005). We speculate that at 2dpi the widespread release of ATP induced by the seizures would be more attenuated than at 1dpi, accounting for the dissimilar results on microglial motility. Overall, our data showed that the reduction in microglial motility was one of the cellular mechanisms underlying the defect in microglial phagocytosis in MTLE mice.

7.3.7. Additional mechanisms in microglial phagocytosis impairment

In addition to the defect in motility, we observed a large proportion of non-phagocytosed apoptotic cells localized in direct apposition to microglial processes in MTLE, which led us to speculate that there could be an additional defect in the apoptotic cell recognition and phagocytosis initiation. In fact, we found that microglia downregulated the expression of several receptors involved in phagocytosis, such as triggering receptor expressed on myeloid cells 2 (TREM2) (Kawabori et al., 2015), complement receptor 3 (CR3) (Noda and Suzumura, 2012), Mer tyrosine kinase (MerTK) (Caberoy et al., 2012), and the G protein coupled receptor GPR34 (Preissler et al., 2015) at 1dpi KA (Abiega et al., 2016). Therefore, the seizure-induced phagocytosis impairment is a complex phenomenon that likely implies other mechanisms in addition to the ATP widespread release. For instance, seizures affect many other signalling molecules released by neurons that control microglial function, such as CX3CL1 (Paolicelli et al., 2014; Xu et al., 2012) or endocannabinoids (Alger, 2014; Bisogno and Di Marzo, 2010). CX3CL1 is upregulated in the serum and cerebrospinal fluid of epileptic patients as well as in a lithium-pilocarpine rat model (Ali et al., 2015), and an increase in CX3CL1 receptor expression is detected between 1 and 6h and begins to decline by 3 days following seizures (Ali et al., 2015; Yeo et al., 2011). However, following intrastriatal KA treatment, fractalkine receptor expression remained unchanged in microglia despite evident neuronal loss (Hughes et al., 2002). In addition, status epilepticus triggers an early energy depletion at the seizure focus followed by a series of metabolic alterations in the long term (Otahal et al., 2014) that affect the mitochondrial function (Zsurka and Kunz, 2015), on which phagocytosis heavily relies, at least in macrophages (Park et al., 2011). Microglial motility and injury response also depend on energy sources, as these functions are early reduced in postmortem mouse tissue (Dibaj et al., 2010). Therefore some of these mechanisms are likely to play additional roles in regulating microglial phagocytosis efficiency at different stages of the disease.

7.4. MECHANISMS OF MICROGLIAL PHAGOCYTOSIS-APOPTOSIS UNCOUPLING IN EPM1

7.4.1. Microglial phagocytosis-apoptosis uncoupling is unrelated to seizures in EPM1 mice

To understand whether the phagocytosis-apoptosis uncoupling we observed in EPM1 mice was related to seizures, we assessed EPM1 mice at PND14, an age that precedes seizure onset. Importantly, even though PND14 mice do not have seizures, electrophysiological recordings of PND7 Cstb KO cerebellar Purkinje cells have revealed a shift towards decreased

inhibition due to reduced GABAergic signalling (Joensuu et al., 2014). These results suggest that Cstb KO mice could have an altered connectivity well before the age of seizure onset, leading to their hyperexcitable phenotype and possibly affecting microglial function. From PND14 on, microglia were found to show increased immunostaining by F4/80 (a murine macrophage antibody) in the DG compared to WT mice (Tegelberg et al., 2012). To our surprise, we observed that EPM1 mice already showed a microglial phagocytosis-apoptosis uncoupling at PND14. PND14 EPM1 mice did not show changes in microglial morphology, differently to what we observed in PND30 mice. Nevertheless, PND14 mice microglia proliferated and increased their Ph capacity, consequentially increasing the net phagocytosis, similar to PND30 mice. Furthermore, the microglial phagocytic potentiation in EPM1 mice was insufficient to match the increase in apoptotic cell numbers at PND14, similar to what occurred at PND30 (**Figure 33**). Importantly, the phagocytosis-apoptosis uncoupling was more severe at PND30, which was probably due to the additional impairment induced by seizures. Thus, microglial phagocytosis showed a very similar behavior both before and after seizure onset, which suggested that the phagocytosis-apoptosis uncoupling in EPM1 mice was not caused by seizures.

7.4.2. Effects of the lack of cystatin B on microglial phagocytosis

Because seizures were not the sole cause of microglial phagocytic uncoupling found in EPM1 mice, we speculate that the lack of Cstb may be directly related to the phagocytosis impairment. Cstb, also known as stefin B, is a member of the cystatins, a type of lysosomal cysteine protease inhibitors (Abrahamson et al., 2003; Turk et al., 2008; Turk et al., 2012), whose main function is the intracellular and extracellular regulation of the extralysosomal activities of cathepsins, a type of lysosomal cysteine proteases (Stoka et al., 2016). Among them, the pathogenesis of EPM1 mice has been largely linked to cathepsin B (CatB). Microglia is known to be a major source of CatB in the brain (Hayashi et al., 2013; von Bernhardi et al., 2015; Wendt et al., 2008) which has been shown to be neurotoxic, inducing neuronal apoptosis in the context of neurodegenerative diseases (Gan et al., 2004; Kim et al., 2007; Kingham and Pocock, 2001). Upon induction of apoptosis by an intracellular stimuli, cathepsins leak out from lysosomes and the lack of Cstb regulation starts a biochemical cascade that leads to mitochondrial membrane permeabilization, caspase activation, and apoptosis (Stoka et al., 2016). Besides, neuroinflammation has also been pointed as a possible contributor to EPM1 pathophysiology (Korber et al., 2016).

Although the effects of Cstb and CatB and their connection to microglia have been studied regarding the neurodegeneration and pathophysiology of EPM1, the effects of the lack

of Cstb over microglial phagocytosis are largely unknown. Interestingly, cystatins in immune cells have been reported to participate in many processes including phagocytosis, expression of cytokines, and release of nitric oxide, thus suggesting that cystatins play a significant role in the immune response (Okuneva et al., 2015; Turk et al., 2008; Verdot et al., 1996). In the present thesis we have not had the time to analyze the mechanisms underlying the microglial phagocytosis uncoupling in EPM1 mice, which we intend to do in the future. Nonetheless, we speculate that the lack of Cstb could affect either the finding, engulfing, and/or degradation stages of microglial phagocytosis.

Several mechanisms could underlie a potential deficit in the finding stage of phagocytosis. For instance, EPM1 mice have been reported to have a diminished number of GABAergic terminals and reduced ligand binding to GABAA receptors in the cerebellum (Joensuu et al., 2014), and have also been shown to have an increased neuronal excitability when treated with KA (Franceschetti et al., 2007). This latent hyperexcitability could potentially affect microglial phagocytosis in EPM1 mice by partially disrupting “find-me” signals in the brain parenchyma. Interestingly, microglia in EPM1 mice have also been shown to have an elevated chemotaxis for ATP (Okuneva et al., 2015) and an overexpression of chemotaxis related genes (Korber et al., 2016). Our results are in agreement with this data, as we found that microglia phagocytosed more cells in EPM1 mice than in WT mice, even though it was not enough to maintain the phagocytosis-apoptosis coupling. Another major “find-me” signal regulated by Cstb that could potentially affect apoptotic cell engulfment is CX3CL1. CX3CL1 neutralization or the deficiency of its receptor has been shown to prevent microglia from finding apoptotic cells (Sokolowski et al., 2014). The cleavage of fractalkine by CatS provokes its detachment from the membrane into a soluble form (Clark and Malcangio, 2012). Therefore, the lack of regulation of CatS in EPM1 mice could provoke a massive release of the soluble CX3CL1 fraction which could alter the CX3CL1 microgradients, possibly blinding microglia to this signal.

Cstb could also also affect mechanisms modulating microglial engulfment. For instance, a study carried in yeast showed that Cstb binds a number of cytoplasmic proteins that are involved in the regulation of cytoskeletal functions (Di Giaimo et al., 2002). Accordingly, PND7 cultured cerebellar granule cells of Cstb KO mice have been shown to differentially express cytoskeleton related genes (Joensuu et al., 2014). These changes could also occur in microglia and impair phagocytosis, as a properly functioning cytoskeleton is key for the correct engulfment and posterior intracellular transport of the phagosomes.

Finally, Cstb could affect the degradation of the ingested apoptotic cells. Cstb is a cytosolic inhibitor of cathepsins (Stoka et al., 2016) and thus, it does not regulate the intralysosomal function of cathepsisns, which suggests that Cstb does not directly affect the degradation stage of phagocytosis in EPM1 mice. Nevertheless, P7 cultured cerebellar granule cells of Cstb KO mice have also been shown to differentially express intracellular transport genes (Joensuu et al., 2014), which could possibly happen in microglia as well, affecting their intracellular transport of organelles involved in the degradation of phagocytosed cells.

Overall, the mechanisms underlying the microglial phagocytosis-apoptosis uncoupling in EPM1 mice remain unknown. Moreover, it is important to note that Cstb is not the only cystatin regulating CatB or CatS (Bromme et al., 1991) and other cystatins could be compensating for the lack of Cstb in this pathways, such as cystatin C (Paraoan et al., 2009; Sun et al., 2008). Future experiments will be carried out to elucidate the specific role of Cstb on microglial phagocytosis.

7.5. MICROGLIAL PHAGOCYTOSIS IMPAIRMENT HAS DETRIMENTAL CONSEQUENCES FOR THE BRAIN

7.5.1. Microglial phagocytosis impairment correlates with the development of an inflammatory response in MTLE

We finally analyzed the functional consequences of the microglial phagocytosis impairment in the pharmacological model of MTLE. Phagocytosis is a vital process for the tissue. First, it prevents the apoptotic cells from losing membrane integrity and the subsequent leakage of potentially toxic intracellular contents into the surrounding parenchyma (Arandjelovic and Ravichandran, 2015). These intracellular contents engage receptors for damage associated molecular patterns and contribute to immune responses to self antigens (Arandjelovic and Ravichandran, 2015). Accordingly, defects in the clearance of apoptotic cells by macrophages have been attributed to the onset of persistent inflammatory disorders and autoimmunity (Lauber et al., 2004). In addition, clearance of apoptotic cells by phagocytes actively suppresses the initiation of inflammatory and immune responses, in part through the release of anti-inflammatory cytokines (Byrne and Reen, 2002; Huynh et al., 2002), thus preventing an immune response against the processed proteins of the apoptotic debris. Because microglial phagocytosis was severely impaired in MTLE, we hypothesized that this should result in an accumulation of apoptotic cells and that it could correlate with the development of an inflammatory response.

Importantly, a strong body of in vitro data on macrophages and microglia has shown that phagocytosis of apoptotic cells is actively anti-inflammatory (Sierra et al., 2013). The anti-inflammatory role of phagocytosis in microglia in vitro has been shown to involve the release of anti-inflammatory cytokines such as transforming growth factor beta (TGFβ) and trophic factors such as nerve growth factor (NGF) (De Simone et al., 2003; Fraser et al., 2010) that may potentially facilitate the functional recovery of the surrounding compromised neurons. Therefore, an impairment in phagocytosis would release the brake imposed on the inflammatory response. As we expected, impairment of microglial phagocytosis correlated with the expression of pro- and anti-inflammatory cytokines in hippocampal tissue, although the signal/s which initiate this response in the epileptic brain remain to be determined. As we have shown that inflammation per se did not impair phagocytosis, this data suggest that the impairment of phagocytosis could lead to the development of an inflammatory response (**Figure 33**). Importantly, we observed that the same hippocampal microglial population that exhibited impaired phagocytosis also had a strong pro-inflammatory profile. Increased expression of pro-inflammatory cytokines has already been observed in experimental and human MTLE tissue (Kan et al., 2012; Vezzani et al., 1999; Vezzani et al., 2011b). Because pro-inflammatory interleukin 1 beta (IL-1β) enhances NMDA excitatory currents, it is speculated to contribute to the development of chronic seizures (Kleen and Holmes, 2010), and drugs designed to prevent IL-1β activation and signalling are currently in clinical trials to prevent epileptogenesis (Vezzani et al., 2011a). Our data strongly support that this inflammation may at least in part originate from the microglial phagocytosis impairment, but whether this dysfunction contributes to seizures remains to be determined (Diaz-Aparicio et al., 2016).

7.5.2. Microglial phagocytosis impairment induces a delayed clearance of apoptotic cells in MTLE

We hypothesized that the microglial phagocytosis impairment would lead to an accumulation of non-phagocytosed apoptotic cells. To analyze the clearance of apoptotic cells, we estimated the clearance time of well identified cell populations undergoing apoptosis in the adult neurogenic cascade in the subgranular zone (SGZ) of the DG. In fact, the majority of newborn cells undergo apoptosis within the first 1–4 days of cell birth, in what is called the early critical period of survival, a cell death that continues in a lesser scale in the late critical period of survival (1-3 weeks) (Sierra et al., 2010; Tashiro et al., 2006). As our data showed that the majority of apoptotic cells were located in the SGZ at 1dpi after KA, we studied the effect of KA-induced seizures on the apoptosis and survival of 3do and 8do newborn cells by labeling them with the proliferative marker BrdU. Comparing both the 3do an 8do populations, we

found that KA did not affect the survival of the newborn cells. Thus, we assessed survival and apoptosis of the 3do population of newborn cells and found no changes in the survival of these cells but a puzzling increase in the numbers of apoptotic 3do cells. Moreover, this increase in apoptotic 3do cells was not due to an increase in their proliferation. Importantly, we found that the increased number of 3do apoptotic cells found in the SGZ neurogenic niche after KA injection was not due to de novo apoptosis of this population induced by KA but instead was related to an accumulation of 3do newborn cells that undergo apoptosis under physiological conditions and are not phagocytosed by the impaired microglia (**Figure 33**). Thus, the impairment of phagocytosis during MTLE led to an overestimation of the number of apoptotic cells induced by KA and an increased apoptotic clearance time of 6.3h.

Therefore, we demonstrated that the efficiency of phagocytosis determined apoptosis dynamics in epilepsy and possibly in other brain diseases as well. Moreover, the accumulation of non-phagocytosed apoptotic cells in the brain parenchyma is of critical importance, as these cells could evolve into secondary necrotic cells that lose membrane integrity and start leaking out intracellular contents (Savill et al., 2002), contributing to the damage of the surrounding tissue. In fact, recent data provided direct evidence of the beneficial effects of microglial phagocytosis, as transgenic silencing of the phagocytic receptor TREM2 impaired microglial phagocytosis in vitro and exacerbated ischemic damage in experimental stroke (Kawabori et al., 2015). Therefore, the detrimental features associated with microglial phagocytosis/apoptosis uncoupling such as inflammation, and accumulation of apoptotic cells, could exacerbate the pathology in brain diseases (Diaz-Aparicio et al., 2016).

7.6. MICROGLIAL PHAGOCYTOSIS MODULATION AS A NOVEL THERAPEUTIC TOOL IN NEURODEGENERATION AND BRAIN INJURY

To this day, most therapies aimed at treating neurodegenerative diseases have focused on preventing neuronal death. For example, some strategies have aimed at inhibiting caspases, the enzymes responsible for executing apoptosis (Troy and Jean, 2015); eliminating amyloid beta (Aβ) plaques in Alzheimer's disease (AD); or repressing the oxidative injury caused by ischemia (Patel, 2016). While the results in animal models are promising, many of these candidate strategies have failed in human clinical trials (Ginsberg, 2007; Snow et al., 2010). We suggest that in addition to reducing neuronal damage and death, a complementary therapeutical strategy could involve enhancing the "self-cleaning" mechanisms of the brain, such as microglial phagocytosis.

Similar to what we have reported in epilepsy in this thesis (Abiega et al., 2016), it is possible that microglial phagocytosis is impaired in other brain diseases (Diaz-Aparicio et al., 2016). Inflammation and/or neuronal death are hallmarks of many other neurodegenerative and neurological disorders, such as Alzheimer´s and Parkinson´s disease, multiple sclerosis, ischemia/stroke, and mood disorders (Cappellano et al., 2013; Ransohoff, 2016). Because we have observed that the phagocytosis impairment induced the delayed clearance of apoptotic cells and the development of an inflammatory response, we speculate that the increase in apoptosis and the pro-inflammatory profile classically described in neurological and neurodegenerative diseases could be the consequence of an undetected phagocytosis impairment. Therefore, modulating microglial phagocytosis could be key in the treatment of brain injury and neurodegenerative diseases. Moreover, the comprehension of the mechanisms that regulate phagocytosis, such as “find-me” signals coming from damaged neurons or apoptotic cells, or phagocytic receptors in microglia, will be crucial for the development of new therapies based on the modulation of microglial phagocytosis. Novel pharmacological approaches aimed at enhancing or restoring microglial phagocytosis efficiency would accelerate the clearance of apoptotic cells and promote an anti-inflammatory response. We propose that the modulation of microglial phagocytosis is a novel and yet unexplored therapy to accelerate functional brain recovery from neurodegenerative and neurological diseases (Diaz-Aparicio et al., 2016).

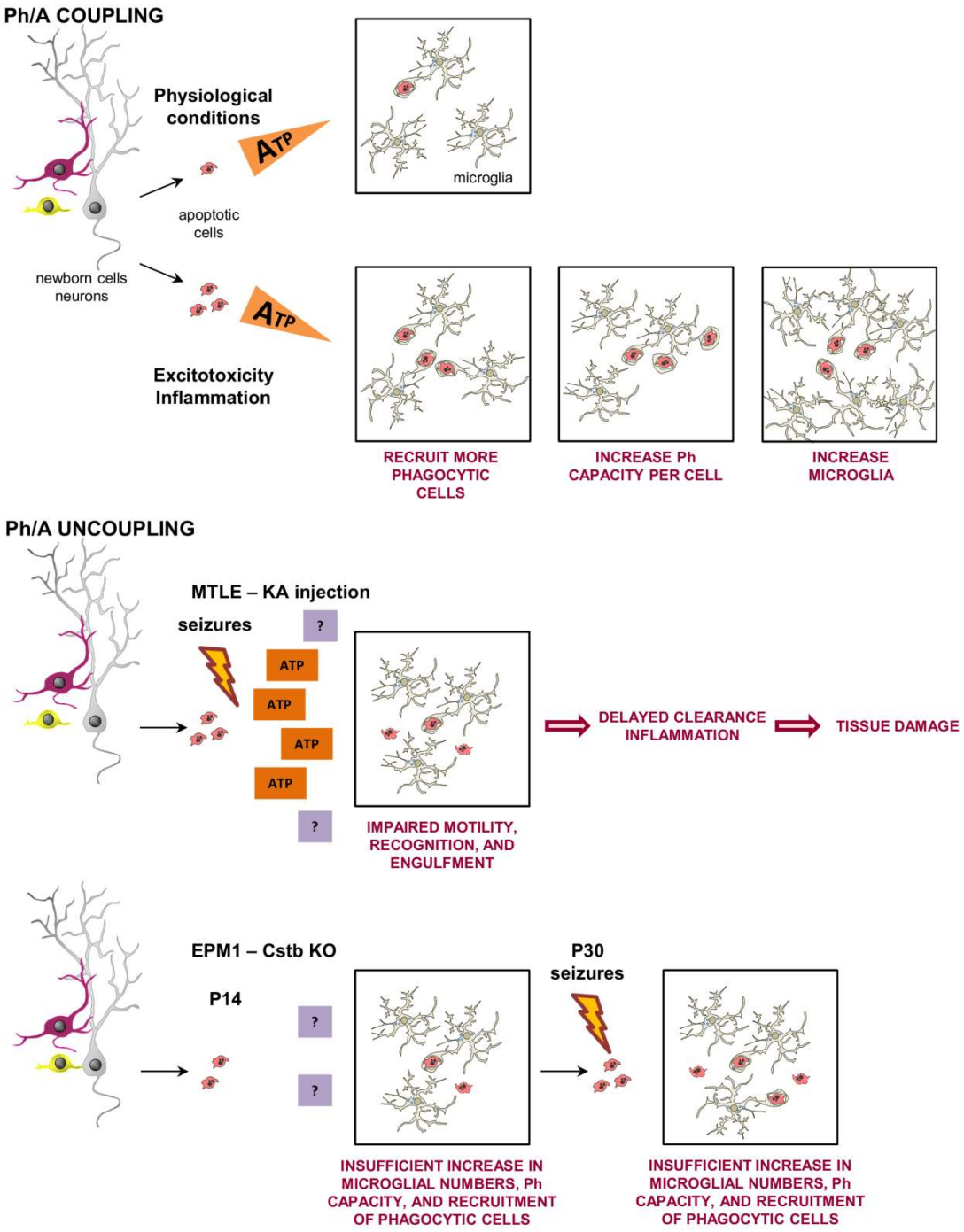

Figure 33. Microglial phagocytosis/apoptosis coupling in health and disease. In physiological conditions as well as during excitotoxicity and inflammation, microglial phagocytosis is tightly coupled to apoptosis due to "find-me" signals released by apoptotic cells, such as ATP. Microglia display a combination of three adaptation strategies to boost their phagocytosis efficiency: recruit more phagocytic cells, increase the phagocytic capacity per cell, and/or increase the number of cells. In contrast, a model of KA induced MTLE provokes seizures that lead to a widespread release of ATP, among other possible signals, and interfere with the ability of microglia to find, recognize and engulf apoptotic cells, resulting in their delayed clearance. Because phagocytosis is actively anti-inflammatory, the phagocytosis impairment was associated with the production of pro-inflammatory, epileptogenic cytokines. Moreover, constitutive KO of Cstb induced seizures at PND30 and microglial phagocytosis impairment as early as

PND14, even though microglial numbers and Ph capacity increased. The mechanisms inducing the Ph/A uncoupling in Cstb KO mice remain unknown. Adapted from (Abiega et al., 2016).

8 CONCLUSIONS

8. CONCLUSIONS

1. MICROGLIAL PHAGOCYTOSIS IS COUPLED TO APOPTOSIS IN PHYSIOLOGICAL AND PATHOLOGICAL CONDITIONS

- Microglial phagocytosis is coupled to cell apoptosis during excitotoxicity in vitro because the Ph capacity increases proportionally to the increase in apoptosis.
- Microglial phagocytosis is coupled to cell apoptosis during acute inflammation in vivo because the Ph capacity increases proportionally to the increase in apoptosis.
- Microglial phagocytosis is coupled to cell apoptosis during chronic inflammation in vivo because microglial numbers and the Ph capacity increase proportionally to the increase in apoptosis.
- Microglia have a large phagocytic reservoir because they can boost their phagocytic potential by combining three adaptation strategies: recruit more phagocytic cells, increase the Ph capacity per cell and/or increase the numbers of microglia.

2. SEIZURES INDUCE A MICROGLIAL PHAGOCYTOSIS-APOPTOSIS UNCOUPLING IN EPILEPSY

- Microglial phagocytosis is uncoupled from apoptosis following seizures in vivo in a pharmacological (MTLE) and a genetic (EPM1) model of epilepsy because MTLE microglia become non-phagocytic and EPM1 microglia increase their microglial numbers and Ph capacity in a way that is not proportional to the increase in apoptosis.
- Microglia remain the most determinant phagocytes during phagocytosis-apoptosis uncoupling in MTLE and EPM1 mice.
- Microglia become multinucleated in EPM1 mice.
- Microglial phagocytosis-apoptosis uncoupling could be a widespread phenomenon in the epileptic brain.

3. MICROGLIA SENSE SEIZURES VIA ATP

- Microglial phagocytosis impairment is unrelated to a direct effect of KA on microglia.
- Microglia respond to ATP released during seizures via purinergic receptors.

4. DISRUPTION OF ATP GRADIENTS IMPAIRS MICROGLIAL PHAGOCYTOSIS

- ATP overload impairs microglial phagocytosis in vitro and in vivo.
- ATP induced phagocytosis impairment is unrelated to microglial viability.
- Pannexin expression is unrelated to microglial phagocytosis impairment.

5. MICROGLIAL PHAGOCYTOSIS IMPAIRMENT IS RELATED TO REDUCED MOTILITY IN MTLE

- KA induced seizures cause a reduction in microglial motility ex vivo and in vivo.

6. MICROGLIAL PHAGOCYTOSIS-APOPTOSIS UNCOUPLING IS UNRELATED TO SEIZURES IN EPM1 MICE

- Microglial phagocytosis-apoptosis uncoupling precedes the onset of seizures in EPM1 mice, suggesting that Cstb might modulate microglial phagocytosis.

7. MICROGLIAL PHAGOCYTOSIS IMPAIRMENT HAS DETRIMENTAL CONSEQUENCES FOR THE BRAIN

- Microglial phagocytosis impairment correlates with the development of an inflammatory response in MTLE.
- Microglial phagocytosis impairment induces a delayed clearance of apoptotic cells in MTLE.
- Microglial phagocytosis efficiency critically affects the dynamics of apoptosis, which urges to routinely assess the microglial phagocytosis efficiency in neurodegenerative disorders.
- Since neuronal death and inflammation are hallmarks of all major neurodegenerative diseases, harnessing microglial phagocytosis may serve to control tissue damage and inflammation as a novel strategy to accelerate brain recovery.

9 BIBLIOGRAPHY

9. BIBLIOGRAPHY

A

Abiega, O., Beccari, S., Diaz-Aparicio, I., Nadjar, A., Laye, S., Leyrolle, Q., Gomez-Nicola, D., Domercq, M., Perez-Samartin, A., Sanchez-Zafra, V.*, et al.* (2016). Neuronal Hyperactivity Disturbs ATP Microgradients, Impairs Microglial Motility, and Reduces Phagocytic Receptor Expression Triggering Apoptosis/Microglial Phagocytosis Uncoupling. PLoS Biol *14*, e1002466.

Abrahamson, M., Alvarez-Fernandez, M., and Nathanson, C.M. (2003). Cystatins. Biochem Soc Symp, 179-199.

Aguzzi, A., Barres, B.A., and Bennett, M.L. (2013). Microglia: scapegoat, saboteur, or something else? Science *339*, 156-161.

Ahl, M., Avdic, U., Skoug, C., Ali, I., Chugh, D., Johansson, U.E., and Ekdahl, C.T. (2016). Immune response in the eye following epileptic seizures. Journal of neuroinflammation *13*, 155.

Akahoshi, N., Murashima, Y.L., Himi, T., Ishizaki, Y., and Ishii, I. (2007). Increased expression of the lysosomal protease cathepsin S in hippocampal microglia following kainate-induced seizures. Neurosci Lett *429*, 136-141.

Alberts, B., Johnson, A., Lewis, J., Raff, M., Roberts, K., and Walter, P. (2002). The adaptive immune system. In Molecular biology of the cell (Garland Science).

Alger, B.E. (2014). Seizing an opportunity for the endocannabinoid system. Epilepsy currents / American Epilepsy Society *14*, 272-276.

Ali, I., Chugh, D., and Ekdahl, C.T. (2015). Role of fractalkine-CX3CR1 pathway in seizure-induced microglial activation, neurodegeneration, and neuroblast production in the adult rat brain. Neurobiol Dis *74*, 194-203.

Amor, S., Puentes, F., Baker, D., and van der Valk, P. (2010). Inflammation in neurodegenerative diseases. Immunology *129*, 154-169.

Andreasson, K.I., Bachstetter, A.D., Colonna, M., Ginhoux, F., Holmes, C., Lamb, B., Landreth, G., Lee, D.C., Low, D., Lynch, M.A.*, et al.* (2016). Targeting innate immunity for neurodegenerative disorders of the central nervous system. J Neurochem *138*, 653-693.

Antony, J.M., Paquin, A., Nutt, S.L., Kaplan, D.R., and Miller, F.D. (2011). Endogenous microglia regulate development of embryonic cortical precursor cells. Journal of neuroscience research *89*, 286-298.

Aquino, D.A., Padin, C., Perez, J.M., Peng, D., Lyman, W.D., and Chiu, F.C. (1996). Analysis of glial fibrillary acidic protein, neurofilament protein, actin and heat shock proteins in human fetal brain during the second trimester. Brain Res Dev Brain Res *91*, 1-10.

Arandjelovic, S., and Ravichandran, K.S. (2015). Phagocytosis of apoptotic cells in homeostasis. Nature immunology *16*, 907-917.

Armstrong, A., and Ravichandran, K.S. (2011). Phosphatidylserine receptors: what is the new RAGE? EMBO Rep *12*, 287-288.

Arnold, T., and Betsholtz, C. (2013). The importance of microglia in the development of the vasculature in the central nervous system. Vasc Cell *5*, 4.

Arnoux, I., Hoshiko, M., Mandavy, L., Avignone, E., Yamamoto, N., and Audinat, E. (2013). Adaptive phenotype of microglial cells during the normal postnatal development of the somatosensory "Barrel" cortex. Glia *61*, 1582-1594.

Aronica, E., van Vliet, E.A., Mayboroda, O.A., Troost, D., da Silva, F.H., and Gorter, J.A. (2000). Upregulation of metabotropic glutamate receptor subtype mGluR3 and mGluR5 in reactive astrocytes in a rat model of mesial temporal lobe epilepsy. Eur J Neurosci *12*, 2333-2344.

Askew, K., Li, K., Olmos-Alonso, A., Garcia-Moreno, F., Liang, Y., Richardson, P., Tipton, T., Chapman, M.A., Riecken, K., Beccari, S.*, et al.* (2017). Coupled Proliferation and Apoptosis Maintain the Rapid Turnover of Microglia in the Adult Brain. Cell Rep *18*, 391-405.

Atagi, Y., Liu, C.C., Painter, M.M., Chen, X.F., Verbeeck, C., Zheng, H., Li, X., Rademakers, R., Kang, S.S., Xu, H.*, et al.* (2015). Apolipoprotein E Is a Ligand for Triggering Receptor Expressed on Myeloid Cells 2 (TREM2). J Biol Chem *290*, 26043-26050.

Avignone, E., Lepleux, M., Angibaud, J., and Nagerl, U.V. (2015). Altered morphological dynamics of activated microglia after induction of status epilepticus. Journal of neuroinflammation *12*, 202.

Avignone, E., Ulmann, L., Levavasseur, F., Rassendren, F., and Audinat, E. (2008). Status epilepticus induces a particular microglial activation state characterized by enhanced purinergic signaling. J Neurosci *28*, 9133-9144.

B

Babb, T.L., Pereira-Leite, J., Mathern, G.W., and Pretorius, J.K. (1995). Kainic acid induced hippocampal seizures in rats: comparisons of acute and chronic seizures using intrahippocampal versus systemic injections. Ital J Neurol Sci *16*, 39-44.

Banerjee, M., Sasse, V.A., Wang, Y., Maulik, M., and Kar, S. (2015). Increased levels and activity of cathepsins B and D in kainate-induced toxicity. Neuroscience *284*, 360-373.

Barber, G.N. (2001). Host defense, viruses and apoptosis. Cell Death Differ *8*, 113-126.

Baron, R., Babcock, A.A., Nemirovsky, A., Finsen, B., and Monsonego, A. (2014). Accelerated microglial pathology is associated with Abeta plaques in mouse models of Alzheimer's disease. Aging Cell *13*, 584-595.

Ben-Ari, Y., and Cossart, R. (2000). Kainate, a double agent that generates seizures: two decades of progress. Trends Neurosci *23*, 580-587.

Ben-Ari, Y., and Lagowska, J. (1978). [Epileptogenic action of intra-amygdaloid injection of kainic acid]. C R Acad Sci Hebd Seances Acad Sci D *287*, 813-816.

Benveniste, E.N. (1992). Inflammatory cytokines within the central nervous system: sources, function, and mechanism of action. American Journal of Physiology - Cell Physiology *263*, C1-C16.

Beppu, K., Kosai, Y., Kido, M.A., Akimoto, N., Mori, Y., Kojima, Y., Fujita, K., Okuno, Y., Yamakawa, Y., Ifuku, M.*, et al.* (2013). Expression, subunit composition, and function of AMPA-type glutamate receptors are changed in activated microglia; possible contribution of GluA2 (GluR-B)-deficiency under pathological conditions. Glia *61*, 881-891.

Bisogno, T., and Di Marzo, V. (2010). Cannabinoid receptors and endocannabinoids: role in neuroinflammatory and neurodegenerative disorders. CNS & neurological disorders drug targets *9*, 564-573.

Block, M.L., and Hong, J.S. (2005). Microglia and inflammation-mediated neurodegeneration: multiple triggers with a common mechanism. Prog Neurobiol *76*, 77-98.

Bolmont, T., Haiss, F., Eicke, D., Radde, R., Mathis, C.A., Klunk, W.E., Kohsaka, S., Jucker, M., and Calhoun, M.E. (2008). Dynamics of the microglial/amyloid interaction indicate a role in plaque maintenance. J Neurosci *28*, 4283-4292.

Bonfoco, E., Krainc, D., Ankarcrona, M., Nicotera, P., and Lipton, S.A. (1995). Apoptosis and necrosis: two distinct events induced, respectively, by mild and intense insults with N-methyl-D-aspartate or nitric oxide/superoxide in cortical cell cultures. Proc Natl Acad Sci U S A *92*, 7162-7166.

Boucsein, C., Zacharias, R., Farber, K., Pavlovic, S., Hanisch, U.K., and Kettenmann, H. (2003). Purinergic receptors on microglial cells: functional expression in acute brain slices and modulation of microglial activation in vitro. Eur J Neurosci *17*, 2267-2276.

Bouilleret, V., Ridoux, V., Depaulis, A., Marescaux, C., Nehlig, A., and Le Gal La Salle, G. (1999). Recurrent seizures and hippocampal sclerosis following intrahippocampal kainate injection in adult mice: electroencephalography, histopathology and synaptic reorganization similar to mesial temporal lobe epilepsy. Neuroscience *89*, 717-729.

Boyd-Tressler, A., Penuela, S., Laird, D.W., and Dubyak, G.R. (2014). Chemotherapeutic drugs induce ATP release via caspase-gated pannexin-1 channels and a caspase/pannexin-1-independent mechanism. J Biol Chem *289*, 27246-27263.

Bromme, D., Rinne, R., and Kirschke, H. (1991). Tight-binding inhibition of cathepsin S by cystatins. Biomed Biochim Acta *50*, 631-635.

Buss, A., Brook, G.A., Kakulas, B., Martin, D., Franzen, R., Schoenen, J., Noth, J., and Schmitt, A.B. (2004). Gradual loss of myelin and formation of an astrocytic scar during Wallerian degeneration in the human spinal cord. Brain *127*, 34-44.

Busse, B. MultiStackReg v1.45 (http://bradbusse.net/sciencedownloads.html).

Bustin, S.A., Benes, V., Garson, J.A., Hellemans, J., Huggett, J., Kubista, M., Mueller, R., Nolan, T., Pfaffl, M.W., Shipley, G.L.*, et al.* (2009). The MIQE guidelines: minimum information for publication of quantitative real-time PCR experiments. Clinical chemistry *55*, 611-622.

Butovsky, O., Siddiqui, S., Gabriely, G., Lanser, A.J., Dake, B., Murugaiyan, G., Doykan, C.E., Wu, P.M., Gali, R.R., Iyer, L.K.*, et al.* (2012). Modulating inflammatory monocytes with a unique microRNA gene signature ameliorates murine ALS. J Clin Invest *122*, 3063-3087.

Byrne, A., and Reen, D.J. (2002). Lipopolysaccharide induces rapid production of IL-10 by monocytes in the presence of apoptotic neutrophils. J Immunol *168*, 1968-1977.

C

Caberoy, N.B., Alvarado, G., and Li, W. (2012). Tubby regulates microglial phagocytosis through MerTK. Journal of neuroimmunology *252*, 40-48.

Cacheaux, L.P., Ivens, S., David, Y., Lakhter, A.J., Bar-Klein, G., Shapira, M., Heinemann, U., Friedman, A., and Kaufer, D. (2009). Transcriptome profiling reveals TGF-beta signaling involvement in epileptogenesis. J Neurosci *29*, 8927-8935.

Calandria, J.M., Marcheselli, V.L., Mukherjee, P.K., Uddin, J., Winkler, J.W., Petasis, N.A., and Bazan, N.G. (2009). Selective survival rescue in 15-lipoxygenase-1-deficient retinal pigment epithelial cells by the novel docosahexaenoic acid-derived mediator, neuroprotectin D1. J Biol Chem *284*, 17877-17882.

Cámara-Lemarroy, C.R., Guzmán-de la Garza, F.J., and Fernández-Garza, N.E. (2010). Molecular Inflammatory Mediators in Peripheral Nerve Degeneration and Regeneration. Neuroimmunomodulation *17*, 314-324.

Capani, F., Ellisman, M.H., and Martone, M.E. (2001). Filamentous actin is concentrated in specific subpopulations of neuronal and glial structures in rat central nervous system. Brain Research *923*, 1-11.

Cappellano, G., Carecchio, M., Fleetwood, T., Magistrelli, L., Cantello, R., Dianzani, U., and Comi, C. (2013). Immunity and inflammation in neurodegenerative diseases. Am J Neurodegener Dis *2*, 89-107.

Casano, A.M., and Peri, F. (2015). Microglia: multitasking specialists of the brain. Developmental cell *32*, 469-477.

Cendes, F. (2005). Mesial temporal lobe epilepsy syndrome: an updated overview. Journal of Epilepsy and Clinical Neurophysiology *11*, 141-144.

Cipriani, R., Domercq, M., and Matute, C. (2014). Ischemia and Stroke. In Microglia in Health and Disease, M.-È. Tremblay, and A. Sierra, eds. (New York, NY: Springer New York), pp. 413-435.

Clark, A.K., and Malcangio, M. (2012). Microglial signalling mechanisms: Cathepsin S and Fractalkine. Exp Neurol *234*, 283-292.

Cossart, R., Tyzio, R., Dinocourt, C., Esclapez, M., Hirsch, J.C., Ben-Ari, Y., and Bernard, C. (2001). Presynaptic kainate receptors that enhance the release of GABA on CA1 hippocampal interneurons. Neuron *29*, 497-508.

Coull, J.A., Beggs, S., Boudreau, D., Boivin, D., Tsuda, M., Inoue, K., Gravel, C., Salter, M.W., and De Koninck, Y. (2005). BDNF from microglia causes the shift in neuronal anion gradient underlying neuropathic pain. Nature *438*, 1017-1021.

Crain, J.M., Nikodemova, M., and Watters, J.J. (2009). Expression of P2 nucleotide receptors varies with age and sex in murine brain microglia. Journal of neuroinflammation *6*, 24.

Crespel, A., Coubes, P., Rousset, M.C., Brana, C., Rougier, A., Rondouin, G., Bockaert, J., Baldy-Moulinier, M., and Lerner-Natoli, M. (2002). Inflammatory reactions in human medial temporal lobe epilepsy with hippocampal sclerosis. Brain Res *952*, 159-169.

Cross, A.K., and Woodroofe, M.N. (1999). Chemokines induce migration and changes in actin polymerization in adult rat brain microglia and a human fetal microglial cell line in vitro. Journal of neuroscience research *55*, 17-23.

Crouch, S.P., Kozlowski, R., Slater, K.J., and Fletcher, J. (1993). The use of ATP bioluminescence as a measure of cell proliferation and cytotoxicity. J Immunol Methods *160*, 81-88.

Crowe, M.J., Bresnahan, J.C., Shuman, S.L., Masters, J.N., and Beattie, M.S. (1997). Apoptosis and delayed degeneration after spinal cord injury in rats and monkeys. Nat Med *3*, 73-76.

Crunelli, V., Carmignoto, G., and Steinhauser, C. (2015). Novel astrocyte targets: new avenues for the therapeutic treatment of epilepsy. Neuroscientist *21*, 62-83.

Cunha, R.A., Sebastiao, A.M., and Ribeiro, J.A. (1998). Inhibition by ATP of hippocampal synaptic transmission requires localized extracellular catabolism by ecto-nucleotidases into adenosine and channeling to adenosine A1 receptors. J Neurosci *18*, 1987-1995.

Cunningham, C.L., Martinez-Cerdeno, V., and Noctor, S.C. (2013). Microglia regulate the number of neural precursor cells in the developing cerebral cortex. J Neurosci *33*, 4216-4233.

Curia, G., Longo, D., Biagini, G., Jones, R.S., and Avoli, M. (2008). The pilocarpine model of temporal lobe epilepsy. Journal of neuroscience methods *172*, 143-157.

Czeh, M., Gressens, P., and Kaindl, A.M. (2011). The yin and yang of microglia. Dev Neurosci *33*, 199-209.

Chekeni, F.B., Elliott, M.R., Sandilos, J.K., Walk, S.F., Kinchen, J.M., Lazarowski, E.R., Armstrong, A.J., Penuela, S., Laird, D.W., Salvesen, G.S.*, et al.* (2010). Pannexin 1 channels mediate 'find-me' signal release and membrane permeability during apoptosis. Nature *467*, 863-867.

Chen, T., Koga, K., Li, X.Y., and Zhuo, M. (2010). Spinal microglial motility is independent of neuronal activity and plasticity in adult mice. Mol Pain *6*, 19.

Cherry, J.D., Olschowka, J.A., and O'Banion, M.K. (2014). Neuroinflammation and M2 microglia: the good, the bad, and the inflamed. Journal of neuroinflammation *11*, 98.

Choi, J., and Koh, S. (2008). Role of brain inflammation in epileptogenesis. Yonsei Med J *49*, 1-18.

Christensen, R.N., Ha, B.K., Sun, F., Bresnahan, J.C., and Beattie, M.S. (2006). Kainate induces rapid redistribution of the actin cytoskeleton in ameboid microglia. Journal of neuroscience research *84*, 170-181.

D

Dahl, G., Qiu, F., and Wang, J. (2013). The bizarre pharmacology of the ATP release channel pannexin1. Neuropharmacology *75*, 583-593.

Dalby, N.O., and Mody, I. (2001). The process of epileptogenesis: a pathophysiological approach. Curr Opin Neurol *14*, 187-192.

Dale, N., and Frenguelli, B.G. (2009). Release of adenosine and ATP during ischemia and epilepsy. Curr Neuropharmacol *7*, 160-179.

Davalos, D., Grutzendler, J., Yang, G., Kim, J.V., Zuo, Y., Jung, S., Littman, D.R., Dustin, M.L., and Gan, W.B. (2005). ATP mediates rapid microglial response to local brain injury in vivo. Nat Neurosci *8*, 752-758.

Davalos, D., Ryu, J.K., Merlini, M., Baeten, K.M., Le Moan, N., Petersen, M.A., Deerinck, T.J., Smirnoff, D.S., Bedard, C., Hakozaki, H.*, et al.* (2012). Fibrinogen-induced perivascular microglial clustering is required for the development of axonal damage in neuroinflammation. Nat Commun *3*, 1227.

Daws, M.R., Sullam, P.M., Niemi, E.C., Chen, T.T., Tchao, N.K., and Seaman, W.E. (2014). Pattern Recognition by TREM-2: Binding of Anionic Ligands. The Journal of Immunology *171*, 594.

Dayer, A.G., Ford, A.A., Cleaver, K.M., Yassaee, M., and Cameron, H.A. (2003). Short-term and long-term survival of new neurons in the rat dentate gyrus. J Comp Neurol *460*, 563-572.

De Simone, R., Ajmone-Cat, M.A., Tirassa, P., and Minghetti, L. (2003). Apoptotic PC12 cells exposing phosphatidylserine promote the production of anti-inflammatory and neuroprotective molecules by microglial cells. J Neuropathol Exp Neurol *62*, 208-216.

De Simoni, A., Allen, N.J., and Attwell, D. (2008). Charge compensation for NADPH oxidase activity in microglia in rat brain slices does not involve a proton current. Eur J Neurosci *28*, 1146-1156.

Desjardins, M., Huber, L.A., Parton, R.G., and Griffiths, G. (1994). Biogenesis of phagolysosomes proceeds through a sequential series of interactions with the endocytic apparatus. J Cell Biol *124*, 677-688.

Devi, L.A. (2000). G-protein-coupled receptor dimers in the lime light. Trends Pharmacol Sci *21*, 324-326.

Di Giaimo, R., Riccio, M., Santi, S., Galeotti, C., Ambrosetti, D.C., and Melli, M. (2002). New insights into the molecular basis of progressive myoclonus epilepsy: a multiprotein complex with cystatin B. Hum Mol Genet *11*, 2941-2950.

Diaz-Aparicio, I., Beccari, S., Abiega, O., and Sierra, A. (2016). Clearing the corpses: regulatory mechanisms, novel tools, and therapeutic potential of harnessing microglial phagocytosis in the diseased brain. Neural Regen Res *11*, 1533-1539.

Dibaj, P., Steffens, H., Nadrigny, F., Neusch, C., Kirchhoff, F., and Schomburg, E.D. (2010). Long-lasting post-mortem activity of spinal microglia in situ in mice. Journal of neuroscience research *88*, 2431-2440.

Dissing-Olesen, L., Ladeby, R., Nielsen, H.H., Toft-Hansen, H., Dalmau, I., and Finsen, B. (2007). Axonal lesion-induced microglial proliferation and microglial cluster formation in the mouse. Neuroscience *149*, 112-122.

Dissing-Olesen, L., LeDue, J.M., Rungta, R.L., Hefendehl, J.K., Choi, H.B., and MacVicar, B.A. (2014). Activation of neuronal NMDA receptors triggers transient ATP-mediated microglial process outgrowth. J Neurosci *34*, 10511-10527.

Domercq, M., Perez-Samartin, A., Aparicio, D., Alberdi, E., Pampliega, O., and Matute, C. (2010). P2X7 receptors mediate ischemic damage to oligodendrocytes. Glia *58*, 730-740.

Domercq, M., Vazquez-Villoldo, N., and Matute, C. (2013). Neurotransmitter signaling in the pathophysiology of microglia. Front Cell Neurosci *7*, 49.

Dong, X.X., Wang, Y., and Qin, Z.H. (2009). Molecular mechanisms of excitotoxicity and their relevance to pathogenesis of neurodegenerative diseases. Acta Pharmacol Sin *30*, 379-387.

Dragunow, M., and Faull, R. (1989). The use of c-fos as a metabolic marker in neuronal pathway tracing. Journal of neuroscience methods *29*, 261-265.

Dube, C.M., Ravizza, T., Hamamura, M., Zha, Q., Keebaugh, A., Fok, K., Andres, A.L., Nalcioglu, O., Obenaus, A., Vezzani, A.*, et al.* (2010). Epileptogenesis provoked by prolonged experimental febrile seizures: mechanisms and biomarkers. J Neurosci *30*, 7484-7494.

Dustin, M.L. (2012). Signaling at neuro/immune synapses. J Clin Invest *122*, 1149-1155.

Duveau, V., Pouyatos, B., Bressand, K., Bouyssieres, C., Chabrol, T., Roche, Y., Depaulis, A., and Roucard, C. (2016). Differential Effects of Antiepileptic Drugs on Focal Seizures in the Intrahippocampal Kainate Mouse Model of Mesial Temporal Lobe Epilepsy. CNS Neurosci Ther *22*, 497-506.

E

Eidet, J.R., Pasovic, L., Maria, R., Jackson, C.J., and Utheim, T.P. (2014). Objective assessment of changes in nuclear morphology and cell distribution following induction of apoptosis. Diagn Pathol *9*, 92.

Ekdahl, C.T., Claasen, J.H., Bonde, S., Kokaia, Z., and Lindvall, O. (2003a). Inflammation is detrimental for neurogenesis in adult brain. Proc Natl Acad Sci U S A *100*, 13632-13637.

Ekdahl, C.T., Mohapel, P., Elmer, E., and Lindvall, O. (2001). Caspase inhibitors increase short-term survival of progenitor-cell progeny in the adult rat dentate gyrus following status epilepticus. Eur J Neurosci *14*, 937-945.

Ekdahl, C.T., Zhu, C., Bonde, S., Bahr, B.A., Blomgren, K., and Lindvall, O. (2003b). Death mechanisms in status epilepticus-generated neurons and effects of additional seizures on their survival. Neurobiol Dis *14*, 513-523.

Elliott, M.R., Chekeni, F.B., Trampont, P.C., Lazarowski, E.R., Kadl, A., Walk, S.F., Park, D., Woodson, R.I., Ostankovich, M., Sharma, P.*, et al.* (2009). Nucleotides released by apoptotic cells act as a find-me signal to promote phagocytic clearance. Nature *461*, 282-286.

Encinas, J.M., Michurina, T.V., Peunova, N., Park, J.H., Tordo, J., Peterson, D.A., Fishell, G., Koulakov, A., and Enikolopov, G. (2011). Division-coupled astrocytic differentiation and age-related depletion of neural stem cells in the adult hippocampus. Cell Stem Cell *8*, 566-579.

Encinas, J.M., Vaahtokari, A., and Enikolopov, G. (2006). Fluoxetine targets early progenitor cells in the adult brain. Proc Natl Acad Sci U S A *103*, 8233-8238.

Engelhardt, B. (2008). Immune cell entry into the central nervous system: involvement of adhesion molecules and chemokines. J Neurol Sci *274*, 23-26.

Eyo, U.B., Gu, N., De, S., Dong, H., Richardson, J.R., and Wu, L.J. (2015). Modulation of microglial process convergence toward neuronal dendrites by extracellular calcium. J Neurosci *35*, 2417-2422.

Eyo, U.B., Murugan, M., and Wu, L.J. (2017). Microglia-Neuron Communication in Epilepsy. Glia *65*, 5-18.

Eyo, U.B., Peng, J., Murugan, M., Mo, M., Lalani, A., Xie, P., Xu, P., Margolis, D.J., and Wu, L.J. (2016). Regulation of Physical Microglia-Neuron Interactions by Fractalkine Signaling after Status Epilepticus. eNeuro *3*.

Eyo, U.B., Peng, J., Swiatkowski, P., Mukherjee, A., Bispo, A., and Wu, L.J. (2014). Neuronal hyperactivity recruits microglial processes via neuronal NMDA receptors and microglial P2Y12 receptors after status epilepticus. J Neurosci *34*, 10528-10540.

F

Fabene, P.F., Bramanti, P., and Constantin, G. (2010). The emerging role for chemokines in epilepsy. Journal of neuroimmunology *224*, 22-27.

Fabene, P.F., Navarro Mora, G., Martinello, M., Rossi, B., Merigo, F., Ottoboni, L., Bach, S., Angiari, S., Benati, D., Chakir, A.*, et al.* (2008). A role for leukocyte-endothelial adhesion mechanisms in epilepsy. Nat Med *14*, 1377-1383.

Falsig, J., van Beek, J., Hermann, C., and Leist, M. (2008). Molecular basis for detection of invading pathogens in the brain. Journal of neuroscience research *86*, 1434-1447.

Fang, K.M., Yang, C.S., Sun, S.H., and Tzeng, S.F. (2009). Microglial phagocytosis attenuated by short-term exposure to exogenous ATP through P2X receptor action. J Neurochem *111*, 1225-1237.

Ferraro, T.N., Dlugos, D.J., Hakonarson, H., and Buono, R.J. (2012). Strategies for studying the epilepsy genome. In Jasper's basic mechanisms od the epilepsies, J.L. Noebels, M. Avoli, M.A. Rogawski, R.W. Olsen, and A.V. Delgado-Escueta, eds. (Oxford university press).

Ferrero-Miliani, L., Nielsen, O.H., Andersen, P.S., and Girardin, S.E. (2007). Chronic inflammation: importance of NOD2 and NALP3 in interleukin-1beta generation. Clin Exp Immunol *147*, 227-235.

Fisher, R.S., Cross, J.H., French, J.A., Higurashi, N., Hirsch, E., Jansen, F.E., Lagae, L., Moshe, S.L., Peltola, J., Roulet Perez, E.*, et al.* (2017). Operational classification of seizure types by the International League Against Epilepsy: Position Paper of the ILAE Commission for Classification and Terminology. Epilepsia *58*, 522-530.

Fisher, R.S., van Emde Boas, W., Blume, W., Elger, C., Genton, P., Lee, P., and Engel, J., Jr. (2005). Epileptic seizures and epilepsy: definitions proposed by the International League Against Epilepsy (ILAE) and the International Bureau for Epilepsy (IBE). Epilepsia *46*, 470-472.

Fontainhas, A.M., Wang, M., Liang, K.J., Chen, S., Mettu, P., Damani, M., Fariss, R.N., Li, W., and Wong, W.T. (2011). Microglial morphology and dynamic behavior is regulated by ionotropic glutamatergic and GABAergic neurotransmission. PLoS One *6*, e15973.

Forstreuter, F., Lucius, R., and Mentlein, R. (2002). Vascular endothelial growth factor induces chemotaxis and proliferation of microglial cells. Journal of neuroimmunology *132*, 93-98.

Fourgeaud, L., Traves, P.G., Tufail, Y., Leal-Bailey, H., Lew, E.D., Burrola, P.G., Callaway, P., Zagorska, A., Rothlin, C.V., Nimmerjahn, A.*, et al.* (2016). TAM receptors regulate multiple features of microglial physiology. Nature *532*, 240-244.

Fox, I.J., Paucar, A.A., Nakano, I., Mottahedeh, J., Dougherty, J.D., and Kornblum, H.I. (2004). Developmental expression of glial fibrillary acidic protein mRNA in mouse forebrain germinal zones--implications for stem cell biology. Brain Res Dev Brain Res *153*, 121-125.

Franceschetti, S., Sancini, G., Buzzi, A., Zucchini, S., Paradiso, B., Magnaghi, G., Frassoni, C., Chikhladze, M., Avanzini, G., and Simonato, M. (2007). A pathogenetic hypothesis of Unverricht-Lundborg disease onset and progression. Neurobiol Dis *25*, 675-685.

Frank-Cannon, T.C., Alto, L.T., McAlpine, F.E., and Tansey, M.G. (2009). Does neuroinflammation fan the flame in neurodegenerative diseases? Mol Neurodegener *4*, 47.

Fraser, D.A., Pisalyaput, K., and Tenner, A.J. (2010). C1q enhances microglial clearance of apoptotic neurons and neuronal blebs, and modulates subsequent inflammatory cytokine production. J Neurochem *112*, 733-743.

Fritsch, B., Reis, J., Gasior, M., Kaminski, R.M., and Rogawski, M.A. (2014). Role of GluK1 kainate receptors in seizures, epileptic discharges, and epileptogenesis. J Neurosci *34*, 5765-5775.

G

Gabrusiewicz, K., Ellert-Miklaszewska, A., Lipko, M., Sielska, M., Frankowska, M., and Kaminska, B. (2011). Characteristics of the alternative phenotype of microglia/macrophages and its modulation in experimental gliomas. PLoS One *6*, e23902.

Gahwiler, B.H., Capogna, M., Debanne, D., McKinney, R.A., and Thompson, S.M. (1997). Organotypic slice cultures: a technique has come of age. Trends Neurosci *20*, 471-477.

Gaitatzis, A., Johnson, A.L., Chadwick, D.W., Shorvon, S.D., and Sander, J.W. (2004). Life expectancy in people with newly diagnosed epilepsy. Brain *127*, 2427-2432.

Gan, L., Ye, S., Chu, A., Anton, K., Yi, S., Vincent, V.A., von Schack, D., Chin, D., Murray, J., Lohr, S.*, et al.* (2004). Identification of cathepsin B as a mediator of neuronal death induced by Abeta-activated microglial cells using a functional genomics approach. J Biol Chem *279*, 5565-5572.

Garin, J., Diez, R., Kieffer, S., Dermine, J.F., Duclos, S., Gagnon, E., Sadoul, R., Rondeau, C., and Desjardins, M. (2001). The phagosome proteome: insight into phagosome functions. J Cell Biol *152*, 165-180.

Gaudet, A.D., Popovich, P.G., and Ramer, M.S. (2011). Wallerian degeneration: gaining perspective on inflammatory events after peripheral nerve injury. Journal of neuroinflammation *8*, 110.

Gautier, E.L., Shay, T., Miller, J., Greter, M., Jakubzick, C., Ivanov, S., Helft, J., Chow, A., Elpek, K.G., Gordonov, S.*, et al.* (2012). Gene-expression profiles and transcriptional regulatory pathways that underlie the identity and diversity of mouse tissue macrophages. Nature immunology *13*, 1118-1128.

Ghorpade, A., Persidsky, Y., Swindells, S., Borgmann, K., Persidsky, R., Holter, S., Cotter, R., and Gendelman, H.E. (2005). Neuroinflammatory responses from microglia recovered from HIV-1-infected and seronegative subjects. Journal of neuroimmunology *163*, 145-156.

Ginhoux, F., Greter, M., Leboeuf, M., Nandi, S., See, P., Gokhan, S., Mehler, M.F., Conway, S.J., Ng, L.G., Stanley, E.R.*, et al.* (2010). Fate mapping analysis reveals that adult microglia derive from primitive macrophages. Science *330*, 841-845.

Ginhoux, F., Lim, S., Hoeffel, G., Low, D., and Huber, T. (2013). Origin and differentiation of microglia. Front Cell Neurosci *7*, 45.

Ginhoux, F., and Prinz, M. (2015). Origin of microglia: current concepts and past controversies. Cold Spring Harb Perspect Biol *7*, a020537.

Ginsberg, M.D. (2007). Life after cerovive: a personal perspective on ischemic neuroprotection in the post-NXY-059 era. Stroke; a journal of cerebral circulation *38*, 1967-1972.

Goh, Y.C., Yap, C.T., Huang, B.H., Cronshaw, A.D., Leung, B.P., Lai, P.B., Hart, S.P., Dransfield, I., and Ross, J.A. (2011). Heat-shock protein 60 translocates to the surface of apoptotic cells and differentiated megakaryocytes and stimulates phagocytosis. Cellular and molecular life sciences : CMLS *68*, 1581-1592.

Gomez-Nicola, D., Fransen, N.L., Suzzi, S., and Perry, V.H. (2013). Regulation of microglial proliferation during chronic neurodegeneration. J Neurosci *33*, 2481-2493.

Gomez-Nicola, D., and Perry, V.H. (2015). Microglial dynamics and role in the healthy and diseased brain: a paradigm of functional plasticity. Neuroscientist *21*, 169-184.

Gomez-Nicola, D.P., V.H. (2014). Neurodegenerative Diseases. In Microglia in Health and Disease, M.E.S. Tremblay, A., ed. (New York: Springer), pp. 437-454.

Grady, M.S., Charleston, J.S., Maris, D., Witgen, B.M., and Lifshitz, J. (2003). Neuronal and glial cell number in the hippocampus after experimental traumatic brain injury: analysis by stereological estimation. J Neurotrauma *20*, 929-941.

Graeber, M.B. (2010). Changing face of microglia. Science *330*, 783-788.

Graeber, M.B., Tetzlaff, W., Streit, W.J., and Kreutzberg, G.W. (1988). Microglial cells but not astrocytes undergo mitosis following rat facial nerve axotomy. Neurosci Lett *85*, 317-321.

Grathwohl, S.A., Kalin, R.E., Bolmont, T., Prokop, S., Winkelmann, G., Kaeser, S.A., Odenthal, J., Radde, R., Eldh, T., Gandy, S.*, et al.* (2009). Formation and maintenance of Alzheimer's disease beta-amyloid plaques in the absence of microglia. Nat Neurosci *12*, 1361-1363.

Green, D.R., and Llambi, F. (2015). Cell Death Signaling. Cold Spring Harb Perspect Biol *7*.

Greve, M.W., and Zink, B.J. (2009). Pathophysiology of traumatic brain injury. Mt Sinai J Med *76*, 97-104.

Gude, D.R., Alvarez, S.E., Paugh, S.W., Mitra, P., Yu, J., Griffiths, R., Barbour, S.E., Milstien, S., and Spiegel, S. (2008). Apoptosis induces expression of sphingosine kinase 1 to release sphingosine-1-phosphate as a "come-and-get-me" signal. FASEB J *22*, 2629-2638.

H

Haas, C.A., and Frotscher, M. (2010). Reelin deficiency causes granule cell dispersion in epilepsy. Exp Brain Res *200*, 141-149.

Hagino, Y., Kariura, Y., Manago, Y., Amano, T., Wang, B., Sekiguchi, M., Nishikawa, K., Aoki, S., Wada, K., and Noda, M. (2004). Heterogeneity and potentiation of AMPA type of glutamate receptors in rat cultured microglia. Glia *47*, 68-77.

Hanisch, U.K., and Kettenmann, H. (2007). Microglia: active sensor and versatile effector cells in the normal and pathologic brain. Nat Neurosci *10*, 1387-1394.

Hayashi, Y., Koyanagi, S., Kusunose, N., Okada, R., Wu, Z., Tozaki-Saitoh, H., Ukai, K., Kohsaka, S., Inoue, K., Ohdo, S.*, et al.* (2013). The intrinsic microglial molecular clock controls synaptic strength via the circadian expression of cathepsin S. Sci Rep *3*, 2744.

Heinrich, A., Ando, R.D., Turi, G., Rozsa, B., and Sperlagh, B. (2012). K+ depolarization evokes ATP, adenosine and glutamate release from glia in rat hippocampus: a microelectrode biosensor study. British journal of pharmacology *167*, 1003-1020.

Heinrich, C., Nitta, N., Flubacher, A., Muller, M., Fahrner, A., Kirsch, M., Freiman, T., Suzuki, F., Depaulis, A., Frotscher, M.*, et al.* (2006). Reelin deficiency and displacement of mature neurons, but not neurogenesis, underlie the formation of granule cell dispersion in the epileptic hippocampus. J Neurosci *26*, 4701-4713.

Hellwig, S., Masuch, A., Nestel, S., Katzmarski, N., Meyer-Luehmann, M., and Biber, K. (2015). Forebrain microglia from wild-type but not adult 5xFAD mice prevent amyloid-beta plaque formation in organotypic hippocampal slice cultures. Sci Rep *5*, 14624.

Hickman, S.E., and El Khoury, J. (2014). TREM2 and the neuroimmunology of Alzheimer's disease. Biochem Pharmacol *88*, 495-498.

Hickman, S.E., Kingery, N.D., Ohsumi, T.K., Borowsky, M.L., Wang, L.C., Means, T.K., and El Khoury, J. (2013). The microglial sensome revealed by direct RNA sequencing. Nat Neurosci *16*, 1896-1905.

Hines, D.J., Hines, R.M., Mulligan, S.J., and Macvicar, B.A. (2009). Microglia processes block the spread of damage in the brain and require functional chloride channels. Glia *57*, 1610-1618.

Hochreiter-Hufford, A., and Ravichandran, K.S. (2013). Clearing the dead: apoptotic cell sensing, recognition, engulfment, and digestion. Cold Spring Harb Perspect Biol *5*, a008748.

Hoeffel, G., Wang, Y., Greter, M., See, P., Teo, P., Malleret, B., Leboeuf, M., Low, D., Oller, G., Almeida, F*., et al.* (2012). Adult Langerhans cells derive predominantly from embryonic fetal liver monocytes with a minor contribution of yolk sac-derived macrophages. The Journal of experimental medicine *209*, 1167-1181.

Hong, S., Dissing-Olesen, L., and Stevens, B. (2016). New insights on the role of microglia in synaptic pruning in health and disease. Curr Opin Neurobiol *36*, 128-134.

Hornik, T.C., Neniskyte, U., and Brown, G.C. (2014). Inflammation induces multinucleation of Microglia via PKC inhibition of cytokinesis, generating highly phagocytic multinucleated giant cells. J Neurochem *128*, 650-661.

Hosmane, S., Tegenge, M.A., Rajbhandari, L., Uapinyoying, P., Kumar, N.G., Thakor, N., and Venkatesan, A. (2012). Toll/interleukin-1 receptor domain-containing adapter inducing interferon-beta mediates microglial phagocytosis of degenerating axons. J Neurosci *32*, 7745-7757.

Hristovska, I., and Pascual, O. (2015). Deciphering Resting Microglial Morphology and Process Motility from a Synaptic Prospect. Front Integr Neurosci *9*, 73.

Hsiao, M.C., Yu, P.N., Song, D., Liu, C.Y., Heck, C.N., Millett, D., and Berger, T.W. (2014). An in vitro seizure model from human hippocampal slices using multi-electrode arrays. Journal of neuroscience methods.

Huang, W.C., Yen, F.C., Shie, F.S., Pan, C.M., Shiao, Y.J., Yang, C.N., Huang, F.L., Sung, Y.J., and Tsay, H.J. (2010). TGF-beta1 blockade of microglial chemotaxis toward Abeta aggregates involves SMAD signaling and down-regulation of CCL5. Journal of neuroinflammation *7*, 28.

Hughes, P.M., Botham, M.S., Frentzel, S., Mir, A., and Perry, V.H. (2002). Expression of fractalkine (CX3CL1) and its receptor, CX3CR1, during acute and chronic inflammation in the rodent CNS. Glia *37*, 314-327.

Huynh, M.L., Fadok, V.A., and Henson, P.M. (2002). Phosphatidylserine-dependent ingestion of apoptotic cells promotes TGF-beta1 secretion and the resolution of inflammation. J Clin Invest *109*, 41-50.

I

Imamoto, K., and Leblond, C.P. (1978). Radioautographic investigation of gliogenesis in the corpus callosum of young rats. II. Origin of microglial cells. J Comp Neurol *180*, 139-163.

Ito, H., and Hamerman, J.A. (2012). TREM-2, triggering receptor expressed on myeloid cell-2, negatively regulates TLR responses in dendritic cells. Eur J Immunol *42*, 176-185.

Ivens, S., Kaufer, D., Flores, L.P., Bechmann, I., Zumsteg, D., Tomkins, O., Seiffert, E., Heinemann, U., and Friedman, A. (2007). TGF-beta receptor-mediated albumin uptake into astrocytes is involved in neocortical epileptogenesis. Brain *130*, 535-547.

J

Jaiswal, M.K., Zech, W.D., Goos, M., Leutbecher, C., Ferri, A., Zippelius, A., Carri, M.T., Nau, R., and Keller, B.U. (2009). Impairment of mitochondrial calcium handling in a mtSOD1 cell culture model of motoneuron disease. BMC Neurosci *10*, 64.

Jensen, F.E. (2011). Epilepsy as a spectrum disorder: Implications from novel clinical and basic neuroscience. Epilepsia *52 Suppl 1*, 1-6.

Jin, X., and Yamashita, T. (2016). Microglia in central nervous system repair after injury. Journal of biochemistry *159*, 491-496.

Jinushi, M., Nakazaki, Y., Dougan, M., Carrasco, D.R., Mihm, M., and Dranoff, G. (2007). MFG-E8-mediated uptake of apoptotic cells by APCs links the pro- and antiinflammatory activities of GM-CSF. J Clin Invest *117*, 1902-1913.

Joensuu, T., Lehesjoki, A.E., and Kopra, O. (2008). Molecular background of EPM1-Unverricht-Lundborg disease. Epilepsia *49*, 557-563.

Joensuu, T., Tegelberg, S., Reinmaa, E., Segerstrale, M., Hakala, P., Pehkonen, H., Korpi, E.R., Tyynela, J., Taira, T., Hovatta, I.*, et al.* (2014). Gene expression alterations in the cerebellum and granule neurons of Cstb(-/-) mouse are associated with early synaptic changes and inflammation. PLoS One *9*, e89321.

Jung, S., Aliberti, J., Graemmel, P., Sunshine, M.J., Kreutzberg, G.W., Sher, A., and Littman, D.R. (2000). Analysis of fractalkine receptor CX(3)CR1 function by targeted deletion and green fluorescent protein reporter gene insertion. Molecular and cellular biology *20*, 4106-4114.

K

Kaindl, A.M., Degos, V., Peineau, S., Gouadon, E., Chhor, V., Loron, G., Le Charpentier, T., Josserand, J., Ali, C., Vivien, D.*, et al.* (2012). Activation of microglial N-methyl-D-aspartate receptors triggers inflammation and neuronal cell death in the developing and mature brain. Ann Neurol *72*, 536-549.

Kalman, M., and Ajtai, B.M. (2001). A comparison of intermediate filament markers for presumptive astroglia in the developing rat neocortex: immunostaining against nestin reveals more detail, than GFAP or vimentin. Int J Dev Neurosci *19*, 101-108.

Kalviainen, R., Khyuppenen, J., Koskenkorva, P., Eriksson, K., Vanninen, R., and Mervaala, E. (2008). Clinical picture of EPM1-Unverricht-Lundborg disease. Epilepsia *49*, 549-556.

Kamphuis, W., Orre, M., Kooijman, L., Dahmen, M., and Hol, E.M. (2012). Differential cell proliferation in the cortex of the APPswePS1dE9 Alzheimer's disease mouse model. Glia *60*, 615-629.

Kan, A.A., de Jager, W., de Wit, M., Heijnen, C., van Zuiden, M., Ferrier, C., van Rijen, P., Gosselaar, P., Hessel, E., van Nieuwenhuizen, O.*, et al.* (2012a). Protein expression profiling of inflammatory mediators in human temporal lobe epilepsy reveals co-activation of multiple chemokines and cytokines. Journal of neuroinflammation *9*, 207.

Kan, A.A., van Erp, S., Derijck, A.A., de Wit, M., Hessel, E.V., O'Duibhir, E., de Jager, W., Van Rijen, P.C., Gosselaar, P.H., de Graan, P.N.*, et al.* (2012b). Genome-wide microRNA profiling of human temporal lobe epilepsy identifies modulators of the immune response. Cellular and molecular life sciences : CMLS *69*, 3127-3145.

Kawabori, M., Kacimi, R., Kauppinen, T., Calosing, C., Kim, J.Y., Hsieh, C.L., Nakamura, M.C., and Yenari, M.A. (2015). Triggering receptor expressed on myeloid cells 2 (TREM2) deficiency attenuates phagocytic

activities of microglia and exacerbates ischemic damage in experimental stroke. J Neurosci *35*, 3384-3396.

Kettenmann, H., Hanisch, U.K., Noda, M., and Verkhratsky, A. (2011). Physiology of microglia. Physiol Rev *91*, 461-553.

Kierdorf, K., Erny, D., Goldmann, T., Sander, V., Schulz, C., Perdiguero, E.G., Wieghofer, P., Heinrich, A., Riemke, P., Holscher, C*., et al.* (2013). Microglia emerge from erythromyeloid precursors via Pu.1- and Irf8-dependent pathways. Nat Neurosci *16*, 273-280.

Kim, S., Ock, J., Kim, A.K., Lee, H.W., Cho, J.Y., Kim, D.R., Park, J.Y., and Suk, K. (2007). Neurotoxicity of microglial cathepsin D revealed by secretome analysis. J Neurochem *103*, 2640-2650.

Kingham, P.J., and Pocock, J.M. (2001). Microglial secreted cathepsin B induces neuronal apoptosis. J Neurochem *76*, 1475-1484.

Kleen, J.K., and Holmes, G.L. (2010). Taming TLR4 may ease seizures. Nat Med *16*, 369-370.

Koizumi, S., Ohsawa, K., Inoue, K., and Kohsaka, S. (2013). Purinergic receptors in microglia: functional modal shifts of microglia mediated by P2 and P1 receptors. Glia *61*, 47-54.

Koizumi, S., Shigemoto-Mogami, Y., Nasu-Tada, K., Shinozaki, Y., Ohsawa, K., Tsuda, M., Joshi, B.V., Jacobson, K.A., Kohsaka, S., and Inoue, K. (2007). UDP acting at P2Y6 receptors is a mediator of microglial phagocytosis. Nature *446*, 1091-1095.

Korber, I., Katayama, S., Einarsdottir, E., Krjutskov, K., Hakala, P., Kere, J., Lehesjoki, A.E., and Joensuu, T. (2016). Gene-Expression Profiling Suggests Impaired Signaling via the Interferon Pathway in Cstb-/- Microglia. PLoS One *11*, e0158195.

Koskenkorva, P., Niskanen, E., Hypponen, J., Kononen, M., Mervaala, E., Soininen, H., Kalviainen, R., and Vanninen, R. (2012). Sensorimotor, visual, and auditory cortical atrophy in Unverricht-Lundborg disease mapped with cortical thickness analysis. AJNR Am J Neuroradiol *33*, 878-883.

Koskiniemi, M., Donner, M., Majuri, H., Haltia, M., and Norio, R. (1974). Progressive myoclonus epilepsy. A clinical and histopathological study. Acta Neurol Scand *50*, 307-332.

Krabbe, G., Halle, A., Matyash, V., Rinnenthal, J.L., Eom, G.D., Bernhardt, U., Miller, K.R., Prokop, S., Kettenmann, H., and Heppner, F.L. (2013). Functional impairment of microglia coincides with Beta-amyloid deposition in mice with Alzheimer-like pathology. PLoS One *8*, e60921.

Kralic, J.E., Ledergerber, D.A., and Fritschy, J.M. (2005). Disruption of the neurogenic potential of the dentate gyrus in a mouse model of temporal lobe epilepsy with focal seizures. Eur J Neurosci *22*, 1916-1927.

Krishan, A. (1975). Rapid flow cytofluorometric analysis of mammalian cell cycle by propidium iodide staining. J Cell Biol *66*, 188-193.

Krysko, D.V., Vanden Berghe, T., D'Herde, K., and Vandenabeele, P. (2008). Apoptosis and necrosis: detection, discrimination and phagocytosis. Methods *44*, 205-221.

Kwan, P., and Brodie, M.J. (2006). Refractory epilepsy: mechanisms and solutions. Expert Rev Neurother *6*, 397-406.

Kwon, M.J., Oh, E., Lee, S., Roh, M.R., Kim, S.E., Lee, Y., Choi, Y.L., In, Y.H., Park, T., Koh, S.S*., et al.* (2009). Identification of novel reference genes using multiplatform expression data and their validation for quantitative gene expression analysis. PLoS One *4*, e6162.

L

Lai, A.Y., and McLaurin, J. (2012). Clearance of amyloid-beta peptides by microglia and macrophages: the issue of what, when and where. Future Neurol *7*, 165-176.

Lai, A.Y., Swayze, R.D., El-Husseini, A., and Song, C. (2006). Interleukin-1 beta modulates AMPA receptor expression and phosphorylation in hippocampal neurons. Journal of neuroimmunology *175*, 97-106.

Lalancette-Hebert, M., Gowing, G., Simard, A., Weng, Y.C., and Kriz, J. (2007). Selective ablation of proliferating microglial cells exacerbates ischemic injury in the brain. J Neurosci *27*, 2596-2605.

Lalioti, M.D., Scott, H.S., Buresi, C., Rossier, C., Bottani, A., Morris, M.A., Malafosse, A., and Antonarakis, S.E. (1997). Dodecamer repeat expansion in cystatin B gene in progressive myoclonus epilepsy. Nature *386*, 847-851.

Lauber, K., Blumenthal, S.G., Waibel, M., and Wesselborg, S. (2004). Clearance of apoptotic cells: getting rid of the corpses. Mol Cell *14*, 277-287.

Lauber, K., Bohn, E., Krober, S.M., Xiao, Y.J., Blumenthal, S.G., Lindemann, R.K., Marini, P., Wiedig, C., Zobywalski, A., Baksh, S., *et al.* (2003). Apoptotic cells induce migration of phagocytes via caspase-3-mediated release of a lipid attraction signal. Cell *113*, 717-730.

Lawrie, A.M., Noble, M.E., Tunnah, P., Brown, N.R., Johnson, L.N., and Endicott, J.A. (1997). Protein kinase inhibition by staurosporine revealed in details of the molecular interaction with CDK2. Nat Struct Biol *4*, 796-801.

Lawson, L.J., Perry, V.H., Dri, P., and Gordon, S. (1990). Heterogeneity in the distribution and morphology of microglia in the normal adult mouse brain. Neuroscience *39*, 151-170.

Lee, J.E., Liang, K.J., Fariss, R.N., and Wong, W.T. (2008a). Ex vivo dynamic imaging of retinal microglia using time-lapse confocal microscopy. Invest Ophthalmol Vis Sci *49*, 4169-4176.

Lee, J.K., Won, J.S., Singh, A.K., and Singh, I. (2008b). Statin inhibits kainic acid-induced seizure and associated inflammation and hippocampal cell death. Neurosci Lett *440*, 260-264.

Lee, T.T., Martin, F.C., and Merrill, J.E. (1993). Lymphokine induction of rat microglia multinucleated giant cell formation. Glia *8*, 51-61.

Lee, W.L., Mason, D., Schreiber, A.D., and Grinstein, S. (2007). Quantitative analysis of membrane remodeling at the phagocytic cup. Mol Biol Cell *18*, 2883-2892.

Legido, A., and Katsetos, C.D. (2014). Experimental studies in epilepsy: immunologic and inflammatory mechanisms. Semin Pediatr Neurol *21*, 197-206.

Leist, M., and Jaattela, M. (2001). Four deaths and a funeral: from caspases to alternative mechanisms. Nat Rev Mol Cell Biol *2*, 589-598.

Lerma, J. (2003). Roles and rules of kainate receptors in synaptic transmission. Nat Rev Neurosci *4*, 481-495.

Levesque, M., and Avoli, M. (2013). The kainic acid model of temporal lobe epilepsy. Neurosci Biobehav Rev *37*, 2887-2899.

Li, Q., Jagannath, C., Rao, P.K., Singh, C.R., and Lostumbo, G. (2010). Analysis of phagosomal proteomes: from latex-bead to bacterial phagosomes. Proteomics *10*, 4098-4116.

Li, T., Pang, S., Yu, Y., Wu, X., Guo, J., and Zhang, S. (2013). Proliferation of parenchymal microglia is the main source of microgliosis after ischaemic stroke. Brain *136*, 3578-3588.

Li, Y., Du, X.F., Liu, C.S., Wen, Z.L., and Du, J.L. (2012). Reciprocal regulation between resting microglial dynamics and neuronal activity in vivo. Developmental cell *23*, 1189-1202.

Liang, K.J., Lee, J.E., Wang, Y.D., Ma, W., Fontainhas, A.M., Fariss, R.N., and Wong, W.T. (2009). Regulation of dynamic behavior of retinal microglia by CX3CR1 signaling. Invest Ophthalmol Vis Sci *50*, 4444-4451.

Liddelow, S.A., Guttenplan, K.A., Clarke, L.E., Bennett, F.C., Bohlen, C.J., Schirmer, L., Bennett, M.L., Munch, A.E., Chung, W.S., Peterson, T.C*., et al.* (2017). Neurotoxic reactive astrocytes are induced by activated microglia. Nature *541*, 481-487.

Litman, G.W., Cannon, J.P., and Dishaw, L.J. (2005). Reconstructing immune phylogeny: new perspectives. Nature reviews Immunology *5*, 866-879.

Liu, J., Bartels, M., Lu, A., and Sharp, F.R. (2001). Microglia/macrophages proliferate in striatum and neocortex but not in hippocampus after brief global ischemia that produces ischemic tolerance in gerbil brain. J Cereb Blood Flow Metab *21*, 361-373.

Liu, S., Liu, Y., Hao, W., Wolf, L., Kiliaan, A.J., Penke, B., Rube, C.E., Walter, J., Heneka, M.T., Hartmann, T*., et al.* (2012). TLR2 is a primary receptor for Alzheimer's amyloid beta peptide to trigger neuroinflammatory activation. J Immunol *188*, 1098-1107.

Liu, Y., Walter, S., Stagi, M., Cherny, D., Letiembre, M., Schulz-Schaeffer, W., Heine, H., Penke, B., Neumann, H., and Fassbender, K. (2005). LPS receptor (CD14): a receptor for phagocytosis of Alzheimer's amyloid peptide. Brain *128*, 1778-1789.

Lu, Z., Elliott, M.R., Chen, Y., Walsh, J.T., Klibanov, A.L., Ravichandran, K.S., and Kipnis, J. (2011). Phagocytic activity of neuronal progenitors regulates adult neurogenesis. Nat Cell Biol *13*, 1076-1083.

Lucas, S.M., Rothwell, N.J., and Gibson, R.M. (2006). The role of inflammation in CNS injury and disease. British journal of pharmacology *147 Suppl 1*, S232-240.

Luhmann, H.J., Dzhala, V.I., and Ben-Ari, Y. (2000). Generation and propagation of 4-AP-induced epileptiform activity in neonatal intact limbic structures in vitro. Eur J Neurosci *12*, 2757-2768.

Llaudet, E., Botting, N.P., Crayston, J.A., and Dale, N. (2003). A three-enzyme microelectrode sensor for detecting purine release from central nervous system. Biosens Bioelectron *18*, 43-52.

M

Madore, C., Joffre, C., Delpech, J.C., De Smedt-Peyrusse, V., Aubert, A., Coste, L., Laye, S., and Nadjar, A. (2013). Early morphofunctional plasticity of microglia in response to acute lipopolysaccharide. Brain Behav Immun *34*, 151-158.

Madry, C., and Attwell, D. (2015). Receptors, ion channels, and signaling mechanisms underlying microglial dynamics. J Biol Chem *290*, 12443-12450.

Magnus, T., Chan, A., Linker, R.A., Toyka, K.V., and Gold, R. (2002). Astrocytes are less efficient in the removal of apoptotic lymphocytes than microglia cells: implications for the role of glial cells in the inflamed central nervous system. J Neuropathol Exp Neurol *61*, 760-766.

Maher, K., Jeric Kokelj, B., Butinar, M., Mikhaylov, G., Mancek-Keber, M., Stoka, V., Vasiljeva, O., Turk, B., Grigoryev, S.A., and Kopitar-Jerala, N. (2014). A role for stefin B (cystatin B) in inflammation and endotoxemia. J Biol Chem *289*, 31736-31750.

Majores, M., Eils, J., Wiestler, O.D., and Becker, A.J. (2004). Molecular profiling of temporal lobe epilepsy: comparison of data from human tissue samples and animal models. Epilepsy Res *60*, 173-178.

Mallat, M., and Chamak, B. (1994). Brain macrophages: neurotoxic or neurotrophic effector cells? J Leukoc Biol *56*, 416-422.

Manninen, O., Koskenkorva, P., Lehtimaki, K.K., Hypponen, J., Kononen, M., Laitinen, T., Kalimo, H., Kopra, O., Kalviainen, R., Grohn, O.*, et al.* (2013). White matter degeneration with Unverricht-Lundborg progressive myoclonus epilepsy: a translational diffusion-tensor imaging study in patients and cystatin B-deficient mice. Radiology *269*, 232-239.

Manninen, O., Laitinen, T., Lehtimaki, K.K., Tegelberg, S., Lehesjoki, A.E., Grohn, O., and Kopra, O. (2014). Progressive volume loss and white matter degeneration in cstb-deficient mice: a diffusion tensor and longitudinal volumetry MRI study. PLoS One *9*, e90709.

Marchi, N., Angelov, L., Masaryk, T., Fazio, V., Granata, T., Hernandez, N., Hallene, K., Diglaw, T., Franic, L., Najm, I.*, et al.* (2007). Seizure-promoting effect of blood-brain barrier disruption. Epilepsia *48*, 732-742.

Marín-Teva, J.L., Navascués, J., Sierra, A., and Mallat, M. (2014). Developmental Neuronal Elimination. In Microglia in Health and Disease, M.-È. Tremblay, and A. Sierra, eds. (New York, NY: Springer New York), pp. 175-192.

Marlatt, M.W., Bauer, J., Aronica, E., van Haastert, E.S., Hoozemans, J.J., Joels, M., and Lucassen, P.J. (2014). Proliferation in the Alzheimer hippocampus is due to microglia, not astroglia, and occurs at sites of amyloid deposition. Neural Plast *2014*, 693851.

Mascalchi, M., Michelucci, R., Cosottini, M., Tessa, C., Lolli, F., Riguzzi, P., Lehesjoki, A.E., Tosetti, M., Villari, N., and Tassinari, C.A. (2002). Brainstem involvement in Unverricht-Lundborg disease (EPM1): An MRI and (1)H MRS study. Neurology *58*, 1686-1689.

Mattson, M.P. (2000). Apoptosis in neurodegenerative disorders. Nat Rev Mol Cell Biol *1*, 120-129.

Matute, C., Alberdi, E., Domercq, M., Perez-Cerda, F., Perez-Samartin, A., and Sanchez-Gomez, M.V. (2001). The link between excitotoxic oligodendroglial death and demyelinating diseases. Trends Neurosci *24*, 224-230.

McKhann, G.M., 2nd, Wenzel, H.J., Robbins, C.A., Sosunov, A.A., and Schwartzkroin, P.A. (2003). Mouse strain differences in kainic acid sensitivity, seizure behavior, mortality, and hippocampal pathology. Neuroscience *122*, 551-561.

McNally, A.K., and Anderson, J.M. (2005). Multinucleated giant cell formation exhibits features of phagocytosis with participation of the endoplasmic reticulum. Exp Mol Pathol *79*, 126-135.

Meyer-Luehmann, M., Spires-Jones, T.L., Prada, C., Garcia-Alloza, M., de Calignon, A., Rozkalne, A., Koenigsknecht-Talboo, J., Holtzman, D.M., Bacskai, B.J., and Hyman, B.T. (2008). Rapid appearance and local toxicity of amyloid-beta plaques in a mouse model of Alzheimer's disease. Nature *451*, 720-724.

Mignone, J.L., Kukekov, V., Chiang, A.S., Steindler, D., and Enikolopov, G. (2004). Neural stem and progenitor cells in nestin-GFP transgenic mice. J Comp Neurol *469*, 311-324.

Mingam, R., Moranis, A., Bluthe, R.M., De Smedt-Peyrusse, V., Kelley, K.W., Guesnet, P., Lavialle, M., Dantzer, R., and Laye, S. (2008). Uncoupling of interleukin-6 from its signalling pathway by dietary n-3-polyunsaturated fatty acid deprivation alters sickness behaviour in mice. Eur J Neurosci *28*, 1877-1886.

Mitchell, C.H., Carre, D.A., McGlinn, A.M., Stone, R.A., and Civan, M.M. (1998). A release mechanism for stored ATP in ocular ciliary epithelial cells. Proc Natl Acad Sci U S A *95*, 7174-7178.

Miura, K., Rueden , C., Hiner, M., Schindelin, J., and Rietdorf, J. (2014). ImageJ Plugin CorrectBleach V2.0.2 (http://zenodo.org/record/30769#.VouRlvnhBaQ).

Miyamoto, A., Wake, H., Moorhouse, A.J., and Nabekura, J. (2013). Microglia and synapse interactions: fine tuning neural circuits and candidate molecules. Front Cell Neurosci *7*, 70.

Mizutani, M., Pino, P.A., Saederup, N., Charo, I.F., Ransohoff, R.M., and Cardona, A.E. (2012). The fractalkine receptor but not CCR2 is present on microglia from embryonic development throughout adulthood. J Immunol *188*, 29-36.

Monier, A., Evrard, P., Gressens, P., and Verney, C. (2006). Distribution and differentiation of microglia in the human encephalon during the first two trimesters of gestation. J Comp Neurol *499*, 565-582.

Moussaud, S., and Draheim, H.J. (2010). A new method to isolate microglia from adult mice and culture them for an extended period of time. Journal of neuroscience methods *187*, 243-253.

Mukherjee, S., Ghosh, R.N., and Maxfield, F.R. (1997). Endocytosis. Physiol Rev *77*, 759-803.

N

Nagata, S., Hanayama, R., and Kawane, K. (2010). Autoimmunity and the clearance of dead cells. Cell *140*, 619-630.

Nardacci, R., Antinori, A., Kroemer, G., and Piacentini, M. (2005). Cell death mechanisms in HIV-associated dementia: the involvement of syncytia. Cell Death Differ *12 Suppl 1*, 855-858.

Nayak, D., Roth, T.L., and McGavern, D.B. (2014). Microglia development and function. Annu Rev Immunol *32*, 367-402.

Nielsen, H.H., Ladeby, R., Fenger, C., Toft-Hansen, H., Babcock, A.A., Owens, T., and Finsen, B. (2009). Enhanced microglial clearance of myelin debris in T cell-infiltrated central nervous system. J Neuropathol Exp Neurol *68*, 845-856.

Nimmerjahn, A., Kirchhoff, F., and Helmchen, F. (2005). Resting microglial cells are highly dynamic surveillants of brain parenchyma in vivo. Science *308*, 1314-1318.

Nitecka, L., Tremblay, E., Charton, G., Bouillot, J.P., Berger, M.L., and Ben-Ari, Y. (1984). Maturation of kainic acid seizure-brain damage syndrome in the rat. II. Histopathological sequelae. Neuroscience *13*, 1073-1094.

Nitta, N., Heinrich, C., Hirai, H., and Suzuki, F. (2008). Granule cell dispersion develops without neurogenesis and does not fully depend on astroglial cell generation in a mouse model of temporal lobe epilepsy. Epilepsia *49*, 1711-1722.

Noda, M., Doi, Y., Liang, J., Kawanokuchi, J., Sonobe, Y., Takeuchi, H., Mizuno, T., and Suzumura, A. (2011). Fractalkine attenuates excito-neurotoxicity via microglial clearance of damaged neurons and antioxidant enzyme heme oxygenase-1 expression. J Biol Chem *286*, 2308-2319.

Noda, M., Nakanishi, H., Nabekura, J., and Akaike, N. (2000). AMPA-kainate subtypes of glutamate receptor in rat cerebral microglia. J Neurosci *20*, 251-258.

Noda, M., and Suzumura, A. (2012). Sweepers in the CNS: Microglial Migration and Phagocytosis in the Alzheimer Disease Pathogenesis. Int J Alzheimers Dis *2012*, 891087.

Nolte, C., Moller, T., Walter, T., and Kettenmann, H. (1996). Complement 5a controls motility of murine microglial cells in vitro via activation of an inhibitory G-protein and the rearrangement of the actin cytoskeleton. Neuroscience *73*, 1091-1107.

Norio, R., and Koskiniemi, M. (1979). Progressive myoclonus epilepsy: genetic and nosological aspects with special reference to 107 Finnish patients. Clin Genet *15*, 382-398.

O

Okuneva, O., Korber, I., Li, Z., Tian, L., Joensuu, T., Kopra, O., and Lehesjoki, A.E. (2015). Abnormal microglial activation in the Cstb(-/-) mouse, a model for progressive myoclonus epilepsy, EPM1. Glia *63*, 400-411.

Olah, M., Amor, S., Brouwer, N., Vinet, J., Eggen, B., Biber, K., and Boddeke, H.W. (2012). Identification of a microglia phenotype supportive of remyelination. Glia *60*, 306-321.

Opal, S.M., and DePalo, V.A. (2000). Anti-inflammatory cytokines. Chest *117*, 1162-1172.

Orr, A.G., Orr, A.L., Li, X.J., Gross, R.E., and Traynelis, S.F. (2009). Adenosine A(2A) receptor mediates microglial process retraction. Nat Neurosci *12*, 872-878.

Orrenius, S., Zhivotovsky, B., and Nicotera, P. (2003). Regulation of cell death: the calcium-apoptosis link. Nat Rev Mol Cell Biol *4*, 552-565.

Otahal, J., Folbergrova, J., Kovacs, R., Kunz, W.S., and Maggio, N. (2014). Epileptic focus and alteration of metabolism. International review of neurobiology *114*, 209-243.

Overstreet, L.S., Hentges, S.T., Bumaschny, V.F., de Souza, F.S., Smart, J.L., Santangelo, A.M., Low, M.J., Westbrook, G.L., and Rubinstein, M. (2004). A transgenic marker for newly born granule cells in dentate gyrus. J Neurosci *24*, 3251-3259.

P

Paloneva, J., Kestila, M., Wu, J., Salminen, A., Bohling, T., Ruotsalainen, V., Hakola, P., Bakker, A.B., Phillips, J.H., Pekkarinen, P.*, et al.* (2000). Loss-of-function mutations in TYROBP (DAP12) result in a presenile dementia with bone cysts. Nat Genet *25*, 357-361.

Paloneva, J., Manninen, T., Christman, G., Hovanes, K., Mandelin, J., Adolfsson, R., Bianchin, M., Bird, T., Miranda, R., Salmaggi, A.*, et al.* (2002). Mutations in two genes encoding different subunits of a receptor signaling complex result in an identical disease phenotype. Am J Hum Genet *71*, 656-662.

Paolicelli, R.C., Bisht, K., and Tremblay, M.E. (2014). Fractalkine regulation of microglial physiology and consequences on the brain and behavior. Front Cell Neurosci *8*, 129.

Paolicelli, R.C., Bolasco, G., Pagani, F., Maggi, L., Scianni, M., Panzanelli, P., Giustetto, M., Ferreira, T.A., Guiducci, E., Dumas, L.*, et al.* (2011). Synaptic pruning by microglia is necessary for normal brain development. Science *333*, 1456-1458.

Paraoan, L., Gray, D., Hiscott, P., Garcia-Finana, M., Lane, B., Damato, B., and Grierson, I. (2009). Cathepsin S and its inhibitor cystatin C: imbalance in uveal melanoma. Front Biosci (Landmark Ed) *14*, 2504-2513.

Pardridge, W.M. (2005). The blood-brain barrier: bottleneck in brain drug development. NeuroRx *2*, 3-14.

Paresce, D.M., Ghosh, R.N., and Maxfield, F.R. (1996). Microglial cells internalize aggregates of the Alzheimer's disease amyloid beta-protein via a scavenger receptor. Neuron *17*, 553-565.

Park, D., Han, C.Z., Elliott, M.R., Kinchen, J.M., Trampont, P.C., Das, S., Collins, S., Lysiak, J.J., Hoehn, K.L., and Ravichandran, K.S. (2011). Continued clearance of apoptotic cells critically depends on the phagocyte Ucp2 protein. Nature *477*, 220-224.

Park, S.K., Solomon, D., and Vartanian, T. (2001). Growth factor control of CNS myelination. Dev Neurosci *23*, 327-337.

Parkhurst, C.N., Yang, G., Ninan, I., Savas, J.N., Yates, J.R., 3rd, Lafaille, J.J., Hempstead, B.L., Littman, D.R., and Gan, W.B. (2013). Microglia promote learning-dependent synapse formation through brain-derived neurotrophic factor. Cell *155*, 1596-1609.

Parnaik, R., Raff, M.C., and Scholes, J. (2000). Differences between the clearance of apoptotic cells by professional and non-professional phagocytes. Curr Biol *10*, 857-860.

Parslow, A., Cardona, A., and Bryson-Richardson, R.J. (2014). Sample drift correction following 4D confocal time-lapse imaging. J Vis Exp.

Patel, M. (2016). Targeting Oxidative Stress in Central Nervous System Disorders. Trends Pharmacol Sci *37*, 768-778.

Pennacchio, L.A., Bouley, D.M., Higgins, K.M., Scott, M.P., Noebels, J.L., and Myers, R.M. (1998). Progressive ataxia, myoclonic epilepsy and cerebellar apoptosis in cystatin B-deficient mice. Nat Genet *20*, 251-258.

Pennacchio, L.A., Lehesjoki, A.E., Stone, N.E., Willour, V.L., Virtaneva, K., Miao, J., D'Amato, E., Ramirez, L., Faham, M., Koskiniemi, M.*, et al.* (1996). Mutations in the gene encoding cystatin B in progressive myoclonus epilepsy (EPM1). Science *271*, 1731-1734.

Peri, F., and Nusslein-Volhard, C. (2008). Live imaging of neuronal degradation by microglia reveals a role for v0-ATPase a1 in phagosomal fusion in vivo. Cell *133*, 916-927.

Pernhorst, K., Herms, S., Hoffmann, P., Cichon, S., Schulz, H., Sander, T., Schoch, S., Becker, A.J., and Grote, A. (2013). TLR4, ATF-3 and IL8 inflammation mediator expression correlates with seizure frequency in human epileptic brain tissue. Seizure *22*, 675-678.

Perry, V.H., Nicoll, J.A., and Holmes, C. (2010). Microglia in neurodegenerative disease. Nat Rev Neurol *6*, 193-201.

Pickering, M., Cumiskey, D., and O'Connor, J.J. (2005). Actions of TNF-alpha on glutamatergic synaptic transmission in the central nervous system. Exp Physiol *90*, 663-670.

Poon, I.K., Lucas, C.D., Rossi, A.G., and Ravichandran, K.S. (2014). Apoptotic cell clearance: basic biology and therapeutic potential. Nature reviews Immunology *14*, 166-180.

Preissler, J., Grosche, A., Lede, V., Le Duc, D., Krugel, K., Matyash, V., Szulzewsky, F., Kallendrusch, S., Immig, K., Kettenmann, H.*, et al.* (2015). Altered microglial phagocytosis in GPR34-deficient mice. Glia *63*, 206-215.

Priel, M.R., and Albuquerque, E.X. (2002). Short-term effects of pilocarpine on rat hippocampal neurons in culture. Epilepsia *43 Suppl 5*, 40-46.

Prinz, M., and Priller, J. (2014). Microglia and brain macrophages in the molecular age: from origin to neuropsychiatric disease. Nat Rev Neurosci *15*, 300-312.

Q

Quan, D.N., Cooper, M.D., Potter, J.L., Roberts, M.H., Cheng, H., and Jarvis, G.A. (2008). TREM-2 binds to lipooligosaccharides of Neisseria gonorrhoeae and is expressed on reproductive tract epithelial cells. Mucosal Immunol *1*, 229-238.

Quinn, M.T., and Schepetkin, I.A. (2009). Role of NADPH oxidase in formation and function of multinucleated giant cells. J Innate Immun *1*, 509-526.

Quirico-Santos, T., Meira, I.D., Gomes, A.C., Pereira, V.C., Pinto, M., Monteiro, M., Souza, J.M., and Alves-Leon, S.V. (2013). Resection of the epileptogenic lesion abolishes seizures and reduces inflammatory cytokines of patients with temporal lobe epilepsy. Journal of neuroimmunology *254*, 125-130.

R

Racine, R.J. (1972). Modification of seizure activity by electrical stimulation. II. Motor seizure. Electroencephalography and clinical neurophysiology *32*, 281-294.

Ransohoff, R.M. (2016). How neuroinflammation contributes to neurodegeneration. Science *353*, 777-783.

Rappold, P.M., Lynd-Balta, E., and Joseph, S.A. (2006). P2X7 receptor immunoreactive profile confined to resting and activated microglia in the epileptic brain. Brain Res *1089*, 171-178.

Rassendren, F., and Audinat, E. (2016). Purinergic signaling in epilepsy. Journal of neuroscience research *94*, 781-793.

Ravichandran, K.S. (2010). Find-me and eat-me signals in apoptotic cell clearance: progress and conundrums. The Journal of experimental medicine *207*, 1807-1817.

Ravizza, T., Balosso, S., and Vezzani, A. (2011). Inflammation and prevention of epileptogenesis. Neurosci Lett *497*, 223-230.

Ravizza, T., Gagliardi, B., Noe, F., Boer, K., Aronica, E., and Vezzani, A. (2008). Innate and adaptive immunity during epileptogenesis and spontaneous seizures: evidence from experimental models and human temporal lobe epilepsy. Neurobiol Dis *29*, 142-160.

Réaux-Le Goazigo, A., Van Steenwinckel, J., Rostène, W., and Mélik Parsadaniantz, S. (2013). Current status of chemokines in the adult CNS. Progress in Neurobiology *104*, 67-92.

Remington, L.T., Babcock, A.A., Zehntner, S.P., and Owens, T. (2007). Microglial recruitment, activation, and proliferation in response to primary demyelination. The American journal of pathology *170*, 1713-1724.

Reubold, T.F., and Eschenburg, S. (2012). A molecular view on signal transduction by the apoptosome. Cell Signal *24*, 1420-1425.

Rezaie, P., Cairns, N.J., and Male, D.K. (1997). Expression of adhesion molecules on human fetal cerebral vessels: relationship to microglial colonisation during development. Brain Res Dev Brain Res *104*, 175-189.

Rezaie, P., Dean, A., Male, D., and Ulfig, N. (2005). Microglia in the cerebral wall of the human telencephalon at second trimester. Cereb Cortex *15*, 938-949.

Rinne, R., Saukko, P., Jarvinen, M., and Lehesjoki, A.E. (2002). Reduced cystatin B activity correlates with enhanced cathepsin activity in progressive myoclonus epilepsy. Ann Med *34*, 380-385.

Robson, S.C., Sevigny, J., and Zimmermann, H. (2006). The E-NTPDase family of ectonucleotidases: Structure function relationships and pathophysiological significance. Purinergic Signal *2*, 409-430.

Roumier, A., Bechade, C., Poncer, J.C., Smalla, K.H., Tomasello, E., Vivier, E., Gundelfinger, E.D., Triller, A., and Bessis, A. (2004). Impaired synaptic function in the microglial KARAP/DAP12-deficient mouse. J Neurosci *24*, 11421-11428.

Roumier, A., Pascual, O., Bechade, C., Wakselman, S., Poncer, J.C., Real, E., Triller, A., and Bessis, A. (2008). Prenatal activation of microglia induces delayed impairment of glutamatergic synaptic function. PLoS One *3*, e2595.

Ruocco, A., Nicole, O., Docagne, F., Ali, C., Chazalviel, L., Komesli, S., Yablonsky, F., Roussel, S., MacKenzie, E.T., Vivien, D.*, et al.* (1999). A transforming growth factor-beta antagonist unmasks the neuroprotective role of this endogenous cytokine in excitotoxic and ischemic brain injury. J Cereb Blood Flow Metab *19*, 1345-1353.

Rutecki, P.A., Lebeda, F.J., and Johnston, D. (1985). Epileptiform activity induced by changes in extracellular potassium in hippocampus. J Neurophysiol *54*, 1363-1374.

S

Safaiyan, S., Kannaiyan, N., Snaidero, N., Brioschi, S., Biber, K., Yona, S., Edinger, A.L., Jung, S., Rossner, M.J., and Simons, M. (2016). Age-related myelin degradation burdens the clearance function of microglia during aging. Nat Neurosci *19*, 995-998.

Santiago, M.F., Veliskova, J., Patel, N.K., Lutz, S.E., Caille, D., Charollais, A., Meda, P., and Scemes, E. (2011). Targeting pannexin1 improves seizure outcome. PLoS One *6*, e25178.

Sasmono, R.T., Oceandy, D., Pollard, J.W., Tong, W., Pavli, P., Wainwright, B.J., Ostrowski, M.C., Himes, S.R., and Hume, D.A. (2003). A macrophage colony-stimulating factor receptor-green fluorescent protein transgene is expressed throughout the mononuclear phagocyte system of the mouse. Blood *101*, 1155-1163.

Savage, N. (2014). Epidemiology: The complexities of epilepsy. Nature *511*, S2-3.

Savill, J., Dransfield, I., Gregory, C., and Haslett, C. (2002). A blast from the past: clearance of apoptotic cells regulates immune responses. Nature reviews Immunology *2*, 965-975.

Schafer, D.P., Lehrman, E.K., Kautzman, A.G., Koyama, R., Mardinly, A.R., Yamasaki, R., Ransohoff, R.M., Greenberg, M.E., Barres, B.A., and Stevens, B. (2012). Microglia sculpt postnatal neural circuits in an activity and complement-dependent manner. Neuron *74*, 691-705.

Schuele, S.U., and Luders, H.O. (2008). Intractable epilepsy: management and therapeutic alternatives. The Lancet Neurology *7*, 514-524.

Schulz, C., Gomez Perdiguero, E., Chorro, L., Szabo-Rogers, H., Cagnard, N., Kierdorf, K., Prinz, M., Wu, B., Jacobsen, S.E., Pollard, J.W*., et al.* (2012). A lineage of myeloid cells independent of Myb and hematopoietic stem cells. Science *336*, 86-90.

Schwartzkroin, P.A. (1986). Hippocampal slices in experimental and human epilepsy. Adv Neurol *44*, 991-1010.

Shankaran, M., Marino, M.E., Busch, R., Keim, C., King, C., Lee, J., Killion, S., Awada, M., and Hellerstein, M.K. (2007). Measurement of brain microglial proliferation rates in vivo in response to neuroinflammatory stimuli: application to drug discovery. Journal of neuroscience research *85*, 2374-2384.

Shannon, P., Pennacchio, L.A., Houseweart, M.K., Minassian, B.A., and Myers, R.M. (2002). Neuropathological changes in a mouse model of progressive myoclonus epilepsy: cystatin B deficiency and Unverricht-Lundborg disease. J Neuropathol Exp Neurol *61*, 1085-1091.

Sharma, A.K., Reams, R.Y., Jordan, W.H., Miller, M.A., Thacker, H.L., and Snyder, P.W. (2007). Mesial temporal lobe epilepsy: pathogenesis, induced rodent models and lesions. Toxicol Pathol *35*, 984-999.

Shorvon, S.D. (2011). The etiologic classification of epilepsy. Epilepsia *52*, 1052-1057.

Sieger, D., and Peri, F. (2013). Animal models for studying microglia: the first, the popular, and the new. Glia *61*, 3-9.

Sierra, A., Abiega, O., Shahraz, A., and Neumann, H. (2013). Janus-faced microglia: beneficial and detrimental consequences of microglial phagocytosis. Front Cell Neurosci *7*, 6.

Sierra, A., Encinas, J.M., Deudero, J.J., Chancey, J.H., Enikolopov, G., Overstreet-Wadiche, L.S., Tsirka, S.E., and Maletic-Savatic, M. (2010). Microglia shape adult hippocampal neurogenesis through apoptosis-coupled phagocytosis. Cell Stem Cell *7*, 483-495.

Sierra, A., Gottfried-Blackmore, A.C., McEwen, B.S., and Bulloch, K. (2007). Microglia derived from aging mice exhibit an altered inflammatory profile. Glia *55*, 412-424.

Sierra, A., Martin-Suarez, S., Valcarcel-Martin, R., Pascual-Brazo, J., Aelvoet, S.A., Abiega, O., Deudero, J.J., Brewster, A.L., Bernales, I., Anderson, A.E., *et al.* (2015). Neuronal hyperactivity accelerates depletion of neural stem cells and impairs hippocampal neurogenesis. Cell Stem Cell *16*, 488-503.

Sierra, A., and Tremblay, M.-È. (2014). Introduction. In Microglia in Health and disease, M.-È. Tremblay, and A. Sierra, eds. (Springer-Verlag New York), pp. 3-6.

Simard, A.R., Soulet, D., Gowing, G., Julien, J.P., and Rivest, S. (2006). Bone marrow-derived microglia play a critical role in restricting senile plaque formation in Alzheimer's disease. Neuron *49*, 489-502.

Simopoulos, A.P. (2002). The importance of the ratio of omega-6/omega-3 essential fatty acids. Biomedicine & pharmacotherapy = Biomedecine & pharmacotherapie *56*, 365-379.

Sinha, R.A., Khare, P., Rai, A., Maurya, S.K., Pathak, A., Mohan, V., Nagar, G.K., Mudiam, M.K., Godbole, M.M., and Bandyopadhyay, S. (2009). Anti-apoptotic role of omega-3-fatty acids in developing brain: perinatal hypothyroid rat cerebellum as apoptotic model. Int J Dev Neurosci *27*, 377-383.

Skaper, S.D., Debetto, P., and Giusti, P. (2010). The P2X7 purinergic receptor: from physiology to neurological disorders. FASEB J *24*, 337-345.

Smolders, I., Khan, G.M., Manil, J., Ebinger, G., and Michotte, Y. (1997). NMDA receptor-mediated pilocarpine-induced seizures: characterization in freely moving rats by microdialysis. British journal of pharmacology *121*, 1171-1179.

Snow, B.J., Rolfe, F.L., Lockhart, M.M., Frampton, C.M., O'Sullivan, J.D., Fung, V., Smith, R.A., Murphy, M.P., Taylor, K.M., and Protect Study, G. (2010). A double-blind, placebo-controlled study to assess the mitochondria-targeted antioxidant MitoQ as a disease-modifying therapy in Parkinson's disease. Mov Disord *25*, 1670-1674.

Sokolowski, J.D., Chabanon-Hicks, C.N., Han, C.Z., Heffron, D.S., and Mandell, J.W. (2014). Fractalkine is a "find-me" signal released by neurons undergoing ethanol-induced apoptosis. Front Cell Neurosci *8*, 360.

Spangenberg, E.E., and Green, K.N. (2017). Inflammation in Alzheimer's disease: Lessons learned from microglia-depletion models. Brain Behav Immun *61*, 1-11.

Stalder, M., Deller, T., Staufenbiel, M., and Jucker, M. (2001). 3D-Reconstruction of microglia and amyloid in APP23 transgenic mice: no evidence of intracellular amyloid. Neurobiol Aging *22*, 427-434.

Stebbing, M.J., Cottee, J.M., and Rana, I. (2015). The Role of Ion Channels in Microglial Activation and Proliferation - A Complex Interplay between Ligand-Gated Ion Channels, K(+) Channels, and Intracellular Ca(2.). Front Immunol *6*, 497.

Stefano, L., Racchetti, G., Bianco, F., Passini, N., Gupta, R.S., Panina Bordignon, P., and Meldolesi, J. (2009). The surface-exposed chaperone, Hsp60, is an agonist of the microglial TREM2 receptor. J Neurochem *110*, 284-294.

Stoka, V., Turk, V., and Turk, B. (2016). Lysosomal cathepsins and their regulation in aging and neurodegeneration. Ageing Res Rev *32*, 22-37.

Stys, P.K., Zamponi, G.W., van Minnen, J., and Geurts, J.J. (2012). Will the real multiple sclerosis please stand up? Nat Rev Neurosci *13*, 507-514.

Sun, B., Zhou, Y., Halabisky, B., Lo, I., Cho, S.H., Mueller-Steiner, S., Devidze, N., Wang, X., Grubb, A., and Gan, L. (2008). Cystatin C-cathepsin B axis regulates amyloid beta levels and associated neuronal deficits in an animal model of Alzheimer's disease. Neuron *60*, 247-257.

Suzumura, A., Tamaru, T., Yoshikawa, M., and Takayanagi, T. (1999). Multinucleated giant cell formation by microglia: induction by interleukin (IL)-4 and IL-13. Brain Research *849*, 239-243.

Swinnen, N., Smolders, S., Avila, A., Notelaers, K., Paesen, R., Ameloot, M., Brone, B., Legendre, P., and Rigo, J.M. (2013). Complex invasion pattern of the cerebral cortex bymicroglial cells during development of the mouse embryo. Glia *61*, 150-163.

Szelényi, J. (2001). Cytokines and the central nervous system. Brain Research Bulletin *54*, 329-338.

T

Takahashi, K., Rochford, C.D., and Neumann, H. (2005). Clearance of apoptotic neurons without inflammation by microglial triggering receptor expressed on myeloid cells-2. The Journal of experimental medicine *201*, 647-657.

Tanaka, T., Ueno, M., and Yamashita, T. (2009). Engulfment of axon debris by microglia requires p38 MAPK activity. J Biol Chem *284*, 21626-21636.

Tashiro, A., Sandler, V.M., Toni, N., Zhao, C., and Gage, F.H. (2006). NMDA-receptor-mediated, cell-specific integration of new neurons in adult dentate gyrus. Nature *442*, 929-933.

Tatum, W.O.t. (2012). Mesial temporal lobe epilepsy. J Clin Neurophysiol *29*, 356-365.

Tay, T.L., Mai, D., Dautzenberg, J., Fernandez-Klett, F., Lin, G., Sagar, Datta, M., Drougard, A., Stempfl, T., Ardura-Fabregat, A*., et al.* (2017). A new fate mapping system reveals context-dependent random or clonal expansion of microglia. Nat Neurosci.

Taylor, R.C., Cullen, S.P., and Martin, S.J. (2008). Apoptosis: controlled demolition at the cellular level. Nat Rev Mol Cell Biol *9*, 231-241.

Tegelberg, S., Kopra, O., Joensuu, T., Cooper, J.D., and Lehesjoki, A.E. (2012). Early microglial activation precedes neuronal loss in the brain of the Cstb-/- mouse model of progressive myoclonus epilepsy, EPM1. J Neuropathol Exp Neurol *71*, 40-53.

Thevenaz, P., Ruttimann, U.E., and Unser, M. (1998). A pyramid approach to subpixel registration based on intensity. IEEE transactions on image processing : a publication of the IEEE Signal Processing Society *7*, 27-41.

Thompson, C.L., Pathak, S.D., Jeromin, A., Ng, L.L., MacPherson, C.R., Mortrud, M.T., Cusick, A., Riley, Z.L., Sunkin, S.M., Bernard, A*., et al.* (2008). Genomic anatomy of the hippocampus. Neuron *60*, 1010-1021.

Thurman, D.J., Beghi, E., Begley, C.E., Berg, A.T., Buchhalter, J.R., Ding, D., Hesdorffer, D.C., Hauser, W.A., Kazis, L., Kobau, R*., et al.* (2011). Standards for epidemiologic studies and surveillance of epilepsy. Epilepsia *52 Suppl 7*, 2-26.

Toscano, C.D., Kingsley, P.J., Marnett, L.J., and Bosetti, F. (2008). NMDA-induced seizure intensity is enhanced in COX-2 deficient mice. Neurotoxicology *29*, 1114-1120.

Traub, R.D., Jefferys, J.G., and Whittington, M.A. (1994). Enhanced NMDA conductance can account for epileptiform activity induced by low Mg2+ in the rat hippocampal slice. J Physiol *478 Pt 3*, 379-393.

Trautmann, A. (2009). Extracellular ATP in the immune system: more than just a "danger signal". Sci Signal *2*, pe6.

Tremblay, M.E., Lecours, C., Samson, L., Sanchez-Zafra, V., and Sierra, A. (2015). From the Cajal alumni Achucarro and Rio-Hortega to the rediscovery of never-resting microglia. Front Neuroanat *9*, 45.

Tremblay, M.E., Lowery, R.L., and Majewska, A.K. (2010). Microglial interactions with synapses are modulated by visual experience. PLoS Biol *8*, e1000527.

Troy, C.M., and Jean, Y.Y. (2015). Caspases: therapeutic targets in neurologic disease. Neurotherapeutics *12*, 42-48.

Truman, L.A., Ford, C.A., Pasikowska, M., Pound, J.D., Wilkinson, S.J., Dumitriu, I.E., Melville, L., Melrose, L.A., Ogden, C.A., Nibbs, R.*, et al.* (2008). CX3CL1/fractalkine is released from apoptotic lymphocytes to stimulate macrophage chemotaxis. Blood *112*, 5026-5036.

Turk, V., Stoka, V., and Turk, D. (2008). Cystatins: biochemical and structural properties, and medical relevance. Front Biosci *13*, 5406-5420.

Turk, V., Stoka, V., Vasiljeva, O., Renko, M., Sun, T., Turk, B., and Turk, D. (2012). Cysteine cathepsins: from structure, function and regulation to new frontiers. Biochim Biophys Acta *1824*, 68-88.

U

Ueno, M., Fujita, Y., Tanaka, T., Nakamura, Y., Kikuta, J., Ishii, M., and Yamashita, T. (2013). Layer V cortical neurons require microglial support for survival during postnatal development. Nat Neurosci *16*, 543-551.

Ulmann, L., Levavasseur, F., Avignone, E., Peyroutou, R., Hirbec, H., Audinat, E., and Rassendren, F. (2013). Involvement of P2X4 receptors in hippocampal microglial activation after status epilepticus. Glia *61*, 1306-1319.

Underhill, D.M., and Goodridge, H.S. (2012). Information processing during phagocytosis. Nature reviews Immunology *12*, 492-502.

V

Vanden Berghe, T., Linkermann, A., Jouan-Lanhouet, S., Walczak, H., and Vandenabeele, P. (2014). Regulated necrosis: the expanding network of non-apoptotic cell death pathways. Nat Rev Mol Cell Biol *15*, 135-147.

Vasek, M.J., Garber, C., Dorsey, D., Durrant, D.M., Bollman, B., Soung, A., Yu, J., Perez-Torres, C., Frouin, A., Wilton, D.K.*, et al.* (2016). A complement-microglial axis drives synapse loss during virus-induced memory impairment. Nature *534*, 538-543.

Verdot, L., Lalmanach, G., Vercruysse, V., Hartmann, S., Lucius, R., Hoebeke, J., Gauthier, F., and Vray, B. (1996). Cystatins up-regulate nitric oxide release from interferon-gamma-activated mouse peritoneal macrophages. J Biol Chem *271*, 28077-28081.

Vezzani, A. (2009). Pilocarpine-induced seizures revisited: what does the model mimic? Epilepsy currents / American Epilepsy Society *9*, 146-148.

Vezzani, A., Aronica, E., Mazarati, A., and Pittman, Q.J. (2013a). Epilepsy and brain inflammation. Exp Neurol *244*, 11-21.

Vezzani, A., Balosso, S., Maroso, M., Zardoni, D., Noe, F., and Ravizza, T. (2010). ICE/caspase 1 inhibitors and IL-1beta receptor antagonists as potential therapeutics in epilepsy. Current opinion in investigational drugs *11*, 43-50.

Vezzani, A., Balosso, S., and Ravizza, T. (2008). The role of cytokines in the pathophysiology of epilepsy. Brain Behav Immun *22*, 797-803.

Vezzani, A., Bartfai, T., Bianchi, M., Rossetti, C., and French, J. (2011a). Therapeutic potential of new antiinflammatory drugs. Epilepsia *52 Suppl 8*, 67-69.

Vezzani, A., Conti, M., De Luigi, A., Ravizza, T., Moneta, D., Marchesi, F., and De Simoni, M.G. (1999). Interleukin-1beta immunoreactivity and microglia are enhanced in the rat hippocampus by focal kainate application: functional evidence for enhancement of electrographic seizures. J Neurosci *19*, 5054-5065.

Vezzani, A., French, J., Bartfai, T., and Baram, T.Z. (2011b). The role of inflammation in epilepsy. Nat Rev Neurol *7*, 31-40.

Vezzani, A., Friedman, A., and Dingledine, R.J. (2013b). The role of inflammation in epileptogenesis. Neuropharmacology *69*, 16-24.

Vezzani, A., and Granata, T. (2005). Brain inflammation in epilepsy: experimental and clinical evidence. Epilepsia *46*, 1724-1743.

Vilček, J. (2003). CHAPTER 1 - The cytokines: an overview A2 - Thomson, Angus W. In The Cytokine Handbook (Fourth Edition), M.T. Lotze, ed. (London: Academic Press), pp. 3-18.

Vinet, J., Weering, H.R., Heinrich, A., Kalin, R.E., Wegner, A., Brouwer, N., Heppner, F.L., Rooijen, N., Boddeke, H.W., and Biber, K. (2012). Neuroprotective function for ramified microglia in hippocampal excitotoxicity. Journal of neuroinflammation *9*, 27.

Viviani, B., Bartesaghi, S., Gardoni, F., Vezzani, A., Behrens, M.M., Bartfai, T., Binaglia, M., Corsini, E., Di Luca, M., Galli, C.L*., et al.* (2003). Interleukin-1β Enhances NMDA Receptor-Mediated Intracellular Calcium Increase through Activation of the Src Family of Kinases. The Journal of Neuroscience *23*, 8692.

Vivien, D., and Ali, C. (2006). Transforming growth factor-beta signalling in brain disorders. Cytokine Growth Factor Rev *17*, 121-128.

Voigt, T. (1989). Development of glial cells in the cerebral wall of ferrets: direct tracing of their transformation from radial glia into astrocytes. J Comp Neurol *289*, 74-88.

von Bernhardi, R., Eugenin-von Bernhardi, L., and Eugenin, J. (2015). Microglial cell dysregulation in brain aging and neurodegeneration. Front Aging Neurosci *7*, 124.

W

Wake, H., Moorhouse, A.J., Jinno, S., Kohsaka, S., and Nabekura, J. (2009). Resting microglia directly monitor the functional state of synapses in vivo and determine the fate of ischemic terminals. J Neurosci *29*, 3974-3980.

Walker, D.G., and Lue, L.F. (2013). Understanding the neurobiology of CD200 and the CD200 receptor: a therapeutic target for controlling inflammation in human brains? Future Neurol *8*.

Wang, K.C., Koprivica, V., Kim, J.A., Sivasankaran, R., Guo, Y., Neve, R.L., and He, Z. (2002). Oligodendrocyte-myelin glycoprotein is a Nogo receptor ligand that inhibits neurite outgrowth. Nature *417*, 941-944.

Wang, S., Cheng, Q., Malik, S., and Yang, J. (2000). Interleukin-1beta inhibits gamma-aminobutyric acid type A (GABA(A)) receptor current in cultured hippocampal neurons. J Pharmacol Exp Ther *292*, 497-504.

Wang, X., Arcuino, G., Takano, T., Lin, J., Peng, W.G., Wan, P., Li, P., Xu, Q., Liu, Q.S., Goldman, S.A*., et al.* (2004). P2X7 receptor inhibition improves recovery after spinal cord injury. Nat Med *10*, 821-827.

Wang, Y., Cella, M., Mallinson, K., Ulrich, J.D., Young, K.L., Robinette, M.L., Gilfillan, S., Krishnan, G.M., Sudhakar, S., Zinselmeyer, B.H*., et al.* (2015). TREM2 lipid sensing sustains the microglial response in an Alzheimer's disease model. Cell *160*, 1061-1071.

Wang, Y., and Qin, Z.H. (2010). Molecular and cellular mechanisms of excitotoxic neuronal death. Apoptosis *15*, 1382-1402.

Watkins, L.R., and Maier, S.F. (2002). Beyond neurons: evidence that immune and glial cells contribute to pathological pain states. Physiol Rev *82*, 981-1011.

Weissberg, I., Wood, L., Kamintsky, L., Vazquez, O., Milikovsky, D.Z., Alexander, A., Oppenheim, H., Ardizzone, C., Becker, A., Frigerio, F.*, et al.* (2015). Albumin induces excitatory synaptogenesis through astrocytic TGF-beta/ALK5 signaling in a model of acquired epilepsy following blood-brain barrier dysfunction. Neurobiol Dis *78*, 115-125.

Wendt, W., Lubbert, H., and Stichel, C.C. (2008). Upregulation of cathepsin S in the aging and pathological nervous system of mice. Brain Res *1232*, 7-20.

Wu, A., Wei, J., Kong, L.Y., Wang, Y., Priebe, W., Qiao, W., Sawaya, R., and Heimberger, A.B. (2010). Glioma cancer stem cells induce immunosuppressive macrophages/microglia. Neuro Oncol *12*, 1113-1125.

Wu, L.J., Vadakkan, K.I., and Zhuo, M. (2007). ATP-induced chemotaxis of microglial processes requires P2Y receptor-activated initiation of outward potassium currents. Glia *55*, 810-821.

Wu, L.J., and Zhuo, M. (2008). Resting microglial motility is independent of synaptic plasticity in mammalian brain. J Neurophysiol *99*, 2026-2032.

X

Xu, J., and Ikezu, T. (2009). The comorbidity of HIV-associated neurocognitive disorders and Alzheimer's disease: a foreseeable medical challenge in post-HAART era. Journal of neuroimmune pharmacology : the official journal of the Society on NeuroImmune Pharmacology *4*, 200-212.

Xu, J., Wang, T., Wu, Y., Jin, W., and Wen, Z. (2016). Microglia Colonization of Developing Zebrafish Midbrain Is Promoted by Apoptotic Neuron and Lysophosphatidylcholine. Developmental cell *38*, 214-222.

Xu, Y., Zeng, K., Han, Y., Wang, L., Chen, D., Xi, Z., Wang, H., Wang, X., and Chen, G. (2012). Altered expression of CX3CL1 in patients with epilepsy and in a rat model. The American journal of pathology *180*, 1950-1962.

Y

Ye, L., Huang, Y., Zhao, L., Li, Y., Sun, L., Zhou, Y., Qian, G., and Zheng, J.C. (2013). IL-1beta and TNF-alpha induce neurotoxicity through glutamate production: a potential role for neuronal glutaminase. J Neurochem *125*, 897-908.

Yeh, F.L., Wang, Y., Tom, I., Gonzalez, L.C., and Sheng, M. (2016). TREM2 Binds to Apolipoproteins, Including APOE and CLU/APOJ, and Thereby Facilitates Uptake of Amyloid-Beta by Microglia. Neuron *91*, 328-340.

Yeo, S.I., Kim, J.E., Ryu, H.J., Seo, C.H., Lee, B.C., Choi, I.G., Kim, D.S., and Kang, T.C. (2011). The roles of fractalkine/CX3CR1 system in neuronal death following pilocarpine-induced status epilepticus. Journal of neuroimmunology *234*, 93-102.

Yoshikawa, K., Kita, Y., Kishimoto, K., and Shimizu, T. (2006). Profiling of eicosanoid production in the rat hippocampus during kainic acid-induced seizure: dual phase regulation and differential involvement of COX-1 and COX-2. J Biol Chem *281*, 14663-14669.

Z

Zeise, M.L., Espinoza, J., Morales, P., and Nalli, A. (1997). Interleukin-1β does not increase synaptic inhibition in hippocampal CA3 pyramidal and dentate gyrus granule cells of the rat in vitro. Brain Research *768*, 341-344.

Zhan, Y., Paolicelli, R.C., Sforazzini, F., Weinhard, L., Bolasco, G., Pagani, F., Vyssotski, A.L., Bifone, A., Gozzi, A., Ragozzino, D.*, et al.* (2014). Deficient neuron-microglia signaling results in impaired functional brain connectivity and social behavior. Nat Neurosci *17*, 400-406.

Zhang, Q., Chen, C., Lu, J., Xie, M., Pan, D., Luo, X., Yu, Z., Dong, Q., and Wang, W. (2009). Cell cycle inhibition attenuates microglial proliferation and production of IL-1beta, MIP-1alpha, and NO after focal cerebral ischemia in the rat. Glia *57*, 908-920.

Zhang, R., Sun, L., Hayashi, Y., Liu, X., Koyama, S., Wu, Z., and Nakanishi, H. (2010). Acute p38-mediated inhibition of NMDA-induced outward currents in hippocampal CA1 neurons by interleukin-1beta. Neurobiol Dis *38*, 68-77.

Zhong, L., Chen, X.F., Zhang, Z.L., Wang, Z., Shi, X.Z., Xu, K., Zhang, Y.W., Xu, H., and Bu, G. (2015). DAP12 Stabilizes the C-terminal Fragment of the Triggering Receptor Expressed on Myeloid Cells-2 (TREM2) and Protects against LPS-induced Pro-inflammatory Response. J Biol Chem *290*, 15866-15877.

Zhuo, L., Sun, B., Zhang, C.L., Fine, A., Chiu, S.Y., and Messing, A. (1997). Live astrocytes visualized by green fluorescent protein in transgenic mice. Dev Biol *187*, 36-42.

Zimmermann, H. (1999). Two novel families of ectonucleotidases: molecular structures, catalytic properties and a search for function. Trends Pharmacol Sci *20*, 231-236.

Zong, W.X., and Thompson, C.B. (2006). Necrotic death as a cell fate. Genes Dev *20*, 1-15.

Zsurka, G., and Kunz, W.S. (2015). Mitochondrial dysfunction and seizures: the neuronal energy crisis. The Lancet Neurology *14*, 956-966.

Zuchero, J.B., and Barres, B.A. (2015). Glia in mammalian development and disease. Development *142*, 3805-3809.